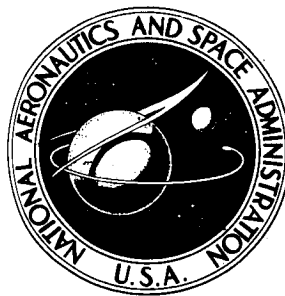


**NASA CONTRACTOR
REPORT**



NASA CR-2383

NASA CR-2383

**CASE FILE
COPY**

**INTEGRATED POWER/ATTITUDE
CONTROL SYSTEM (IPACS) STUDY**

Volume I - Feasibility Studies

by J. E. Notti, A. Cormack III, and W. C. Schmill

Prepared by

ROCKWELL INTERNATIONAL

SPACE DIVISION

Downey, Calif, 90241

for Langley Research Center

NATIONAL AERONAUTICS AND SPACE ADMINISTRATION • WASHINGTON, D. C. • APRIL 1974

1. Report No. NASA CR- 2383		2. Government Accession No.		3. Recipient's Catalog No.	
4. Title and Subtitle INTEGRATED POWER/ATTITUDE CONTROL SYSTEM (IPACS) STUDY- VOLUME I FEASIBILITY STUDIES				5. Report Date April 1974	
				6. Performing Organization Code	
7. Author(s) J.E. NOTTI, A. CORMACK III, and W. C. SCHMILL				8. Performing Organization Report No. SD 73-SA-0101-1	
9. Performing Organization Name and Address Rockwell International Space Division Downey, CA.				10. Work Unit No. 999-74-35-01	
				11. Contract or Grant No. NAS1-11732	
12. Sponsoring Agency Name and Address National Aeronautics and Space Administration Washington, D. C. 20546				13. Type of Report and Period Covered Contractor Report	
				14. Sponsoring Agency Code	
15. Supplementary Notes This is a final report.					
16. Abstract An Integrated Power/Attitude Control System (IPACS) concept consisting of an array of spinning flywheels, with or without gimbals, capable of performing the dual function of power storage and generation, as well as attitude control has been investigated. This system provides attitude control through momentum storage, and replaces the storage batteries onboard the spacecraft. The results of the investigation are presented in two volumes. Volume I contains the trade-off studies performed to establish the feasibility, cost effectiveness, required level of development, and boundaries of application of IPACS to a wide variety of spacecraft. Volume II presents the conceptual designs for a free-flying research application module (RAM), and for a tracking and data relay satellite (TDRS). Volume II also contains results from dynamic analyses and simulations of the IPACS conceptual designs.					
17. Key Words (Suggested by Author(s)) Integrated Power/Attitude Control System Attitude control Power storage and generation Battery replacement Weight, volume, and cost savings				18. Distribution Statement UNCLASSIFIED- UNLIMITED	
19. Security Classif. (of this report) UNCLASSIFIED		20. Security Classif. (of this page) UNCLASSIFIED		21. No. of Pages 301	
				22. Price* \$7.00	

FOREWORD

This report was prepared by the Space Division of Rockwell International for the National Aeronautics and Space Administration's Langley Research Center in accordance with the requirements of Exhibit A of Contract NAS1-11732. The contract directed a 13-month study of spacecraft integrated electrical power and attitude control subsystems which utilize flywheels to perform the dual functions of energy storage and attitude control.

The results of this study are presented in two volumes. Volume I, Feasibility Studies (SD 73-SA-0101-1), presents feasibility and cost-effectiveness comparison studies defining the use of integrated power and attitude control subsystems for seven spacecraft missions. Volume II, Conceptual Design (SD 73-SA-0101-2), presents specific designs for a satellite and a Shuttle research and application module mission.

The Aerospace Instruments and Control System Department of the General Electric Company performed a major subcontract effort in support of the integrated power and attitude control subsystem study. The subcontract effort included support to feasibility studies, component development program definition and cost estimation, and the preparation of flywheel rotating assembly designs including electronics.

The authors would like to acknowledge the substantial contributions of Mr. S. B. Hamilton and Mr. R. C. Wells of General Electric to both the study and the final report.

Acknowledgement is given to the following individuals for their participation in the conduct of the study:

F. B. Cauchon	-	Controls Analysis
B. J. Call	-	Rotor Design
W. Cooper	-	Cost Comparisons
F. J. Darnes	-	Rotor Design
J. J. Jandrasi	-	Controls Analysis
E. J. Mulcahy	-	Rotor Design
V. Van Camp	-	Electrical Power
P. W. Welch	-	Dynamic Analysis

CONTENTS

	Page
SUMMARY	1
INTRODUCTION	3
Background	3
IPACS Concept	4
Study Objectives	4
Study Scope and Qualifications	4
Report Organization	6
MODULE 1 - TECHNICAL FEASIBILITY ANALYSIS	
Requirements Definition	7
Mission/vehicle selections	7
Spacecraft requirements	7
Power and control requirements	7
IPACS design criteria	10
Competitive Power and Control Subsystems	10
Feasibility Trade Study	10
Component Trades	15
Motor/generators	15
Isotropic rotors	24
Composite rotors	30
Spin bearing	40
Housing and gimbal	52
Energy Storage Elements and Subsystems	59
Energy storage elements	59
Energy storage subsystems	62
System Trades	70
Wheel array evaluations	70
Array selection methodology	76
Array selections	76
Electrical mechanizations	80
IPACS Concepts	86
RAM system description	86
TDRS system description	89
MSS system description	92
MJS system description	95
EOS system description	98
Extended shuttle system description	98
IPACS and Competitive System Performance Comparisons	102
Quantitative performance comparisons	102
Qualitative considerations	110
Feasibility Analysis Summary	115
References	116

APPENDIX 1-A - SELECTION OF MISSION CLASS REPRESENTATIVE VEHICLES	117
APPENDIX 1-B - SPACECRAFT REQUIREMENTS	129
APPENDIX 1-C - COMPETITIVE ELECTRICAL POWER AND ATTITUDE CONTROL SUBSYSTEMS DEFINITION	133

MODULE 2 - CRITICAL COMPONENT DEVELOPMENT

Development Requirements	167
Present Technology Extensions	167
Ball bearings and lubrication systems	167
High-speed and power permanent magnet motor/generator	170
Rotor balancing and induced vibration	171
Advanced Technology Developments	172
High-speed magnetic suspension bearings	172
Composite rotors	173
Recommended Development Priority	173
First priority developments	173
Second priority development	174
Third priority developments	174

MODULE 3 - COST ANALYSIS

Introduction and Summary	175
Costing Groundrules and Assumptions	177
Common costs	178
Cost-effectiveness factors	178
Work breakdown structure	178
Costing approach	180
TDRS Cost Data	181
General	181
Equipment cost	184
Cost-effectiveness	188
Total cost comparison	189
RAM Cost Data	189
General	189
Equipment cost	191
Cost-effectiveness	199
Total cost comparison	199
MSS Cost Data	200
General	200
Equipment cost	200
Cost-effectiveness	206
Total cost comparison	207
30-Day Shuttle Sortie Cost Data	207
General	207
Equipment cost	210
Cost-effectiveness	214
Total cost comparison	214
Conclusions	215

MODULE 4 - APPLICATIONS BOUNDARIES

Introduction	217
Power Rating	217
Energy Storage	219
Angular Momentum Storage	219
Pointing	220
Vibration	220
Excess angular momentum	223
Control non-linearities	225
Power interaction with control	226
Pointing summary	226
System Cost Comparisons	226
Summary	228
Standardization Considerations	228
Requirements	229
Design considerations	230
Potential standardized configurations	232
Standardization summary and recommendations	234

MODULE 5 - SPACE SHUTTLE ADVANCED TECHNOLOGY LABORATORY APPLICATIONS

Advanced Technology Laboratory Requirements	235
Study requirements	235
Mission requirements	235
Competitive Power and Control Concepts	241
Battery energy storage assembly parametric analysis	241
Advanced energy storage devices	249
Competitive electrical power characteristics	251
Competitive control concept and characteristics	254
IPACS ATL Concept	257
ATL IPACS design	259
IPACS and Competitive System Comparisons	262
Physical characteristics comparison	264
Performance characteristics comparison	264
Operational consideration comparisons	266
System comparison summary	266
ATL Systems Cost Analysis	268
General	268
Equipment cost	268
Cost-effectiveness tradeoffs	276
Total cost comparison	278
ATL Summary	278
References	279
APPENDIX 5-A - CRITERIA FOR SORTIE LAB BACKUP POWER	281

MODULE 6 - FEASIBILITY STUDY CONCLUSIONS AND RECOMMENDATIONS

Feasibility Study Conclusions	285
Recommendations	287

ILLUSTRATIONS

Figure		Page
I-1	Integrated Power and Control System Concept	5
1-1	Feasibility Study Trade Tree	14
1-2	Motor Efficiency Versus Slip	16
1-3	Motor Torque Versus Slip	16
1-4	Brushless dc Motor-Generator Optimum Design Weights	19
1-5	Brushless dc Motor-Generator Optimum Design Weights (Extended Range)	20
1-6	Brushless dc Motor-Generator Optimum Design Volumes	21
1-7	Efficiencies for Brushless dc Motor-Generator - Peak Efficiencies at Rated Torque	22
1-8	Efficiencies for Brushless dc Motor-Generator - Peak Efficiency at 1/3 Rated Torque	23
1-9	Isotropic Wheel Shape Factors	27
1-10	Isotropic Rotor Maximum Operating Speeds	29
1-11	Circular Brush Configuration	31
1-12	Tape-Wound Configuration	34
1-13	Composite Rotor Weight Versus Kinetic Energy	35
1-14	Composite Rotor Weight Versus Radius	36
1-15	Composite Rotor Speed Versus Radius	36
1-16	Bearing Trades - Design Considerations	41
1-17	Ball Bearing Operation	42
1-18	Ball Bearing Life Data, 38H Bearing	45
1-19	Ball Bearing Life Data, 206H Bearing	46
1-20	Relationship of Fatigue Life to L_{10} Life	46
1-21	Ball Bearing Friction, 38H Bearing	48
1-22	Ball Bearing Friction, 206H Bearing	48
1-23	Magnetic Journal Bearing	49
1-24	Magnetic Bearing Weight	53
1-25	Magnetic Bearing Power	53
1-26	Magnetic Bearing Volume	54
1-27	Operating Speed Cross-Over Points for Ball and Magnetic Suspension Bearings	56
1-28	Outer Gimbal Weight	58
1-29	NiCd Battery Cycle Life	61
1-30	Current Technology Energy-Momentum Wheel	64
1-31	Advanced Technology Energy-Momentum Wheel	65
1-32	Energy Storage Subsystem Capability and Potential	68
1-33	Energy Density Variation with Orbit Altitude and Mission Duration	69
1-34	TDRS Energy-Momentum Sizing	70
1-35	Energy-Momentum Change	71
1-36	Skewed Array of Five Nongimbaled Units	73

1-37	Sketch of Skewed Array of Five Single Gimballed Units	74
1-38	Sketch of Hybrid Array	76
1-39	IPACS Systems Array Options	77
1-40	First Screen Rejections of Array Options	77
1-41	IPACS Array Selections	78
1-42	Mechanization Alternatives	81
1-43	Brushless DC Motor/Generator Electronics Efficiency	83
1-44	Evaluation of Solar Array Voltage Effects	85
1-45	RAM Functional Block Diagram	87
1-46	IPACS Concept of TDRS	91
1-47	MSS Functional Block Diagram	94
1-48	IPACS Concept for MJS	96
1-49	Extended Shuttle Functional Block Diagram	100
1-50	Charge-Discharge Efficiency and Bearing Loss	103
1-51	Generic Power and Control Reliability Chain	112
1-C-1	EOS Control Concept Functional Block Diagram	134
1-C-2	Functional Block Diagram - TDRS Control Concept	135
1-C-3	MJS Attitude Control Subsystem Functional Block Diagram	138
1-C-4	30-Day Shuttle Payload Control Concept	140
1-C-5	Shuttle CMG Control Software Flow	141
1-C-6	Free-Flying RAM Control Concept	143
1-C-7	MSS G&C Functional Block Diagram	146
1-C-8	MSS Momentum Exchange Assembly	148
1-C-9	Modular Space Station Electrical Power Subsystem Functional Block Diagram	152
1-C-10	Block Diagram - Series Regulator Type System (Airlock Module Hardware)	154
1-C-11	Sortie RAM Electrical Power Subsystem Schematic	156
1-C-12	TDRS Electrical Power Subsystem Block Diagram	158
1-C-13	MJS77 Power System Functional Block Diagram	161
1-C-14	EOS Electrical Power Subsystem Block Diagram	163
3-1	Summary Work Breakdown Structure (WBS) - Typical	179
3-2	IPACS Work Breakdown Structure for TDRS	182
3-3	TDRS IPACS Development Schedule	183
3-4	IPACS Work Breakdown Structure - RAM	190
3-5	Free-Flying RAM IPACS Development Schedule	192
3-6	RAM Mission Logistics	194
3-7	IPACS Work Breakdown Structure - Modular Space Station	201
3-8	MSS IPACS Development Schedule	202
3-9	IMPCS Work Breakdown Structure - Shuttle Sortie - 30-Day	208
3-10	30-Day Shuttle Sortie IPACS Development Schedule	209
4-1	Normalized Non-Recurring Cost of PM Motor-Generators Versus Power Level	218
4-2	Normalized Recurring Cost of PM Motor-Generators Versus Power Level	218
4-3	Usable Energy Per Unit Versus Low Speed Angular Momentum	221
4-4	CMG Vibration Effects	221
4-5	Single Gimbal IPACS With Compliance	224

Figure		Page
4-6	System Cost Comparison	227
4-7	Power Versus Energy Storage Requirements	231
5-1	Representative Advanced Technology Lab Payload Power Requirements	237
5-2	Estimated Emergency Requirements	240
5-3	Battery Cycle Life and Total Energy Characteristics	242
5-4	ATL Electrical Power Subsystem Schematic With Peaking Batteries	252
5-5	ATL Electrical Power Subsystem Schematic With IPACS	258
5-6	Gimbal Drive Power Weight Trade	260
5-7	ATL Program Work Breakdown Structure	269
5-8	ATL Program IPACS Development Schedule	270
5-A-1	Power-Down Timeline	283

LIST OF TABLES

Table		Page
1-I	Representative Mission/Vehicles Requirements Summary	8
1-II	Power and Control Requirements Summary	9
1-III	IPACS Design Criteria	11
1-IV	Competitive Control Subsystem Summary	12
1-V	Competitive Electrical Power Subsystems Summary	13
1-VI	Motor/Generator Comparison	24
1-VII	Homogeneous Material Properties	26
1-VIII	Wheel Properties Summary	28
1-IX	TDRS Rotor Design Comparison	32
1-X	Tape Material Properties	37
1-XI	RAM Rotor Design Comparison	38
1-XII	Anisotropic and Isotropic Design Comparison	39
1-XIII	Speed Limits for Ball Bearings	41
1-XIV	Spin Bearing Options	44
1-XV	Fatigue Life Requirements	45
1-XVI	Magnetic Bearing Characteristics for IPACS Missions	55
1-XVII	Sizing of Gimbal Drive and Sensor	58
1-XVIII	Energy Density for Example Storage Elements	60
1-XIX	Spacecraft Energy Storage Subsystem Weights	62
1-XX	Subsystems Energy Density	63
1-XXI	TDRS Design Characteristics Comparison (Per Flywheel Unit)	79
1-XXII	RAM Design Characteristics Comparison (Per Inner Gimbal Unit)	80
1-XXIII	Series/Parallel/Hybrid Electrical Mechanization Efficiencies	82
1-XXIV	RAM IPACS Design Characteristics	88
1-XXV	Weight Breakdown for RAM IPACS Unit	89
1-XXVI	Motor/Generator Design Characteristics - TDRS	90
1-XXVII	IPACS Unit Weight Breakdown	92
1-XXVIII	MSS IPACS Design Characteristics	93
1-XXIX	Weight Breakdown for MSS IPACS Unit	95
1-XXX	MSS IPACS Design Characteristics	97
1-XXXI	Weight Breakdown for MJS IPACS Unit	97
1-XXXII	EOS IPACS Design Characteristics	99
1-XXXIII	Weight Breakdown for EOS IPACS Unit	99
1-XXXIV	Extended Shuttle IPACS Design Characteristics	101
1-XXXV	Weight Breakdown for Extended Shuttle IPACS Unit	102
1-XXXVI	Weight Comparison between IPACS and Competitive Systems	104
1-XXXVII	Volume Comparison between IPACS and Competitive Systems	105
1-XXXVIII	Effect of IPACS on Solar Array Size	107
1-XXXIX	Induced Vibration Comparison	109

1-XXXX	Failure Rate Comparison for IPACS Versus CMG's	113
1-XXXXI	Heating From M/G Losses	114
1-A-I	Near Earth Satellite Missions	119
1-A-II	Geosynchronous Missions	120
1-A-III	Planetary Missions	121
1-A-IV	30-Day Shuttle Missions	123
1-A-V	RAM Free-Flyer Missions	125
1-A-VI	Space Station Missions	125
1-A-VII	Mission Class Comparison	127
1-C-I	Competitive System Weight and Power Summary	135
1-C-II	TDRS Attitude Control Subsystem Component Physical Characteristics Summary	137
1-C-III	RAM Control Component Physical Characteristics	144
1-C-IV	G&C Physical Characteristics	150
1-C-V	MSS (Regenerative Fuel Cell) EPS Weight Characteristics	153
1-C-VI	Free-Flying RAM EPS Weight Summary	155
1-C-VII	30-Day Sortie Electrical Power Subsystem Weights	157
1-C-VIII	TDRS Electrical Power Subsystem Weights	159
1-C-IX	MJS Electrical Power System Weight Summary	162
1-C-X	EOS Electrical Power Subsystem Weight Summary	164
2-I	Development Requirements Summary by Mission	168
3-I	Cost Summary and Comparison	176
3-II	Cost Summary - TDRS	185
3-III	Cost Breakdown - Components Deleted - TDRS	186
3-IV	Cost Breakdown - TDRS IPACS Units Added	187
3-V	IPACS Annual Funding Schedule - TDRS	188
3-VI	Cost-Effectiveness Tradeoff	188
3-VII	Total Cost	189
3-VIII	RAM Cost Summary	193
3-IX	Mission Operations Costs - RAM Components Deleted	193
3-X	Mission Operations Costs - RAM IPACS Units Added	194
3-XI	Replacement Parts Weight	195
3-XII	Cost Breakdown, RAM Components Deleted	197
3-XIII	Cost Breakdown, RAM IPACS Components Added	198
3-XIV	RAM IPACS Annual Funding	199
3-XV	Cost-Effectiveness Tradeoff	199
3-XVI	Total Cost	199
3-XVII	MSS Cost Summary	203
3-XVIII	Cost Breakdown, MSS Components Deleted	204
3-XIX	Cost Breakdown, MSS IPACS Units Added	205
3-XX	MSS IPACS Annual Funding Schedule	206
3-XXI	Cost-Effectiveness Tradeoff	206
3-XXII	Total Cost	207
3-XXIII	Shuttle Sortie Cost Summary	210
3-XXIV	Cost Breakdown, Shuttle Sortie Components Deleted	211
3-XXV	Cost Breakdown, Shuttle Sortie IPACS Components Added	212
3-XXVI	Shuttle Sortie IPACS Annual Funding Schedule	213
3-XXVII	Cost-Effectiveness Tradeoff	214
3-XXVIII	Total Cost	214

Table		Page
4-I	IPACS Performance Boundaries	228
4-II	Range of Requirements by Mission Class	229
4-III	Population Density by Region	232
4-IV	Standard IPACS for Region A	233
4-V	Standard IPACS for Region C	234
5-I	ATL Payload Energy Storage Requirements	238
5-II	Energy Storage Requirements Summary	239
5-III	Battery Cycle Life Estimation, ATL No. 3 Payload Based on Maximum 60-Percent Depth of Discharge	243
5-IV	ATL Payload Peak Power Approaches (Design Point)	245
5-V	ATL Payload Peak Power Approaches (Modular)	245
5-VI	ATL Payload Peak Power Approach Weight Comparison	247
5-VII	ATL Payload Peak Power Approach Cost Comparison (Modularized)	248
5-VIII	Battery Cell Costs and Cost Relationships	248
5-IX	Advanced Energy Storage Devices for ATL No. 3 Payload	250
5-X	ATL Payload Electrical Power Subsystem Weights (Mission)	253
5-XI	ATL Payload Electrical Power Subsystem Weights (Program)	255
5-XII	Secondary Power Subsystem Components Physical Characteristics	256
5-XIII	ATL IPACS Weight Summary	257
5-XIV	ATL Weight Estimate	261
5-XV	Power Requirements	262
5-XVI	CMG Size and Volume	263
5-XVII	Performance Characteristics	263
5-XVIII	Physical Characteristics Comparison	265
5-XIX	Performance Characteristics Comparison	265
5-XX	Hardware Requirements - Flight and Spare	267
5-XXI	Pre-Flight Operations Comparison	267
5-XXII	Cost Summary - ATL	271
5-XXIII	Mission Operations Cost - Components Deleted - ATL	272
5-XXIV	Mission Operations Costs - IPACS Added - ATL	272
5-XXV	Flight Replacement Hardware - ATL	273
5-XXVI	Cost Breakdown, Components Deleted - ATL	274
5-XXVII	Cost Breakdown - IPACS Components Added - ATL	275
5-XXVIII	IPACS Annual Funding Schedule - ATL	276
5-XXIX	Cost-Effectiveness Tradeoff	277
5-XXX	Transportation Weight Summary	277
5-XXXI	Total Cost Comparison	278
5-A-I	Baseline Considerations	281
5-A-II	Summary of Crew Actions and Functions	282

INTEGRATED POWER/ATTITUDE CONTROL SYSTEM (IPACS) STUDY
VOLUME I - FEASIBILITY STUDIES

by

J.E. Notti, A. Cormack III,
W. C. Schmill

Space Division, Rockwell International Corporation

SUMMARY

A study has been conducted to evaluate the concept of an integrated power and attitude control system (IPACS) for spacecraft. The IPACS is defined as a system capable of performing the functions of power generation, energy storage, power conditioning and distribution, and momentum exchange attitude control. The primary feature of the IPACS concept is the use of spinning flywheels to perform the dual functions of storing electrical energy and providing momentum exchange for attitude control.

The major objectives of the study were: determine the feasibility and cost effectiveness of the concept, establish boundaries of application for manned and unmanned spacecraft, identify hardware developments required for the conceptual designs and, prepare conceptual designs for two missions.

Feasibility was evaluated by comparing the physical and performance characteristics of candidate IPACS designs with comparable characteristics of the baseline electrical power and attitude control subsystems as defined in previous studies. Seven spacecraft/missions were studied: a low orbit satellite (Earth Observations Satellite - EOS); a geosynchronous vehicle (Tracking and Data Relay Satellite - TDRS); a planetary spacecraft (Mariner Jupiter/Saturn - MJS); an extended duration (30-day) shuttle sortie mission; a free-flying shuttle research and applications module (RAM); a Modular Space Station (MSS); and a seven-day shuttle sortie mission with the Advanced Technology Laboratory (ATL) payload.

Simultaneous electrical energy storage and attitude control by means of flywheel arrays appeared technically feasible for all missions studied. Both electrical power and attitude control performance requirements can be satisfied by high-speed flywheel energy-momentum units utilized in conventional gimbaled or non-gimbaled arrays.

The IPACS systems are predicted to weigh less than conventional electrical power and attitude control systems utilizing batteries or fuel cells for all missions except the planetary. As electrical energy storage elements, high speed energy-momentum units are predicted to produce about twice the energy

density of spacecraft battery systems at comparable development levels. The weight advantage of flywheel units increases as mission life and the number of charge-discharge cycles increases.

Systems of two development levels are postulated. In the current technology systems the use of high speed ball bearings and permanent magnet motors is defined. The applications require development testing for design verification. The advanced technology flywheel systems require the continued development of composite rotors and an extension of the current magnetic suspension bearing design technology to the high speed operating regime.

The studies did not show any inherent power, energy, or control boundaries which limit IPACS in spacecraft applications. Power levels to 80 KW and energy storage to 70 KW-hr are obtainable for designs sized to spacecraft dimensional constraints. Attitude control dynamic range and pointing accuracy is expected to be approximate that of current control moment gyros.

Cost effectiveness was evaluated by comparing estimated costs of IPACS designs with the original cost estimates of the designs for the conventional power and control subsystems. IPACS appeared cost competitive for all missions except the planetary MJS mission and the particular 30-day shuttle sortie mission studied. The shuttle mission was characterized by a short term 60 KW power requirement for a few cycles. The planetary mission was characterized by a low energy storage requirement for three discharge cycles at planet encounter. In both cases, IPACS development costs exceeded costs of a short life, high energy density battery system. IPACS was shown to promise significant cost advantages for spacecraft with extended life missions or a recurring mission usage such as the RAM and ATL shuttle missions. In extended life missions IPACS development costs were similar to those required for conventional systems and operational cost significantly better by reason of the predicted life and refurbishment advantages of the flywheel systems.

Dynamic analyses and digital computer simulations were performed for both the RAM and TDRS conceptual designs. This work confirmed analytical predictions and demonstrated the feasibility of revising generic control laws to operate the flywheels for simultaneous energy transfer and attitude control. Control response in the presence of energy charge-discharge cycles was shown equivalent to conventional response for both gimbale and non-gimbale systems. Digital computer simulations of the solar array, power bus and motor generator system were performed. Motor-generator loop stability and power response in the presence of solar array output changes and load variations were shown to be satisfactory.

INTRODUCTION

Background

During the last several years a number of different approaches to electrical power subsystems have been identified and studied for the postulated spacecraft of NASA mission models. In practically all designs the energy storage function is performed by use of rechargeable battery systems. Designs have emphasized the performance aspects of energy storage capability and charge - discharge cycles because of their direct relationship to the more important factors of battery subsystem weight and life. Cycle life factors are of particular importance to batteries which have an inherent characteristic of decreasing life with an increasing number of charge - discharge cycles.

The requirement for spacecraft lifetimes in excess of five years or the requirement for long quiescent periods, both characteristic of Shuttle era designs, results in relatively high battery subsystem weight. Achievable energy storage densities vary appreciably among spacecraft designs. Battery subsystems commonly constitute 30 percent of an electrical power system weight and have, in specific designs, approached 50 percent.

Developments of recent years have shown that spinning flywheel designs can be made to provide higher energy densities than can be expected from several conventional electrochemical devices. The spinning flywheel is studied herein as a potential competitor for spacecraft electrical energy storage as well as attitude control. In spacecraft applications, the flywheel concept is enhanced in that even parity in energy density between the flywheel and battery subsystems may result in significant advantage for the flywheel subsystem. This is because many spacecraft designs currently employ spinning flywheels in reaction and momentum exchange attitude control systems. If a flywheel subsystem can be designed to perform efficiently the dual functions of electrical energy storage and momentum storage for attitude control, advantage can accrue through deletion of batteries and associated electronics.

The purpose of this study was to determine the mission applications of an integrated power and attitude control system (IPACS) which uses spinning flywheels for both electrical energy storage and attitude control. Applicability was to be determined by studying feasibility, cost-effectiveness, and specific designs for selected mission/vehicles from the spacecraft mission classes of unmanned satellites, extended Space Shuttle sortie missions, Shuttle research and applications modules, and space stations. The study was to determine the extent to which the IPACS concept is practical considering both current and anticipated technology developments.

IPACS Concept

The IPACS concept consists of solar cell arrays, energy-momentum (E-M) wheel subassemblies, gimbals, gimbal actuators and sensors, power conditioning and distribution components, and all computer electronics associated with power and attitude control functions. Figure I-1 illustrates the system concept. Electrical power is supplied directly from the solar array to the loads through a regulated spacecraft bus. Electrical energy is stored in the rotating wheel and discharged to the loads when required. Spacecraft attitude control is accomplished simultaneously by changing the angular momentum state of the flywheel. Momentum changes for attitude control torque generation can be accomplished by conventional means. The energy-momentum wheel is either used in the reaction mode (in which applied motor torques change the spin speed of the wheel and react upon the vehicle) or the gimballed mode (in which the wheel angular momentum vector is precessed to generate vehicle torques).

The central power and control electronics element controls both electrical power and attitude control functions. A single dc permanent magnet unit acts as both a motor to store energy and a generator to provide energy to the loads. Electrical power is regulated by detecting the difference between main bus voltage and the reference voltage and using the difference signal to switch motor-generator modes.

The system utilizes no batteries and performs all the functions of conventional spacecraft power and control subsystems.

Study Objectives

The objectives of the IPACS study as structured under the direction of NASA/LRC were: (1) to determine the feasibility and cost-effectiveness of a solar array energy wheel system capable of dual functions of spacecraft electrical energy storage and attitude control; (2) to establish the boundaries of application of this system for both manned and unmanned spacecraft; (3) to identify hardware components considered critical to the viability of the concept and to define the level of development required; and (4) to generate conceptual designs for two specific systems to be selected at the conclusion of the feasibility analysis. A contract change authorization issued after mid-term review provided an additional objective of studying the feasibility and cost-effectiveness of the IPACS concept as applied to the Langley Research Center Application and Technology Laboratory (ATL) seven-day Shuttle sortie mission.

Study Scope and Qualifications

The study began with a definition of missions for the four mission classes of the statement of work. Spacecraft and subsystem requirements for electrical power and attitude control were then compiled and analyzed. Specific candidate

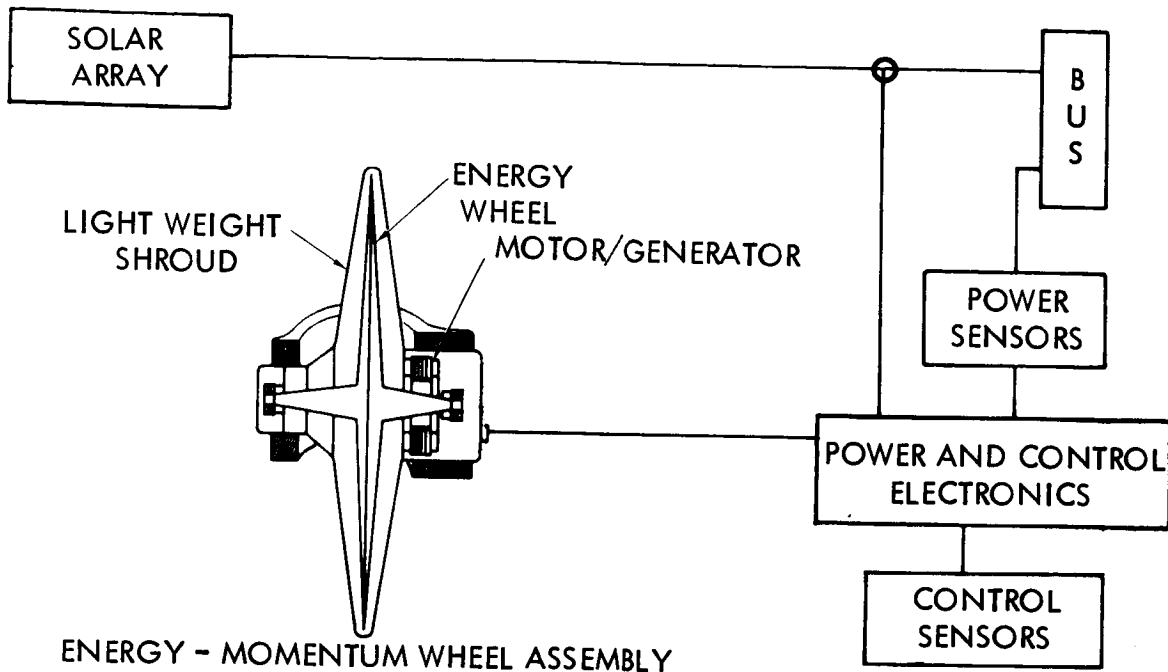


Figure I-1. Integrated Power and Control System Concept

mission/spacecraft were selected as representative for each mission class. The selections were an astronomy mission (A303B) for the research and application module (RAM), the Rockwell modular space station (MSS) design, and the Rockwell 30-day Shuttle sortie mission design. In the unmanned satellite mission class the variety of requirements dictated that more than one mission/spacecraft be studied to typify the class as a whole. In this case, three mission/spacecraft were selected for study: the Rockwell tracking and data relay satellite (TDRS) Phase B design for a geosynchronous satellite; a low earth orbit design for the earth observatory satellite (EOS) mission; and a Rockwell design for the Mariner Jupiter/Saturn (MJS) flyby spacecraft. Each mission/spacecraft selected had previously been defined by extensive contract or research study efforts.

IPACS candidate conceptual designs were developed through component trade and system synthesis studies. These studies established the more efficient components to be used in the flywheel rotating assembly for both current and projected technology. Projected technology developments were analyzed and programs defined. The more efficient flywheel assemblies were then combined in different system configurations and screened for performance. The more efficient systems within each technology classification were then selected and compared with the conventional power and control designs in performance.

Cost-effectiveness studies were performed by comparing system and penalty costs developed for IPACS against the costs determined in the Phase B studies for the competitive systems. Cost studies represented approximately 3 percent of the total effort.

The development of system conceptual designs for the TDRS and RAM missions comprised approximately 50 percent of the contract effort. The conceptual designs present element sizing, dimensioning, material selection, electronic schematics, system design, spacecraft integration, and dynamic performance studies. The designs define two distinct prototype flywheel energy storage subassemblies. The subassemblies incorporate high energy density isotropic wheels with permanent magnet motor-generators.

The depth of technical analyses and accuracy of data are considered appropriate for the comparisons made between IPACS and competitive systems. Study scope did not permit iterations and optimizations of the IPACS designs. In this respect, design decisions were made such that the IPACS advantages which are predicted in the performance comparisons can be considered conservative and may be improved.

The feasibility study also identified interesting alternative studies which were beyond the scope of the reported effort. Potential areas for further study are discussed in the conclusions and recommendations sections of Volume I.

Report Organization

The report is presented in two volumes, each of which is modularized. The modules contain the results of specific sets of tasks performed to satisfy study objectives. This volume, which presents the feasibility, cost-effectiveness, and applications studies, consists of the following six modules:

- (1) Technical Feasibility Analysis
- (2) Critical Component Developments
- (3) Cost Analysis
- (4) Applications Boundaries
- (5) Space Shuttle Advanced Technology Laboratory Applications
- (6) Feasibility Study Conclusions

MODULE 1 - TECHNICAL FEASIBILITY ANALYSIS

Requirements Definition

Mission/vehicle selections and spacecraft requirements are summarized for the six representative mission/vehicles of the IPACS studies. Power and control subsystems requirements and applicable design criteria and constraints are also discussed.

Mission/vehicle selections.- Vehicle selection was directed toward two objectives. First, each vehicle was to be representative of the given mission class. Performance requirements peculiar to that mission class had to be present in the vehicle representing that class. Second, each vehicle was to expose IPACS to as many design issues as possible. Selected vehicles were to show a spectrum of performance requirements to meet this objective. The requirements of the six missions selected for study are summarized in Table 1-I.

The selected vehicles meet both of the original objectives of being representative of the individual mission classes and exposing IPACS to a broad cross section of issues. Table 1-I shows how well the selected vehicles exposed the IPACS to design issues. The EOS satellite provided the coarsest pointing vehicle. It also required study of the effects of sun-synchronous orbit conditions on IPACS design. The planetary vehicle allowed examination of the usefulness of IPACS with a constant power generation concept. The Shuttle mission determined the IPACS effectiveness with a very large vehicle. The RAM mission exposed the IPACS to extremely fine pointing requirements. Finally, the modular space station examined the impact of large electrical energy requirements and pitted the IPACS against the regenerative fuel cells, another promising energy storage alternative to the NiCd battery. Appendix 1-A presents a discussion of the missions evaluated, selection criteria, and final selection procedure.

Spacecraft requirements.- Spacecraft requirements are summarized in Appendix 1-B.

Power and control requirements.- The power and control requirements for the representative missions are summarized in Table 1-II. The requirements are presented on a total vehicle basis except where specifically noted. Rate control requirements have not been established for the TDRS and EOS vehicles as the control problem is adequately defined by the pointing accuracy. In the momentum storage requirements column the term "planar" is used to denote cases where the major momentum storage requirement occurs within a single plane and the requirement normal to the plane is relatively small. The term "bias" refers to the bias momentum associated with the attitude control concept used on TDRS and EOS.

TABLE 1-1. - REPRESENTATIVE MISSION/VEHICLES REQUIREMENTS SUMMARY

	Launch date	Mission duration	Manning	Orbit inclination altitude Rad (deg) km/(nm)	Spacecraft weight, kg (lb)	Pointing accuracy rad (deg)	Momentum storage/ transfer requirement n-m-sec (ft-lb-sec)	Power level (W)
Near earth satellite: earth observations satellite	1978	2 yr	Unmanned	$\boxed{\text{Sun-synch}}$ 1100 (600)	770 (1700)	0.0174 $\boxed{(1.0)}$	-	100
Geosynchronous satellite: tracking & data relay satellite	$\boxed{1977}$	3 yr	Unmanned	$\boxed{(0^\circ)}$ 35 700 (19 300)	1230 (2717)	0.016 (0.9)	$\boxed{16.95}$ (12.5)	$\boxed{300/180}$
Planetary/spacecraft: Mariner-Jupiter/Saturn	$\boxed{1977}$	4 yr	Unmanned	0.52 (30°) $\boxed{1.43 \times 10^8}$ (9.5 A.U.)	$\boxed{680}$ (1500)	0.0008 (0.05)	-	400
Shuttle 30-day mission: earth observation & contamination technology & material science	1979	$\boxed{30 \text{ days}}$	Manned	0.95 (55°) $\boxed{185}$ (100)	$\boxed{97 500}$ (215 000)	0.0087 (0.5)	$\boxed{7118}$ (5250)	61 000
RAM: advanced solar observatory	$\boxed{1986}$	4-6 yr	Unmanned ops, manned mainten- ance	0.78-0.95 (45 - 55°) 500 (270)	12 200 (27 000)	4.8×10^{-6} $\boxed{1 \text{ sec}}$	2038 (1500)	3400
Modular space station: Rockwell design	1985	$\boxed{10 \text{ yr}}$	Manned	0.95 (55°) 500 (270)	81 500 (180 000)	0.0043 (0.25)	3000 (2200)	$\boxed{19 000}$

TABLE 1-II. - POWER AND CONTROL REQUIREMENTS SUMMARY

Mission	Control													Energy storage		Power	
	Pointing accuracy			Rate control		Control torque		Momentum storage		Charge/ discharge cycles	Energy/ cycle W-hr	Power output W	Bus regulation				
	rad	deg	rad/sec	deg/sec	N-m	ft-lb	N-m-sec	ft-lb-sec									
RAM	4.85×10^{-6}	1 sec	8.24×10^{-8} per 0.75 hr	0.017 sec per 0.75 hr	9.5 (per torquer)	7 (per torquer)	2034 (planar)	1500 (planar)	27.8 K	2500	4800	+5%					
TDRS	0.016	0.9	--	--	0.021 (per axis)	3 in.-oz (per axis)	16.9 (bias)	12.5 (bias)	450	285	237	+1 volt					
EOS	0.017	1.0	--	--	0.049 (per axis)	7 in.-oz (per axis)	24.4 (bias)	18 (bias)	10.2 K	460	1048	+2%					
MJS	0.00087	0.05	0.00035	0.02	0.014 (par axis)	2 in.-oz (per axis)	0.068	0.05	10	360	20	+1%					
MSS	0.0044	0.25	0.00087	0.05	678 (par axis)	500 (per axis)	2758 (planar)	2034 (planar)	52.6 K	14 900	20 000	+2.5%					
30-day Shuttle	0.0087	0.5	0.00017	0.01	163 (par torquer)	120 (per torquer)	7118 (planar)	5250 (planar)	10 K	6100	61 000	+5%					

IPACS design criteria.- Design criteria relevant to the formulation of IPACS concepts and designs are summarized in Table 1-III. Note that in some cases the power function life is significantly different than the control function life. This occurs for TDRS, a synchronous vehicle which experiences solar eclipse for only 90 days per year and MJS, which requires energy storage for only the planet encounter phases of the mission. These mission characteristics allow IPACS units to run at relatively low speeds for the greater part of the mission when only control is required.

Unit size constraints were established by a review of existing vehicle configurations. The 0.38-m (15-in.) overall dimension was selected as a reasonable size limit for the smaller vehicles such as TDRS, EOS, and MJS. The size constraint for the larger vehicles is derived from hatch size considerations.

Failure requirements were established through an evaluation of the failure mode performance capability of the competitive systems. Thus IPACS designs formulated to meet or exceed these requirements would have comparable failure mode performance.

Competitive Power and Control Subsystems

The characteristics of electrical power and attitude control subsystems for each of the six reference missions are summarized in Tables 1-IV and 1-V. These are termed the competitive subsystems and represent the designs which candidate IPACS configurations were compared with and traded against. In all cases design data were extracted from original mission design documents and utilized without change. Appendix I-1-B presents a description of each subsystem including a functional block diagram, discussion of operation, physical characteristics, performance data, and references.

Feasibility Trade Study

The feasibility of IPACS was established through synthesizing candidate conceptual designs for the various missions and comparing these designs in physical and performance factors against conventional systems.

Synthesizing the candidate designs was performed by use of both system and component level trade studies. Figure 1-1 shows the feasibility trade studies performed.

Component-level trade studies were performed to define the preferred components and component combinations which would result in the more efficient energy-momentum flywheel assembly. As shown in Figure 1-1 component trades were primarily efficiency trades performed for the rotors, motor-generators, bearings, housings, and gimbal assemblies.

TABLE 1-III. - IPACS DESIGN CRITERIA

Mission	Duration (yr)	Operating Life (yr)	Service Interval	Size Constraints	Single Failure Requirement	
					Control	Energy Storage
TDRS	5	Control 5 yr Power 450 days	None	↑ 0.38m (15 in.) max overall ↓	Full performance	50%
EOS	2	2	None		Degraded performance	75%
MJS	3.5	Control 3.5 yr Power 100 days	None		Revert to RCS	No requirement
RAM	5	5	6 months	↑ 1.016m (40 in.) overall ↓	Revert to RCS	85%
30-day Shuttle	30 (days)	50 flights 1500 days	30 days		Revert to RCS	100%
MSS	10	10	As required		Full momentum exchange	100%

TABLE 1-IV. - COMPETITIVE CONTROL SUBSYSTEM SUMMARY

Spacecraft	Control design	Sensors	Computer	Weight, kg (lb)	On-orbit average power consumed, (w)	Pointing accuracy, rad (deg)	Design control torque, n-m (ft-lb)	Design momentum storage, n-m-sec (ft-lb-sec)
EOS	2 reaction wheels 'v' momentum bias + GN2 jets + magnetic torquers	Integrated Horizon sensors Rate gyros Sun sensor	Dedicated	46.8 (103)	65	0.017 (1.0)	0.049 (7 in.-oz) (per axis)	24.4 (18) (bias)
TDRS	2 Reaction wheels + dual function gyro augmented 'v' mom bias system + hydrazine jets	Integrated Horizon sensor Sun sensors Yaw gyro	Dedicated	26.2 (57.7) without jets	95.5	0.016 (0.9)	0.049 (7 in.-oz) (per axis)	16.9 (12.5) (bias)
30-day Shuttle	Orthogonal 3 DG CMG's + experiment platforms	Orbiter	Orbiter	612 (1350)	144	0.0087 (0.5)	163 (120) (per torquer)	7118 (5250) (planar)
RAM	3 DG CMG's + 3 reaction wheels + magnetic torquer + hydrazine jets	IMU Star trackers Sun sensor Magnetometer Rate gyros	Centralized processor	470.3 (1035) without jets	223	4.85×10^{-6} (1 sec)	14.9 (11) (per torquer)	2034 (1500) (planar)
MSS	3 DG CMG's + H ₂ & O ₂ jets	Strapdown IRU Star trackers Horizon tracker Sextant/scope	Central processor + preprocessor	668 (1470) without jets	487	0.0044 (0.25)	678 (500) (per torquer)	2758 (2034) (planar)
MJS	3 momentum gyros + hydrazine jets	Sun Sensors Accelerometer Canopus tracker Planet encounter sensor	Central processor	*	*	0.00087 (0.05)	0.014 (2 in.-oz) (per axis)	0.068 (0.05)
*Data not available.								

TABLE 1-V. - COMPETITIVE ELECTRICAL POWER SUBSYSTEMS SUMMARY

Spacecraft	Power source			Energy storage			Conditioning and distribution				EPS
	Type	Weight, kg (lb)	Generated power W	Type*	Weight, kg (lb)	Capacity W-hr	Type	Bus voltage (vdc)	Source voltage	Weight, kg (lb)	
MSS	650 m ² (7000 ft ²) solar array	3026 (6676)	47 000	1	2253 (4966)	11 700	On-array switching + inverter	+112	112 vdc	1712 (3768)	6900 (15 410)
RAM	98.5 m ² (1060 ft ²) solar array	291 (640)	6890	2	441 (972)	1380	Buck regulator	28	52 vdc	414 (913)	1146 (2525)
30-day Shuttle	Fuel cells	1746 (3840)	Up to 5 kW from Shuttle fuel cell	3	284 (625)	5000	Series regulator + inverter	29	27-31 vd vdc	785 (1724)	2815 (6189)
TDRS	4.2 m ² (45 ft ²) solar array	27.1 (59.6)	400	2	20.1 (44.3)	266	Shunt regulator	28	30.8 vdc (EOL) 40°C	23.9 (52.7)	71 (156)
MJS	Radioisotope thermoelectric generator	113.4 (249.7)	360	4	2.27 (5)	Transients only	Shunt regulator	29	30 vdc	31.0 (68.7)	146.7 (322.8)
EOS	15.6 m ² (168 ft ²) solar array	112.8 (248)	1280	2	79.1 (174)	430	Shunt regulator	28	31 vdc	40 (88)	232 (510)
*Energy storage type: 1 - Regenerative fuel cell 2 - NiCd batteries 3 - Ag Zn batteries 4 - Radioisotope thermoelectric generator											

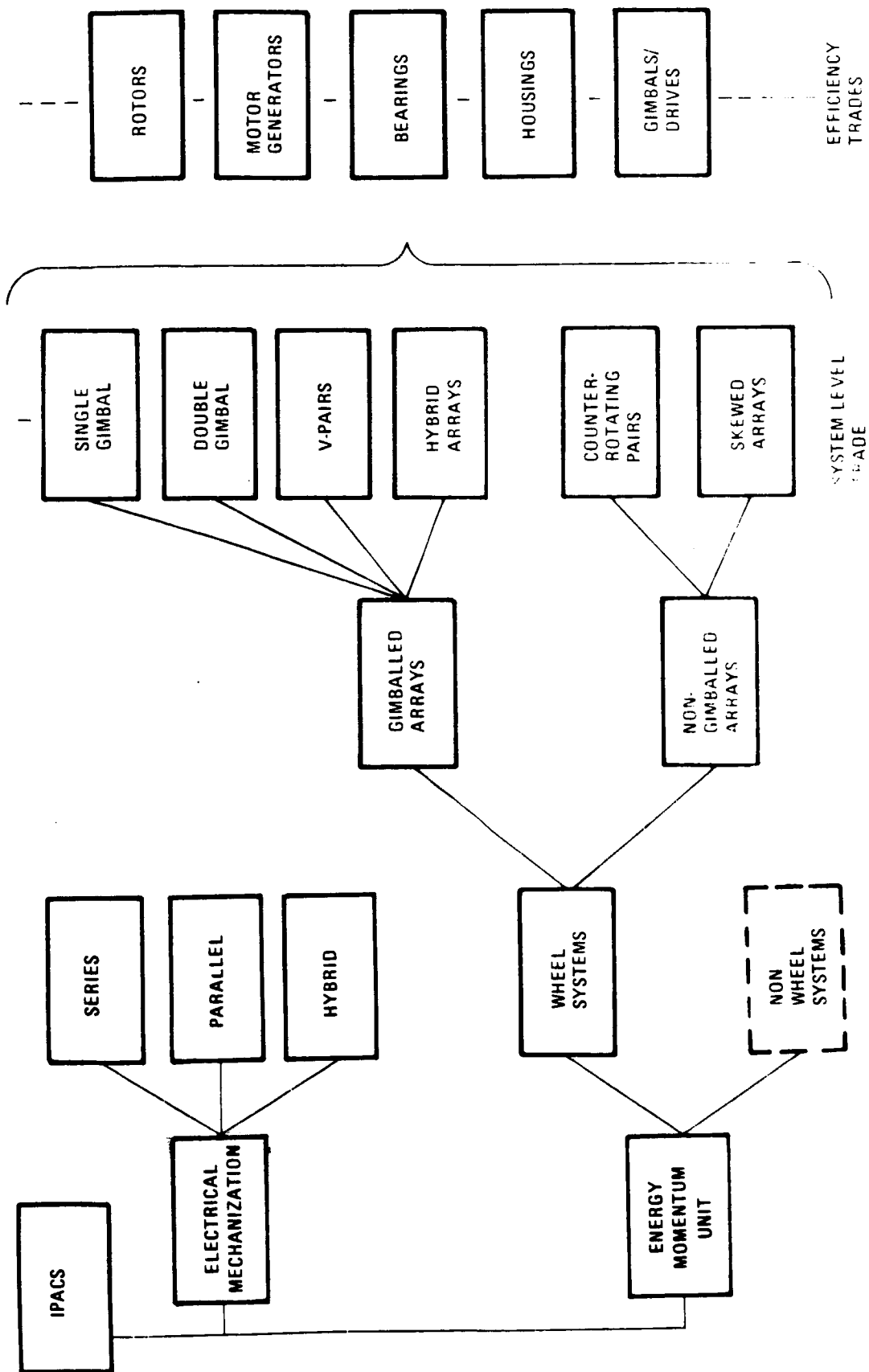


Figure 1-1. Feasibility Study Trade Tree

Component Trades

Component trades were conducted in the areas of motor/generators, rotors, bearings, housings and gimbals.

Motor/generators.— Three type of spin motors were considered, two of which were ac and one dc. The dc brushless motor was selected over both the ac induction and ac servo motor because of its superior efficiency and torque over the speed range of interest. Four generic machine designs were then analyzed and a trade-off was made to determine the desired motor-generator combination. The selected system is an integral unit that serves as both a motor and a generator.

Ac-dc spin motor comparison:

Motor generic types The ac induction motors differ primarily in the selection of the breakdown point in the speed torque curve. The two extremes are the motor having a low resistance and good regulation (typically used for constant speed operation) and a high resistance rotor with poor regulation but improved starting torque (servomotor). The former type ac induction motor is only controllable by changing the excitation voltage with the torque proportional to the square of the current (with constant impedance). The efficiency at any excitation will be nearly constant since copper and core losses also vary with the square of the current. The ac servomotor, on the other hand, sacrifices good regulation for high starting torque. It has a two-phase winding and for any fixed phase excitation, the output torque is proportional to the control phase current (assuming constant impedance). During starting the dc induction motor has large phase differences between currents and flux developed. Starting currents may be 5 to 7 times rated current with only a moderate torque developed.

Ac-dc motor tradeoff The advantages of the brushless dc machine over the two primary types of ac motor/generators are apparent when comparing torque and efficiency over the expected range of operating speeds (percentage slip from design speed). Efficiencies versus slip are plotted for the two types of ac motors and compared with the brushless dc motor. (Figure 1-2). Note that for the speed range where one-half the energy is extracted from the wheel (0 to 30 percent slip), the efficiency of the induction motor with good regulation is somewhat better than that of the servomotor. However, brushless dc motor efficiencies are well above those of either ac motor over all speed ranges.

The torque versus slip is plotted for the three motor types in Figure 1-3. Available torque is reduced significantly near synchronous speed for the induction motor.

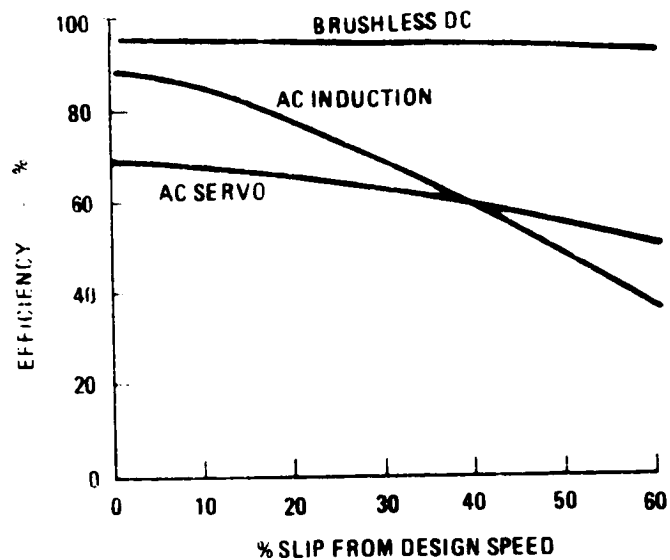


Figure 1-2. Motor Efficiency Versus Slip

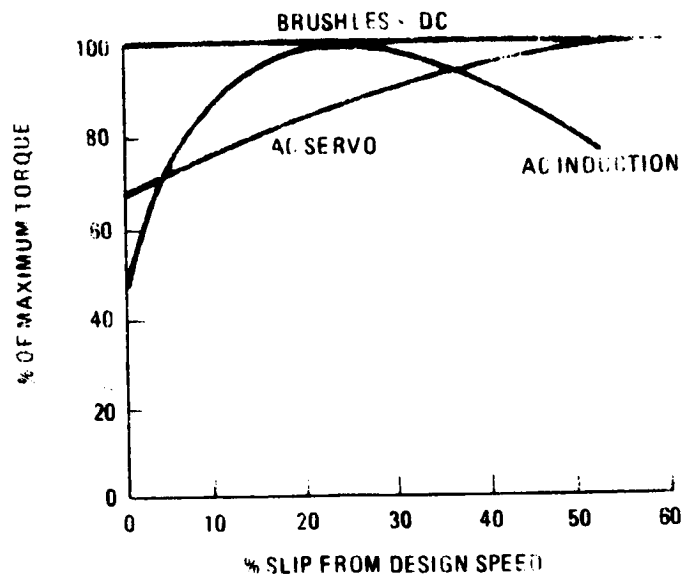


Figure 1-3. Motor Torque Versus Slip

Some improvement in ac efficiencies and torque dropoff with speed variation can be made by utilizing an electronic commutation which changes field current frequency with speed variations. With this method, torque can be maintained essentially constant but efficiencies are 4 to 7 percent lower than dc motor/generator efficiencies. The requirement for high efficiencies over wide (50 percent) speed reductions favors brushless dc motors.

Generic dc machine design trades In the previous section the dc spin motor was selected over the two ac alternatives. In this section four generic types of brushless designs are analyzed. These machines may be used as either generators or motors.

The designs considered are:

- . Permanent Magnet Rotor - Permanent magnets, mounted on the rotor, provide the field. The power windings are located on the stator in the conventional manner.
- . Wound Rotor - The field is produced by current in the rotor windings. Rotor current may be provided through slip rings, commutators, or by a rotor excitation winding and rectifier.
- . Solid Rotor Inductor - Field and main windings are on the stator. Field variations are produced by permeance variations in the air gap and do not reverse.
- . Solid Rotor Lundell - The field and main windings are also on the stator. The rotor has an interdipital magnetic circuit with N-S poles and a sinusoidally varying air gap flux.

Characteristics and special features of each were analyzed to determine applicability to IPACS.

The permanent magnet design is the simplest of the four types and the more reliable. The active rotor parts are soft iron or laminations and permanent magnet material. Use of the new rare earth magnet material has provided a significant improvement to this machine type. Rotor size and inertia are reduced, air gaps have been increased and accidental demagnetization has been prevented. The permanent magnet generator and brushless dc motor can be the same unit serving the dual function of energy storage and extraction. The mechanical strength of the rotor limits maximum speed to approximately 50 000 rpm and 5-10 kW output at this speed due to rotor diameter limitations and increased axial length at higher output power. Higher speeds are possible at lower power levels. Voltage regulation cannot be as easily obtained in this device since the field is not controllable. Major losses in this machine are I^2R and core losses. An efficiency of 95-97 percent is realizable. Magnet limitations (cost, size, stresses) limit outputs to the 10 kW range.

The wound rotor design is the more conventional approach; however, the slip rings or commutator normally used to supply dc current to the rotor

field windings are replaced by a brushless exciter. This consists of generator windings on the rotor to provide ac power which is rectified on the rotor to supply current to the rotor field windings. Increased size and complexity result. Major losses are I^2R , core, and field I^2R . Efficiency is high but cannot approach that of the permanent magnet machine in the smaller sizes (5 kW and below).

The solid rotor induction type is a machine with both field and main windings on the stator. The rotor is shaped to provide a sinusoidal varying permeance and flux. This field does not reverse, however, so that the induction machine is not as efficient as the permanent magnet and wound rotor machines. In addition, the copper in the stator cannot be used as effectively. Principal losses are stator and field I^2R , core losses, pole face losses, and stray load losses. An efficiency of 88.9 percent is realizable. The solid rotor machines must run at 2 to 3 times the speed of the wound rotor or permanent magnet design to achieve the same output in a comparable size.

The Lundell design also is a solid rotor machine and its characteristics are similar to the induction device with one major exception. The sinusoidal field flux reverses in sign. This is accomplished by doubling the air gap reluctance (4 air gaps rather than 2) and by using a rotor design with high flux leakage paths. The field and main windings are on the stator and the rotor is an interdigitated magnetic circuit configuration with magnetic and nonmagnetic materials. The rotor design is not as strong as the inductor rotor. The Lundell is axially shorter than the inductor machine. Size, weight, and efficiencies are comparable for both solid rotor machines.

The four design types are compared in Table 1-VI. The more critical factors in the selection are:

1. High efficiency
2. Simplicity and high reliability
3. Suitability for selected speed range
4. Small overall motor-generator package

The permanent magnet design appears as the best choice on all four counts.

Permanent magnet motor/generator characteristics: Parametric weight and volume data are presented in figures 1-4, 1-5, and 1-6 as functions of power output. These data are based on existing motors in the 10 000-rpm range and preliminary designs for the 50 000 rpm range. The volume data include consideration of shape factors compatible with operation at the higher speeds. These data and the efficiency data shown in figures 1-7 and 1-8 are based on use of the rare earth permanent magnets. The peak efficiency point can be shifted by design of the unit to give equal core and iron losses at different torque levels. Two different cases are shown in figures 1-7 and 1-8. In figure 1-7 the peak efficiency is at rated torque while peak efficiency occurs at 1/3 rated torque in figure 1-8. Note that the efficiency for the machine of figure 1-8 drops off rapidly with speed near rated torque. High efficiency is retained, however, at very low torque levels.

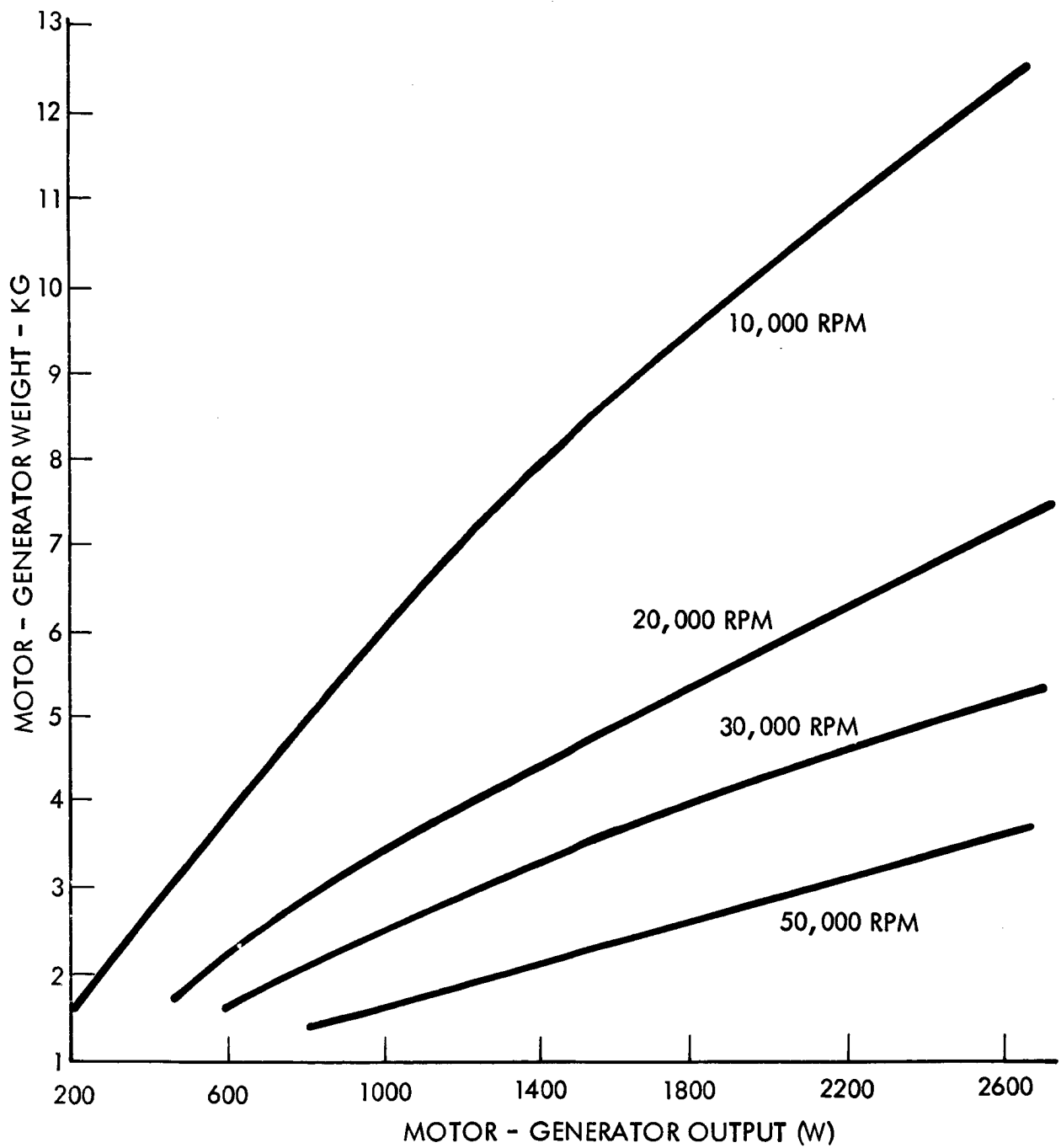


Figure 1-4. Brushless dc Motor-Generator Optimum Design Weights

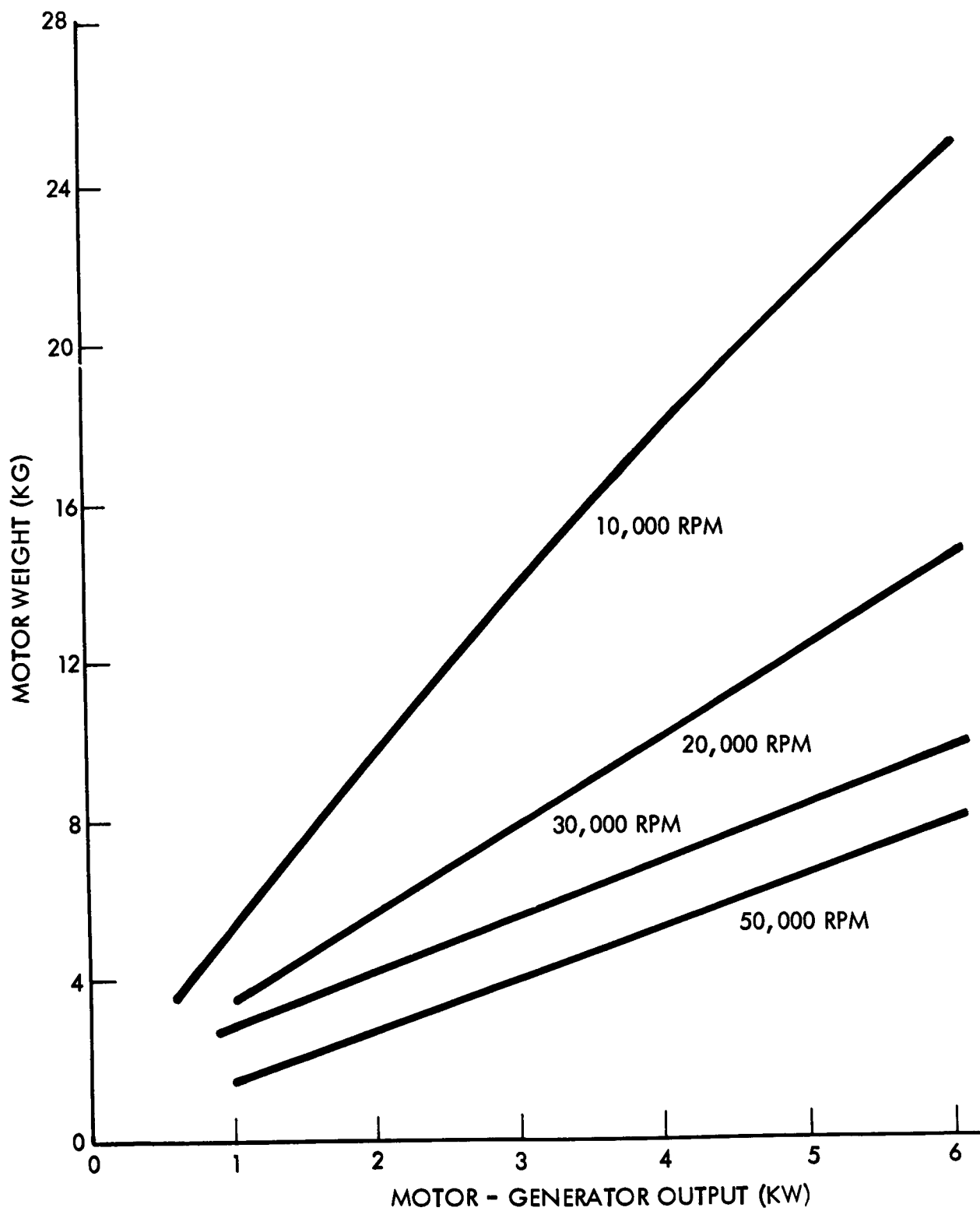


Figure 1-5. Brushless dc Motor-Generator Optimum Design Weights
(Extended Range)

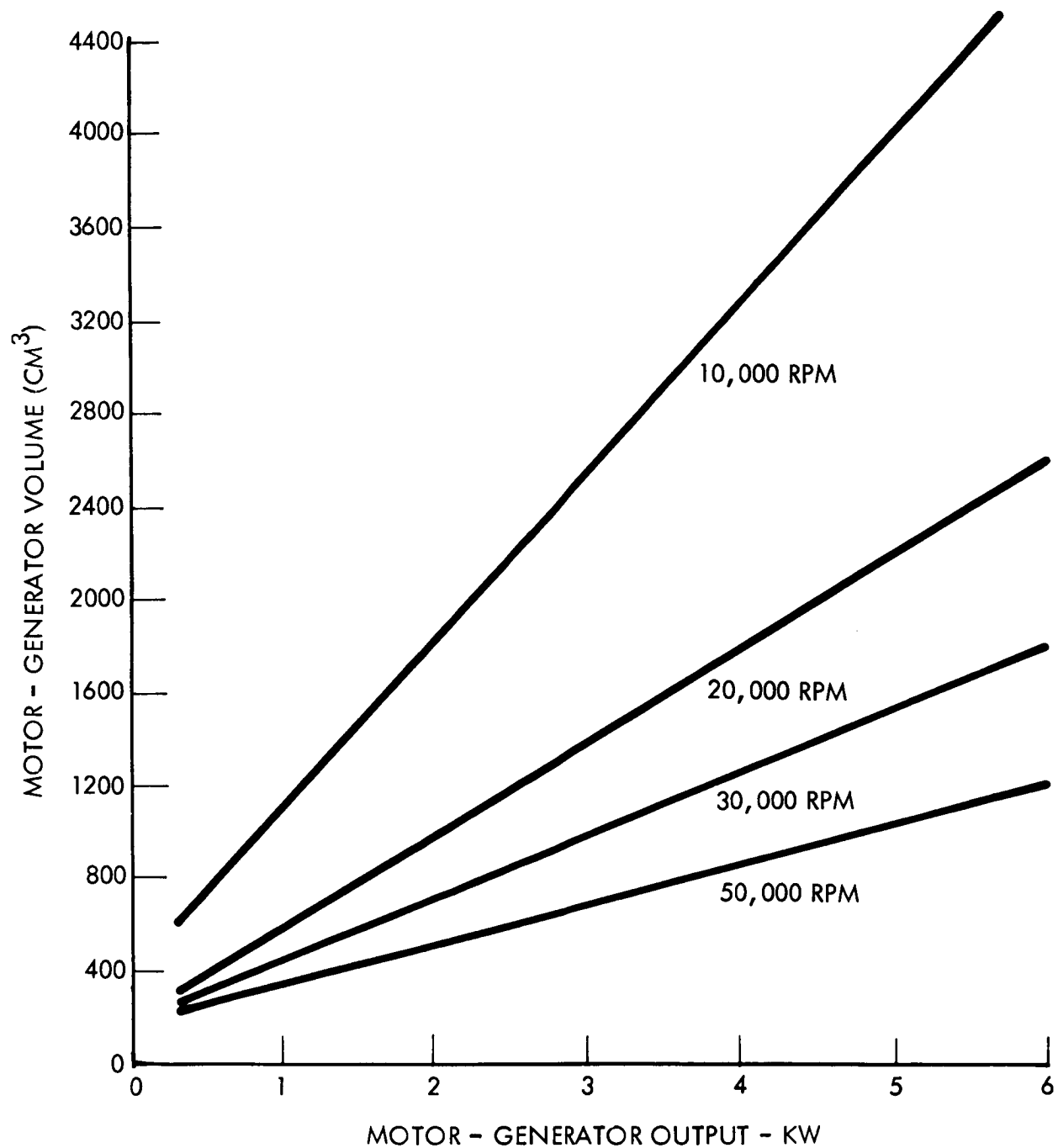


Figure 1-6. Brushless dc Motor-Generator Optimum Design Volumes

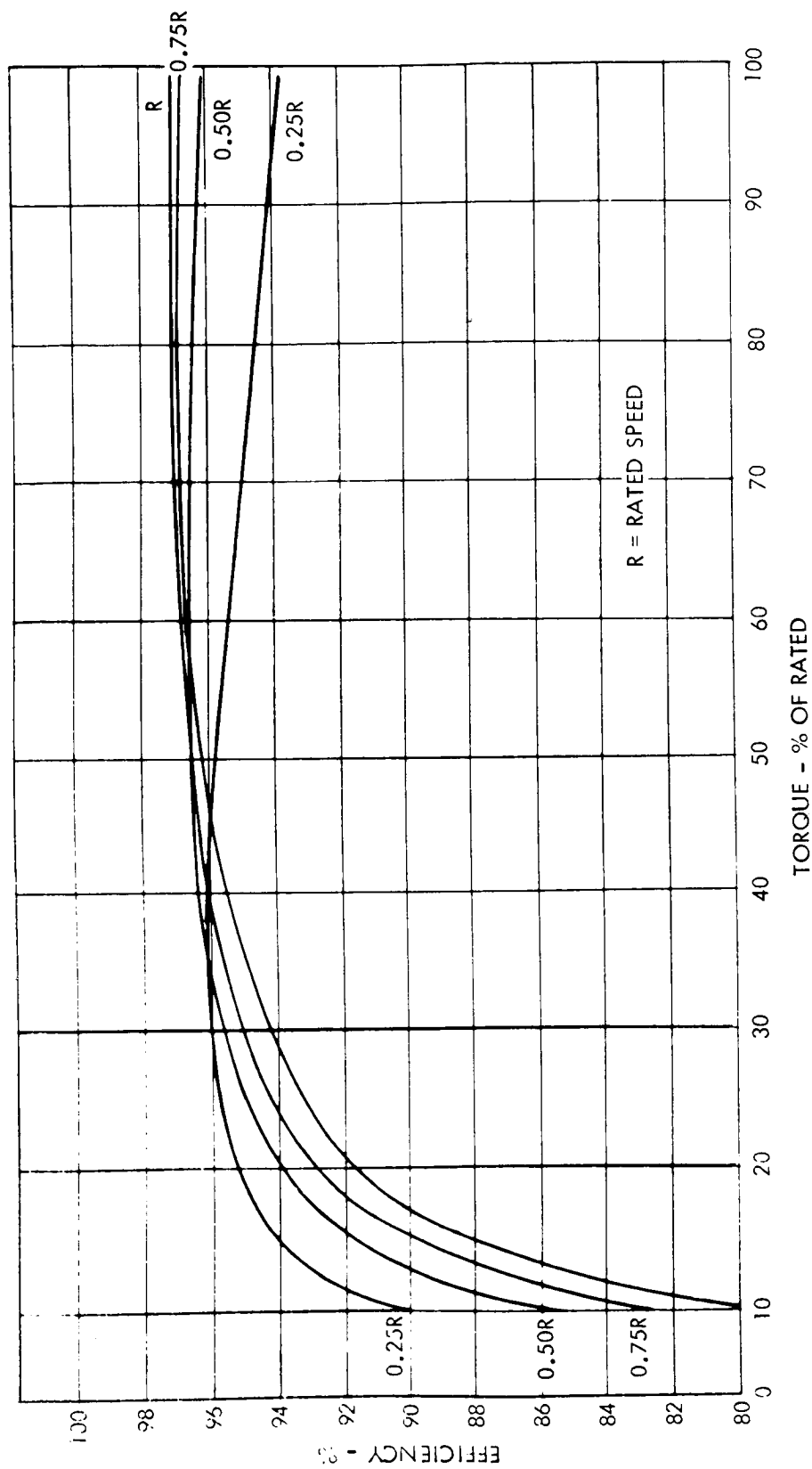


Figure 1-7. Efficiencies for Brushless dc Motor-Generator-Peak Efficiencies at Rated Torque

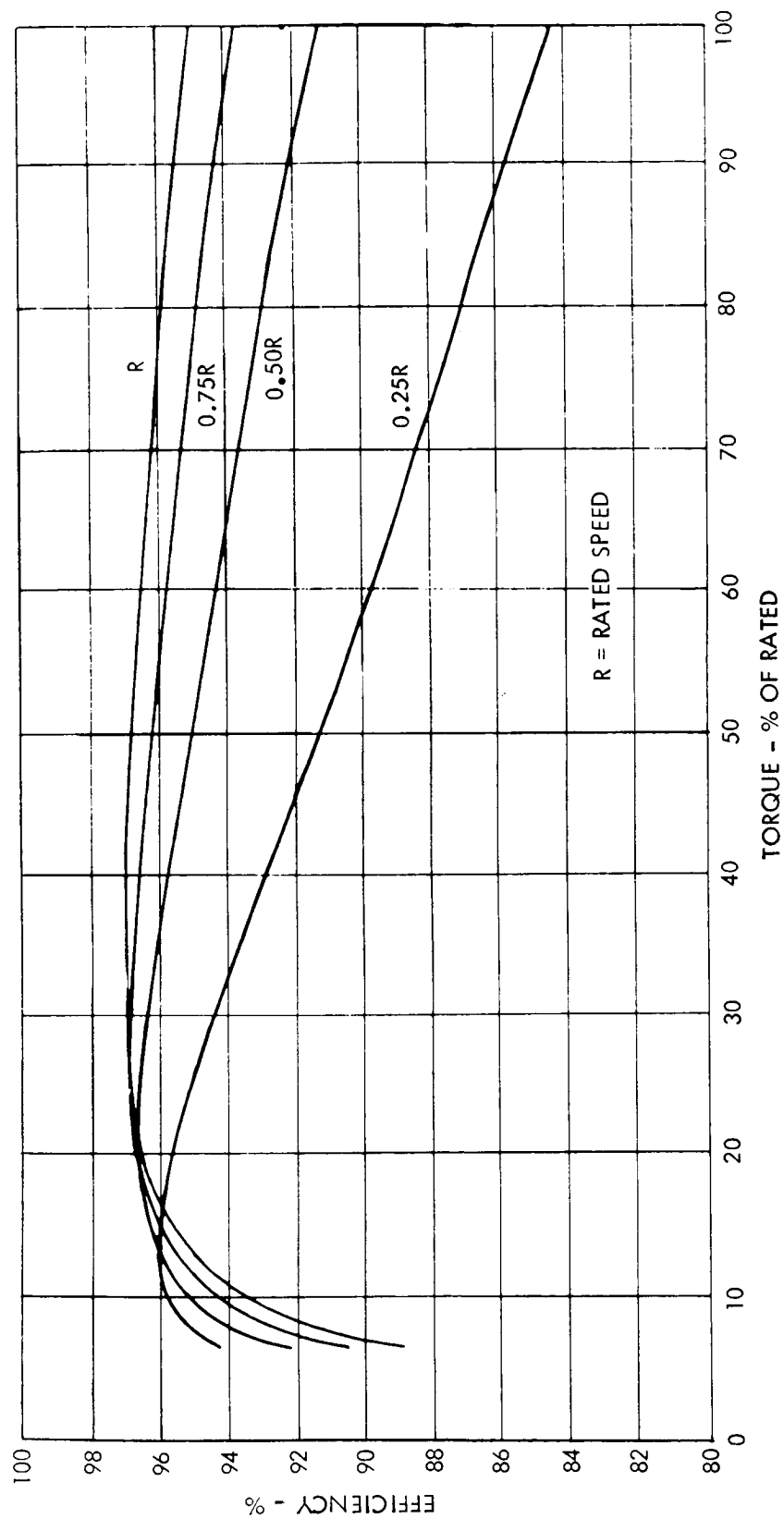


Figure 1-8. Efficiencies for Brushless dc Motor-Generator - Peak Efficiency at 1/3 Rated Torque

TABLE 1-VI.- MOTOR/GENERATOR COMPARISON

Item	Permanent Magnet Rotor	Wound Rotor	Solid Rotor	
			Inductor	Lundell
Efficiency (1-5 KVA)	95-97%	90-93%	88-90%	88-93%
Relative size (at same speed)	X	1.2X	1.5X	X
Relative complexity	X	1.2X	1.2X	1.2X
Relative complexity of electronics	X	X	.8X	X
Relative cost	X	1.5X	1.2X	1.5X
Operating speed range (in thd rpm)	to 50	to 20	30 to 120	50 to 100
Best rated size (KWA)	to 10	1+	5+	5+
Relative size of overall package	X	1.2X	1.3X	X

Isotropic rotors.- Recent development work in the area of flywheel energy storage systems can be categorized in two areas depending on the rotor material and construction. One group, termed isotropic rotors, uses materials in which the strength properties remain the same regardless of the direction of measurement. These are the more common metallic rotors built from steel, titanium, or similar materials. The second group, termed anisotropic or composite rotors (references 1-1 and 1-2), is based on utilization of some of the very high strength anisotropic materials. These materials are commonly used in filament form and include such materials as boron, glass, graphite, and organics.

Relevant work in the isotropic rotor field includes the work by Rockwell conducted under contract to the Air Force. This work established numerically optimized constant stress rotor shapes and proceeded through the design, fabrication, and test of an energy storage substation. This work formed the basis for the IPACS program analyses in the isotropic rotor area. Other studies (reference 1-3) have addressed the isotropic rotor problem and established other numerically optimized rotor profiles which are comparable in efficiency to the Rockwell constant stress design.

Energy density function: Stress analyses for representative isotropic flywheel shapes indicate that the energy storage potential of the wheel can be expressed in the form

$$\frac{KE}{W} = K_s \frac{\sigma}{\rho}$$

where

KE = Kinetic energy stored in the wheel at the maximum speed

W = Wheel weight

K_s = Dimensionless shape factor

σ = Allowable stress in material

ρ = Material density defined as weight per unit volume

The above expression assumes that the only constraint on the operation of the wheel is the allowable stress in the material. A lightweight wheel designed for efficient energy storage would then be fabricated from a material with a high strength to density ratio and with a form characterized by a relatively high shape factor K_s . Each of these subjects is discussed below.

Isotropic materials: Table 1-VII summarizes the significant properties for various homogeneous materials. The allowable stress data have been specified to allow 100 000 stress cycles on the rotor. A Goodman diagram is used to establish the allowable stress for isotropic materials.

For purposes of the feasibility study, high-strength steel was conservatively selected as the rotor material. Both 300M tool steel and Republic HP9-4-.45 are seen to have essentially equivalent properties. The HP9-4-.45 material was used in the 50 000-rpm rotors built and tested under Air Force contract by the Los Angeles Division of Rockwell. The 300M material is currently readily available and is in common use. The HP9-4-.45 steel is currently available only on special order.

As can be noted, titanium has the high stress to density ratio desired for rotor materials. It further has the property of being nonmagnetic which is required for the permanent magnet motor ball bearing isolation required in IPACS designs. The lower density, however, requires a corresponding increase in rotor diameter over that of high-strength steel for storing comparable amounts of energy at the same speeds.

Shape factor: Figure 1-9 presents sketches of typical flywheel shapes together with the associated shape factor. The shape factor has a theoretical maximum of 1.0 as indicated for the top configuration in the figure. As noted,

TABLE 1-VII.- HOMOGENEOUS MATERIAL PROPERTIES

Material	Weight Density		Ultimate Tensile Strength		Recommended Working Stress		Strength to Density Ratio	
	(kg/m ³)	(lb/in ³)	Ksi	N/m ²	Ksi	N/m ²	in. x10 ⁻⁶	$\frac{Nm}{kg}$
Republic Steel HP9-4-45	7889	0.285	283	195 x 10 ⁷	160	110 x 10 ⁷	0.561	139,400
Tool Steel 300M	7833	0.283	280	193 x 10 ⁷	160	110 x 10 ⁷	0.565	139,500
Titanium 6Al-4V	4429	0.160	130	89.6 x 10 ⁷	120	83 x 10 ⁷	0.750	187,400
Titanium 6Al-6V-2Sn	4540	0.164	150	103 x 10 ⁷	128	88 x 10 ⁷	0.781	193,800
Maraging Steel 300 grade	8000	0.289	270	186 x 10 ⁷	120	83 x 10 ⁷	0.415	103,800
Maraging Steel 250 grade	8000	0.289	245	169 x 10 ⁷	120	83 x 10 ⁷	0.415	103,800
*Based upon 100,000 fatigue cycles								





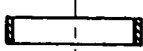


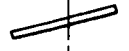

WHEEL TYPE	SHAPE	SHAPE FACTOR
CONSTANT STRESS $R \rightarrow \infty$		-1.0
CONSTANT STRESS		-0.834
CONICAL DISK		-0.806
FLAT DISK		-0.606
THIN RIM		-0.50
SHAPED BAR		-0.50
RIM AND WEB		-0.40
STRAIGHT ROD		-0.333
DISK WITH HOLE		-0.305

Figure 1-9. Isotropic Wheel Shape Factors

this theoretical wheel requires an infinite radius to obtain the perfect constant stress configuration. A practical constant stress design (as designed built and tested by the Los Angeles Division of Rockwell) is characterized by a shape factor of 0.834. Rockwell computer studies and manufacturing experience would show this the maximum realizable shape factor. Other shapes are less efficient such as the theoretical thin rim at a value of 0.5 or a rim and web such as the rotors built for control moment gyros with a shape factor of 0.4.

From an energy density standpoint, a constant-stress wheel built from a high strength to density ratio material is optimum.

Rim-disc-constant stress comparison: Studies were conducted to investigate some of the other properties for representative wheel shapes. Three shapes were considered: rim, disc, and constant stress. The rim wheel was assumed to be defined with an inside radius equal to nine-tenths of the outside radius. The hub and web or spokes were assumed to increase the weight of the theoretical rim by 20 percent without benefit of increased energy storage. The disc and constant-stress wheels were assumed to have no hole at the center. Stress analyses of each of these shapes led to the characteristics summarized in Table 1-VIII. These properties assume that the wheel is operated at the speed which loads the material at $110 \times 10^7 \text{ N/m}^2$ (160 ksi).

TABLE 1-VIII. - WHEEL PROPERTIES SUMMARY - STEEL AT
 $110 \times 10^7 \text{ N/m}^2$ (160,000 PSI)

	Kinetic Energy KE_{TOT}^* W-hr	Angular Momentum H_{TOT} N-m-sec	Maximum** Thickness cm	Diameter x rpm
Disc	23.5 (wt)	$1.61 \times 10^6 \frac{\text{wt}}{\text{rpm}}$	$40.4 \frac{\text{wt}}{\text{radius}^2}$	1 112 500
Rim	16.15 (wt)	$1.108 \times 10^6 \frac{\text{wt}}{\text{rpm}}$	$176.8 \frac{\text{wt}}{\text{radius}^2}$	713 700
Constant stress	32.4 (wt)	$2.22 \times 10^6 \frac{\text{wt}}{\text{rpm}}$	$105.4 \frac{\text{wt}}{\text{radius}^2}$	1 706 800
*At the maximum wheel speed **Thickness at the hub Units: Wt ~ kg Diameter ~ cm Radius ~ cm				

Several conclusions can be drawn by inspection of the foregoing mathematical relationships:

- (1) Flywheel weight is established by the requirements for kinetic energy. In this regard, the constant-stress design will provide the lightest flywheel for a given kinetic energy requirement.
- (2) Considered at a maximum operating stress level, the disk and rim type flywheels will provide more H for a given diameter than the constant-stress flywheel. H can be increased or decreased without a direct change in flywheel weight.
- (3) The thickness dimension of the rim flywheel may limit its use to applications that do not require as much kinetic energy storage as can be provided by the disk flywheel or the constant stress flywheel.

Figure 1-10 illustrates the speed-size characteristics for typical isotropic rotors operated at the recommended working stress. For a limited rotor size, the constant-stress design will operate at the highest speed. With a limited operational speed, the constant-stress profile will require the largest diameter. Operation of a specific design in the region under the curve would mean that the wheel stresses are below the design value and therefore the rotor is being used inefficiently.

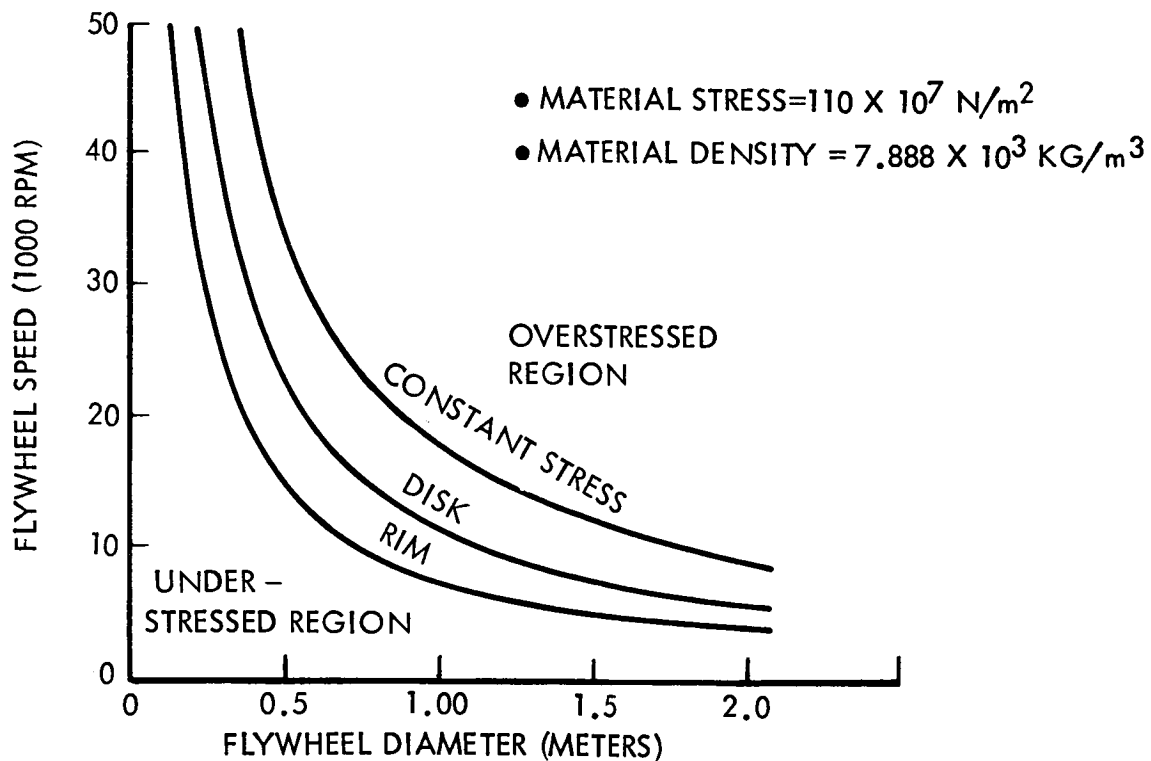


Figure 1-10. Isotropic Rotor Maximum Operating Speeds

Design constraints and optimization considerations: Rotor size constraints were recognized in the design of units to satisfy specific mission requirements. The constraint for the larger vehicles (MSS, 30-day Shuttle, and RAM) was assumed to be 102 cm (40 in.) overall. The constraint for the smaller vehicles was set for the smaller vehicles was set at 38.1 cm (15 in.). The large vehicle constraint was derived from hatch size limitations on the modular space station. The 38.1-cm (15-in.) constraint was derived from a review of representative satellite layout drawings.

The principal design objective used in IPACS flywheel sizing was minimum weight. There are several general factors established in the study which have an influence on the flywheel design and weight. These factors and their influence are as follows:

(1) Flywheel diameter -

- a. The minimum flywheel diameter results in the lightest gimbal cover and support weight, provided the axial length of the rotating group does not exceed the flywheel diameter.
- b. The minimum flywheel diameter results in the highest rotational speed, which yields the largest contact bearing losses.
- c. The minimum flywheel diameter results in the maximum axial length for the rotating group.

(2) Flywheel speed reduction -

- a. The speed reduction of a flywheel in supplying its kinetic energy to a generator is limited by the design of the generator.
- b. A large speed reduction results in minimum flywheel weight.
- c. A large speed reduction results in a maximum generator weight, since full power must be provided at the minimum flywheel speed.
- d. Motor/generator studies have shown a 50-percent speed reduction to be reasonable.

The units must be operated at speeds which will permit satisfactory bearing life and reasonable drag losses. These considerations require compromises as low unit weight is contingent upon the wheels operating at speeds which fully stress the rotor material.

Composite rotors.- Composite rotor designs for IPACS were developed by computer stress studies of three candidate designs selected from the results of research into current anisotropic rotor technology. The preferred concept, a tape-wound design utilizing PRD-49-III filament, was developed by Rockwell studies. The design is predicted to provide 71 W-hr/kg (32.3 W-hr/lb). The computer program for predicting wheel performance has been submitted under NASA Technology Utilization X60020-Composite Flywheel Tape Wound Design.

The first of the three design concepts studied was a constant thickness orthotropic disk employing circumferentially wound high-strength graphite fibers. The second design considered a circular brush design using unidirectional high-strength boron fibers. The third concept, the selected tape-wound design, considered fiber materials being made into tapes, then wound into a disk. The materials considered for the third concept are PDR-49-III (an organic fiber) and graphite fibers.

Circular brush design: A circular brush concept employing unidirectional high-strength boron fibers is illustrated in the sketch on figure 1-11. The flywheel consists of boron fiber elements and a hub.

The brush elements are made up of 0.01 cm (0.004 in.) diameter boron fibers, equally spaced on the hub, and having the following properties:

Modulus of elasticity (E)	$40 \times 10^{10} \text{ N/m}^2$ ($58 \times 10^6 \text{ psi}$)
Density (ρ)	$2.6 \times 10^3 \text{ kg/m}^3$ (0.094 lb/in.^3)
Ultimate tensile strength (F_{tu})	$3.45 \times 10^9 \text{ N/m}^2$ ($500,000 \text{ psi}$)
Allowable fatigue stress, based on 100,000 cycles	$2.42 \times 10^9 \text{ N/m}^2$ ($350,000 \text{ psi}$)

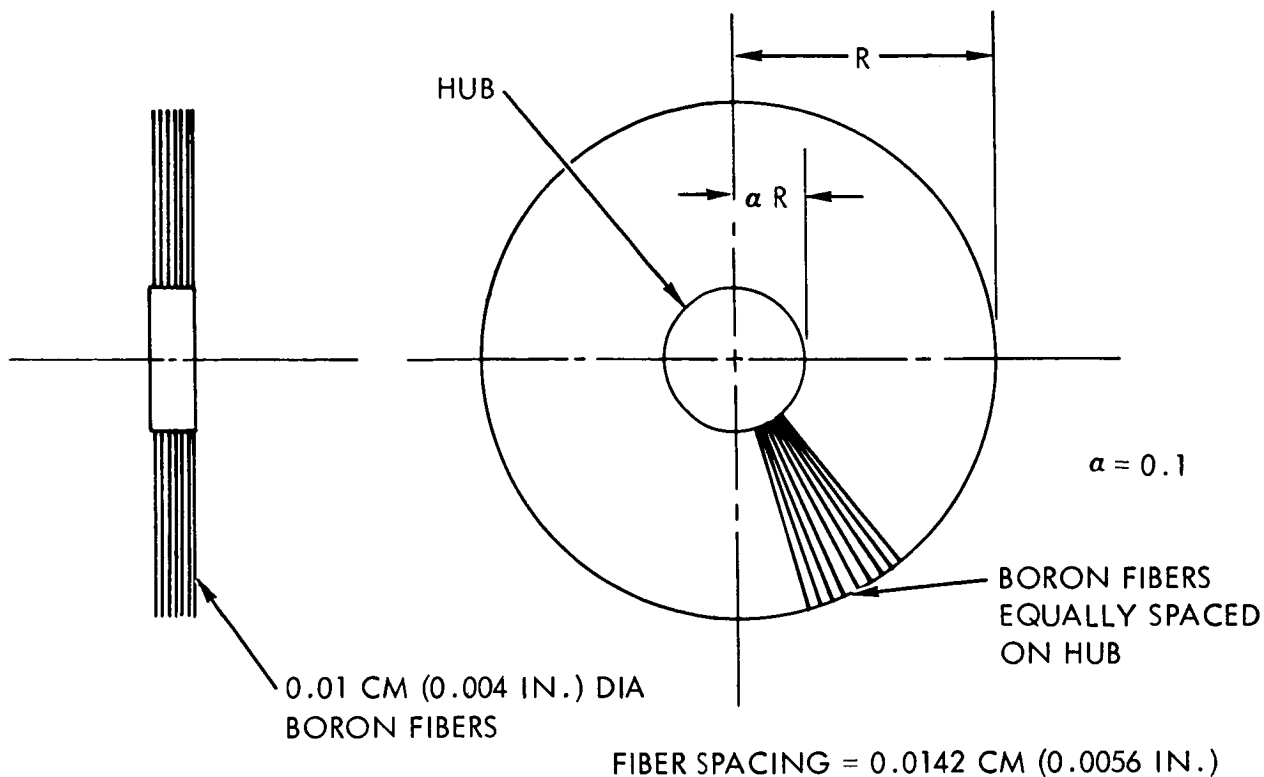


Figure 1-11. Circular Brush Configuration

The hub, as assumed for the analysis, is made of 300M steel.

The method of analysis assumes the boron fibers to be uniaxially stressed and the hub to be acting as a disk. The spacing of boron fibers is limited by the allowable stress for the hub section. The interface loads between the boron fiber and the hub will be transferred by shear action in the bonding compound, which normally, is not the weak area.

Analysis of the above design indicates that the specific energy is 67.7 W-hr/kg (30.8 W-hr/lb) on a total energy basis (zero to maximum speed).

Table 1-IX shows a comparison of weights required by the TDRS rotor using the boron design in comparison to an isotropic material, titanium 6Al-4V. The shaft weight is not included in the composite design weight. The energy requirement for TDRS rotor is taken as 94.7 W-hr.

A steel hub was assumed for purposes of the analysis. A more practical design from a manufacturing standpoint is a sandwich hub, where the boron fibers and resin are sandwiched between aluminum spacers. The assembly is bonded together by a pressure and temperature cure.

TABLE 1-IX.- TDRS ROTOR DESIGN COMPARISON

	Circular brush design	Isotropic design
Radius cm (in.)	32.5 (12.8)	17 (6.70)
Width cm (in.)	1.575 (0.62)	0.761 (0.30)
Speed (rpm)	39 000	50 470
Specific energy W-hr/kg (W-hr/lb)	67.6 (30.76)	37.2 (16.91)
Material	Boron fibers	Titanium 6Al-4V
Cycles	10^5	10^5
Weight kg (lb)	1.4 (3.08)*	2.54 (5.6)
*Shaft weight not included.		

Constant-thickness orthotropic disk: A constant-thickness orthotropic disk employing circumferentially wound high-strength graphite fibers was investigated. The specific energy was found to vary between 28.2 to 29.4 W-hr/kg (12.82 to 13.34 W-hr/lb) depending on the hub size (αR). For a hub size of $\alpha = 0.1$, the specific energy is 28.2 W-hr/kg (12.82 W-hr/lb). This design approach for a composite flywheel gives a specific energy less than that obtainable by isotropic materials. The weakness of the design is that it fails to make full use of the high uniaxial strength of the graphite fibers. Manufacturing difficulties are encountered in winding fibers circumferentially at the correct and uniform tension. Other investigations have shown that the specific energy can be increased by increasing the filler (resin) density.

Tape-wound design: The use of a tape-wound design employing a high strength and a high modulus organic fiber (PDR-49-III) will give a specific energy of 71 W-hr/kg (32.28 W-hr/lb). A sketch of the flywheel design is shown in figure 1-12. Figures 1-13, 1-14, and 1-15 present graphs for the specific energy, weight, wheel radius, and rotating speed. Also plotted on figures 1-13, 1-14, and 1-15 is the case for using high-strength graphite fiber tape. For graphite the specific energy is found to be 60.4 W-hr/kg (27.41 W-hr/lb).

The analysis for the tape-wound flywheel was programmed for computer solution. The equations used are taken from "Anisotropic Plates" by S. G. Lekhnitskii, translated from the second Russian edition by S. W. Tsai and T. Sheron. The equations are for a rotating non-homogeneous curvilinearly anisotropic disk and have been modified to account for the flywheel thickness and the directional properties varying with radial position. The disk is divided into a number of cylindrical rings, each ring varying in its elastic properties. The rings are joined at their respective boundaries, subjected to the compatibility conditions that the radial displacement at the respective contact surfaces are equal. From the compatibility conditions the interface pressures are found which gives the allowable stress coefficients for the ring elements.

The program calculates at each ring section the tangential and radial stress coefficients ($\sigma/R^2\omega^2$) where σ is actual stress, R is flywheel outer radius, and ω is flywheel angular speed. From the stress coefficients and allowable stress, the value $R^2\omega^2$ is found for each ring element. The lowest value of $R^2\omega^2$ is used for determining the specific energy, weight, angular speed, and flywheel radius. The material properties used in the program solution are given in Table 1-X.

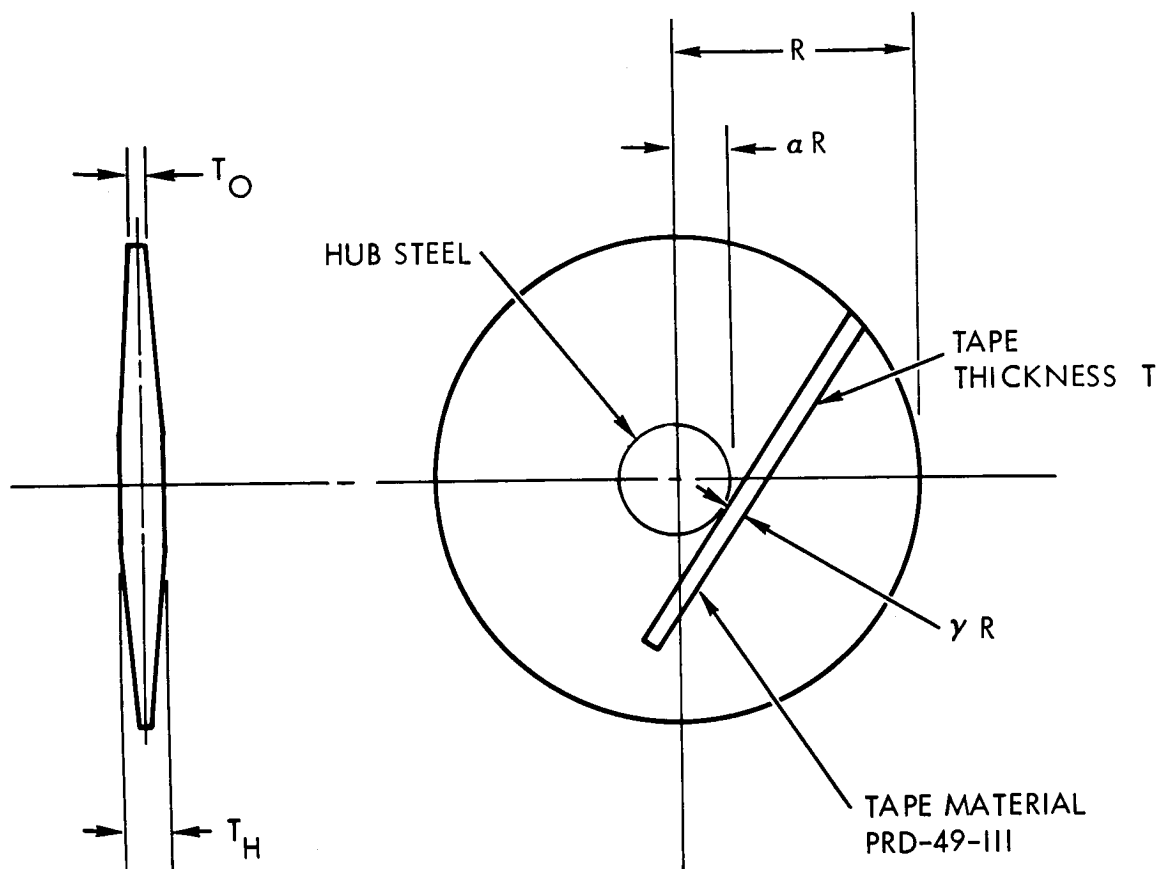
The tape wound design assumes the flywheel will be made by symmetrically winding the tape around a mandrel. After curing, the part is cut and the mandrel is removed. The two disk halves and hubs are assembled by bonding.

In analyzing the tape-wound composite disk for stresses, it is assumed that the hub is not attached to the disk; that is, the radial stress at the hub and disk interface is zero. This assumption is considered conservative. It is expected that a hollow thin metal hub connected to the disk will

TAPE ALLOWABLE STRESSES:

$$F_L = 1.38 \times 10^9 \text{ N/M}^2 \text{ (200 KSI)}$$

$$F_T = 3.45 \times 10^7 \text{ N/M}^2 \text{ (5 KSI)}$$



$$T_H = 2.59 \text{ CM (1.001 IN.)}$$

$$\rho_H = 8.3 \times 10^3 \text{ KG/M}^3 \text{ (0.3 LB/IN.}^3\text{)}$$

$$\rho_C = 1.39 \times 10^3 \text{ KG/M}^3 \text{ (0.05 LB/IN.}^3\text{)}$$

$$a = 0.254 \text{ CM (0.100 IN.)}$$

$$\gamma = 0.508 \text{ CM (0.200 IN.)}$$

$$T_O = 0.391 \text{ CM (0.154 IN.)}$$

$$T = 0.0978 \text{ CM (0.0385 IN.)}$$

Figure 1-12. Tape-Wound Configuration

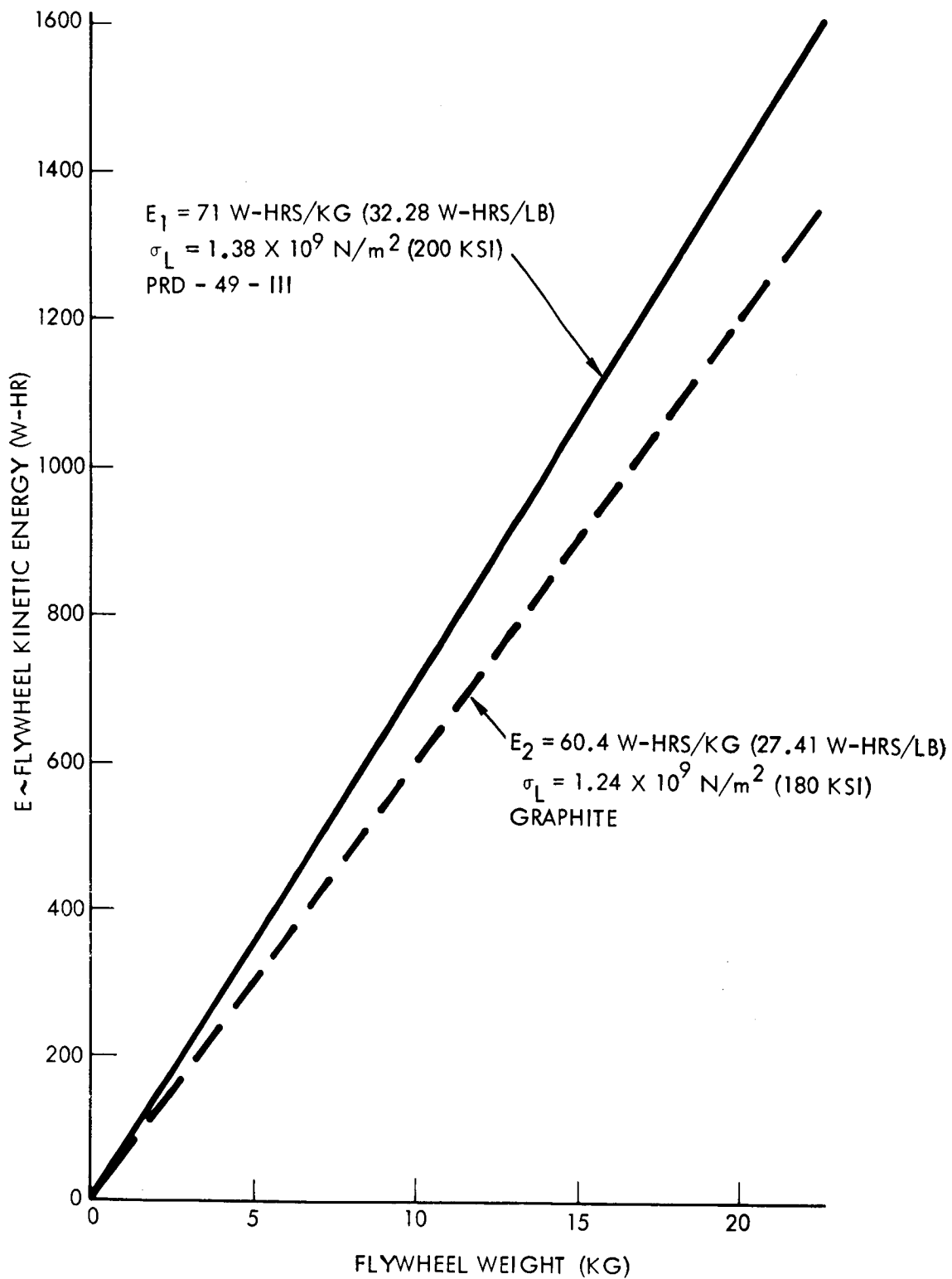


Figure 1-13. Composite Rotor Weight Vs Kinetic Energy

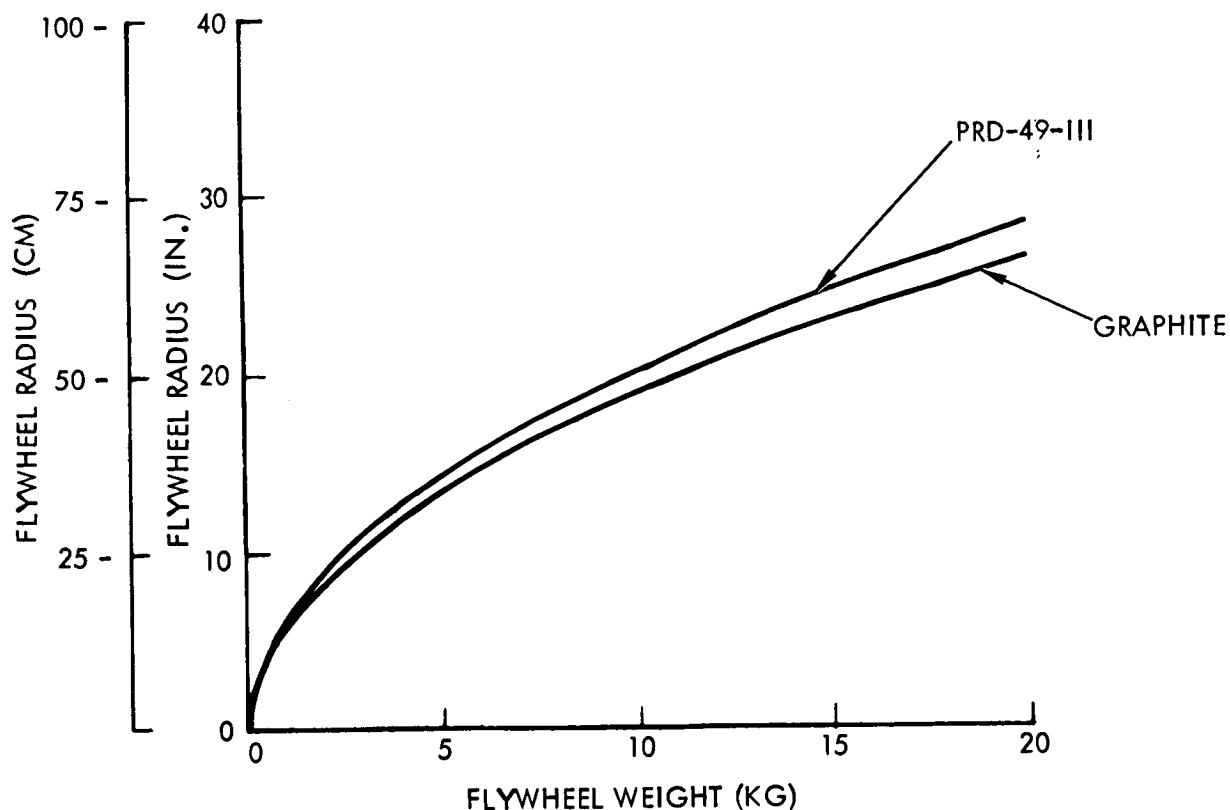


Figure 1-14. Composite Rotor Weight Vs Radius

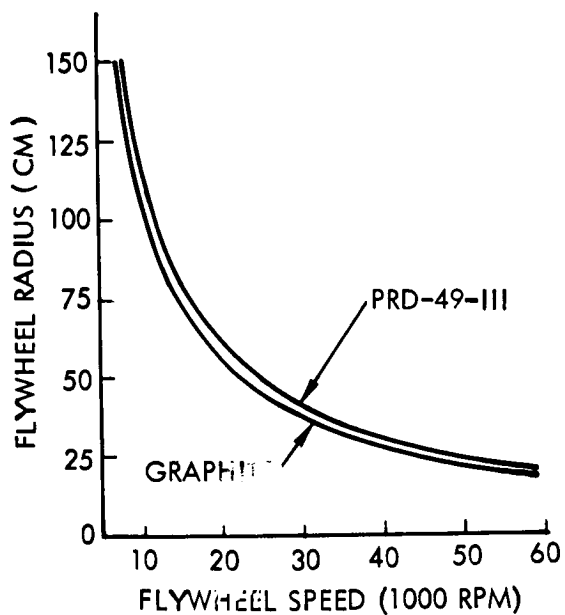


Figure 1-15. Composite Rotor Speed Vs Radius

TABLE 1-X.- TAPE MATERIAL PROPERTIES

Item	PDR-49-III 60% fiber	Graphite epoxy
Modulus of elasticity		
Longitudinal (E_L)	$75.9 \times 10^9 \text{ N/m}^2$ ($11 \times 10^6 \text{ psi}$)	$13.52 \times 10^{10} \text{ N/m}^2$ ($19.6 \times 10^6 \text{ psi}$)
Transverse (E_T)	$5.52 \times 10^9 \text{ N/m}^2$ ($0.8 \times 10^6 \text{ psi}$)	$7.59 \times 10^9 \text{ N/m}^2$ $1.1 \times 10^6 \text{ psi}$
Density - tape	$1.39 \times 10^3 \text{ kg/m}^3$ (0.05 lb/in^3)	$1.61 \times 10^3 \text{ kg/m}^3$ (0.058 lb/in^3)
Poisson's ratio		
V_{LT}	0.34	0.240
V_{TL}	0.025	0.0090
Allowable stress - tape		
Longitudinal (F_L)	$1.38 \times 10^9 \text{ N/m}^2$ (200 ksi)	$1.24 \times 10^9 \text{ N/m}^2$ (180 ksi)
Transverse (F_T)	$3.45 \times 10^7 \text{ N/m}^2$ (5 ksi)	$3.45 \times 10^7 \text{ N/m}^2$ (5 ksi)
Shear modulus	$2.07 \times 10^9 \text{ N/m}^2$ ($0.3 \times 10^6 \text{ psi}$)	$5.58 \times 10^9 \text{ N/m}^2$ ($0.81 \times 10^6 \text{ psi}$)
Allowable shear stress	$6 \times 10^7 \text{ N/m}^2$ (8.7 ksi)	$6.21 \times 10^7 \text{ N/m}^2$ (9 ksi)
Allowable stress - hub	$110 \times 10^7 \text{ N/m}^2$ (160 ksi)	$110 \times 10^7 \text{ N/m}^2$ (160 ksi)
Density - hub	$8.3 \times 10^3 \text{ kg/m}^3$ (0.3 lb/in^3)	$8.3 \times 10^3 \text{ kg/m}^3$ (0.3 lb/in^3)

approximate this condition and at the same time give a small increase in specific energy. The program solution showed low tangential stress at the inner radius of the composite disk. These low allowable stresses are attributed to the generalized method of the material properties derivations in the complex structural area where the tapes are stacked. Changing the computer program to have a finer grid in this area and adding the hub should increase the allowable stresses and decrease the actual stresses in the tangential directions.

For the analysis it is assumed that the material properties are not degraded in the process of manufacturing the rotor.

Table 1-XI, using figures 1-13, 1-14, and 1-15, compares rotor properties for the RAM mission between the tape-wound composite design and the isotropic material design.

TABLE 1-XI.- RAM ROTOR DESIGN COMPARISON

	Composite tape-wound design	Isotropic design speed constrained	Isotropic design optimum speed
Radius cm (in.)	27.9 (11.0)	18.9 (7.45)	18.9 (7.45)
Width cm (in.)	16.5 (6.50)	13.5 (5.30)	<13.5 (<5.3)
Speed (rpm)	45,000	45,000	55,050
Material	PDR-49-III	Titanium 6Al-4V	Titanium 6Al-4V
Cycles	10^5	10^5	10^5
Weight* kg (lb)	20.6 (45.4)	45.9 (101.0)	30.6 (67.34)
*Shaft weight not included			

Comparison of concepts: Table 1-XII presents a summary of the various specific energies for anisotropic designs and, for comparison, two cases for isotropic design employing titanium 6Al-4V and steel 300M.

No optimization study has been made with respect to weight variation and flywheel dimensions. For the same specific energy, a decrease in radius requires an increase in angular speed and flywheel width. It is anticipated that for a given weight, there is an optimum flywheel radius and hub width which would give a minimum volume.

Composite considerations: Although the composites offer significant weight saving advantages, they are not without their disadvantages. Associated with the composites are problems pertaining to the following:

- (1) Fabrication techniques
- (2) Properties of composite materials, particularly the lack of data on fatigue life for resin and filament.

- (3) Variation of resin viscosity during winding.
- (4) Holding uniform tension of fibers during winding.
- (5) Lack of relative geometric symmetry in manufacturing.
- (6) Difficulties in obtaining optimum shapes.
- (7) Residual stresses.
- (8) Inspection of wheel for quality assurance.
- (9) Compatibility of shaft with disk material.
- (10) Disk repair impractical.
- (11) Dynamic balancing.
- (12) Verification of the method of analysis.

Looking at this list, one might conclude that disadvantages outweigh the advantages. However, it should be noted that many of the problems associated with composites are presently being investigated. Preliminary results indicate that they are solvable or will be solvable in the near future.

TABLE 1-XII.- ANISOTROPIC AND ISOTROPIC DESIGN COMPARISON

Design	Material	Specific Energy W-hrs/kg (W-hrs/lb)
Circular brush	Boron	67.75 (30.76)
Orthotropic disk	Graphite	28.24 (12.82)
Tape wound	PDR-49-III	71.10 (32.28)
	Graphite	60.37 (27.41)
Isotropic	Titanium 6Al-4V	47.75 (21.68)
Isotropic	Steel 300M	34.34 (15.59)

Summary: Flywheels made of composite materials will give higher specific energies than the isotropic materials. This study shows two possible designs - the tape-wound and the circular brush concepts - that have the feasibility of offering weight saving for IPACS.

The circular brush concept, although shown to have a lower specific energy than the tape-wound concept, has excellent future possibilities. Advances in technology promise fibers with strengths two to three times the present-day composites. Combine this potential with solutions to the fiber-hub attachment and manufacturing difficulties, and tremendous weight saving advantages result for flywheel energy storage systems.

For IPACS systems development the tape-wound concept is recommended and has been used in the feasibility analysis of advanced concepts. This is based on the following:

- (1) Highest specific energy.
- (2) Manufacturing procedures would follow techniques developed for filament-wound vessels.
- (3) Dynamic balancing obtainable by machining.
- (4) Less potential of damage during fabrication and handling.

Spin bearing.— The types of bearings included in the trade studies that were conducted are shown in figure 1-16, together with the primary design requirements. These requirements include long life at high speed with low friction losses. Bearing stiffness is important to lessen the coupling of a compliant rotor assembly into the primary control loops. Both contact and non-contact bearing types were considered. The hydrodynamic type includes both gas and grease bearings.

A preliminary trade screening was conducted to narrow the potential bearing candidates. The results of this analysis are summarized in figure 1-16. All types except the ball and magnetic bearings were eliminated from consideration for this application, in the main by reason of the limiting characteristics shown in the accented blocks.

Ball bearings: In the IPACS application, the requirements imposed upon the bearings include long life at high speed with low friction losses. Bearing loads can be maintained low and temperatures of the bearings benign. In such applications, the more significant factor is bearing life as rotational and surface speeds increase.

The criterion of normal bearing life is the metal fatigue of the contacting surfaces. This fatigue results from repeated high stresses on the ball and raceways and is evidenced by material flaking and surface breakup. If a bearing is allowed to run long enough, fatigue is unavoidable, but the number of revolutions the bearing makes before flaking starts is a function of bearing load and speed and resulting Hertzian stress level. If a large group of apparently identical bearings is tested to fatigue failure under the same conditions of load and speed, a variation in bearing lives will be noted. The distribution of failures within such a test group follows a probability curve. The form and proportions of the curve are typical of fatigue distributions and remain much the same for all sizes, types, and makes of ball bearings.

BEARING TYPE	MAX SPEED	LOAD CAPACITY	STIFFNESS	POWER	BRG LIFE	IMPACT ON IPACS DESIGN
BALL	30 TO 80,000 RPM	MORE THAN ADEQUATE	HIGH $1.75 \times 10^8 \text{ N/M}$ (10^6 LB/IN.)	POWER IS MAJOR FACTOR ABOVE 30-50000 RPM 10-100 WATTS	ADEQUATE WITHIN DESIGN SPEEDS	MIN
ROLLER	30000 RPM MAX	HIGHER THAN BALL BEARING	EXCESSIVE $1.75 \times 10^9 \text{ N/M}$ (10^7 LB/IN.)	HIGH RELATIVE TO BALL BRGS 3 TO 10X	INSUFFICIENT FOR ROLLER TYPE REQUIRED (TAPERED)	MIN
HYDRODYNAMIC ¹	SPEED LIMITED BY HIGH POWER ABOVE 30000 RPM	MORE THAN ADEQUATE	HIGH $1.75 \times 10^8 \text{ N/M}$ (10^6 LB/IN.)	HIGHER THAN BALL BRGS ABOVE 20-40000 RPM	ADEQUATE	MIN
MAGNETIC	LIMITED BY SERVO BANDWIDTH ²	ADEQUATE	ADEQUATE $1.75 \times 10^7 \text{ N/M}$ (10^5 LB/IN.)	LOW 1-2 WATT MAX (DRAG)	ADEQUATE WITH REDUNDANT ELECTRONICS	MODERATE
ELECTROSTATIC	LIMITED BY SERVO BANDWIDTH ²	INSUFFICIENT FOR HIGHER LOAD RANGE	ADEQUATE	LOW	ADEQUATE WITH REDUNDANT ELECTRONICS	MAJOR
CRYOGENIC	100,000 RPM RANGE	ADEQUATE	LOW	LOW	ADEQUATE AS PASSIVE BRG	MAJOR

NOTES:

1. SELF ENERGIZED JOURNAL AND THRUST PLATE
2. DEVELOPMENT REQD ABOVE 10-20K RPM
3. ACTIVE CONTROL WOULD IMPROVE STIFFNESS

Figure 1-16. Bearing Trades - Design Considerations

A conventional method of indicating the severity of ball bearing usage is the DN factor which is calculated as the product of bearing size in millimeters multiplied by the rotational speed in rpm. The DN numbers are surface speed numbers and are affected by bearing design characteristics which include surface finish, retainer strength, friction properties, and internal clearances. Table 1-XIII lists general DN limits for ball bearings as defined in reference 1-6.

TABLE 1-XIII.- SPEED LIMITS FOR BALL BEARINGS

Lubrication	DN limit (mm x rpm)
Oil	
Conventional bearing designs	300 000 to 350 000
Special finishes and separators	1 000 000 to 1 500 000

The expected range of IPACS applications is 0.4 to 1.5×10^6 DN and, as such, falls within the specified limits. Figure 1-17 illustrates several current bearing applications as a function of DN range. As can be noted, the jet aircraft engine applications result in higher DN values than those of IPACS with higher bearing loads and more severe temperature environment.

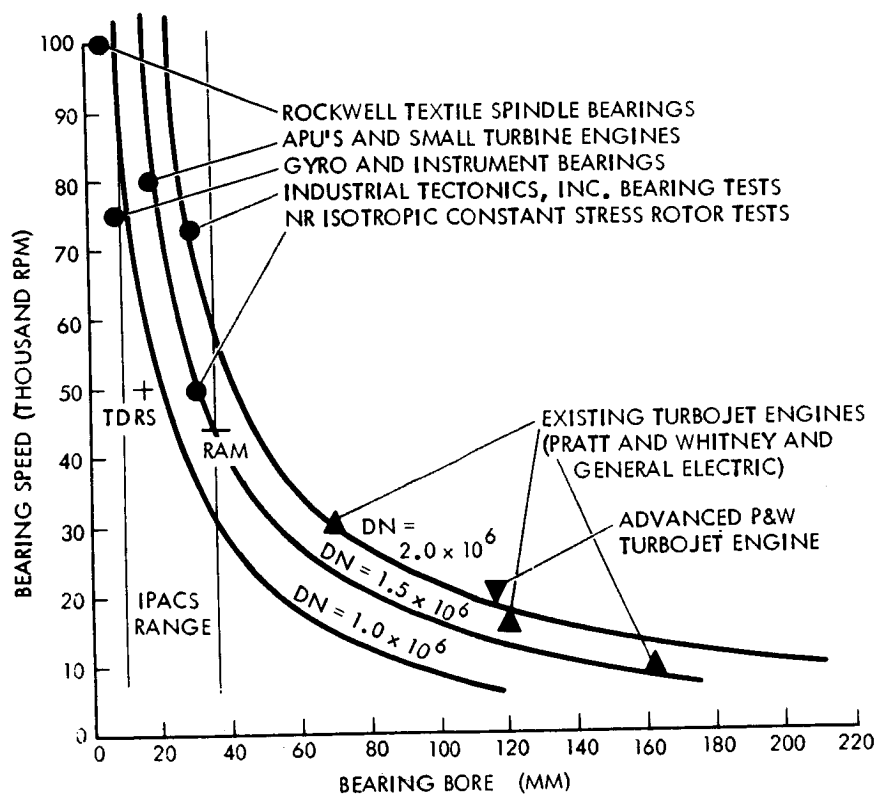


Figure 1-17. Ball Bearing Operation

However, the DN values can only be considered an indicator of probable bearing life and applicability. As stated, the values only reflect surface speeds and related fatigue failure which is the more improbable failure mode noted in high-precision, high-speed spin-axis bearings. The more probable failure mode is due to retainer problems or lubricant breakdowns.

Lubrication is expected to be the more important design factor in achieving adequate ball bearing life for the high-speed IPACS applications. Most of the high DN designs illustrated in figure 1-17 utilize recirculating spray or oil mist lubrication systems which flood the bearings, carrying away heat and wear particles. These designs are undesirable for IPACS because of their power losses (both in pumping and in viscous friction) which would lower charge-discharge efficiency. As will be subsequently shown, heating calculations indicate flooded bearings are not required in IPACS for thermal stabilization of the bearings. The high efficiency of the motor generators and low bearing loads result in heat loads which are readily stabilized through conduction and radiation of flywheel elements. As in conventional designs, it is necessary to match thermal expansion coefficients of the rotor shaft, bearings, and housings and provide for preload adjustment.

With spray lubrication neither required nor desired, grease and grease-oil lubricants were considered. Much experimental work has been performed upon bearings to test the suitability of various lubricants. Grease and solid lubricants have been thoroughly investigated and, to date, they have not yielded the life of many oil lubricants. Results show, for a long, continuous application an oil should be used. Tests show that ball bearings can operate for years when lubricated with select low-vapor-pressure oils. The centrifugal oiler was selected for use in IPACS designs. The oiler is a self-contained unit precharged with lubricant sufficient for several mission times. The oiler housing rotates with the shaft and meters a low amount of oil through a calibrated leak. The oil is gathered in a collector on the rotor side of the bearing and labyrinth seals prevents appreciable leakage into the housing.

Such oilers have been demonstrated in CMG systems at speeds to 10 000 rpm. Design calculations indicate them suitable for IPACS speeds.

The IPACS missions can be categorized in two groups (Table 1-XIV). Several bearings were selected as candidates and are listed at the bottom of Table 1-XIV. A bearing was selected for each group based on fatigue life and friction. For Group 1, the 38H bearing was chosen and the 206H bearing was picked for Group 2 missions.

As shown in figure 1-18, longer life (as well as reduced drag) is achieved with reduced preload. The preloads utilized are the minimum recommended by bearing manufacturers and verified by General Electric Company experience.

The principal load in orbit is the bearing preload which should be approximately 22 N (5 lb) minimum for the 38H bearing application and 133 N (30 lb) minimum for the 206H bearing application. High preload values reduce life and increase bearing friction while low preload values cause noise and vibration.

Figure 1-18 is a plot of bearing life versus speed for the 38H bearing and figure 1-19 is a similar plot for the 206H bearing suitable for Group 2 missions. The L_{10} life plotted is the fatigue life for 10 percent failure (L_5 indicates a 5 percent failure). If the L_{10} life is 8760 hours, bearing reliability is Q90 for one year. Figure 1-20 allows conversion to other fatigue life values.

TABLE 1-XIV.- SPIN BEARING OPTIONS

Mission		Slew loads N-m ft-lb		Approx. design load N lb		Approx. bearing preload N lb	
Group 1	EOS	<1.3	<1	445	100	22.3	5
	TDRS	<1.3	<1	445	100	22.3	5
	MJS	<6.8	<5	445	100	22.3	5
Group 2	Shuttle	<13	<10	4450	1000	223	50
	RAM	<26	<20	4450	1000	223	50
	MSS	<13	<10	4450	1000	223	50
<p style="text-align: center;">Spin bearings considered:</p> <p style="text-align: center;">Group 1 - R36, R-4, Z114, 38BX2, 38H</p> <p style="text-align: center;">Group 2 - 204H, 206H, 207H, 304H</p> <p style="text-align: center;">Spin bearings selected:</p> <p style="text-align: center;">Group 1 - 38H</p> <p style="text-align: center;">Group 2 - 206H</p>							

To determine the L_{10} life at other points, the following relationships may be used:

$$L_{10} \propto \frac{1}{RP^3} \quad (38H \text{ bearing})$$

$$L_{10} \propto \frac{1}{R^{.92}P^3} \quad (206H \text{ bearing})$$

where R = Wheel speed (rpm)

P = Bearing preload (lb)

The design life for each mission is indicated on figures 1-18 and 1-19. This is based on the L_{10} life as determined from Table 1-XV.

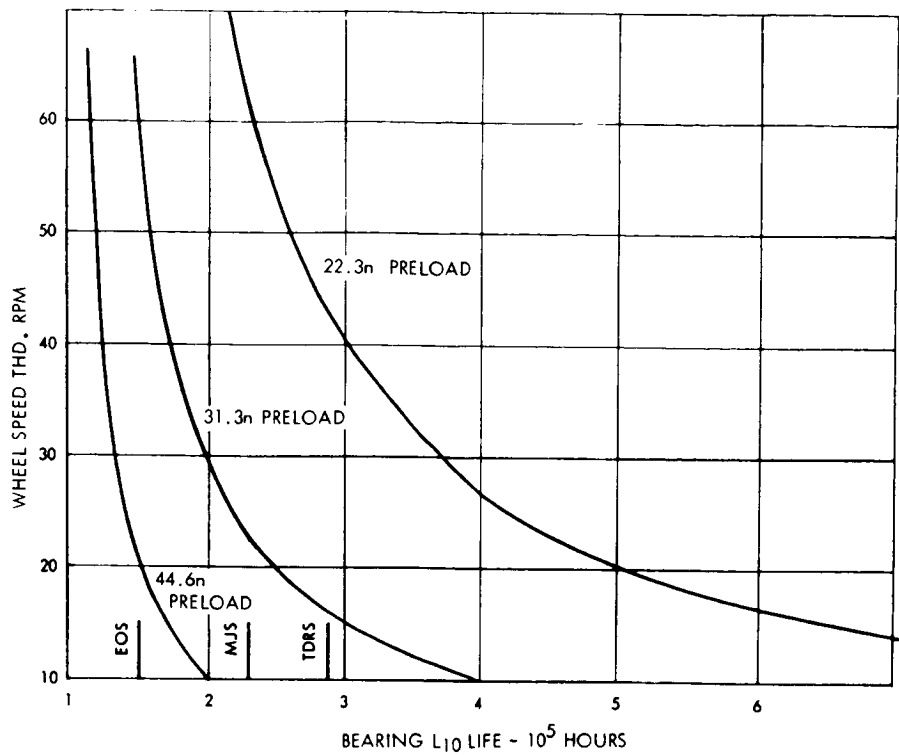


Figure 1-18. Ball Bearing Life Data, 38H Bearing, Mission 1, 2, 3 (Group 1)

TABLE 1-XV. - FATIGUE LIFE REQUIREMENTS

Mission	Life	Est bearing reliability reqmts	Estimated bearing life reqmts hr	
1. EOS	2 yr	0.98	L ₂ -17 500	L ₁₀ -49 400
2. TDRS	5 yr	0.99	L ₁ -43 800	L ₁₀ -186 300
3. MJS	3-1/2 yr	0.99	L ₁ -30 600	L ₁₀ -130 400
4. Shuttle	30 days	0.99	L ₁ -720	L ₁₀ -3070
5. RAM	5 yr	0.95	L ₅ -43 800	L ₁₀ -73 000
6. MSS	10 yr	0.95	L ₅ -87 600	L ₁₀ -166 000

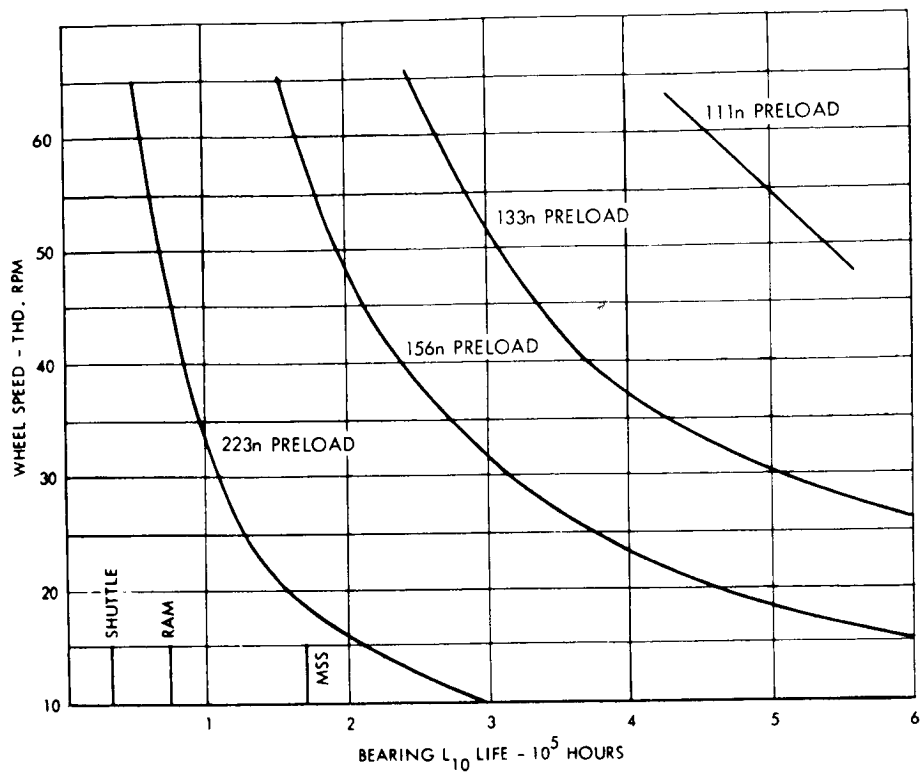


Figure 1-19. Ball Bearing Life Data, 206H Bearing, Mission 4, 5, 6 (Group 2)

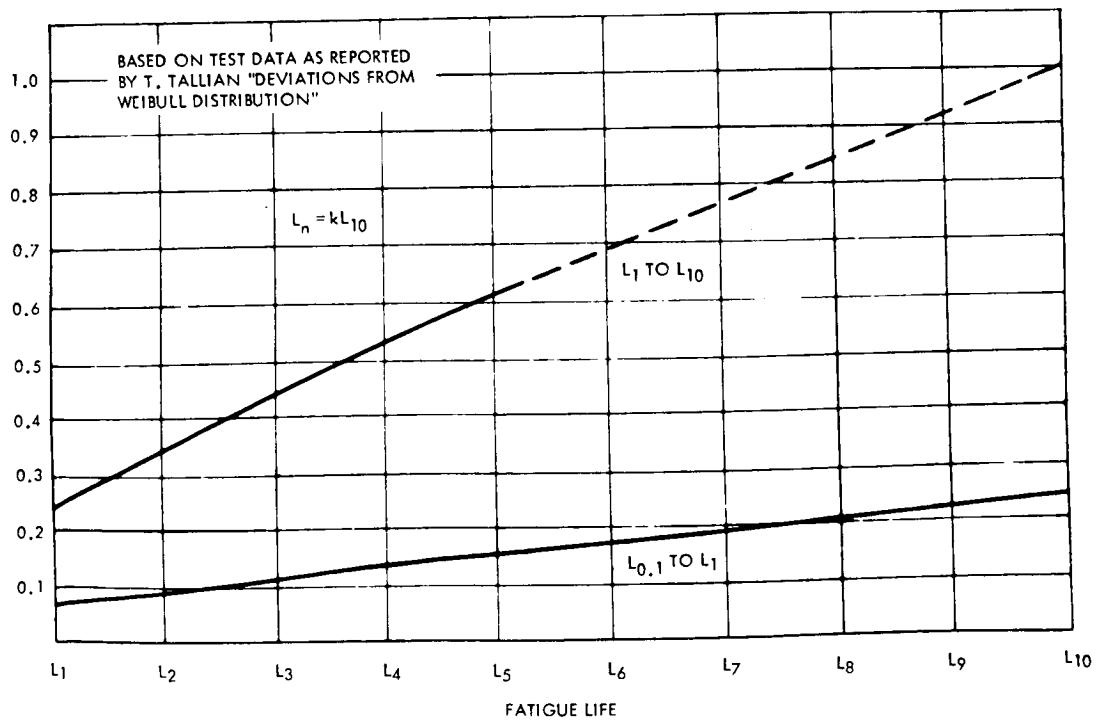


Figure 1-20. Relationship of Fatigue Life to L_{10} Life

The bearing friction is a combination of load friction and viscous drag with:

Viscous drag $\propto R^{.666}$

Load friction $\propto R^{.143}$

Figure 1-21 is a plot of bearing friction versus speed for the 38H bearings for Group 1 missions and figure 1-22 gives bearing friction for the 206H bearings suitable for Group 2 missions.

Magnetic bearing: The magnetic suspension bearing is a noncontact bearing suitable for IPACS use which is expected to operate at lower losses than conventional contact bearings for an indefinite life. Several bearings have been developed and tested. More notably, the Aircraft Equipment Division of the General Electric Company built a 101.68 N-m (75 ft-lb-sec) momentum wheel assembly suspended by magnetic bearings under contract NAS5-11440 to NASA/GSFC. A sketch of this type of bearing is presented in figure 1-23.

The stator of the bearing consists of a stack of four-pole punchings and two shell-type flux return sections. Each pole piece is equipped with a control winding and diametrically opposite windings are connected in series, thus forming two separate control circuits. The shell-type sections enclose the punchings as shown and they may be provided with a flange for purposes of mounting.

The rotor consists of alternately stacked rings of iron and ring-shaped permanent magnets which are axially magnetized. The magnets are polarized such that their flux enters from both sides into the central ring-section which is also preferably composed of a stack of punchings and located directly underneath the four-pole pieces of the stator. The solid soft iron rings at the left and right end of the bearing provide, in combination with the shell-type structure of the stator, a return path for the fluxes of the two permanent magnets and at the same time serve to furnish passive axial support of the bearing. To achieve satisfactory axial stiffness, part of the surface of these iron rings as well as the inner surface of the circular end-opening of the shells are recessed by machining one or several grooves into their surfaces. In this manner, a high flux density (β) level in the airgap around these narrow ring sections is obtained. Since the force which is required to displace the shaft axially is proportional to β^2 and the number of ring-sections, a high degree of stiffness can be achieved. The magnet material to be used should belong to the family of rare-earth-cobalt magnets which

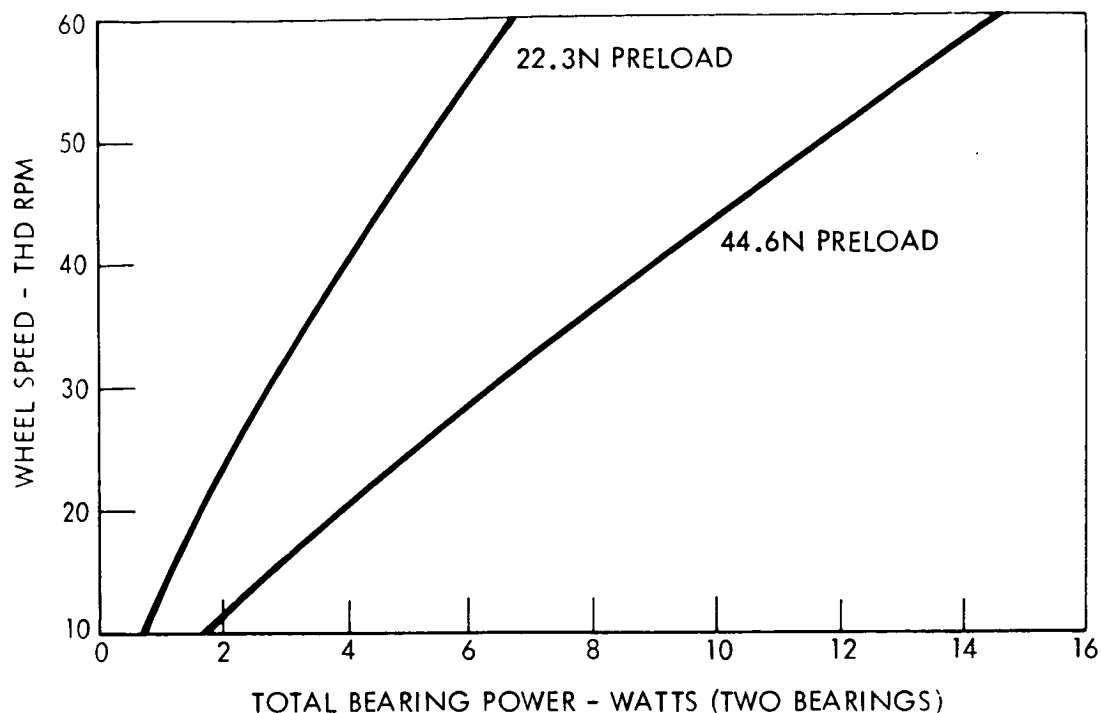


Figure 1-21. Ball Bearing Friction, 38H Bearing, Mission 1, 2, 3 (Group 1)

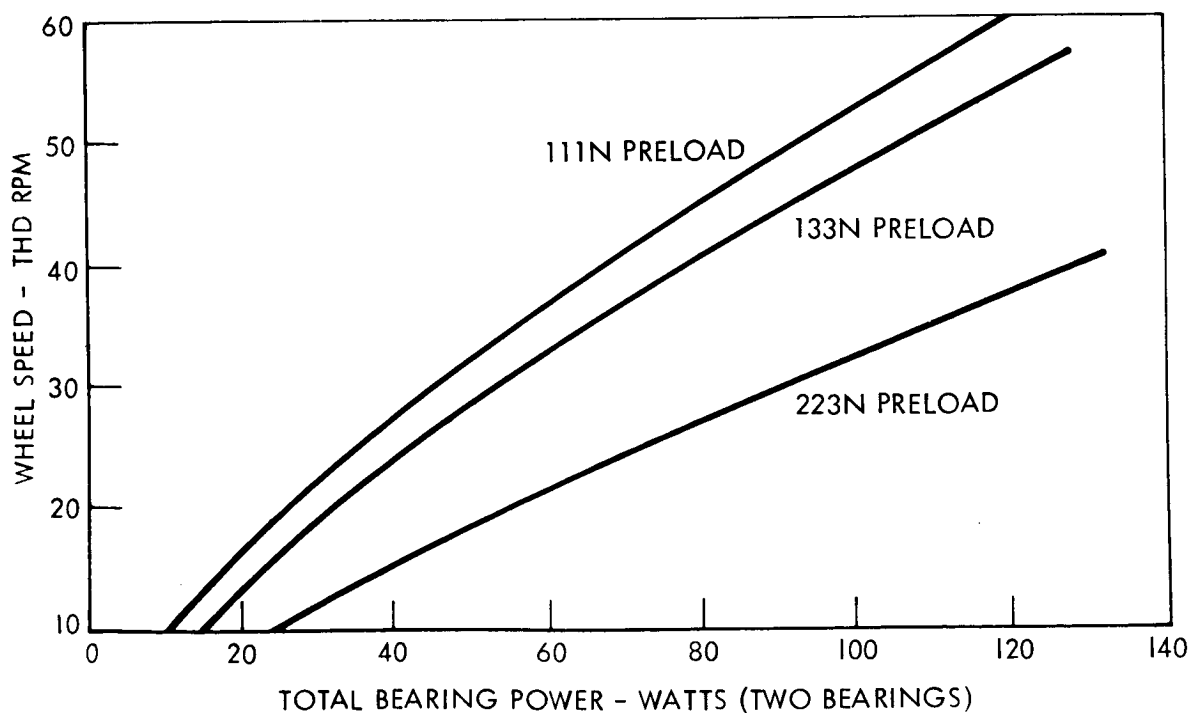


Figure 1-22. Ball Bearing Friction, 206H Bearing, Mission 4, 5, 6 (Group 2)

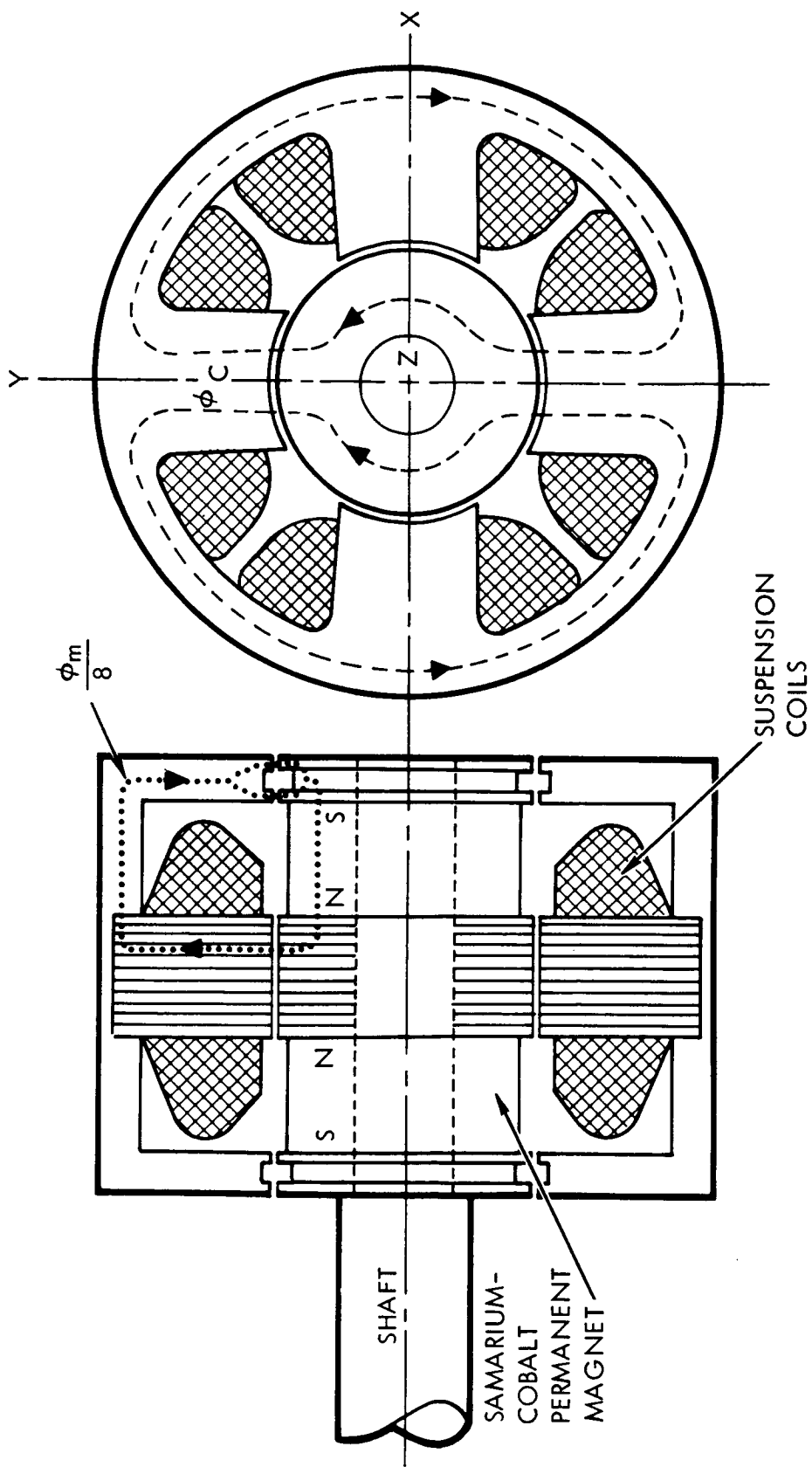


Figure 1-23. Magnetic Journal Bearing

exhibit a very large coercive force and, therefore, can be designed to have a short axial length and relatively large cross-section which contribute to a compact design of the bearing.

The total flux of the permanent magnets enters and leaves the stator in the radial direction in eight distinguishable flux paths which converge through the cylindrical housing towards the circular airgaps of the axial support ring sections. One of these flux paths is shown as a dotted line in figure 1-23. There are four such flux paths in both vertical and horizontal planes.

It is easily understood that the flux ϕ_m of the permanent magnets cannot provide a stable support of the rotor, and therefore, the shaft, since an infinitely small radial displacement from its theoretical zero position will cause it to be attracted to any one of the four-pole pieces. Stability can be achieved by provision of control ampere turns in each axis via the control windings. The flux path of the controlling flux ϕ_c is shown as dashed lines in figure 1-23 for the case of the vertical axis and one may observe that as indicated it causes a decrease in flux density in the airgap of the lower pole while, at the same time, the flux density in the upper gap will be increased resulting in an upward directed total force. Reversal of this flux results in a reversal of the direction of this force. Thus, any radial load exerted upon the shaft can be supported by suitable control of the control winding currents.

In order to arrive at a stable support, these currents must, in both axes, be proportional to the radial displacement components. To achieve this, position detectors are required in both axes which convert the magnitudes of displacement into electrical signals. These signals are then amplifiers, containing suitable networks for dynamic stabilization, and thus converted into currents within the control windings. Capacitive, inductive, Hall-effect, magneto-resistive, or photo-electrical position sensors can be employed.

Magnetic bearing physical characteristics: Parametric weight, power, and volume data are determined as a function of bearing load capacity. The bearing load capacity varies as the pole face area and for a similar design, the pole length varies as $\sqrt{\text{AREA}}$. Then the load capacity is proportional to l^3 , VOLUME, and WT.

$$W = 5.18 \times 10^{-3} (L)$$

$$W = 0.0092(L)^{0.9} \quad \text{for an improved design}$$

$$V = 217 W$$

L = Bearing load capacity - Newtons

V = Magnetic bearing volume - cm³

For bearing power assume that the gap g is proportional to $\ell^{1.3}$
(based on data and adequate heat transfer surface).

$$I = \frac{10\beta g}{4\pi N} \propto \ell^{1.3} \quad (\text{for constant flux density } \beta \text{ and a single turn } N = 1)$$

but

$$R \propto \frac{\ell}{\ell^2} \propto \frac{1}{\ell}$$

Then

$$P = I^2 R \propto \frac{\ell^{2.6}}{\ell} \propto \ell^{1.6}$$

but bearing load $L \propto \ell^3$

Then

$$P \propto (\text{LOAD})^{\frac{1.6}{3}} \propto (\text{LOAD})^{0.534}$$

and

$$\frac{P}{\text{RADIATING AREA}} \propto \frac{1}{\ell^{0.4}}$$

This is satisfactory since heat transfer per unit area is lower on larger unit.

Based on two present designs:

$$P_{\text{MAX}} = 0.27 (L_{\text{MAX}})^{0.534} \text{ power in watts per bearing}$$

and for operation at fractional load k ($L = k L_{\text{MAX.}}$)

$$P = P_{\text{MAX}}(k)^{.5}$$

In the above expressions:

- W - Bearing weight, kg
- β - Flux density
- g - Air gap, cm
- N - Turns per coil
- R - Coil resistance, ohms
- P - Power, watts
- ℓ - Representative dimensions of bearing, cm
- D - Bearing drag, N-m
- L - Bearing load capacity, lb
- I - Current - amps

The electronics power is:

$$P_E = I + 0.00598 L_{MAX} \text{ watts per bearing}$$

Bearing drag is a function of the magnetic material and is independent of speed in range up to 10 000 rpm.

$$D = 2.21 \times 10^{-7} (L_{MAX}) \text{ Newtons per bearing}$$

Figure 1-24 is a plot of bearing weights and figure 1-25 shows bearing power. Average power will be very nearly that of the electronics since the duty cycle is low. Figure 1-26 indicates magnetic bearing volume.

Table 1-XVI gives weight, power, and bearing drag (per bearing) for a magnetic bearing suitable for each mission.

In an attempt to define the range of operation of the magnetic bearing versus the ball bearing, figure 1-27 indicates the speeds at which magnetic bearing power and ball bearing spin power is equal. Any speed above this point will have lower power losses if a magnetic bearing is used. If we neglect weight of the bearings, the lower points are obtained. If we consider weight and assign 6.6 W/kg (3 W/lb), we obtain the higher points.

Housing and gimbal - parametric data. - The data used to estimate the housing and gimbal weights for the IPACS units are presented below.

Weights of IPACS wheel housing and supports - The wheel housing or supports will depend on the type of attitude control required. For the gimballed units, the stiffness requirements will result in a housing of

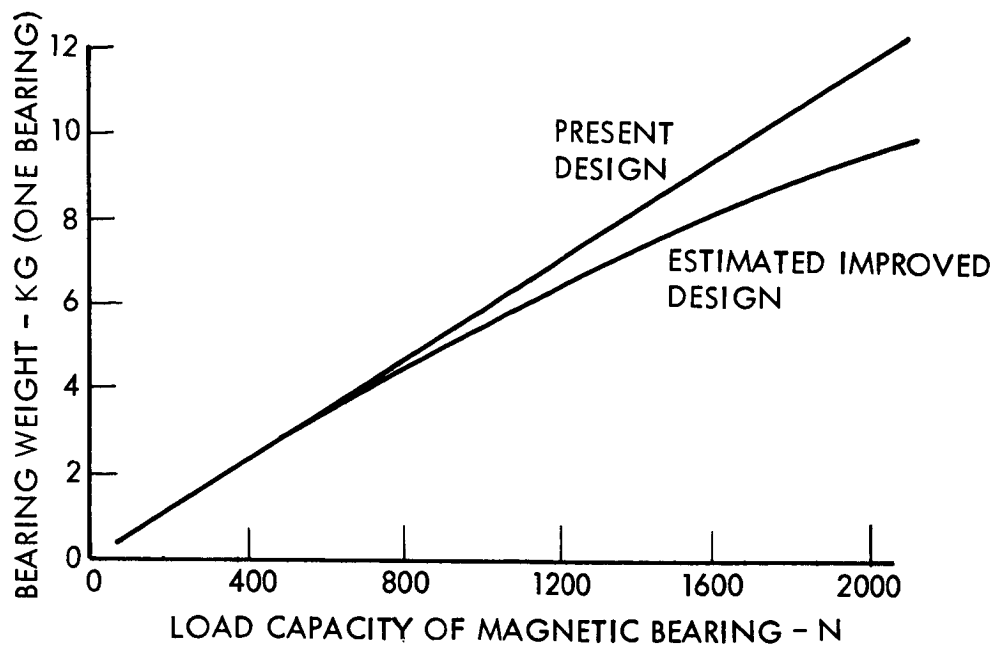


Figure 1-24. Magnetic Bearing Weight

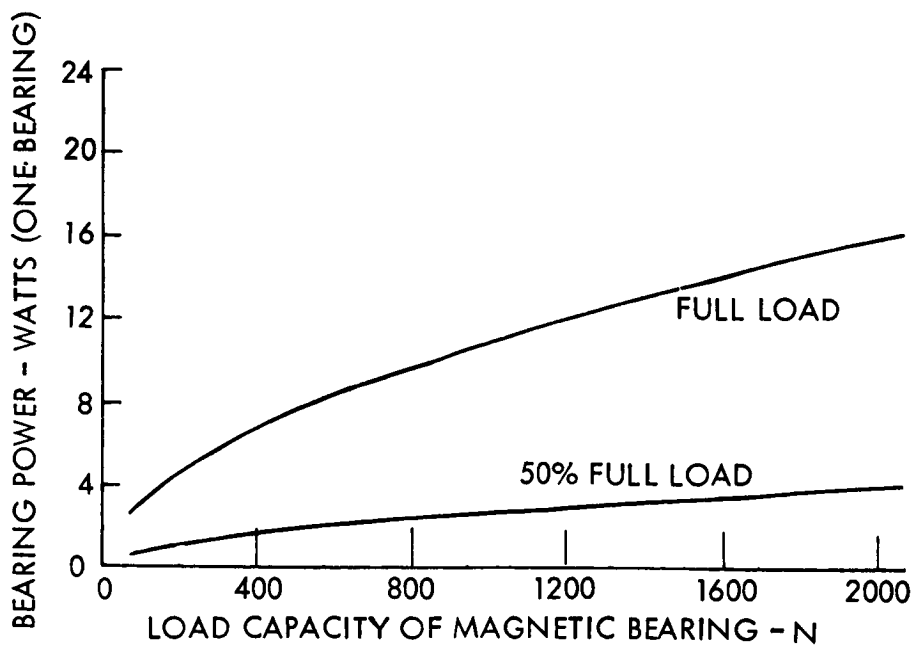


Figure 1-25. Magnetic Bearing Power

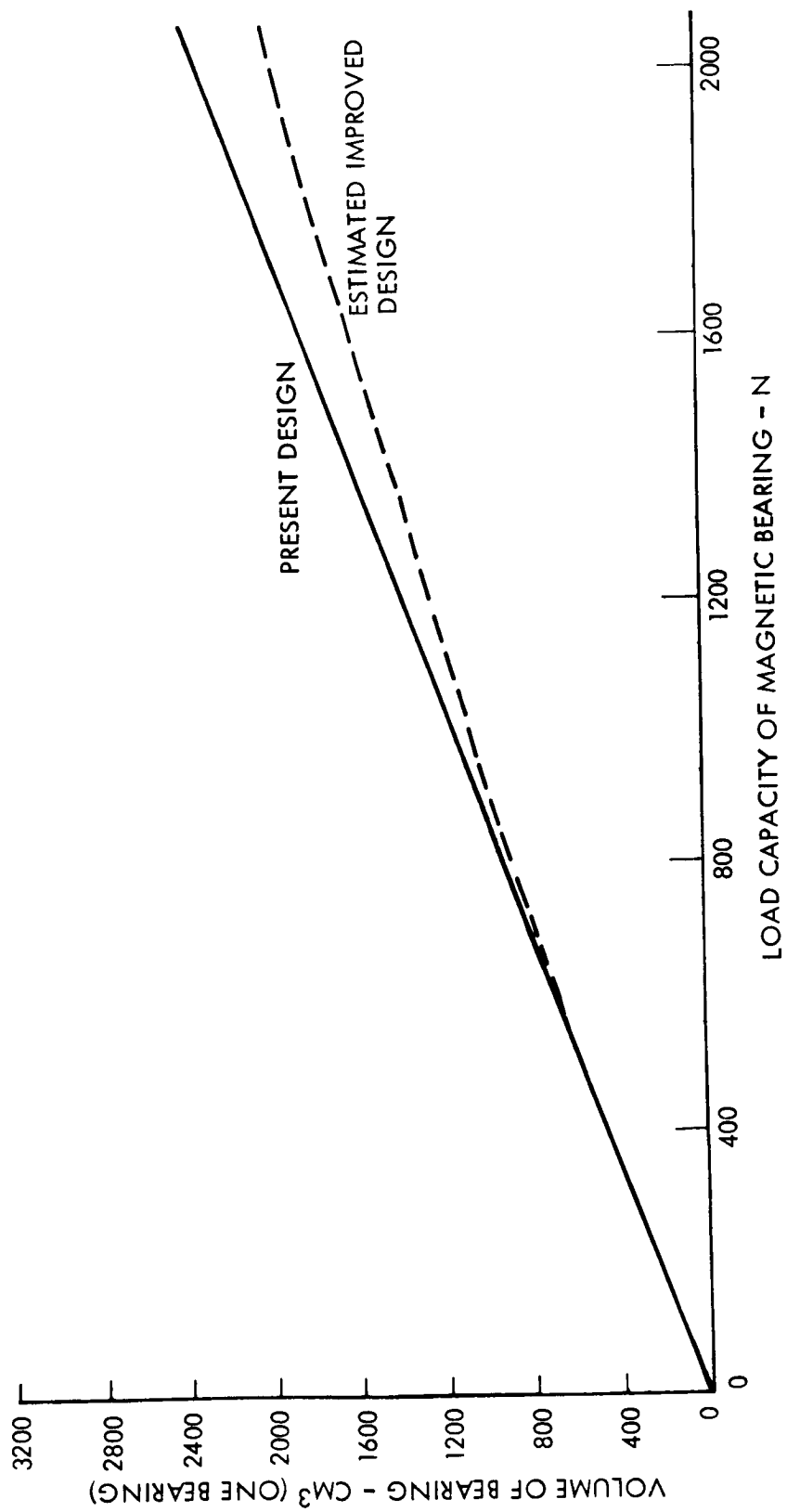


Figure 1-26. Magnetic Bearing Volume

TABLE 1-XVI.- MAGNETIC BEARING CHARACTERISTICS FOR IPACS MISSIONS

Mission	Load capacity, N lb	Bearing weight kg lb	*Avg power, W	Peak power, W	Bearing drag N-m (in-oz)	Bearing drag (at 5240 rad/sec), Watts
TDRS	44 (10)	0.23 (0.5)	1.6	3.3	9.2 (0.0013)	0.048
EOS	44 (10)	0.23 (0.5)	1.6	3.3	9.2 (0.0013)	0.048
MJS	44 (10)	0.23 (0.5)	1.6	3.3	9.2 (0.0013)	0.048
RAM	220 (50)	1.13 (2.5)	3.0	7.2	46.6 (0.0066)	0.244
Shuttle	534 (120)	2.77 (6.1)	5.4	11.9	113 (0.016)	0.590
MSS	1480 (333)	7.63 (16.8)	11.1	22.1	314 (0.0445)	1.65
*10% duty cycle (10% peak power) would generally be lower						

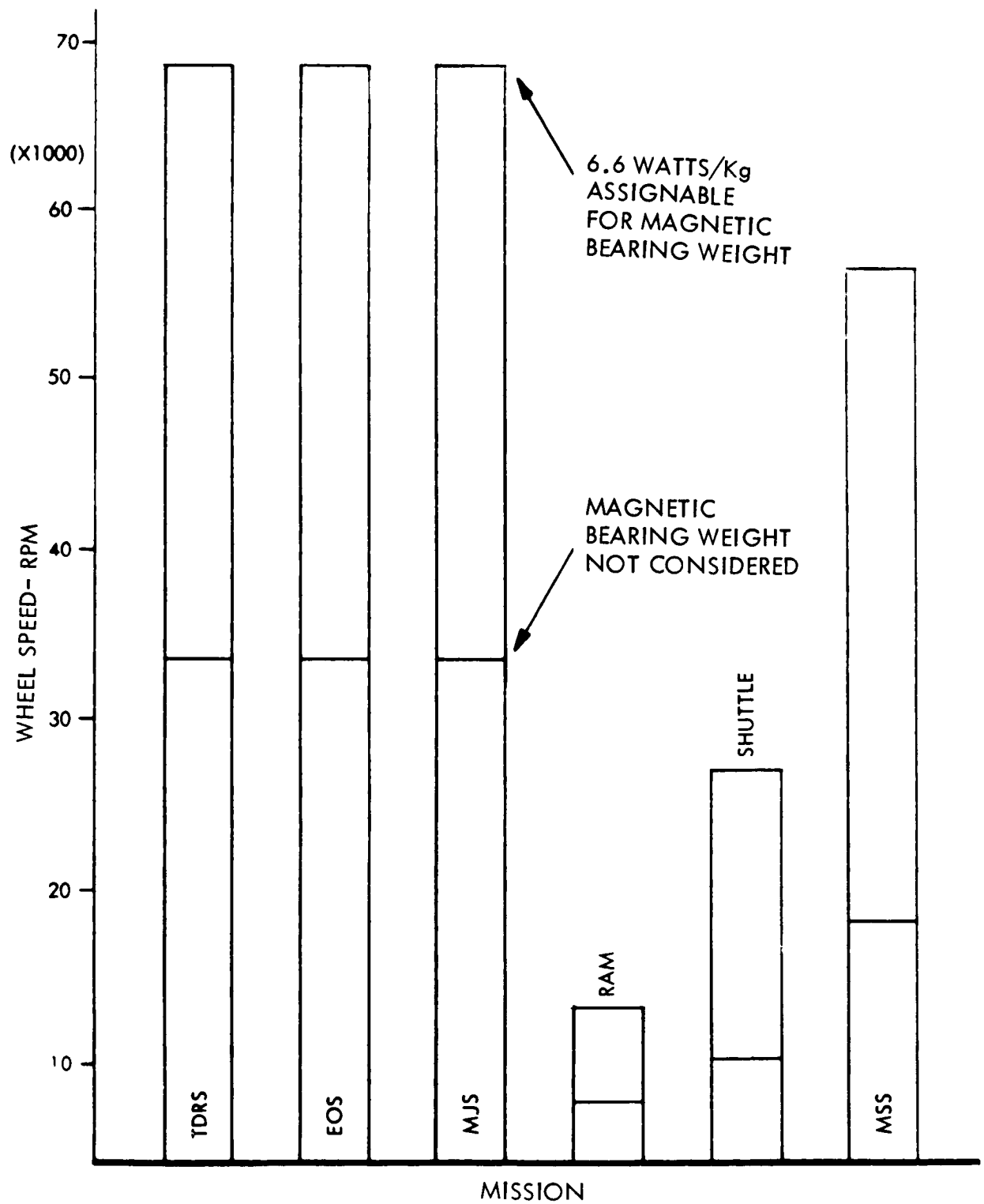


Figure 1-27. Operating Speed Cross-Over Points for Ball and Magnetic Suspension

significant weight. An approximate expression based on several existing CMG's is given below. Note that a term has been included to allow for varying axial length requirements.

For a reaction/momentum wheel which can be operated in the vacuum of space, open wheel supports can be used which reduce unit weight.

The third possible approach, again for reaction/momentum wheels, uses wheel supports and a light weight case.

CMG inner gimbal

$$W_{IG} = 0.0045d^2 + 0.000646d^{1.3} \quad L = \text{inner gimbal weight in kg}$$

d = Wheel diameter in cm

$L = L_W + L_B + L_{MG} + L_C$ - axial length in cm

L_W = axial length of wheel in cm

$L_B = 2.54 + 0.1d$ - bearing axial length in cm

L_{MG} = total axial length of motor generator units in cm

$L_C = 0.15d$ - axial clearance in cm

Open wheel supports

$$W_{SU} = 0.0883d^{1.5} (L_B) + 0.1W_{MG} \text{ - support weight in kg}$$

W_{MG} = weight of motor-generator units in kg

Case and supports

$$W_{CS} = W_{SU} + 0.1W_{IG} = \text{Case and support weight in Kg}$$

Note: Wheel shaft extensions and ball bearings are included. Only wheel weights and motor-generator weights must be added to determine momentum of the reaction wheel unit or CMG inner gimbal.

Outer gimbal weight: The outer gimbal weight for a double gimbal CMG is given in figure 1-28 as a function of wheel diameter.

Gimbal drive and sensor: The gimbal drives and sensors are given in Table 1-XVII for applicable missions. The single gimbal torquer size is based on adequate acceleration of an equivalent gimbal inertia.

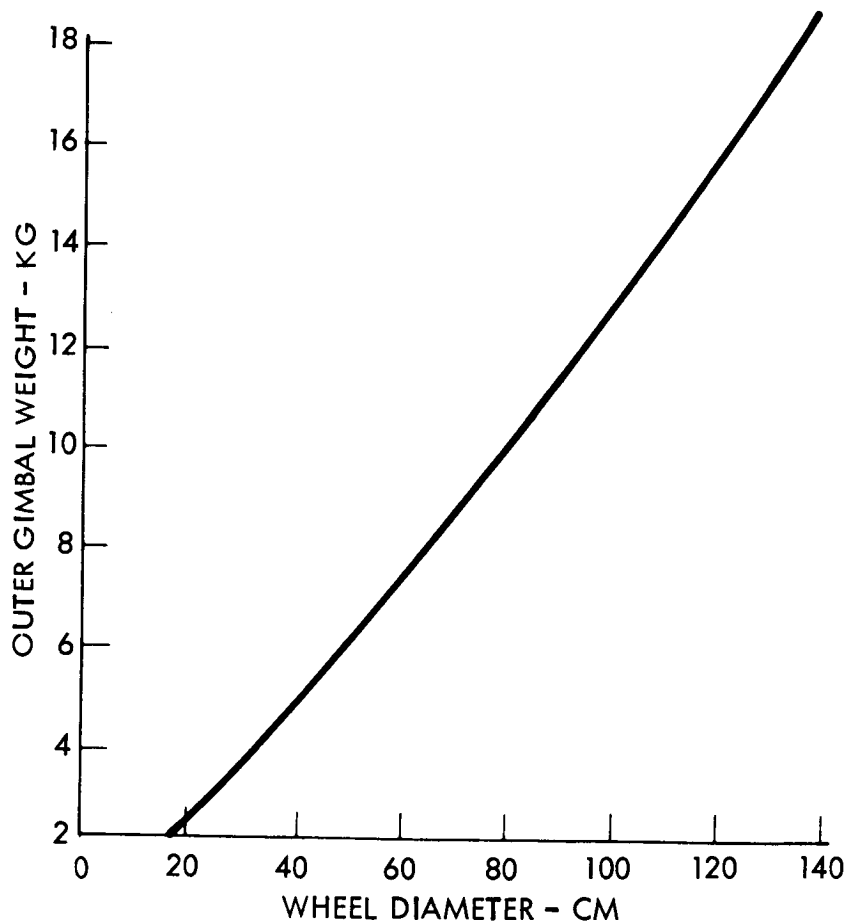


Figure 1-28. Outer Gimbal Weight (Stiffness = 1.36×10^5 n-m/rad)

TABLE 1-XVII.- SIZING OF GIMBAL DRIVE AND SENSOR

Mission	CMG array*	Gimbal torque		Gimbal drive weight		Gimbal gear Ratio	Sensor weight		Approx. axial length	
		N-m	(ft-lb)	kg	(lb)		kg	(lb)	drive cm in	sensor cm in
TDRS	2SG	0.049	(7 in.-oz)	0.45	(1)	1	0.45	(1)	5.08	(2)
RAM	3 DG	14.9	(11)	3.1	(7)	10	1.82	(4)	10.2	(4)
RAM	4 SG	1.35	(1)	1.82	(4)	1	1.82	(4)	10.2	(4)
Shuttle	3 DG	163	(120)	11.3	(25)	10	2.3	(5)	17.8	(7)
MSS	5 SG	27.1	(20)	5	(11)	5	2.3	(5)	12.7	(5)
EOS-MJS	None	-	-	-	-	-	-	-	-	-

*DG - Double gimbal
SG - Single gimbal

Energy Storage Elements and Subsystems

Conventional spacecraft battery and fuel cell elements are discussed and differences between element and subsystem energy density noted. Flywheel systems synthesized from the component trade analysis are presented in their energy density relationships and compared with the conventional systems.

Energy storage elements.- Spacecraft energy storage designs have been dominated by rechargeable, or secondary, batteries subsystems. Over the years battery technology has been well developed and the silver-zinc (AgZn), silver-cadmium (Ag-Cd), and nickel-cadmium (Ni-Cd) cells have seen wide application.

The AgZn battery is characterized by high-energy density, up to 132 W-hr/kg (60 W-hr/lb) for low cycle rates, and good discharge rate performance. Its short cycle life has proven a limitation. The Ni-Cd battery is a relatively long-life, highly reliable system with a high discharge rate capability that has been the predominant battery in spacecraft designs. Its cell energy density is a relatively low 26 W-hr/kg (12 W-hr/lb), and projected improvements of approximately 60 percent. The Ag-Cd battery has energy density and cycle life characteristics between those of Ag-Zn and NiCd and consequently has seen little spacecraft use.

Some recent spacecraft designs have been based on use of regenerative fuel cells as energy storage devices. The regenerative fuel cell consists of hydrogen and oxygen electrode plates separated by electrolyte. Gaseous hydrogen and oxygen are contained on the appropriate sides of the electrodes and pressure is maintained by the container. In the "charged" condition the electrolyte and electrodes are "dry". Electrical energy is released by reaction of hydrogen and oxygen to produce power, heat, and water. The water appears as increased moisture in the electrolyte and within the hydrogen electrode matrix. Power output decreases as moisture content approaches saturation. When power is applied to the electrode terminals, the moisture in the system is converted back into hydrogen and oxygen. Although fuel cells have been proven in space applications, fuel cells with the regenerative feature have only been tested under laboratory conditions for a limited number of cycles. Energy densities to 55 W-hr/kg (25 W-hr/lb) have been demonstrated in the laboratory and values as high as 110 W-hr/kg (50 W-hr/lb) are predicted. Cycle life characteristics are unproven, however, and development costs are estimated to be high.

The component trade studies have shown the spinning flywheel to be a viable competitor for spacecraft electrical energy storage. Designs with current technology, in fact, achieve higher energy densities than can be expected from conventional electrochemical devices. Steel and titanium rotor designs were studied which are expected to be capable of approximately

48 W-hr/kg (22 W-hr/lb). Advanced rotor designs utilizing high-strength filaments in a composite matrix are expected to achieve 70 W-hr/kg (32 W-hr/lb) with improvements of nearly 100 percent postulated. The development of high efficiency motor-generators and associated electronics selected will allow the extraction of rotor energy at efficiency levels required for spacecraft.

Pragmatically the ultimate test of an energy storage design lies in its delivered energy density, efficiency, and life as measured on a subsystem basis in a specific design. The factor between energy density of an element and delivered energy density of a subsystem is not only significant but is also strongly affected by other subsystem variables.

Table 1-XVIII presents some typical energy density values for example energy storage elements.

TABLE 1-XVIII.- ENERGY DENSITY FOR EXAMPLE STORAGE ELEMENTS

Energy storage element	Energy density, W-hr/kg (W-hr/lb)	
PRD-49 filaments	422	(192)
Boron filaments	310	(141)
E-glass filaments	255	(116)
Ag-Zn cell	132	(60)
PRD-49 composite flywheel	70	(32)
Steel flywheel	48	(22)
Titanium flywheel	46	(21)
Advanced NiCd cell	44	(20)
Current NiCd cell	26	(12)

The energy density values of Table 1-XVIII have been compiled to illustrate the relative energy densities of typical materials and energy storage elements. Flywheels are seen to rank highly with respect to battery cells. A number of factors influencing the values presented should be noted.

The values, for example, for filament energy density were calculated from the recommended working rather than the ultimate tensile stress value. Design calculations defining the composite laminate geometry, matrix strength properties, and wheel shape factors reduces the PRD-49 from an ultimate value of approximately 508 W-hr/kg (231 W-hr/lb) to a value of 70 W-hr/kg (32 W-hr/lb) for the useable rotor. In a similar manner the ultimate storage capability of 63 W-hr/kg (28.6 W-hr/lb) for the titanium material reduces to 46 W-hr/kg (21 W-hr/lb) for the rotor rated at the working stress and including shape factor.

The values quoted for current NiCd battery cells are developed from an average sampling of test data for a 1 KW-hr system. Values for advanced Ni-Cd cells are derived from reported test results on high rate Sub C cell types currently being developed. In each case, battery cycle life is dependent upon depth of discharge, cell temperature, and duration of power cycling as shown in figure 1-29. These interrelationships result in significantly different energy density values for energy storage subsystems as opposed to the individual cells.

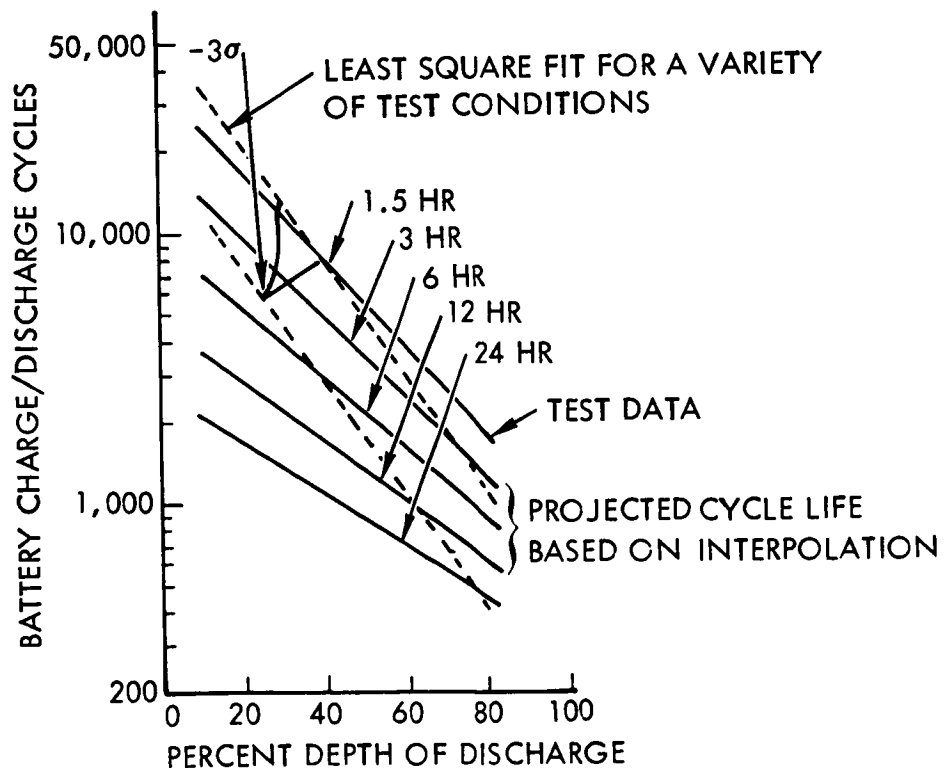


Figure 1-29. NiCd Battery Cycle Life

Energy storage subsystems.- An energy storage subsystem is defined herein as capable of receiving, storing, and discharging power and includes electronics required for the energy storage function but excludes conditioning and distribution equipment. For the battery storage subsystems this definition would include battery cells, case, mounts, connectors, meters, charger electronics, and load controller. For the flywheel systems introduced herein the definition would include motor, housing, seals, mounts, motor generators, and control and regulation electronics. For equitable comparisons of energy density between the two types, charge/discharge losses to the terminals are included.

Battery and fuel cell subsystems: Table 1-XIX presents energy storage subsystem weights and percentages for the six conventional designs designated as the competitive systems.

TABLE 1-XIX.- SPACECRAFT ENERGY STORAGE SUBSYSTEM WEIGHTS

Mission	Weight, kg (lb)	Percentage of power system weight
EOS	91.5 (201)	40
TDRS	27.1 (59.6)	38
MJS	4.5 (10)	3
30-day Shuttle	284 (625)	10
RAM	441 (972)	39
MSS	1776 (3911)	28

The effects of cycle life and power on storage weight is indicated by the low-energy storage percentage for missions with low discharge cycles. The MJS system, for example, provides only a small amount of peaking power for the three periods at planet encounter. In the more representative satellite and RAM missions energy storage weight is clearly seen to be a large percentage of power system weight. Specific energy density values are presented in Table 1-XX for the same designs where the effect of a large number of charge/discharge cycles is evident in the delivered subsystem energy density.

TABLE 1-XX.- SUBSYSTEMS ENERGY DENSITY

Mission	Storage System	Energy density, W-hr/kg (W-hr/lb)		Nominal depth of discharge, %
TDRS	NiCd	9.24	(4.2)	54
EOS	NiCd	3.78	(1.72)	26
MSS	Regenerative Fuel Cell	6.62	(3.01)	30
RAM	NiCd	4.81	(2.19)	25
30-day Shuttle	Ag-Zn	17.60	(8.0)	17
MJS	NiCd	11.00	(5.0)	100

Flywheel energy-momentum subsystems: The component trade studies resulted in the synthesis of two generic energy momentum subsystems. The two designs differed in the degree of technology development required and the achievable energy density and life performance.

The first level design is illustrated in figure 1-30. The assembly uses components of current technology which require moderate extensions to prove their applicability to the IPACS.

The current technology energy-momentum wheel utilizes constant-stress rotors of isotropic materials, ball bearings, centrifugal oilers and permanent magnet motor generators. Component development requirements are discussed in Module 2 - Critical Component Developments and include high speed motor-generators and bearing assembly verification and demonstration of precise balancing over a speed range.

The advanced technology energy-momentum wheel synthesized is illustrated in figure 1-31. This unit utilizes a composite rotor and magnetic suspension bearings which are integrated with the permanent magnet motor-generators. Both rotors and magnetic bearings have been demonstrated but are development items for the high-speed applications.

Studies were performed to establish flywheel ancillary equipment weights, typical losses, and speed reduction factors. These data were derived for the six mission designs which were synthesized and compared with the conventional subsystems.

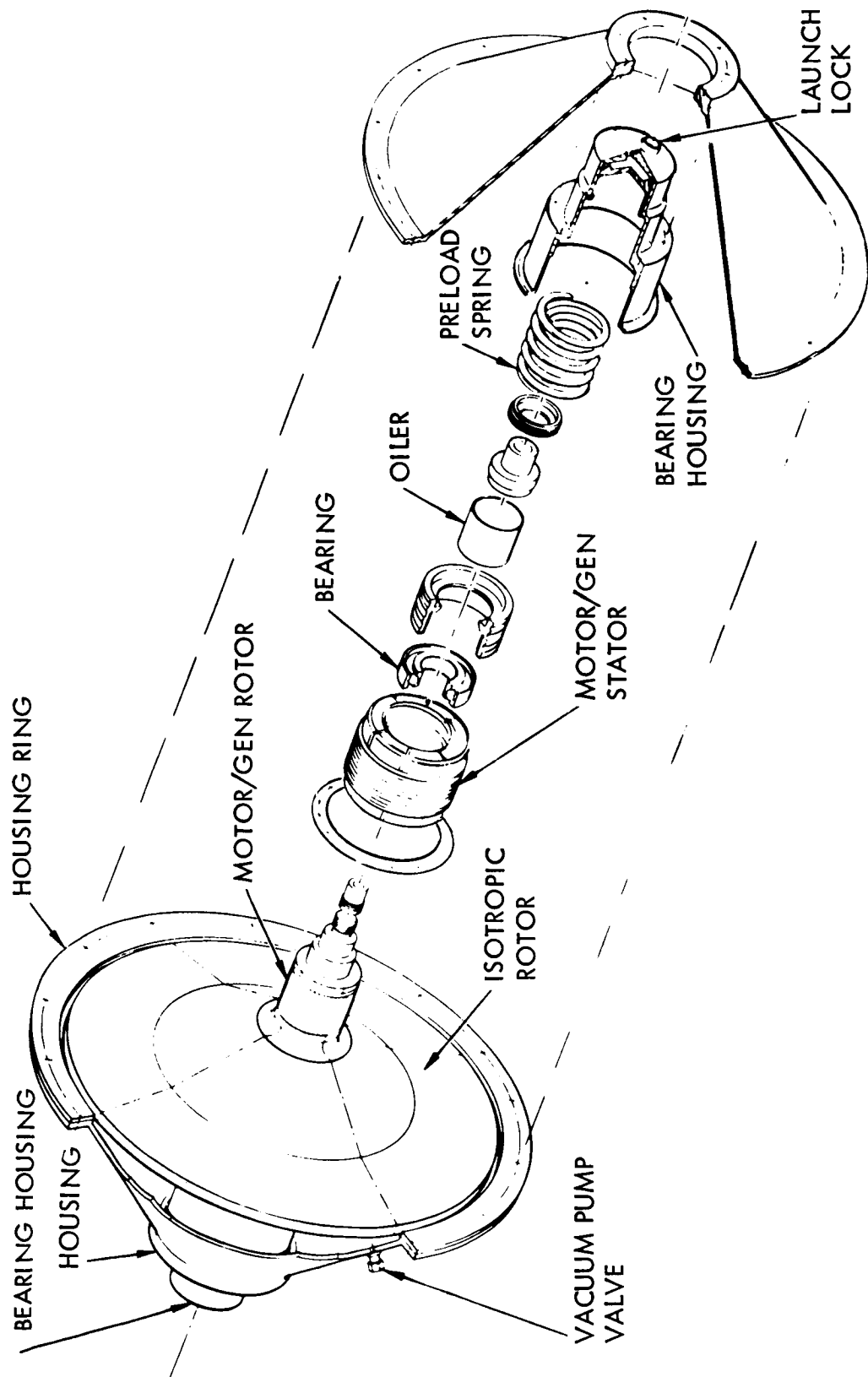


Figure 1-30. Current Technology Energy-Momentum Wheel

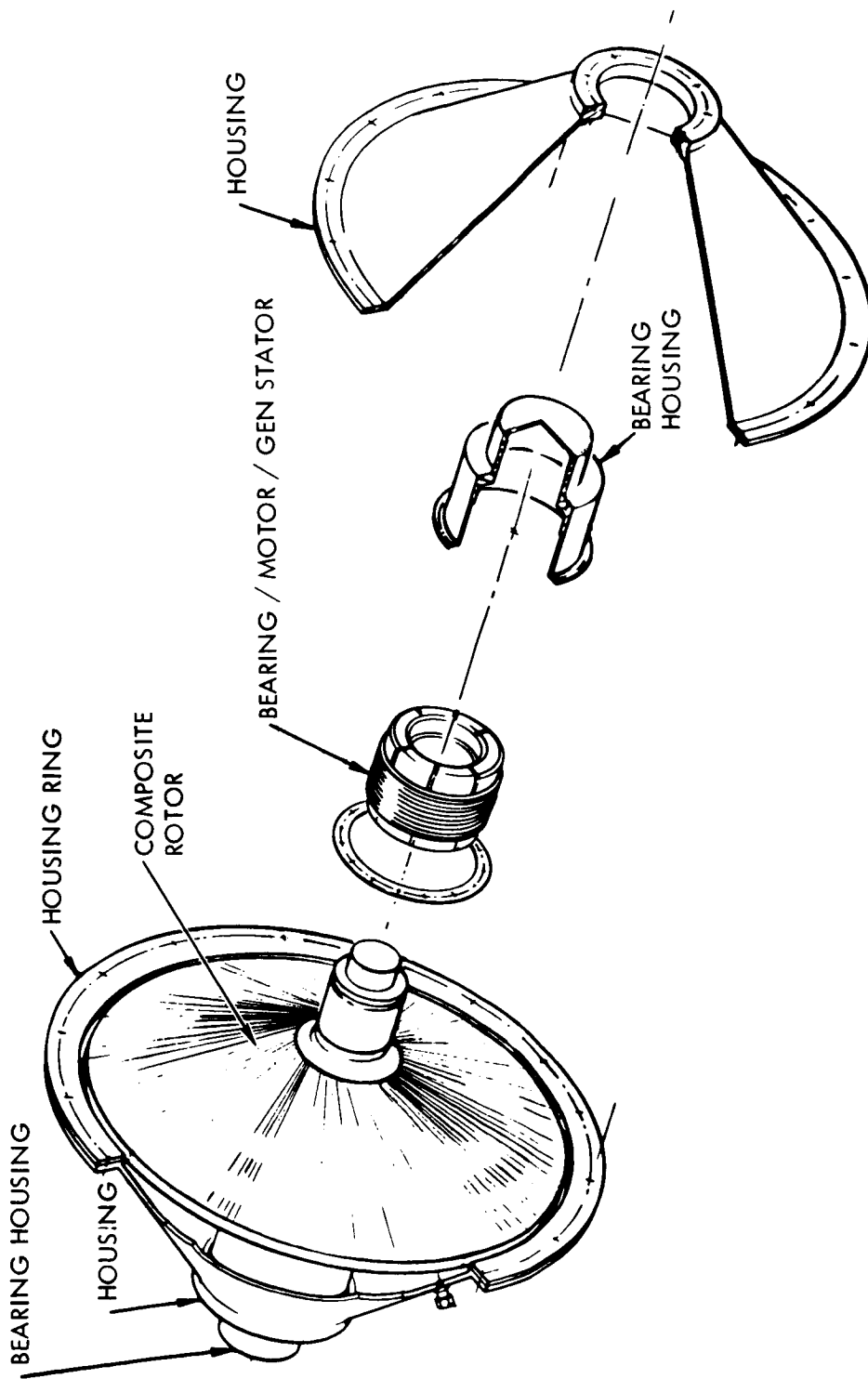


Figure 1-31. Advanced Technology Energy-Momentum Wheel

The energy density of the rotor must be modified by charge-discharge losses, the allowable speed-reduction, spin losses, and weight of ancillary equipment to reflect the usable energy density of a flywheel subsystem. In equation form:

$$E_{DS} = E_{DR} \eta_{CD} \eta_S f$$

where

E_{DS} = Subsystem energy density - W-hr/kg

E_{DR} = Rotor energy density at rated working stress - W-hr/kg

η_{CD} = Charge-discharge efficiency

η_S = Spin efficiency

f = Speed reduction factor

As shown in the performance comparison section, charge-discharge efficiency for the motor-generators and electronics selected for spacecraft flywheel applications approximate 70 percent.

Spin losses cannot be generalized but were found to vary from about 12 percent for small energy units with ball bearings to less than 4 percent for large units with magnetic suspension bearings. Since rotors of 66 W-hr/kg (30 W-hr/lb) travel at tip speeds of about 1150 m/sec (3800 ft/sec) regardless of material, losses of the above magnitude require having pressures on the order of 10^{-5} torr in the vicinity of the rotor.

Speed reduction factors were evaluated in terms of minimum weight and charge-discharge efficiency over the speed range. Studies indicate a 50-percent reduction ($f = 0.75$) the better compromise for all missions studied. Although some optimization can be expected for specific mission applications, the speed reduction value appears relatively constant for the gimbaled IPACS case where some residual momentum is required for control. In reaction wheel control IPACS applications lower speed reductions may prove effective in specific instances. It can be noted that significant increases in energy density can be achieved with higher speed reductions which specific missions can allow.

Data from the feasibility studies were used to develop figure 1-32 as representative of the range of expected energy densities for spacecraft energy storage subsystems. Values shown represent usable energy at the subsystem output, including losses and weight of ancillary equipment. The data ranges were developed utilizing a fixed 50-percent speed reduction and 46 to 70 W-hr/kg (21 to 32 W-hr/lb) rotors for the current and advanced technology designs respectively. Current technology flywheel systems employing isotropic rotors and conventional ball bearings are shown to compare well with advanced NiCd batteries. Advanced technology flywheel units employing composite rotors and noncontact magnetic suspension bearings are estimated to exceed advanced NiCd batteries and regenerative fuel cell technology which has been demonstrated but not qualified. Advanced regenerative fuel cell technology is expected to have higher development costs than other systems shown. If rotor energy densities were to reach the 132 to 143 W-hr/kg (60-65 W-hr/lb) values predicted by some researchers (reference 1-1), the dashed lines of figure 1-32 show the advanced flywheel system to be competitive with the predictions for advanced fuel cells. The high-energy density shown for the silver zinc battery is clearly for low charge-discharge cycles and does not represent a competitor for the majority of missions. Reference points which show the specific values for the conventional and IPACS designs are shown. It should be noted that whereas the range for battery densities is primarily affected by charge/discharge cycles, the flywheel density variations are more dependent upon material selections, speed reductions, and system technology. This relative insensitivity of IPACS to mission cycles is illustrated in figure 1-33 where a conventional NiCd subsystem is compared with current technology IPACS subsystems with two different rotor materials.

The rotor materials shown are titanium 6Al-4V and 300M tool steel. As can be noted, both materials result in comparable delivered energy density at the subsystem level and are relatively insensitive to orbit altitude (charge-discharge cycles) for one-year missions. The strength to density ratio values are similar for both materials at a low number of stress cycles. As stress cycles increase the titanium rotor has a clear advantage of a higher allowable working stress resulting in higher energy densities. Both systems can achieve higher energy densities than the NiCd subsystem.

The data shown for nickel cadmium (NiCd) batteries are based on a 56.7-kg (125-lb) energy storage subsystem having a 1000 W-hr capacity (100 percent depth of discharge). Battery life data used for this analysis are based on tests conducted by the Quality Evaluation Laboratory of the Naval Ammunition Depot, Crane, Ind. These data take into account long periods between cycling which occurs at geosynchronous altitude. The increase in usable energy density at the higher altitudes is due to higher usable depths of discharge permitted by a reduction in charge-discharge cycles required. For example at 200 nm there are 5,960 eclipse periods in a year and at geosynchronous there are 90.

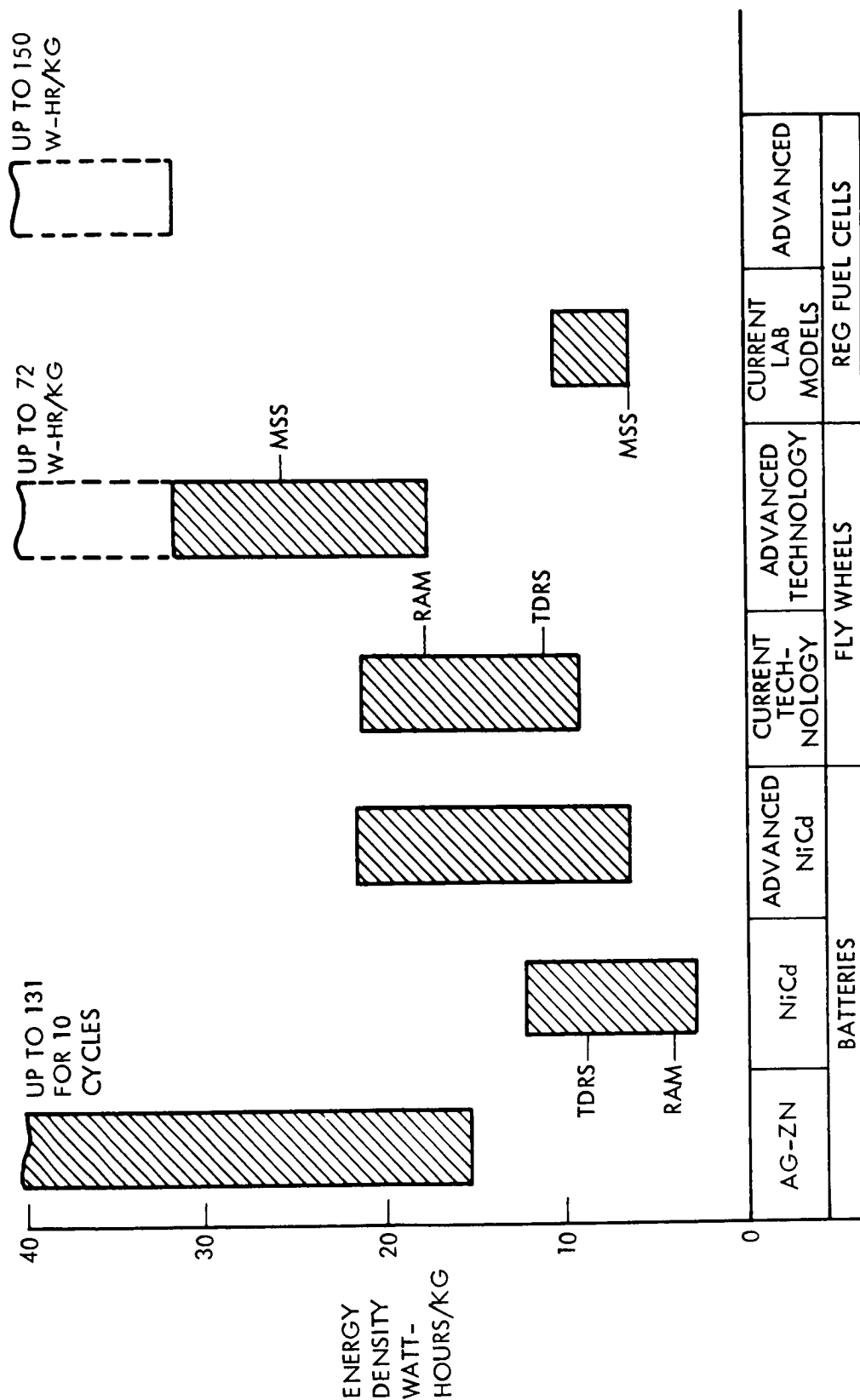


Figure 1-32. Energy Storage Subsystem Capability and Potential

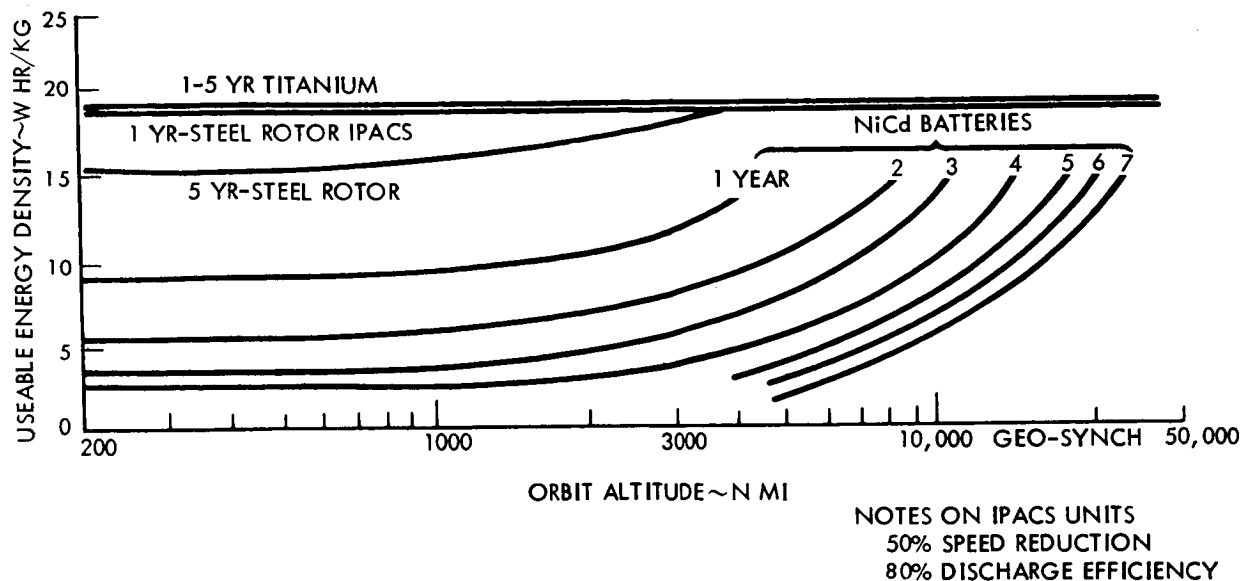


Figure 1-33. Energy Density Variation With Orbit Altitude and Mission Duration

A lifetime advantage for flywheel systems is indicated by calculations which show relatively little impact in the number of charge-discharge cycles below 10^5 . This advantage is predicated upon the validity of life calculations for ball bearings used at high speed and with low lubrication. The advantage for the advanced technology magnetic noncontact bearing is considered apparent.

In general, the advanced technology IPACS units are expected to deliver at least twice the energy density of current units with projections to increases of three to four not improbable.

The above data show the flywheel assemblies competitive with both batteries and fuel cells as an energy storage element for the given designs. The design ground rule for this study was that integrated system designs satisfy both electrical power and attitude control functions simultaneously with the same equipment. In the calculation of energy density, the additional capability of the flywheels and ancillary equipment to provide the attitude control functions must be considered. If the equivalent weight of IPACS components utilized for control were removed from the IPACS weight, the energy storage capability comparison would be even more favorable toward IPACS.

The next section presents the system wheel array options and selections for control use of the energy-momentum assembly.

System Trades

System-level trade studies were conducted to evaluate IPACS energy-momentum wheel array options and alternative electrical mechanizations. Preferred gimbaleed or nongimbaleed array selections were made for each mission. The preferred electrical mechanizations among the solar array, conditioning equipment, and the energy-momentum wheel were established. The efficiency benefits of higher voltage array systems have been noted.

Wheel array evaluations.— The wheel arrays studied included nongimbaleed and gimbaleed type wheels and hybrid arrays which combine both types.

Nongimbaleed arrays: With flywheels sized to the energy requirement, excess angular momentum was characteristic of the nongimbaleed, or reaction control applications. These systems are commonly designed to operate near zero angular momentum (H) in three-axis applications and about some low nominal H value for momentum bias systems. In both cases, control momentum is stored in wheel speed to some maximum value and then dumped by means of external counter torques. Studies showed that control momentum requirements represented a small percentage of available momentum at maximum energy. For example, each wheel of the TDRS design, sized to the 71 Watt-hour energy requirement, contained 10 times the H bias requirement of the satellite. The excess H of this magnitude dictated that wheels be operated in counter rotating pairs. For the TDRS case, the momentum bias requirements were easily satisfied by a 10 percent underspeed in one wheel (Figure 1-34).

The electrical power required for control torques at high rotational speeds is of significance in reaction wheel applications. The preferred control for energy-momentum flywheels used in counter rotating pairs results in transferring energy as well as momentum among the wheels. This requires that one unit act as a generator driving the other as a motor. Figure 1-35 presents the change in state. The power requirements for control torques, then,

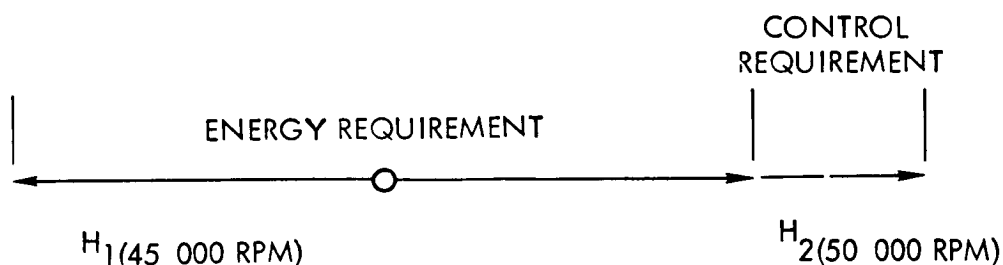


Figure 1-34. TDRS Energy-Momentum Sizing

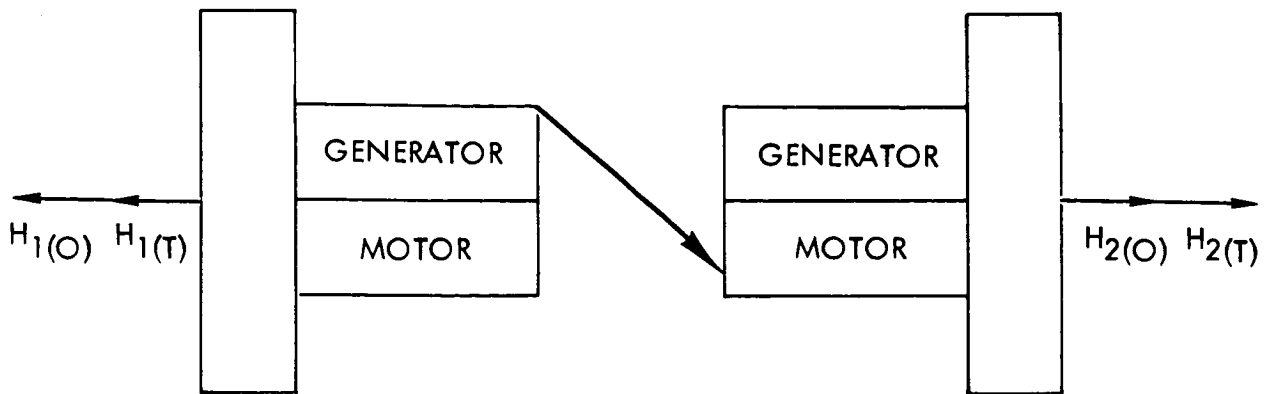


Figure 1-35. Energy-Momentum Change

amount to the discharge-charge losses of the generator-motor set. As will be shown in subsequent designs, typical satellite wheels rated at 120 watts maximum with an 85 percent charge (or discharge) efficiency can deliver a maximum torque of 0.0438 Newton-meters (6.25 in-oz) at 29 watts. Efficiency in this instance is comparable to current reaction wheels. A specific ATS F and G assembly, for example, delivers 0.07 newton-meter (10 in-oz) at 27 watts. A similar design used on Nimbus can deliver 0.028 newton-meter (4 in-oz) at 18 watts. The IPACS wheels then appear competitive as a control device with the added capability of power storage. Simulation studies show that the major part of momentum wheel operation is at less than a quarter of maximum torque capability in any case and that power usage is minimal.

The use of IPACS energy-momentum wheels in various charge-discharge states, as well as in a reaction control mode only, is possible and appears effective for some missions. A notable example is the geosynchronous mission where occultation occurs for less than one quarter of each year. During these periods, the duration of occultation varies from first shadow to a maximum of 1.2 hours. In missions such as this, IPACS wheels can be employed as low-speed reaction wheels during the major share of the year, increasing speed as energy storage is required.

The following nongimbaled arrays were studied for application to the reference missions.

Two pairs of opposing nongimbaled wheels - The simplest array considered consists of two pairs of opposing wheels. Each wheel pair is nominally operated with the wheels counter-rotating. This array would be used for the momentum bias type attitude control approach as described for the competitive control concept for TDRS in Appendix 1-C. In general, a momentum bias is used along the body axis oriented normal to the orbit plane. This axis will be termed the pitch axis. This momentum bias provides the vehicle with a gyroscopic stiffness in the two axes normal to the bias. Nutation damping is provided in one of the axes (yaw) normal to the bias by

the application of active control torques. Direct active control is provided about the bias or pitch axis. Thus the vehicle is continuously controlled about one axis and restrained through gyroscopic stiffness in the other two axes.

The IPACS mechanization of this concept would utilize the wheels in an orthogonal array. Two wheels would be installed with their spin axes oriented along the vehicle pitch axis. Energy would be stored with the wheels counter-rotating, and the pitch bias would be obtained by operating one of the wheels faster than the other. Active pitch control would be obtained essentially by allowing the bias to vary in response to pitch attitude commands. The remaining pair of wheels would be installed with their spin axes collinear with the vehicle yaw axis. These wheels would nominally store energy through counter-rotation with a net zero angular momentum. Oscillatory torques would be provided from these wheels for nutation damping.

In the case of failure of one wheel, the failed wheel would be shut down and the opposing wheel would be relegated to a control function only. Fifty percent energy storage capability is retained through normal operation of the wheels in the other axis. Depending upon the axis in which a wheel fails, the remaining wheel in that axis will operate with either a nominal speed of zero (yaw wheel failure) or that speed required to provide the pitch bias momentum (pitch wheel failure).

Skewed arrays of nongimbaled wheels - Various skewed arrays of nongimbaled units were considered. A typical array can be visualized with the aid of the sketch on Figure 1-36 which illustrates a five-skew array. Note that the spin axes are constrained to lie upon the faces of a five-sided polygon. The faces of the polygon may be either inclined to the base plane or normal to it. The orientation of an individual spin vector within the plane is defined by an angle γ as indicated in the sketch and measured from a line parallel to the base of the figure. In an array with five units, two wheels would be oriented with a positive γ , two with a negative γ , and the fifth wheel with $\gamma = 0$. On an array with an even number of units, none would require the zero γ angle mount.

The array concept can be generalized to range from four units on a four-sided figure up through six or more units on the corresponding geometric figures.

Since the units are nongimbaled, the only degrees of freedom available for energy storage and attitude control are the individual wheel speeds. To perform an energy storage function, the individual wheels are torqued such that the resultant angular momentum is zero. Attitude control commands are superimposed upon the energy commands resulting in a perturbation of the zero momentum state to obtain the required momentum exchange control function. Arrays of this type with an adequate number of units can provide simultaneous energy storage and independent three axis attitude control.

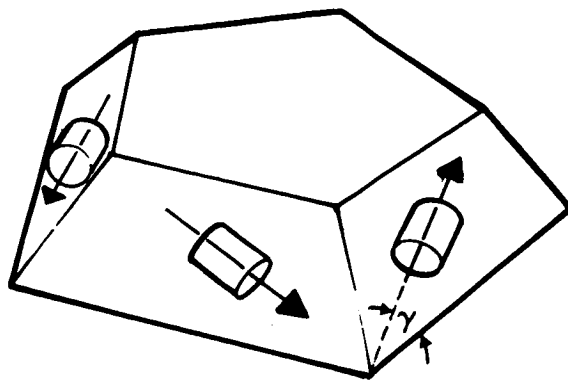


Figure 1-36. Skewed Array of Five Nongimbaled Units

Three pairs of opposing nongimbaled wheels - This array concept is an extension of the type discussed previously and termed as two pairs of opposing nongimbaled wheels. The array is orthogonal with a pair of wheels oriented with their spin vectors along each vehicle axis. Each pair of wheels nominally operates in a counter-rotating manner, with net momentum equal to the accumulated secular disturbance torque. The array provides independent, three-axis attitude control together with energy storage in each pair of wheels.

Under failure mode conditions, the failed wheel would be stopped and the remaining wheel in that axis operated as a momentum wheel. The other four units would perform in the normal manner. Two-thirds of the nominal energy storage capacity would be retained.

Gimbaled control applications: Gimbaled control applications for the IPACS energy momentum wheel assembly appeared similar to those of conventional single and double-gimbaled control moment gyros.

Sizing and control aspects can differ somewhat. In the IPACS, momentum storage requirements are scaled to the discharge state of the wheels. The result is that the wheels have an excess of H from the charged state. For the 50-percent speed reduction of this study, the H can be twice that required. The implications of varying H to control appear as loop gain variations as a function of orbit position which must be compensated for or shown to be acceptable. As will subsequently be shown in Volume II, Module 3, digital simulations of a double-gimbaled control energy-momentum gyro (CEMG) as sized for the RAM mission showed acceptable performance over the 50-percent speed reduction and in the presence of maximum charge and discharge rates.

Another factor of the IPACS is providing for the gimbal torque power required to compensate for induced charge-discharge disturbances. The wheel speed changes associated with power transfer result in sensed disturbance torques on the vehicle. The torque and vehicle rate feedback loops of the vehicle respond by commanding stabilizing torques from the gimbal torquers.

These torques can be superimposed upon vehicle disturbances in the worst case sense to change nominal torque scaling. The torque required of the gimbals is a complex function of the initial momentum state of the vehicle and not easily characterized. RAM simulations for expected adverse initial states showed discharge-charge torques required to be less than 40 percent of total available. It can be postulated that a sophisticated study of a particular vehicle and mission could result in optimizations where the torques required to counter external disturbances would approximate those required to maintain stabilization in the presence of charge and discharge cycles. The power required for vehicle control may approach a minimum.

Skewed single gimbaled arrays- Various arrays of single gimbaled units were studied. Typical arrays of this type are represented by the sketch on figure 1-37. The spin vectors are constrained to remain within the face planes of the polygon; however with gimbal freedom, the spin vector can be reoriented within the mount plane. The additional degrees of freedom (gimbal angles in addition to wheel speed), in general, make possible the use of a smaller number of units or provide improved failure mode performance compared with arrays of nongimbaled units.

These arrays would be operated around a nominal null momentum state for energy storage. In charging or discharging the array, the gimbal angles would be varied as required to maintain the instantaneous momentum state. It may or may not be desirable to drive the wheels with identical speed commands. The system is less complex with all wheel speeds maintained the same, but potential degrees of freedom are sacrificed.

V-pair arrays- Pairs of single-gimbaled units that are gimbaled simultaneously have been developed as control devices with the intent of eliminating the cross coupling inherent within the operation of a single gimbaled control moment gyro. The potential of these arrays for IPACS was briefly considered. They were in general, found to be more complex and heavier than the skewed arrays of single gimbal units considered.

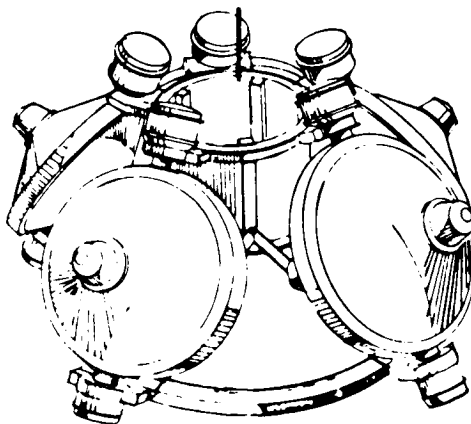


Figure 1-37. Sketch of Skewed Array of Five Single Gimbaled Units

Double gimbaledd arrays- Orthogonal and planar arrays of double gimbaledd units were considered. For the mission applications under study, the planar array was considered more suitable due to the planar nature of the momentum requirements (Table 1-II). The planar array is the type described within the competitive control section for the modular space station, Appendix 1-A and Section 3 of Volume II.

Counter-rotating double gimbaledd arrays- These arrays consist of units wherein the inner gimbal assembly includes counter-rotating wheels. In these units energy can be stored within a single device with zero net momentum or some resultant momentum required to satisfy the attitude control function. Contrasted with the arrays described above, this is the only one wherein energy can be stored within a single device without creating an attitude disturbance. The device complexity is also greatest in this case.

In general these arrays were rejected in favor of the non-counter-rotating double gimbaledd arrays. The latter were found to have adequate degrees of freedom to perform the energy-storage and attitude-control functions simultaneously. Thus for the missions studied, the standard double-gimbaledd arrays were chosen as being the least complex. It should be noted that the counter-rotating double gimbaledd device may be more applicable to missions other than those studied in this contract.

Hybrid arrays- A hybrid array, for this study, is defined as one including dissimilar energy-momentum devices. An example hybrid array contains two single-gimbaledd units and one nongimbaledd unit. A significant disadvantage of this array type is that it potentially requires development of two different devices for a single vehicle application. All the other arrays were formulated to use identical devices. The potential advantage of the hybrid array is that it enables the elimination of one device when considered for applications such as TDRS and EOS, which utilize the momentum bias control concept; three wheels can be used in place of the four required in an array of opposing pairs of nongimbaledd units.

The hybrid concept using two single gimbaledd units and one nongimbaledd unit is illustrated in figure 1-38. The system would be used in a momentum bias application in the following manner. The x axis wheel is nongimbaledd and used as a control wheel only. It operates at a nominal speed to provide the required bias momentum. The other two wheels are gimbaledd, but nominally operate as opposed nongimbaledd units for energy storage and nutation damping. The gimbal feature of these units is only used under failure mode conditions. If the x axis wheel fails, then the gimbal capability is used to absorb the x axis control function within the y axis wheels. If a y axis wheel fails, then the remaining y axis wheel is gimbaledd to be nominally collinear with the x axis wheel and these wheels are then run opposed for energy storage, and the gimbal is torqued to provide y axis nutation damping.

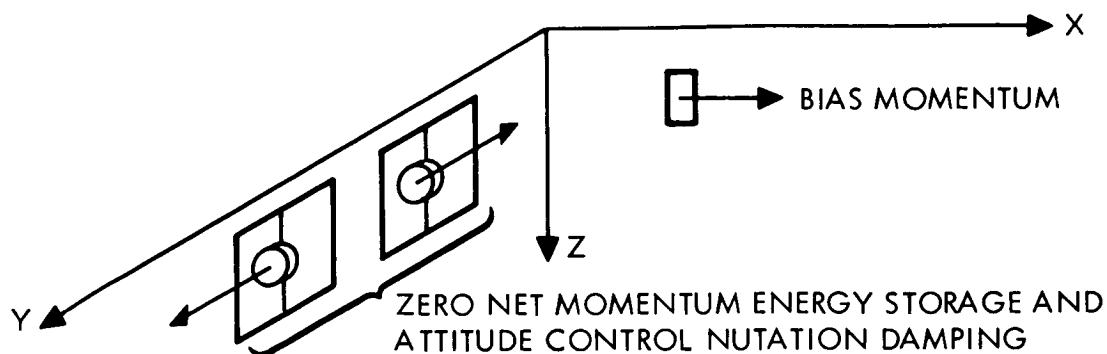


Figure 1-38. Sketch of Hybrid Array

Array selection methodology.— A limited study was performed to evaluate the array candidates defined above for the reference missions to expose the potential IPACS advantages and disadvantages for each type array. It was not considered necessary to study all array types for all missions. In general, candidate arrays were identified for each mission based primarily upon prior experience which indicated array candidates and their ability to satisfy the functional requirements and minimum complexity considerations. The arrays chosen for evaluation on each mission are identified in matrix form in figure 1-39.

Array selections.— The IPACS array selections of the feasibility study were determined by a first and second order screening process. The first order screening was performed by studies of weight, complexity, and failure mode performance. In the second screen, sizing, weight, volume, and operational factors were evaluated to determine the final selections. The candidates rejected in the first screen are identified by the shaded blocks in figure 1-40.

For the TDRS and EOS missions, the 4-skew array was rejected because of its relatively poor failure mode performance as compared with the other two candidates. In the case of the MJS mission, the 4-skew array will meet the failure mode criteria; it was selected over the other candidates because it is the least complex. For the 30-day Shuttle mission, the array of three double-gimbaled units was selected over a skewed array of five nongimbaled wheels and a skewed array of five single-gimbaled wheels. The nongimbaled array was rejected because of its relatively poor momentum delivery capability and the high control torque requirements which favor the use of gimbaled units.

MISSION VEHICLE	MOMENTUM WHEELS				CMG ARRAYS			HYBRID	V PAIRS
	2 OPPOS- ING PAIRS	4 SKEW	5 SKEW	3 OPPOS- ING PAIRS	4 SKEW SG	5 SKEW SG	3 DG	2 SG + MW	3 V PAIRS
TDRS	X	X						X	
EOS	X	X						X	
MJS		X	X	X					X
SHUTTLE			X			X	X		
MSS						X	X		
RAM					X		X		X

X ARRAYS STUDIED

Figure 1-39. IPACS Systems Array Options

MISSION VEHICLE	MOMENTUM WHEELS				CMG ARRAYS			HYBRID	V PAIRS
	2 OPPOS- ING PAIRS	4 SKEW	5 SKEW	3 OPPOS- ING PAIRS	4 SKEW SG	5 SKEW SG	3 DG	2 SG + MW	3 V PAIRS
TDRS	X	X						X	
EOS	X	X						X	
MJS		X	X	X					X
SHUTTLE			X			X	X		
MSS						X	X		
RAM					X		X		X

X ARRAYS STUDIED



FIRST SCREEN REJECTIONS

Figure 1-40. First Screen Rejections of Array Options

In order to make possible a comparison between the 5-skew single gimbal array and the 3-double gimbal array, one was selected for extended shuttle and the other for modular space station. The final mission in the table is RAM. The array of 3 V pairs was rejected on the basis of both weight and complexity factors.

The remaining array candidates were then subjected to a second-level screen considering detailed sizing, weight, volume, and operational factors. The study results are presented in figure 1-41. The rejected candidates are shown boxed.

The TDRS selection was based primarily on weight. Weight is critical on this mission, and the higher volume of the selected concept is acceptable. The balance comment in the figure relates to a comparison of the induced vibration potential between the two arrays. The rotors in both cases turn at the same maximum speed; however, a rotor in the hybrid array is nearly twice as heavy as a rotor in the opposed wheel array (see Table 1-XXI). Thus, on an individual unit basis, the induced vibration would be expected to be more severe for the hybrid array. On a total system basis (four units in the opposed array, compared with three in the hybrid) the hybrid array still loses.

MISSION	WHEEL ARRAYS	SYSTEM WEIGHT KG (LB)	SYSTEM VOLUME M ³ (FT ³)	FAILURE PERFORMANCE	COMMENTS
TDRS*	TWO OPPOSING MOMENTUM WHEEL PAIRS	37.8 (83.2)	0.082 (2.91)	NO DEGRADATION	<ul style="list-style-type: none"> • SINGLE DEVELOPMENT • BALANCE PROBLEM LESS SEVERE
	TWO SINGLE GIMBAL + MOMENTUM WHEEL	42.4 (93.4)	0.062 (2.18)	SOME ATTITUDE CONTROL DEGRADATION	<ul style="list-style-type: none"> • DUAL DEVELOPMENT • LESS TOTAL PARTS • GIMBAL ONLY USED IN FAILURE MODE
RAM	THREE DOUBLE GIMBALED	233 (514)	0.085 (3.00)	ENERGY MODE WITH LIMITED ATTITUDE CONTROL	<ul style="list-style-type: none"> • ADEQUATE LIFE • HIGHER BEARING POWER
	FOUR SKEWED SINGLE GIMBAL	242 (534)	0.44 (15.51)	ENERGY MODE ONLY	<ul style="list-style-type: none"> • LOWER SPEED • BALANCE PROBLEM LESS SEVERE
MSS	FIVE SKEWED SINGLE GIMBAL	903 (1990)	0.53 (18.69)	FULL CAPABILITY	<ul style="list-style-type: none"> • MINIMUM NUMBER OF WHEELS • LEAST COMPLEX
30-DAY SHUTTLE	THREE DOUBLE GIMBAL	688 (1516)	0.27 (9.49)	ENERGY MODE WITH LIMITED ATTITUDE CONTROL	
MJS	FOUR SKEWED MOMENTUM WHEEL	17.3 (38)	0.017 (.62)	NO ENERGY STORAGE PARTIAL ATTITUDE CONTROL	

*SELECTION APPLICABLE TO EOS

Figure 1-41. IPACS Array Selections

The RAM selection was made primarily on a volume basis; the weight difference in this case is not considered significant. The volume difference is in part due to the larger rotor diameter associated with the single gimbal units (see Table 1-XXII). The larger diameter and lower speed are characteristics of optimized rotors designed to meet a higher momentum to energy ratio. The failure mode performance of the double-gimbaled array is considered to be slightly better than that for the single-gimbaled array because of the operational flexibility provided by the additional gimbal freedom.

TABLE 1-XXI.- TDRS DESIGN CHARACTERISTICS COMPARISON
(PER FLYWHEEL UNIT)

Design Parameter	Array of two opposing pairs	Hybrid array Two single gimbaled and one non-gimbaled
Rotor weight kg (lb)	3.9 (8.6)	6.9 (15.2)
Rotor diam m (in.)	0.34 (13.4)	0.34 (13.4)
Max speed rad/sec (RPM)	5240 (50 000)	5240 (50 000)
Low speed angular momentum N-m-sec (ft-lb-sec)	16.9 (12.5)	16.9 (12.5)
Deliverable/ energy watt hrs	71.3	142
Bearing losses - watts	3.7	3.7

TABLE 1-XXII.- RAM DESIGN CHARACTERISTICS COMPARISON
(PER INNER GIMBAL UNIT)

	3 DG array		4 skew SG array	
Design parameter				
Rotor wt kg (lb)	45.2	(99.5)	30.1	(66.3)
Rotor diam m (in.)	0.378	(14.9)	0.494	(23.4)
Max speed rad/sec (RPM)	4710	(45 000)	3040	(29 000)
Low speed angular momentum N-m-sec (ft-lb-sec)	1115	(822)	1168	(860)
Deliverable energy watt-hr	1095		730	
Bearing losses - watts	65		37	

Electrical mechanizations.- The preferred IPACS electrical mechanization was determined through two trade studies. The first considered three different concepts of energy storage and transfer. The second trade study evaluated the impact of source voltage on system efficiencies as measured by solar array area requirements.

Series-parallel-hybrid tradeoff: Three basic generic energy storage and recovery concepts were analyzed for the IPACS electrical power subsystem. (See figure 1-42)

The series scheme routes all power through the motor-rotor-generator to the loads. The parallel mechanization transfers power directly from the power source to the loads. The difference between the parallel and hybrid scheme is that the latter is a source of either ac or dc power. In this case all the ac power passes through the motor-rotor-generator. A mix of ac and dc power for the series and parallel mechanization will require addition of an inverter or a converter to the IPACS.

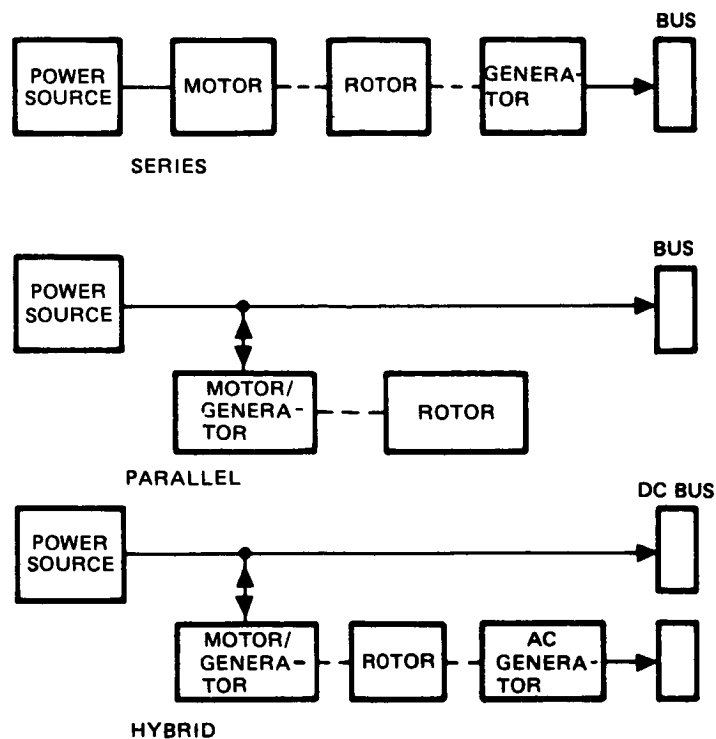


Figure 1-42. Mechanization Alternatives

Table 1-XXIII summarizes the efficiency of the various IPACS mechanizations considered. Primary variables considered were source voltage, percent AC or DC power delivered to the loads, and orbit altitude. Load power was assumed constant for the analysis. The index of efficiency used for comparison is the solar array area required for each energy storage concept. Component efficiencies were fixed for the analysis at approximately maximum values, as follows:

Component efficiencies

Motor/generator	= .95
Alternator	= .95
Inverter	= .93
Cycloconverter	= .90
Motor/generator electronics	= .95

TABLE 1-XXIII.- SERIES/PARALLEL/HYBRID ELECTRICAL
MECHANIZATION EFFICIENCIES

Energy Storage Concept	Load		AC Source	Relative Solar Array Area	
				Geosynch Orbit	500 km (270 NM) Orbit)
	% ac	% dc			
Series	100	0	Alt	1.28	1.20
	0	100	-	1.21	1.13
Parallel	100	0	Alt	1.08	1.08
	0	100	-	1.0	1.0
	0	100	-	-	1.04(1)
	0	100	-	-	1.16(2)
Hybrid					
Parallel	10	90	Inv	-	1.01
Parallel	90	10	Inv	-	1.07
Parallel	10	90	Alt	-	1.02
Parallel	90	10	Alt	-	1.17
Series	10	90	Inv	-	1.27
Notes: Solar array voltage 100 V except for: (1) = 50 V (2) = 25 V					

Solar array area required has been normalized to the concept requiring the smallest array. This is the parallel mechanization delivering 100 percent DC power to the loads. Relative solar array areas are shown for two orbital altitudes, geosynchronous and 500 km (270 nm). The series concept drives source power up by imposing a loss on all electrical energy supplied to the loads. This loss is relatively greater at geosynchronous altitude due to the larger time spent in sunlight than at the 500 km altitude. The series scheme has higher losses than the parallel at all values of eclipse-to-daylight ratios, and it was therefore rejected as an IPACS candidate.

The ac loads always require larger solar arrays than the dc loads because of inverter losses. The data shown are based on an inverter efficiency of 0.93. Using an alternator for an IPACS generator will not improve the ac efficiency trade because a cycloconverter ($\eta = 0.90$) will be required to provide a fixed frequency at the loads.

Source voltage tradeoff- Source voltage has major impact on distribution losses as well as efficiency of the brushless dc motor/generator electronics selected for IPACS designs. These electronics consist of two dc power amplifiers and the necessary low level conversion circuitry. The power amplifiers perform the function of linear amplification and apply power to the motor windings. Figure 1-43 shows the equation for electronics efficiency which is

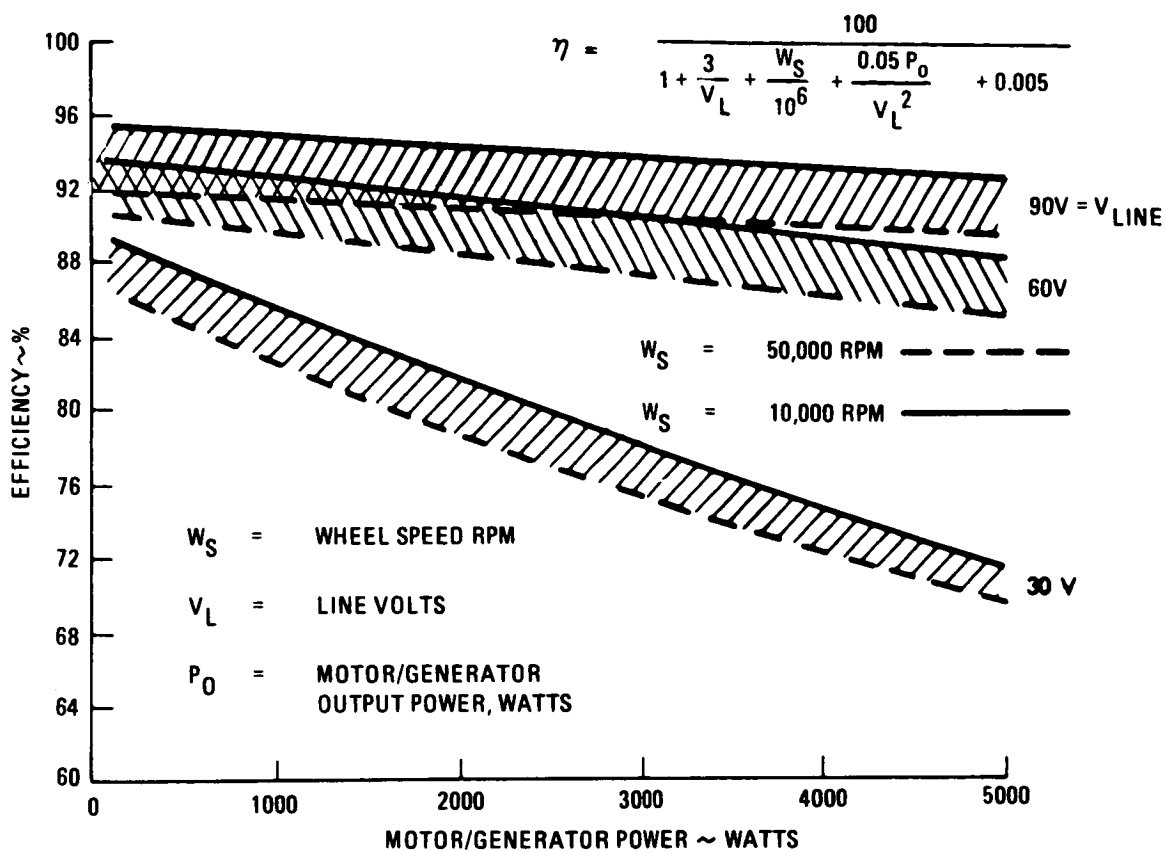


Figure 1-43. Brushless DC Motor/Generator Electronics Efficiency

presented graphically for three different values of line voltage. The term $3/V_L$ represents the 3 volt switching transistor loss. The P_o/V_L^2 term is the I^2R loss and the .005 constant is a driver loss.

At low powers the transistor loss is predominant; however, at high powers and low voltages the I^2R loss becomes prevailing. The data shown by figure 1-43 indicates that line voltages of 60 and larger result in decreasing electronics efficiency loss. The effect of solar array voltage on relative solar array area is considered next.

In order to determine the overall effect of source voltage on charge-discharge efficiency and solar array area, the mechanizations shown by figure 1-44 were analyzed. All mechanizations are based on the energy storage function being in parallel with distribution of load power. Two solar array sources were considered. One assumes the whole array to be configured for a minimum 30-volt output. The other considers an array switching of cell strings to permit delivery of power at 90 volts to the motor/generator electronics and 30-volt power to the loads. All of the candidate mission loads are nominally 28 volts except the modular space station. To design the complete array for 90-volt output requires a dc-dc converter in series with the array and the loads. At a converter efficiency of approximately 90 percent, a larger array is again required. Another approach is to dedicate a fixed part of the array to 90 volt output. However, this type of mechanization does not lend itself to varying load requirements.

The solar array voltage shown for the RAM is the minimum given for the competitive baseline electrical power subsystem. The subsystem buck-regulator is shown in the schematic but is not included in the charge-discharge efficiency. By the same token there are no allowances for bus-regulation losses in the efficiencies for the other mechanizations. It is assumed the same bus regulation losses would result for all schemes. Hybrid array voltages would be obtained by on-array switching of solar cell strings to change string output from 30 volts to 90 volts and vice versa. Logic for string switching would be incorporated into the IPACS computer. The efficiency column shown by the chart lists the charge efficiency (η_{CH}) first, then discharge efficiency (η_{DIS}) and finally the product ($\eta_{CH} - DIS$). In the instance of the TDRS (case II and III) the increase of charge efficiency made possible by higher solar array voltages is nullified by losses in converting 90 volt discharge voltage to the 28 volts required by the loads. The ratio of power to the load (P_L) to required solar array power (P_{SA}) is the same for the TDRS cases considered. However, Case III proved to be the most efficient for the free-flying RAM. This is partly due to the decrease in brushless DC motor electronics efficiency by increasing electronics rating from 250 watts (TDRS) to 2500 watts for the RAM. Case III incorporates a 90 volt alternator ($\eta = .917$) with a transformer rectifier ($\eta = .94$) to interface with the 28 volt loads. The increased power required by RAM results in an improved alternator efficiency over TDRS. Despite the increased efficiency shown for larger array voltages for RAM, standard 28 volt arrays (52 volts for RAM) have been used in the IPACS systems studies for direct comparison with baseline systems.

In each case the candidate mission baseline solar array and load voltages are retained as originally proposed in the baseline documents. The rationale for this approach is summarized below.

MISSION	CASE	IPACS MECHANIZATION	HCH NOIS HCH-DIS	PL/PSA	RELATIVE SOLAR AR- RAY AREA
TORS	I		0.840 0.826 0.694	0.930	1.002
	II		0.875 0.795 0.695	0.930	1.002
	III		0.875 0.794 0.695	0.930	1.002
FREE FLYER RAM	I		0.838 0.790 0.661	0.525	1.05 (2)
	II		0.860 0.790 0.680	0.531	1.04
	III		0.860 0.862 0.740	0.552	1.00

(2) BASELINE BUCK REG NOT INCLUDED
(1) CANDIDATE CONCEPT MIN ARRAY VOLTAGE

Figure 1-44. Evaluation of Solar Array Voltage Effects

- (1) Maintaining baseline voltage causes minimum impact on the baseline electrical power subsystems, thus making more accurate comparison possible.
- (2) The higher voltage level would also provide some advantage to the competitive subsystems which could not be estimated within the scope of the present effort. For an equitable comparison therefore the IPACS was designed to operate at the nominal voltage.

It can be noted that the IPACS penalty for lower source voltage is probably more severe than that of the competitive subsystem since both systems benefit from lower distribution losses at the higher source voltage.

IPACS Concepts

This section defines the IPACS concept selected for each reference mission, including sizing requirements, concept description and functional block diagram, design characteristics, and operating concept.

RAM system description.- The selected IPACS concept for RAM is described below. The recommended concept employs a present technology energy storage unit.

Sizing requirements: The IPACS system for RAM is required to store 2500 watt-hours and to deliver a total power output of 4820 watts. Under failure conditions, momentum exchange attitude control is not required, and the control function may be assumed by the reaction control system. The energy storage function, however, must be maintained under failure conditions. The system must be capable of storing 7/8 of the nominal energy storage requirement and delivering full power with one rotor unit inoperable. This requirement establishes the energy storage capacity of a single wheel at 1095 w-hr with a power rating of 2410 watts. The attitude control sizing requirements include an angular momentum storage capacity of 2034 N-m-sec (1500 ft-lb-sec) with a control torque requirement of 9.5 N-m (7 ft-lbs) per torquer.

Design concept: The IPACS concept for RAM is shown in functional block diagram form on figure 1-45. Energy storage and attitude control are provided by a planar array of three double-gimbaled units. These units replace the three double gimbaled CMG's and the battery subsystem in the competitive attitude control design. The remainder of the baseline control concept is retained, including the sensors, RCS, magnetic torquers for desaturation, and reaction wheels for precision control. Three reaction wheels with an angular momentum of 4.07 N-m-sec (3 ft-lb-sec) each and a torque capability of 1.36 N-m (1 ft-lb) per wheel are used in an orthogonal array.

Buck regulators are used in both the IPACS concept and the competitive power subsystem. The IPACS units operate with a solar array voltage ranging from a maximum of 75 to a minimum of 52 volts. Buck regulators drop the voltage to 28 volts for distribution on the busses. Power switching functions are performed within the processor and power control unit. Computational functions performed within this unit are supplemented by those performed within the vehicle central processor.

Design characteristics: The more significant design characteristics for the motor/generator/wheel units are presented in Table 1-XXIV.

The weight breakdown for a single unit is shown in Table 1-XVV.

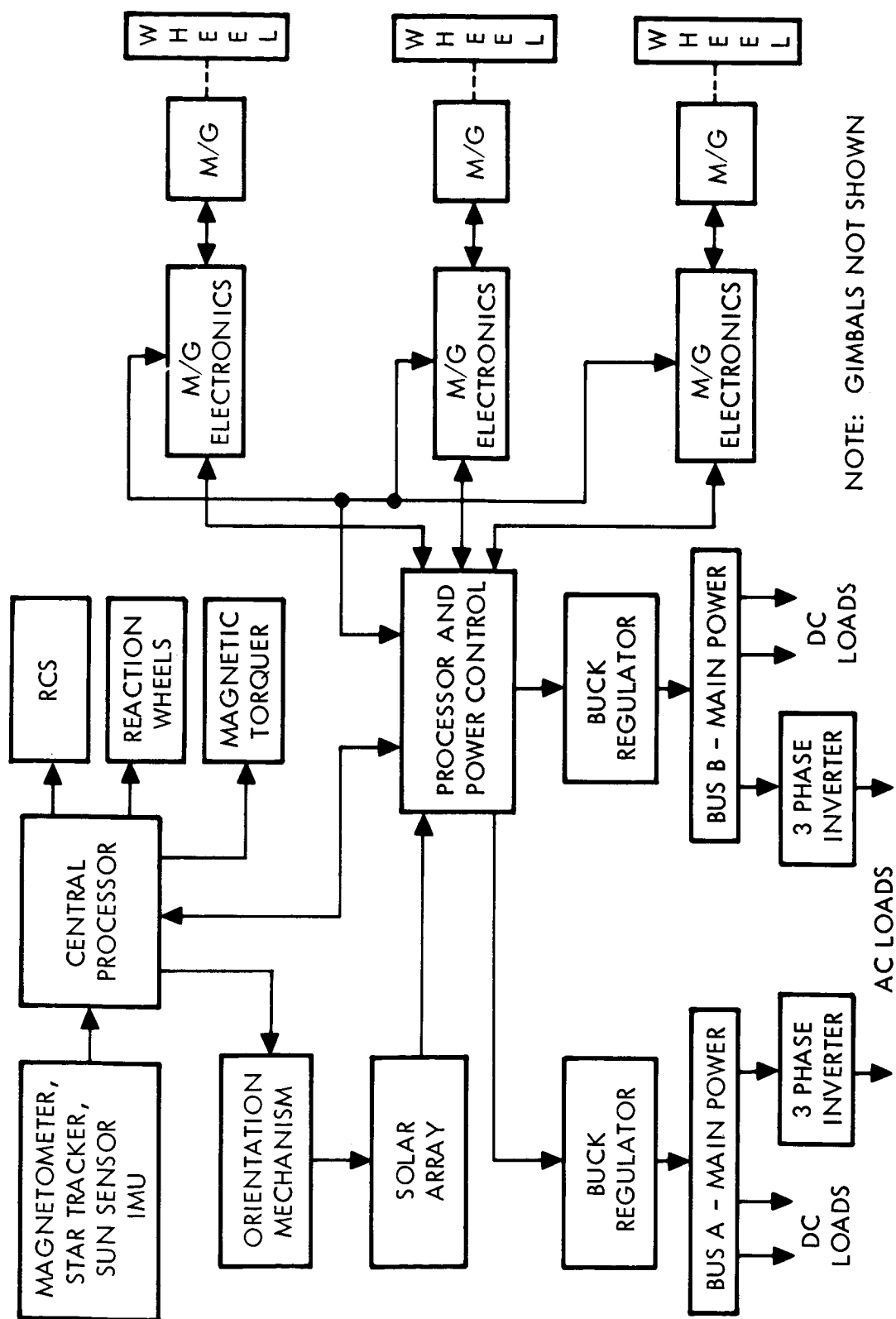


Figure 1-45. RAM Functional Block Diagram

TABLE 1-XXIV.- RAM IPACS DESIGN CHARACTERISTICS

Rotor

Material: high strength steel
Geometry: constant stress profile
Diameter: 37.9 cm (14.9 in.)
Maximum width: 13.5 cm (5.3 in.)
Tip width: .814 cm (0.32 in.)
Minimum angular momentum: 1115 N-m-sec (822 ft-lb-sec)
Unit energy storage: 1095 watt-hr

Bearing characteristics:

133.2N (30 lb) preload

$L_{10} = 4.2 \times 10^5$ hr

Drag power - 65 watts/bearing pair (average)

Motor/generator

Maximum design speed: 45 000 rpm
Speed reduction: 50 percent
Volume: $1.082 \times 10^{-3} \text{ m}^3$ (66 in.³)
Minimum axial length: 13.7 cm (5.4 in.)
Weight: 6.13 kg (13.5 lb)
Unit power rating: 2410 watts

Other

Gimbal torque limit: 9.5 N-m (7 ft-lb)
Unit weight: 75 kg (165 lb)

TABLE 1-XXV.- WEIGHT BREAKDOWN FOR RAM IPACS UNIT

Element	Weight	
	kg	lb
Wheel	45.2	99.5
Motor generator	6.1	13.5
Electronics	1.0	2.2
Housing/bearings	9.0	19.8
Drives and sensors	10.0	22.0
Outer gimbal	3.6	8.0
	74.9	165.1

Operating concept: The three energy units are mounted in the vehicle as a planar array with the outer gimbal axes parallel and aligned with the longitudinal axis of the vehicle which is the minor inertia axis. Thus, the three outer gimbal torques act in parallel. The deliverable torque about the transverse axes is dependent upon the instantaneous gimbal configuration but in general will be equal to or greater than the output of a single torquer.

Energy is stored in all three wheels under normal operating conditions. The gimbals are torqued as required to minimize the effects of torques produced by rotor speed changes. Under failure mode conditions, the two remaining units are slewed to a position where the spin axes of the rotors are collinear. The rotors are counter rotated to provide torque-free energy storage. The primary attitude control function is assumed by the reaction control system supplemented by the energy units where possible.

TDRS system description - The selected IPACS concept for TDRS is described briefly below.

Sizing requirement- The IPACS is sized for a total energy storage capacity of 285 watt-hours with a total power capability of 240 watts. The system must be capable of storing 50 percent of the nominal energy and delivering full rated power with one of the four units failed. The individual units are, therefore, sized to store approximately 71 watt-hours and deliver 120 watts. The attitude control sizing requirements include a maximum angular momentum requirement of 16.95 N-m-sec (12.5 ft-lb-sec) and a torque level of approximately 0.049 N-m (7 in-oz) (each on a per axis basis). The system is required to provide nominal attitude control performance with one unit failed.

Design concept - The concept for TDRS is presented in system block diagram form on figure 1-46. Energy storage and attitude control is provided by an array of four identical, nongimbaled, variable speed units. Each unit includes a permanent magnet brushless dc motor-generator and a constant stress geometry, titanium flywheel.

The IPACS concept retains a significant portion of the existing baseline design. For example, the baseline attitude control sensors are retained with the exception of the horizon sensors used during the normal on-station operation. In the baseline control system, the horizon sensors are integrated with the momentum wheels which provide the rotational motion for the scan function. In the IPACS concept, a separate solid-state horizon sensor is required because of the inability of the sensor chips to respond to the high modulating speeds of the IPACS wheels. The selected sensor is a flight qualified unit that weighs approximately 3.3 kg (7.2 lb).

The logic which governs operation of the system is contained in the central processor unit. Power switching functions are provided by the central power control unit. The shunt dissipator consists of transistor switches and resistive loads on radiator plates physically located on the solar array panels. These elements can be switched on command by the power control logic to dissipate excess solar array power. The dissipator also serves as an overvoltage regulator for the array.

Design characteristics - The more significant design characteristics for the motor/generator-wheel units are presented in Table 1-XXVI.

TABLE 1-XXVI.- MOTOR/GENERATOR DESIGN CHARACTERISTICS - TDRS

Rotor material - titanium
Rotor geometry - constant stress profile
Rotor diameter - 34 cm (13.4 in.)
Rotor maximum width - 1.42 cm (0.56 in.)
Rotor tip width - 0.099 cm (0.039 in.)
Maximum speed - 50 000 rpm
Speed reduction - 50 percent
Angular momentum reserved for control - 16.95 N-m-sec (12.5 ft-lb-sec)
Unit torque rating - .049 N-m (7 in-oz)
Unit energy storage - 71.3 watt-hr
Unit power rating - 120 watts
Array weight (4 units) - 25.97 kg (57.2 lb)
Bearing characteristics
22.2 N (5 lb) preload
$L_{10} = 2.2 \times 10^5$ hr
Drag power - 3.7 watts/bearing pair

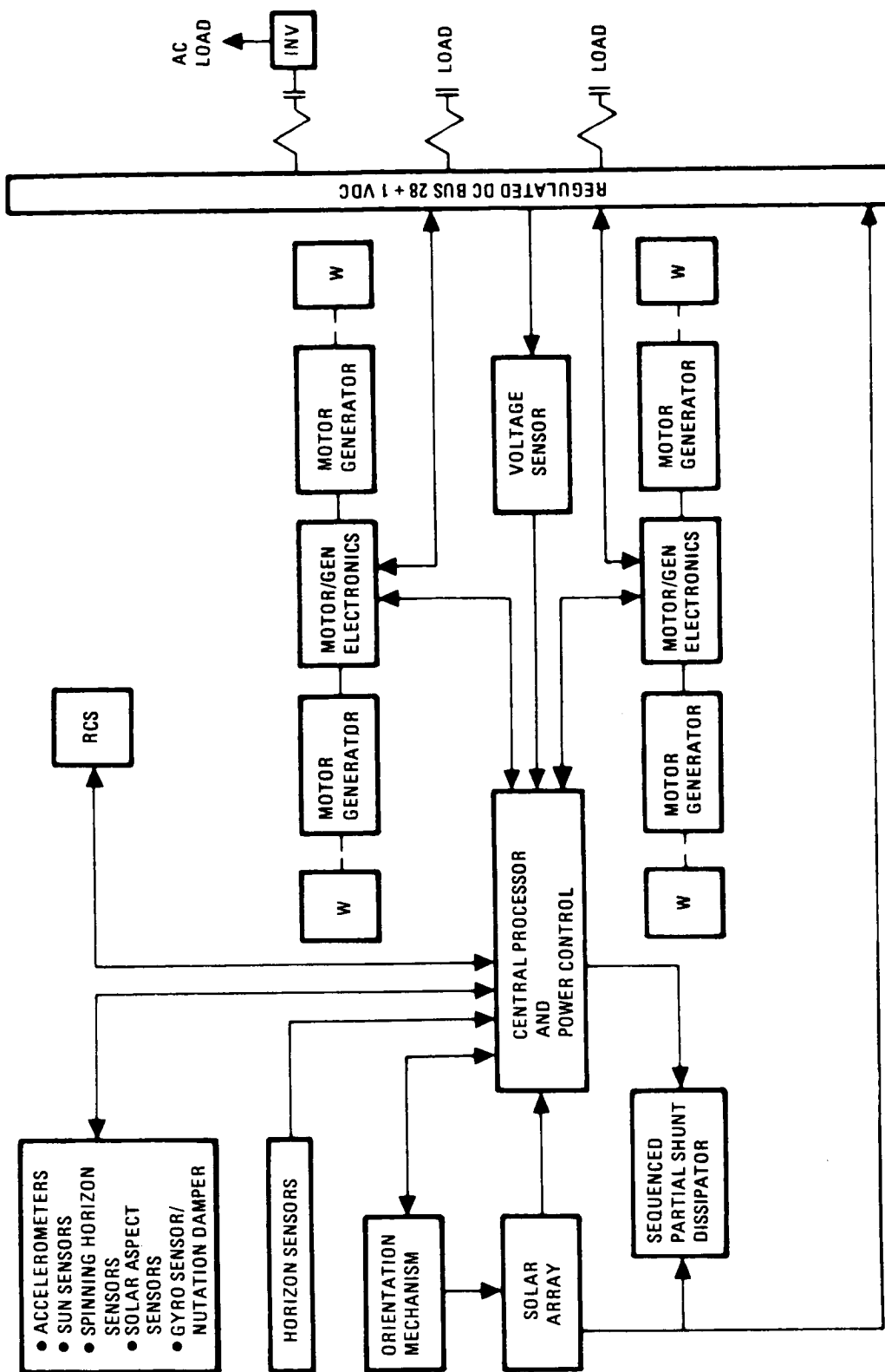


Figure 1-46. IPACS Concept of TDRS

The weight breakdown for a single wheel unit is shown in Table 1-XXVII. Weight is minimized in this design by not enclosing the flywheels.

TABLE 1-XXVII.- IPACS UNIT WEIGHT BREAKDOWN

Item	kg	lb
Wheel	3.90	8.6
Motor/generator	0.45	1.0
Electronics	0.99	2.2
Supports and bearings	1.14	2.5
Total	6.48	14.3

Operating concept: The four motor/generator-wheel units are mounted in the vehicle in pairs to deliver torques directly along the vehicle pitch and yaw axes. The pitch axis wheels are operated with a momentum bias perpendicular to the plane of the orbit. Energy is stored in both the pitch axis and yaw axis wheels by counter-rotating the wheels. Pitch axis control may be obtained by torquing either or both of the pitch axis wheels as required. The yaw axis wheels are nominally operated with zero net angular momentum but are torqued to provide active nutation damping.

Under failure mode conditions, where one unit has failed, energy is stored in the pair of units which remain operational. The operative wheel in the failed axis is used for control only. Thus, control performance with one unit failed for IPACS is equivalent to the unfailed baseline system. In the baseline TDRS design, control performance degradation is the result of a wheel failure.

MSS system description.- The selected IPACS concept for modular space station is described briefly below.

Sizing requirement: The IPACS array is sized for a total energy storage capacity of 14 900 watt hours, with a maximum power delivery capability of 20 000 watts. The system must be capable of meeting the above requirements with one IPACS unit failed. Each of the units in the five unit array is therefore sized to store 3730 watt hours and deliver 5000 watts. Attitude control requirements include an array momentum storage capability of 2760 N-m-sec (2034 ft-lb-sec) with one unit failed. The selected array consists of five single-gimbaled units. The momentum delivery capability with one unit failed is assumed to be 150 percent of the momentum capacity of a single unit. The individual wheel is therefore required to have a minimum angular momentum of 1762 N-m-sec (1350 ft-lb-sec). A rotor sized to provide the required energy storage will actually exceed the required momentum storage capacity.

Design concept - The IPACS design concept for MSS is shown in functional block diagram form on figure 1-47. A skewed array of five single-gimbaled IPACS units provides momentum exchange and energy storage.

The solar array design of the baseline vehicle is retained along with the attitude control sensors and reaction control subsystem. The high voltage design of the baseline vehicle is also retained. The major vehicle loads are supplied 120/208 vac with 56 vdc also available.

The major computation functions required to support the IPACS are performed within the IPACS preprocessor. Mode commands are generated within the ISS multiprocessor and transmitted via the inter-connecting data link to the IPACS preprocessor.

The more significant design characteristics for the MSS system are presented in Table 1-XXVIII.

TABLE 1-XXVIII.- MSS IPACS DESIGN CHARACTERISTICS

Rotor
Rotor material: composite PRD-49-III and epoxy
Diameter: 57.9 cm (22.8 in.)
Maximum speed: 35 000
Speed reduction: 50 percent
Minimum angular momentum: 5690 N-m-sec (4200 ft-lb-sec)
Unit energy storage: 3730 watt-hrs
Bearing characteristics:
Magnetic suspension bearings
Average power per bearing pair: 22 watts
Motor/generator
Unit volume: $2.51 \times 10^3 \text{ m}^3$ (153 in. ³)
Minimum axial length: 18.55 cm (7.3 in.)
Other
Gimbal torquer rating: 27.1 N-m (20 ft-lbs)
Torquer gear ratio: 5 to 1

The weight breakdown for a single unit is shown in Table 1-XXIX.

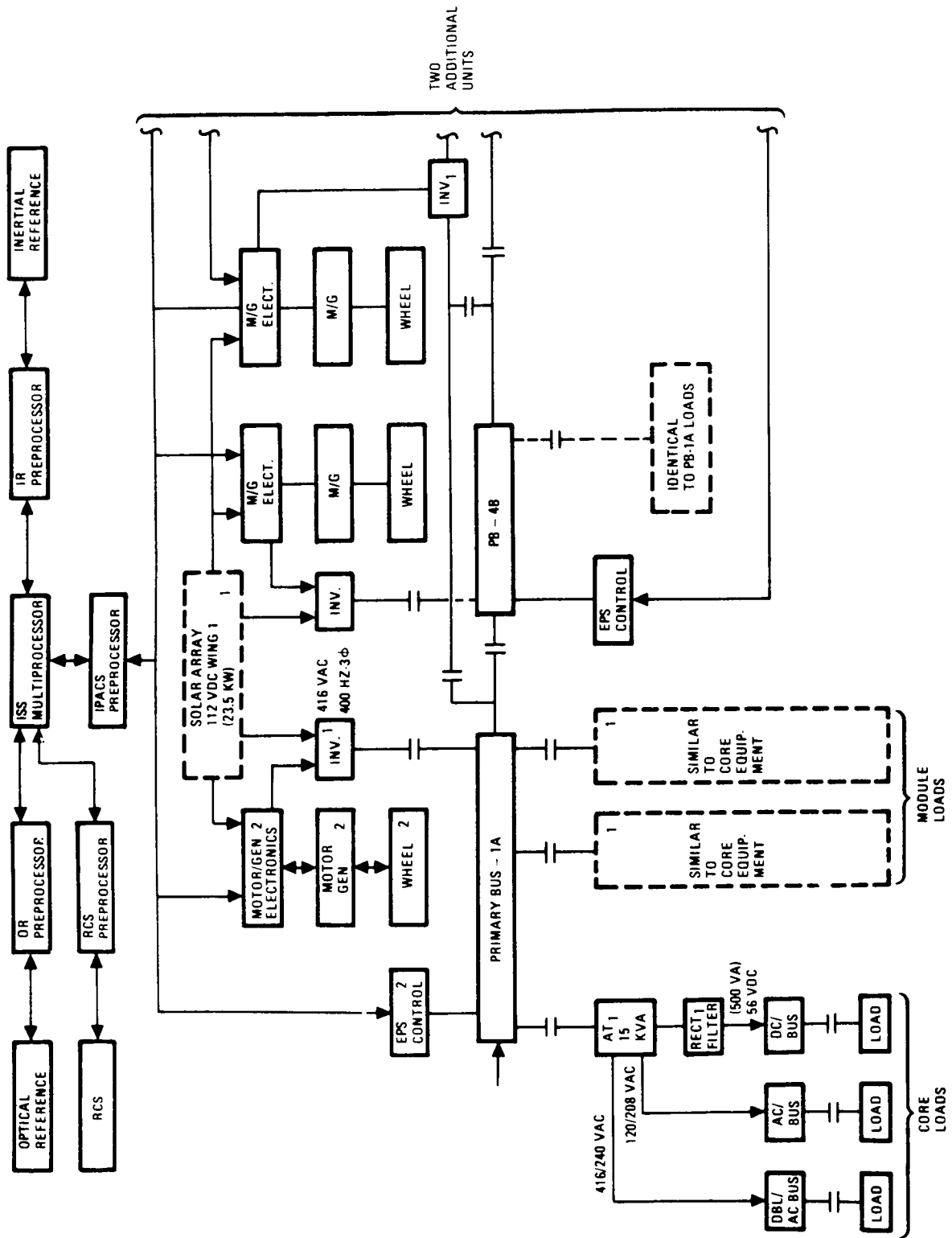


Figure 1-47. MSS Functional Block Diagram

TABLE 1-XXIX.- WEIGHT BREAKDOWN FOR MSS IPACS UNIT

Element	Weight	
	kg	lb
Wheel	94.0	207
Motor/generator	14.3	31.6
Gimbal drive	5.0	11
Sensors	2.3	5
Electronics	1.2	2.6
Housing and supports	14.1	31
Bearings	15.3	33.6
Unit weight	146.2	321.8

Operating concept - The five single-gimbaled IPACS units are mounted as a skewed array. All units are normally in operation. In case of a failure in one IPACS unit, the energy storage and momentum exchange functions are continued with the four operable units and the other unit is shut-down for repair. On-orbit repair is performed through part replacement at the module level. Typical modules are an electronics package, an inner gimbal assembly, or a sensor package.

MJS system description.- The selected IPACS concept for MJS is described briefly below.

Sizing requirements - The IPACS array is required to deliver a total of 360 watt-hours at a power level of 20 watts. Under failure mode conditions, the system is not required to store energy or deliver power. Thus, each wheel is sized to store 90 watt-hours. Since the weight penalty is low, the motors are sized to deliver 10 watts rather than 5 watts, the minimum possible. The momentum storage requirements are extremely small, 0.068 N-m-sec (0.05 ft-lb-sec) per axis. For a skewed array of four nongimbaled units, the individual axis requirement translates to a per wheel requirement of 0.076 N-m-sec (0.056 ft-lb-sec.)

Design concept - The IPACS concept for MJS is shown in functional diagram form on figure 1-48. A skewed array of four nongimbaled units is used. The baseline vehicle radioisotope thermoelectric generator (RTG) power source is retained. Excess power, not required by either the spacecraft loads or for

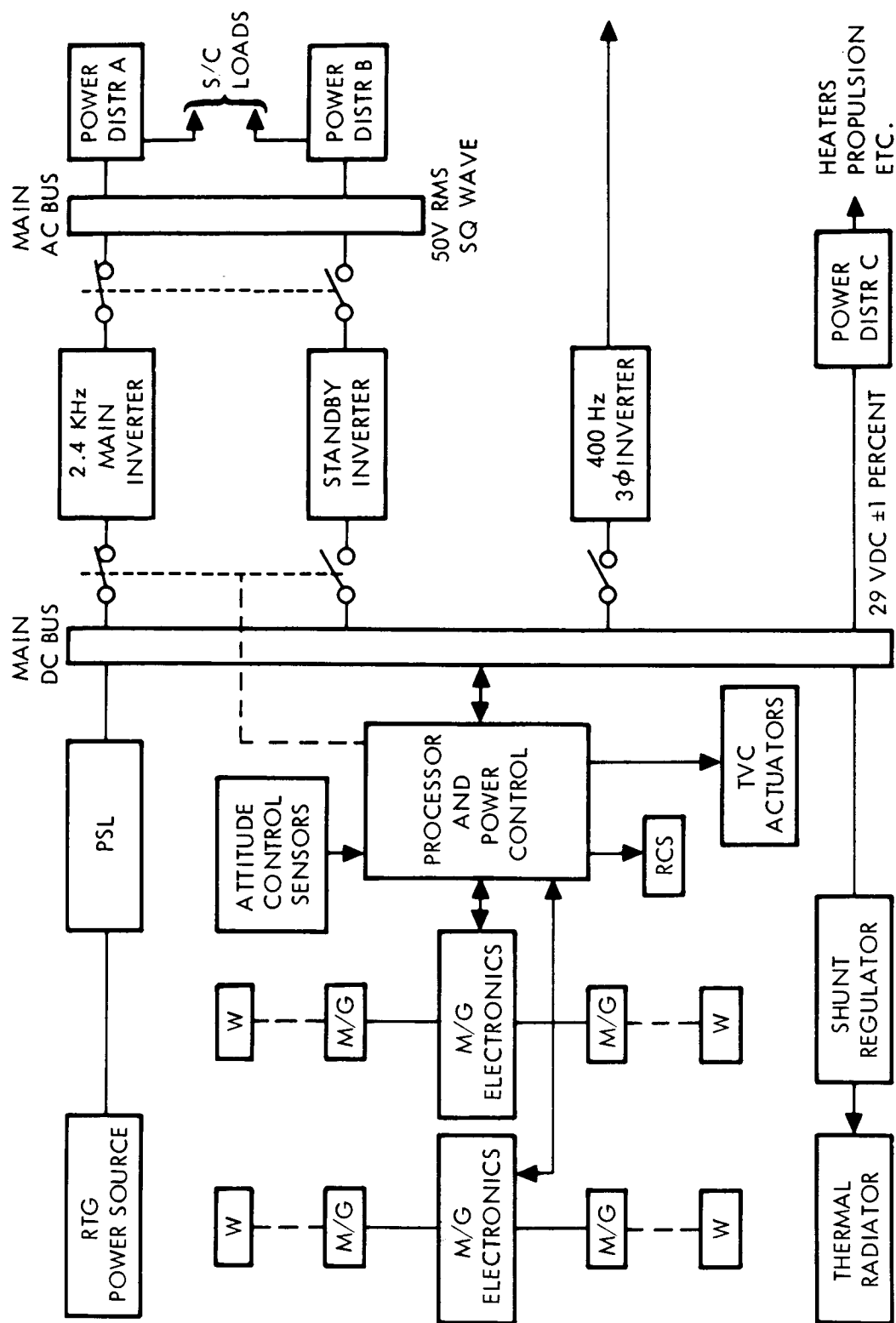


Figure 1-48. IPACS Concept for MJS

storage in the IPACS wheels, is dissipated through the shunt regulator and ultimately the thermal radiator. The IPACS units complement the shunt regulator.

Power and control logic functions are performed within the processor and power control unit. The RCS and TVC concepts of the baseline vehicle are retained.

Design characteristics - The more significant design characteristics for the MJS system are presented in Table 1-XXX.

TABLE 1-XXX.- MJS IPACS DESIGN CHARACTERISTICS

Rotor	
Rotor material: Composite PRD-49-III and epoxy	
Diameter: 20.3 cm (8 in.)	
Maximum speed: 100 000	
Speed reduction: 50 percent	
Unit energy storage: 90 watt-hours	
Bearing characteristics:	
Magnetic suspension bearings	
Average power per bearing pair: 3.2 watts	
Motor/generator	
Unit volume: $4.1 \times 10^5 \text{ m}^3$ (2.5 in. ³)	
Minimum axial length: 2.54 cm (1.0 in.)	

The weight breakdown for a single unit is shown in Table 1-XXXI.

TABLE 1-XXXI.- WEIGHT BREAKDOWN FOR MJS IPACS UNIT

Element	Weight	
	kg	lb
Wheel	2.27	5.0
Motor/generator	0.14	0.3
Electronics	1.00	2.2
Supports	0.45	1.0
Bearings	0.45	1.0
Total unit weight	4.31	9.5

Operating concept - The skewed array of four IPACS units provides three-axis, mass conservative momentum exchange and energy storage. The primary requirement for the energy storage function occurs during the planet encounter phases of the mission when experiment power demands potentially exceed the output of the isotope power source. Thus, energy storage in the IPACS units may not be required for the long cruise phases of the mission. The IPACS units, required to provide momentum exchange control only, then have the option of running at relatively low speeds during these cruise phases of the mission. Normal operation in the 50 000 to 100 000 speed range would be resumed to supply energy for planet encounter periods.

Under failure mode conditions, the IPACS energy storage requirement is terminated. The three remaining wheels are used to provide partial momentum exchange attitude control (reaction control may be required in one axis).

EOS system description.- The IPACS concept for EOS is functionally identical to the concept presented for TDRS. Sizing and design characteristics which differ are presented below.

Sizing requirements - The IPACS array under normal operating conditions is required to store 460 watt-hours and deliver 1048 watts. The individual wheels in the array are sized by the failure criterion which requires storage of 345 watt-hours with one of the four wheels in the array failed. Since failure of a single wheel forces loss of that wheel pair for energy storage, the 345 watt-hours must be stored in a single wheel pair. Thus, each wheel is sized to store 173 watt-hours and deliver 525 watts.

The momentum exchange allocation within the 50 percent operating speed range for a single wheel yields a momentum bias or storage capability of 24.4 N-m-sec (18 ft-lb-sec).

Design concept - The IPACS concept for EOS is the same as that described for TDRS and illustrated in functional diagram form on figure 1-46.

Design characteristics - The more significant design characteristics for the IPACS EOS design are presented in Table 1-XXXII.

The weight breakdown for a single unit is shown in Table 1-XXXIII.

Operating concept - The IPACS operating concept for EOS is the same as that for TDRS.

Extended Shuttle system description.- The selected IPACS concept for the 30-day shuttle is described briefly below.

TABLE 1-XXXII.- EOS IPACS DESIGN CHARACTERISTICS

Rotor	
Rotor material: Composite PRD-49-III and epoxy	
Diameter: 33.8 cm (13.3 in.)	
Maximum speed: 60 000 rpm	
Speed reduction: 50 percent	
Angular momentum reserved for control: 24.4 N-m-sec (18 ft-lb-sec)	
Unit energy storage: 173 watt-hours	
Bearing characteristics:	
Magnetic suspension bearings	
Average power per bearing pair: 3.2 watts	
Motor/generator	
Unit volume: $3.06 \times 10^4 \text{ m}^3$ (18.7 in. ³)	
Minimum axial length: 6.35 cm (2.5 in.)	

TABLE 1-XXXIII.- WEIGHT BREAKDOWN FOR EOS IPACS UNIT

Element	Weight	
	kg	lb
Wheel	5.58	12.3
Motor/generator	1.32	2.9
Electronics	1.00	2.2
Housing and supports	1.13	2.5
Bearings	0.45	1.0
Unit weight	9.48	20.9

Sizing requirements The IPACS array, under normal operating conditions, is required to store 6100 watt-hours and deliver a total of 61 000 watts. Full energy/power performance is required with one of the three units failed. Thus, each unit is sized to store 3050 watt-hours and deliver power at 30 500 watts. The wheel will be charged at a rate of 2000 watts.

The attitude control requirements include a momentum storage capability of 7120 N-m-sec (5250 ft-lb-sec) and a torque requirement of 163 N-m (120 ft-lb) per torquer. Under IPACS failure conditions, the attitude control function reverts to the orbiter RCS. Thus, each IPACS rotor is sized such that the minimum angular momentum is 2370 N-m-sec (1750 ft-lb-sec).

Design concept - The IPACS concept for extended shuttle is shown in functional block diagram form on figure 1-49. The IPACS array is a planar array of three double-gimbaled units. Note that the individual units are mounted with the outer gimbal axes parallel. These units provide momentum exchange attitude control for the entire vehicle.

The IPACS units for this design include a separate motor and generator for each wheel due to the large difference between the charge and discharge

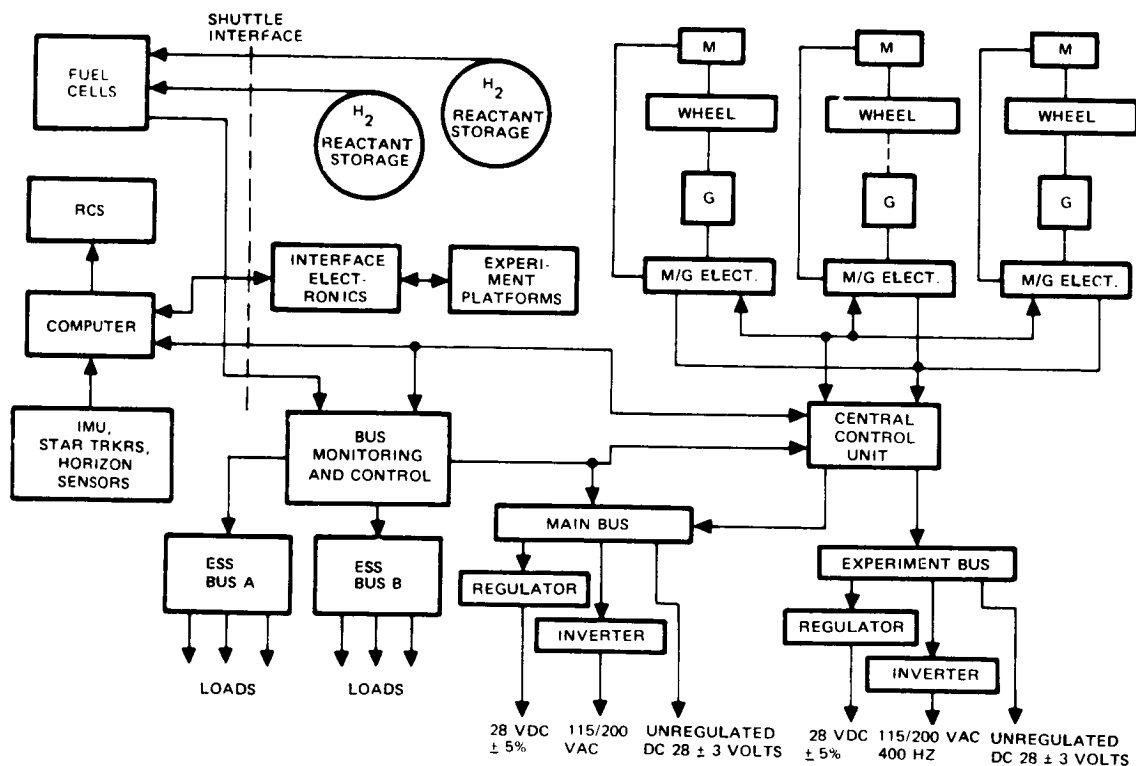


Figure 1-49. Extended Shuttle Functional Block Diagram

power levels (2 kW and 30.5 kW). The generator is an inside-out design. The inside-out design has the permanent magnets located on the exterior portion of the motor and the windings on a non-rotating shaft. A conventional design generator was evaluated and found to be impractical from a length standpoint.

The orbiter fuel cells serve as the power source with added reactant tankage provided in the payload bay. The orbiter attitude control sensors, computer, and RCS are utilized. Experiment servo platforms are retained from the competitive control design.

Design characteristics - The design characteristics of the extended shuttle IPACS units are summarized in Table 1-XXXIV.

The weight breakdown for a single unit is shown in Table 1-XXXV.

Table 1-XXXIV.- EXTENDED SHUTTLE IPACS DESIGN CHARACTERISTICS

Rotor

Rotor material: Composite PRD-49-III and epoxy
Diameter: 56.6 cm (22.3 in.)
Maximum speed: 35 500 rpm
Speed reduction: 50 percent
Minimum angular momentum: 3930 N-m-sec (2900 ft-lb-sec)
Unit energy storage: 3050 watt-hours
Bearing characteristics:
 Magnetic suspension bearings
 Average power per bearing pair: 10.8 watts

Motor

Unit volume: $1.15 \times 10^3 \text{ m}^3$ (70 in.³)
Minimum axial length: 8.6 cm (3.4 in.)

Generator

Unit volume: $1.56 \times 10^2 \text{ m}^3$ (953 in.³)
Minimum axial length: 10.68 cm (4.2 in.)
Inside-out design

TABLE 1-XXXV.- WEIGHT BREAKDOWN FOR EXTENDED SHUTTLE IPACS UNIT

Element	Weight	
	kg	lb
Wheel	77.2	170
Generator	82.6	182
Motor	6.8	15
Electronics	6.4	14
Housing and supports	13.6	30
Bearings	5.4	12
Outer gimbal	5.9	13
Sensors and drivers	27.2	60
Total unit weight	225.1	496

IPACS and Competitive System Performance Comparisons

The performance of the IPACS and competitive systems has been compared. The initial phase of this effort consisted of a quantitative comparison of factors such as weight, volume, solar array area, charge-discharge efficiency, and induced vibration. In addition, qualitative comparisons were made.

Quantitative performance comparisons.-

Weight - Weight comparisons between the IPACS concepts and the competitive concepts are presented in Table 1-XXXVI. The first columns show total power and control subsystem weight on a single vehicle basis. The final columns indicate the magnitude of the weight saving and express this as a percentage of the competitive subsystems weight.

Note that IPACS provides a potential weight saving for all missions except MJS. The saving appears most significant for RAM and EOS - both of which are low-altitude earth orbit missions utilizing solar array power. The saving on TDRS, although a smaller percentage, is perhaps more important. The transportation costs to synchronous orbit are higher (refer to TDRS cost analysis), and the vehicle is performance constrained by weight limitations.

Volume - Volume comparisons between the IPACS and competitive systems are presented in Table 1-XXXVII. The volume estimates for the IPACS energy storage momentum wheel units and the conventional control moment gyros were calculated as the volume of spheres with radii equal to the rotor radii. It is recognized that the actual displacement volumes of the nongimbaled units are significantly different from the spherical estimates; however the spherical volumes perhaps better represent the installation problems and problems with utilization of surrounding volume in the vehicle. The only components included in the IPACS estimates are the energy/momentum units. Competitive system volumes include only the momentum exchange control volumes and battery volumes. Comparison of these numbers yields a fair estimate of the delta volume between the systems. As seen from the table, substantial volume savings are obtained for all missions except TDRS and MJS.

Charge-Discharge Efficiency - Figure 1-50 graphically compares IPACS charge-discharge efficiencies with the competitive systems. The full length of the IPACS bar represents the efficiency of the brushless dc motor/generator and electronics. Bearing losses reduce that efficiency as indicated on the graphs by the shaded regions. In all cases studied, the IPACS systems are seen to be more efficient in performing the charge-discharge operation. The effect of these increased efficiencies are best evaluated through consideration of the solar array requirements - discussed in the next section.

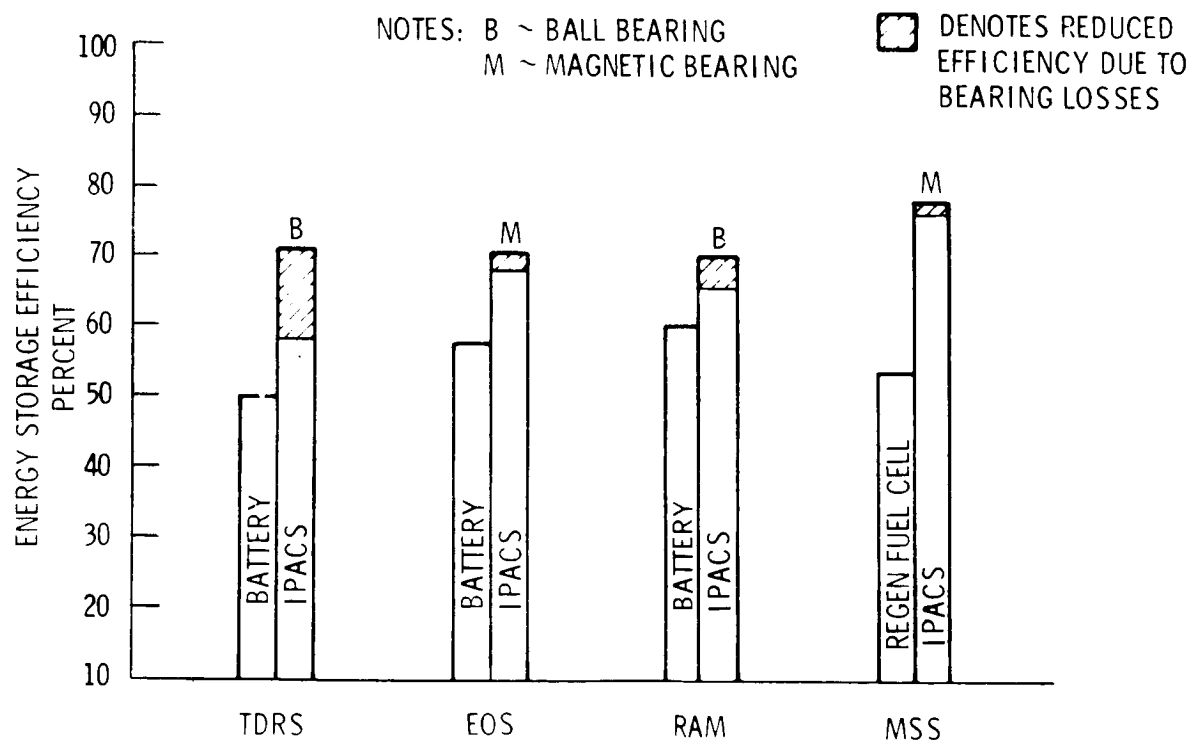


Figure 1-50. Charge-Discharge Efficiency and Bearing Loss

TABLE 1-XXXVI.- WEIGHT COMPARISON BETWEEN IPACS AND COMPETITIVE SYSTEMS

Mission	IPACS weight		Competitive weight		Weight savings with IPACS		Percentage wt savings*
	lb	kg	lb	kg	lb	kg	
TDRS	191.6	86.91	213.7	96.93	22.1	10.02	10
RAM	2464	1118	3560	1615	1096	497	31
MSS	13 322	6043	15 825	7178	2503	1135	16
30-Day Shuttle	7066	3205	7539	3420	473	215	6
EOS	391.4	177.5	613	278.0	221.6	100.5	36
MJS	356.5	161.7	341.5	154.9	-15	-6.8	-4**

* Weight savings with IPACS divided by competitive weight and expressed as a percentage.

**Negative number denotes weight penalty.

TABLE 1-XXXVII.- VOLUME COMPARISON BETWEEN IPACS AND COMPETITIVE SYSTEMS

Mission	IPACS ft ³	Volume		Competitive		Volume		Volume savings with IPACS		Percentage Volume Savings*
		ft ³	m ³	ft ³	m ³	ft ³	m ³	ft ³	m ³	
TDRS	2.9		0.082	1.1	0.031	-1.8	-0.051			Volume penalty
RAM	3.0		0.085	14.6	0.413	11.6	0.33			79
MSS	18.7		0.53	171	4.84	152.3	4.31			89
30-Day Shuttle	9.5		0.27	67	1.90	57.5	1.63			86
EOS	2.9		0.082	3.3	0.093	0.4	0.0113			12
MJS	0.62		0.017	0.23	0.0065	-0.39	-0.011			Volume penalty
*Volume savings with IPACS divided by competitive volume and expressed as a percentage.										

The relatively large effect of bearing loss on the TDRS IPACS efficiency is due to the low power allocated for charging and the resultant long period (≈ 5 hours) to recharge. This also did not include consideration of IPACS bearing losses during the long daylight period (when neither charging nor discharging) nor does it include comparable factors for the battery concepts such as charge circuit losses for battery stand by, trickle charge, or overcharge.

Solar array area - A study was conducted to quantize the significance of charge-discharge efficiency differences between the IPACS concepts and the competitive energy storage systems. The approach taken was to estimate the solar array area required in each case. The area can be estimated once the power requirement is known. For a parallel mechanization, the following expression specifies array power as a function of the efficiencies and orbital parameters.

$$P_{SA} = \left(\frac{P_L T_E}{\eta_{CH-DIS} T_D} + P_L \right) \frac{1}{\eta_{DIST}}$$

where: P_{SA} = required solar array power, watts
 T_E = eclipse time, minutes
 T_D = sunlight time, minutes
 P_L = power to loads, watts
 η_{CH-DIS} = charge discharge efficiency
 η_{DIST} = transmission and conditioning efficiencies

This expression was evaluated for the various missions including consideration of the IPACS bearing losses and the results are shown on Table 1-~~XX~~XVIII.

In the case of the TDRS, a small increase in solar array power is required even though the IPACS has a higher efficiency than the $N_i C_d$ batteries used in the competitive power system. At geosynchronous orbit, the maximum eclipse period is 72 minutes. Based on 85 watts of solar array power available for charging, time required to return the IPACS to 100 percent storage energy is 4.8 hours. The IPACS wheel bearing loss (total) is 14.8 watts when ball bearings are used. The requirement for this fixed power to sustain wheel speed during standby periods results in a 2 percent increase in solar array area for an IPACS TDRS.

TABLE 1-XXXVIII.- EFFECT OF IPACS ON SOLAR ARRAY SIZE

Mission		TDRS		EOS		RAM		MSS	
Parameter		Comp NiCd batt	IPACS 4 opposed wheels	Comp NiCd batt	IPACS 4 opposed wheels	Comp NiCd batt	IPACS 3-double gimbaled	Comp Regen fuel cells	IPACS 5 skewed single gimbal
Energy storage concept									
Charge discharge efficiency		.50	.715	.58	.703	.62	.708	.536	.78
IPACS bearing losses (total) watts		-	14.8	-	10.4	-	195.0	-	90
Solar array power (EOL) watts		374	381	1224	1137	7105	6748	46 500	47 900
Solar array area m ² (ft ²)		4.18 (45)	4.26 (45.9)	14.96 (161)	13.84 (149)	90.1 (970)	85.0 (915)	644 (6930)	661 (7120)
Net change in required solar array power, watts		+7		-87			-357	+1400	
Percent change in solar array area		+2		-7.5			-5.6	+2.7	

In the case of the EOS and RAM, the higher IPACS energy storage efficiency does result in a decrease in required solar array area. For the MSS case analyzed, a 2.7 percent increase in solar array area is required with IPACS. This result is explained by the MSS electrical load profile which is based on a 14-hour work and a 10-hour rest period. The eclipse period powers are approximately 5.4 kw less than the sunlight requirement. If a system is sized to the 14-hour work period profile, a minimum weight results for the energy storage components. However, extra solar array power available during the 10-hour rest period is not utilized. The addition of extra energy storage capacity allows this power to be stored and then used during the 14-hour work period. In the case of the regenerative fuel cells, gaseous hydrogen and oxygen tankage weight required to store 10-hour rest period excess solar array power amounts to 787 kg (1735 lb). Sizing the reactant storage tanks for the 14-hour work period requirements result in a 592 kg (1301 lb) weight reduction. On the other hand, the solar array area required is increased by 122.8m^2 (1320 sq ft), which corresponds to a weight increase of 572 kg (1260 lb). The weight trade is about equal but an operational and cost advantage results by use of the smaller solar array. A minimum IPACS weight of 905 kg (1990 lb) is required to meet 14-hour work eclipse period requirements. By increasing IPACS weight to that required by the baseline regenerative fuel cell system, a reduction in solar array area could be obtained. This must be traded off against the increased IPACS weight and cost. The present concept of sizing the IPACS energy storage system and the solar array to the 14-hour work period eclipse demands allows for power growth requirements such as would be required for multiple shift operations. The system can be operated at maximum power continuously. In order to provide this capability with a regenerative fuel cell energy storage system, a solar array of 769m^2 (8270 ft^2) would be required which is 107m^2 (1150 ft^2) greater than that required for IPACS.

Induced vibration: A preliminary analysis was conducted to compare the IPACS designs with the competitive control units from an induced vibration standpoint. The unbalance force is proportional to $m\epsilon\omega^2$ where m is the rotor mass, ϵ is the equivalent offset in the rotor mass center, and ω is the rotational speed of the rotor. The same rotor balancing technology is assumed for both the IPACS and competitive control units. This assumption is warranted in that the precision of the balancing operation is determined by the test techniques and instrumentation rather than the rotor mass, speed, or other rotor characteristics. Thus it is felt that the techniques used to balance a 28 kg, 3000 rpm CMG rotor to 7.6×10^{-8} meters (3 micro-inches) will also enable the balancing of a 45 kg 45 000 rpm rotor to 7×10^{-8} meters. The induced force or vibration comparison then simplifies to a consideration of the rotor mass and rotational speed of the units. The competitive rotor mass characteristics were estimated in some cases using unit size, angular momentum, and speed data. The results used in deriving the relative force factor are shown in Table XXXIX.

TABLE 1-XXXIX.- INDUCED VIBRATION COMPARISON

Mission	Competitive rotor characteristics			IPACS rotor characteristics			Relative force factor: IPACS force competitive force
	Estimated weight		Speed	Weight		Speed	
	kg	lb	RPM	kg	lb	RPM	
RAM	28.7	63.2	3000	45.2	99.5	45 000	360
MSS	40.9	90	7500	94	207	35 000	50
TDRS	5.0	11	2000	3.9	8.6	50 000	500
Extended shuttle	65.8	145	9100	77.2	170	35 500	20
EOS	7.3	16	2000	5.6	12.3	60 000	700

The study indicates that induced vibration forces will be higher for IPACS than would be expected with the competitive control units. Further studies, documented in Module 4 of this volume address the potential impact of induced vibration with respect to pointing stability. With the incorporation of vibration isolation techniques, it is felt that IPACS induced vibration would not preclude the attainment of precision image motion stabilization such as that required for the free-flying RAM.

Qualitative considerations.-

Safety - The safety consideration for IPACS concerns the high concentration of energy stored in the rotor. Provision must be made for personnel safety and spacecraft protection in the event of flywheel disintegration. The probability can be made arbitrarily small by design derating, material and manufacturing techniques but it cannot, as in the case of pressure vessels, be eliminated completely. Reference 1-9 has shown that containment and energy transfer rings are possible, but that weight penalties, even for ground vehicle use, are unacceptable. Lightweight containment devices can be postulated, but are not of current technology for isotropic wheels.

The problem, for isotropic wheels, is solved for IPACS by adequate design margins, material selection and testing, development testing, rigorous quality control through manufacturing and proper facility provisions. The solutions proposed are seen to be directly analogous to those currently existing for large control moment gyros and pressure vessels and are not considered more difficult or, significantly, more costly to implement.

The design margin is applied through specification of the working stress in the rotor, including consideration of the number of fatigue cycles which the rotor must endure. For this study, the allowable working stress in the rotor was selected from fatigue data allowables equivalent to twice the anticipated cycles for the worst case mission. The worst case mission was space station designed for ten years of operation in low altitude earth orbit.

Material selection requires specification of rotating-grade quality as well as material type. Tests for material homogeneity, purity, and lack of stress concentrations are required.

Development testing is required in several areas. Rotor fatigue cycle tests should be conducted to add confidence to the material fatigue data used in establishing the allowable working stress. Development tests should also include overspeed to destruction on families of rotors with various surface grades and stress notches.

Manufacturing or acceptance tests on every rotor would include over-speed tests to a prespecified stress level as a test of rotor integrity. Rotor inspections should be designed to detect internal imperfections, as well as surface imperfections that could lead to eventual weakening under operating stress.

Facility provisions represent a further aspect of the safety problem. Containment provisions will be required for operations where the rotors are run at design speeds or overspeed. The usual technique is to use a pit where the rotor is mounted below ground level with the plane of rotation parallel to the ground. The construction of the pit should be such that disintegration of a rotor can occur and be totally contained without risk to test personnel. It should be noted that all testing need not be performed in a pit. Functional tests can be performed at speeds well under the maximum design speed. A rotor running at 50 percent design speed experiences only 25 percent of the stress associated with maximum speed operation.

The unique failure properties of the anisotropic rotors would appear to result in less hazard. Testing of various composite rotors has shown that frequently a large part of the rotor energy is dissipated in the destruction of the rotor. For example, some fiber/epoxy designs fail with the fibers essentially delaminating but not breaking loose from the shaft. Other tests with rod type shapes have shown that a significant portion of the kinetic energy is dissipated within the failure mechanism. These conclusions are supported by analysis of containment ring deformation resulting from the impact of rotor segments following rotor overspeed to destruction tests. This failure property is considered to be a significant advantage for the composite rotors over the homogeneous type and represents a further reason for encouraging the development of the composite rotor.

Reliability - Two factors can be considered in reliability. The first is the impact of integrating power and control functions upon overall power and control systems reliability. In the second, an IPACS unit can be compared with a conventional momentum device for reliability.

In the systems sense, conventional power and control reliability functions are chained to give spacecraft reliability. This is because all elements of both systems must work for nominal systems operations. Figure 1-51 shows a generic block diagram of power and control elements. As can be noted, IPACS changes the chain from eight (the number is arbitrary) to seven functional elements with an added change in reliability to the momentum system. If IPACS flywheel assembly reliability can be made equal to that of the original momentum element, IPACS will result in a reliability advantage.

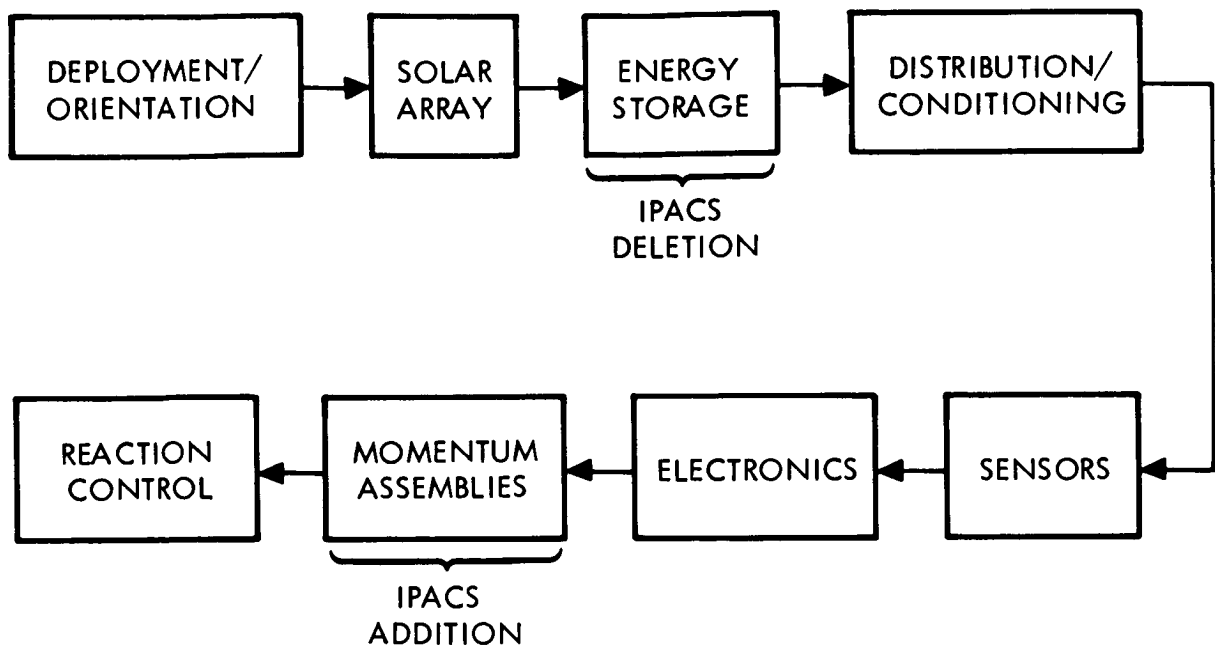


Figure 1-51. Generic Power and Control Reliability Chain

A preliminary study was conducted to compare the estimated reliability between an IPACS unit and a typical control moment gyro. Both the IPACS and CMG were assumed to be double gimbaled units. The results of this study are presented in Table 1-XXXX below. The IPACS unit, representing a "second generation" CMG, is shown to include the benefits of technology/reliability improvements. For example, the IPACS unit includes a brushless direct drive torquer whereas the CMG includes a brush type direct drive torquer. Similarly, brushless sensors are used in the IPACS compared to brush type sensors in the CMG's. Integrated circuit electronics were assumed for both the IPACS and the CMG's. The spin assembly for IPACS is seen to be less reliable than the comparable unit on the CMG for primarily two reasons. The IPACS spin bearings operate at significantly higher speeds and the IPACS unit includes a launch lock to restrain the axial motion of the rotor/preload assembly through the launch environment. This launch lock is characteristic of designs which are not able to use the central rod preload technique.

Table 1-XXXX presents comparative estimates for two electronics concepts - without redundancy and with standby redundancy. The marked reliability improvement for the latter case warrants further investigation. As shown in the table the IPACS unit is estimated to have a slight reliability advantage over the conventional control moment gyro.

TABLE 1-XXXX.- FAILURE RATE COMPARISON FOR IPACS VERSUS CMG'S

	Failures per million hours	
	CMG	IPACS
Spin assembly	2.0	2.6
Spin motor electronics	2.9 (.206) ⁽¹⁾	2.9 (.206)
Gimbal	-	-
Gimbal drive (IG)	0.76 ⁽²⁾	0.31 ⁽³⁾
Drive electronics (IG)	2.9 (.206)	2.9 (.206)
Sensor (IG)	1.0 ⁽⁴⁾	0.32 ⁽⁵⁾
Sensor electronics (IG)	1.2	1.0
Gimbal drive (OG)	0.76	0.31
Drive electronics (OG)	2.9 (.206)	2.9 (.206)
Sensor (OG)	1.0	0.32
Sensor electronics (OG)	1.2	1.0
Outer support	-	-
Total	16.6 (8.5)	14.56 (6.5)
Notes: (1) Assumes standby redundancy (2) Direct drive brush type (3) Direct drive brushless (4) Brush type (5) Brushless (6) Integrated circuit electronics		

Thermal control - The following heat sources have been identified for a representative IPACS energy storage/momentum unit.

- Bearing friction
- Rotor windage
- Motor/generator losses

Torquer duty cycles are expected to be sufficiently low that this heating source is not significant.

The relatively high efficiencies associated with the IPACS units tend to minimize the thermal problems associated with the identified heating sources. The rotors operate in an evacuated housing to minimize the motor power required to overcome windage drag. Considering outgassing, the pressure within the housing is expected to be on the order of 0.1 microns. The associated motor power to overcome the drag is on the order of 1 to 2 watts depending upon the size of the unit. Windage heating is therefore considered to be negligible.

Losses within the permanent magnet motor/generators can be allocated between electronics losses and copper and core losses within the rotating machine itself. The electronics losses do not represent a heating problem as the electronics are mounted in a separate package on the exterior of the rotor housings and can be designed to radiate to the surrounding spacecraft structure.

Assuming motor/generator efficiencies on the order of 97 percent, representative heating rates are presented in Table I-XXXXI.

TABLE I-XXXXI.- HEATING FROM M/G LOSSES

Mission	Power level (watts)	Losses (watts)
MJS	12.5	0.39
TDRS	120	3.7
EOS	525	16
RAM	2410	75
MSS	5000	154
Extended Shuttle	30 500	942

Losses for the MJS, TDRS, and EOS missions are considered to be sufficiently small to not be a problem. For the extended shuttle case, the associated duty cycle is significant. The high power level occurs for a maximum duration of 0.1 hr. Thus the heating pulse is only 94 watt hr.

The last heating source of interest is the bearing friction for conventional ball bearings. This applies to the designs for RAM and TDRS. Magnetic suspension bearings were selected for the other designs, and the average power dissipation of these bearings (11 watts/bearing maximum) is small.

Average ball-bearing friction losses per unit (two bearings) are estimated to be on the order of 65 watts and 3.6 watts for RAM and TDRS. The problem for RAM is expected to be the establishment of thermal stability in the transfer of heat away from the bearing area. Feasibility is not questioned, but this thermal stability will require analysis and test in the design and development phases. The reader is referred to the RAM conceptual design section for a further discussion of this problem.

Orbital storage. -- The orbital storage problem for an IPACS unit is expected to be essentially comparable to the storage problem for present technology control moment gyros. System elements such as the permanent magnet motors, electronics, gimbal drives, and sensors are considered to be equivalent between IPACS and CMG's.

Feasibility Analysis Summary

Energy storage by means of flywheels appears technically feasible for spacecraft applications.

Flywheel energy units can be assembled from either current or advanced technology elements. Both technologies are expected to produce about twice the energy density of NiCd batteries at comparable development levels.

As energy storage elements, current technology flywheels were found to be capable of 48 W-hr/kg with advanced technology wheels producing up to 70 W-hr/kg. This compares with 26 and 41 W-hr/kg for current- and advanced-technology NiCd systems respectively.

The flywheel energy units were found to be readily adaptable to both gimballed and nongimballed control arrays of conventional usage.

Flywheel energy momentum units used in integrated power and attitude control applications were found to be technically feasible for all missions studied.

The advantages of the flywheel systems increased as mission life and charge-discharge cycles increased.

The IPACS units showed weight and efficiency advantages for all missions except the MJS, where the low energy requirement resulted in a weight penalty.

Weight advantages ranged from a low of 6 percent for the 30-day Shuttle mission to 36 percent for the EOS mission. The RAM mission showed a weight savings of 31 percent, and MSS showed 16 percent. Charge-discharge efficiency for the IPACS units exceeded that of competitive battery and fuel cell systems. Current technology IPACS ranged from 58 to 67 percent (with bearing losses) and advanced technology units showed about 70 to 75 percent.

IPACS operational factors were found to be comparable to current systems. Some added rigor is required for insuring safety, but the procedures required parallel current practice. Current technology IPACS units are considered comparable in reliability with the competitive energy storage and control sub-systems.

References

- 1-1. Primary Energy Storage and the Super Flywheel; TG 1081. Technical Memorandum of the Applied Physics Laboratory of the John Hopkins University; D. W. Rabenhorst; Sept. 1969.
- 1-2. Heat-Engine/Mechanical-Energy-Storage Hybrid Propulsion Systems for Vehicles; CP011; Prepared for the Environmental Protection Agency, Office of Air Programs by the Applied Physics Laboratory of John Hopkins University; G. L. Dugger, A. Brandt, J. F. George, et al; March 1972.
- 1-3. Flywheel Feasibility Study and Demonstration Final Report; LMSC-D007915; April 30, 1971; Contract No. EHS 70-104 with Air Pollution Control Office of Environmental Protection Agency; R. R. Gilbert, J. R. Harvey, G. E. Heuer, and L. J. Lawson; Lockheed Missiles and Space Company.
- 1-4. Bower, E. R., "Rolling Versus Sliding Bearings," Prod Eng (April 27, 1969).
- 1-5. GDCA-DDA71-004. Research and Applications Module (RAM) Phase B Study, Vol. II, Appendix A. General Dynamics, Dec. 17, 1971 (Contract NAS 8-27539). GDCA-DDA71-006A. RAM Mass Properties Document General Dynamics, April 10, 1972 (Contract NAS 8-27539).
- 1-6. SD 71-217-4. Modular Space Station Phase B Extension Preliminary System Design. Volume IV. Subsystem Analysis. North American Rockwell, Space Division. January 1972 (Contract NAS 9-9953).
- 1-7. MSC 02471 (SD 71-217-7), Modular Space Station, Phase B, Extension Preliminary System Design Volume VII: Ancillary Studies, NR Space Division, January 1972.
- 1-8. GDCA-DDA72-006, RAM Phase B Study, Vol. III, 4.4 Preliminary Design Appendix A, Trade and Special Studies, GD Convair Aerospace Division, May 12, 1972.
- 1-9. Flywheel Drive System Study, LMSC-D246393, July 31, 1972. R. R. Gilbert, et al.

Appendix 1-A - SELECTION OF MISSION CLASS REPRESENTATIVE VEHICLES

Vehicle selection was directed toward two objectives. First, each vehicle was to be representative of the given mission class. Performance requirements peculiar to that mission class had to be present in the vehicle representing that class. Second, it was desired that each vehicle expose IPACS to as many design issues as possible. Selected vehicles must show a spectrum of performance requirements to meet this objective.

Approach to Vehicle Selection

Input data consisted of the Fleming and von Braun NASA mission models and subsystem performance data for various candidate vehicles. The approach consisted of a two level screening within each mission class and a final screening of candidate vehicles across mission classes.

Missions listed in both mission models were tabulated according to the four defined mission classes. The planetary missions were taken from the von Braun model and most of the satellites were taken from the Fleming plan. Similar vehicles were combined in families to reduce the candidates to be considered. Those missions scheduled earlier than 1975 were excluded because an IPACS could not be incorporated into the design of these missions within the available development time. Non-NASA missions were also excluded because candidate missions among the NASA programs provide as wide a variation of requirements as necessary to ensure in-depth evaluation of IPACS candidates.

Preliminary screening within each mission class consisted of two phases. In the first phase vehicle size, pointing accuracy and power levels were compared with the average characteristics of the mission class. Compatibility of the recommended attitude control and power subsystem concept with IPACS was also examined. If this screening did not provide a clear cut selection, a second screening phase determined the availability of reference data to the study team and was employed as a selection criteria.

Final screening of candidates was accomplished by comparing the candidate vehicles across mission classes. This step was accomplished to ensure establishment of a wide spectrum of design requirements to expose as many IPACS design issues as possible.

Mission Class Evaluation

The unmanned satellite class was subdivided into three subclasses of (a) near-earth orbit, (b) geosynchronous orbit and (c) planetary spacecraft. Each class is considered in the paragraphs to follow.

Near-Earth Orbit Satellites.- Table 1-A-I presents comparative data for 22 satellite vehicles scheduled to fly during the 1975 to 1990 time frame with orbital altitudes ranging from 370 to 1850 kilometers (200 to 1000 n.mi.).

Spin stabilized or dual spin spacecraft were rejected because of the incompatibility of their control configuration with the efficient storage of electrical energy.

The screening of spin and dual spin satellites left twenty missions to be considered. Additionally, the Bioexplorer was rejected because it uses cold gas and extendable booms. The Primate and Plant Experiment satellites were rejected because their power levels are an order of magnitude greater than the range of the rest of the satellites tabulated. The Plasma Physics and Perturbation satellite was rejected because of inadequate data.

The remaining sixteen missions were retained for screening on an overall mission/class basis. By this means the unmanned satellite requirement when considered across all missions, could serve to add to the scope of the overall study and fill in requirements voids which might occur through similarities in the selection of the other spacecraft classes. The final selection is discussed further in the Mission Class Comparison section.

Geosynchronous Orbit Satellites.- Table 1-A-II lists the candidate geosynchronous satellites. This family was more readily screened than the near-earth satellites.

The Tracking and Data Relay Satellite (TDRS) was selected as the candidate geosynchronous satellite for the following reasons: (1) it has design characteristics representative of the class, (2) Rockwell International, Space Division has an in-house study of a three-axis stabilized TDRS providing a convenient source of detailed data, and (3) it provides insight into IPACS applications to communication-type satellites which have been the type most frequently placed in geosynchronous orbit.

Planetary Vehicles.- Table 1-A-III illustrates the planetary missions scheduled in the 1975 to 1990 time frame. The planetary vehicles can be broken down into the subclasses with unique characteristics; the inner and the outer planet missions.

Outer planet missions were selected as the more significant type for IPACS evaluation. Radioisotope/thermal electric power generation (RTG) devices are used instead of solar arrays because of the decrease in solar energy with distance from the sun. This difference will allow determination of the effects of integration of an IPACS with an alternative power source to the solar array.

Planning for outer planet missions centers around the use of Pioneer and Mariner vehicles. Spin stabilization eliminates the Pioneer vehicles from further consideration for reasons explained previously. The Mariner series of vehicles is a family with very similar requirements and characteristics

TABLE 1-A-I.- NEAR EARTH SATELLITE MISSIONS

MISSION/VEHICLE	LAUNCH DATE	MISSION DURATION YEARS	ORBIT CHARACTERISTICS		WEIGHT Kg (L.B)	POINTING		ATTITUDE CONTROL CONCEPT	POWER LEVEL	POWER CONCEPT
			INCLINATION DEGREE	ALT Km(mi)		DIRECTION	ACCURACY			
SMALL ATS	1979	1 YR	POLAR	555-5550 (300-3000)	135 (300)	EXP DEP	10 SEC	3 AXIS N ₂ H ₄	500W	SOLAR ARRAY BATT (SAB)
COOPERATIVE APPS SATELLITE	1979	2 YRS	LOW TO POLAR	555-5550 (300-3000)	90 to 360 (200 to 800)	EARTH	10 SEC	3 AXIS & SPIN N ₂ H ₄	420W	SAB
ORBITAL SUPPORT MISSIONS	--	3 YRS	0->+30	650 (350)	2300 (5080)	SUN & STELLAR	1 SEC	WHEELS	--	SAB
ASTRONOMY EXPLORER A	1979	3 YRS	28.5	500 (270)	340 (860)	SUN & STARS	--	WHEELS & GRAV GRAD	100W	SAB
ORBITING SOLAR OBSERVATORY	1980	1 YR	28.5	650 (350)	860 (1900)		5 SEC	3 AXIS N ₂ H ₄	300W	SAB
BIOEXPLORER	1978	180 DAYS	0->90	465 (250)	190 (420)	--	ARRAY ORIENT- TATION ONLY ± 1°	COLD GAS & BOOMS	150W	SAB
PRIMATE EXPERIMENT	--	1 YR	55°	500 (270)	1065 (2350)	--	--	--	4 KW	--
PLANT EXPERIMENTS	--	UP TO 1 YR	0->90°	500 (270)	2260 (5000)	--	--	--	3.4 KW	--
LOWER MAGNETOSPHERE EXPLORER	1979	1 YR	POLAR	185-3700 (100-2000)	525 (1160)	EARTH	2°	SPIN GRAV GRAD	100W	SAB
PLASMA PHYSICS & PERTURBATION	--	--	55	500 (270)	250 (550)	--	± 0.5°	--	350W	--
GENERAL RELATIVITY (A,C,E)	1981	1 YR	90	555 (300)	670 (1450)	--	1.0 SEC	3 AXIS WHEELS	700W	SAB
EARTH OBSERVATION SATELLITE	1978	2 YRS	SUN SYNCH	925 (500)	900 TO 2700 (2000 to 6000)	EARTH	± .005° TO ± 1°	3 AXIS WHEELS & N ₂ H ₄	450W TO 5 KW	SAB
POLAR EARTH OBSERVATION SATELLITE	1975	2 YRS	SUN SYNCH	925 (500)	1130 (2500)	EARTH	0.07°	3 AXIS WHEELS & N ₂ H ₄	600W	SAB
EARTH PHYSICS SATELLITE	1980	2 YRS	POLAR	740-1850 (400-1000)	260 (580)	EARTH	1 SEC	3 AXIS WHEELS & N ₂ H ₄ OR GRAV GRAD	200W	SAB
TIROS	1976	4 YRS	SUN SYNCH	1300 (700)	450 (1000)	EARTH	1°	3 AXIS	200W	SAB
EARTH PHYSICS SATELLITE -SEA	1980	[1 YR]	30 TO 90	740 (400)	295 (650)	EARTH	30 SEC	3 AXIS WHEELS + N ₂ H ₄	250W	SAB
EARTH PHYSICS SATELLITE - MAGNETIC	1980	[1 YR]	30 TO 90	370 (200)	295 (650)	EARTH	30 SEC	3 AXIS WHEELS + N ₂ H ₄	250W	SAB
SMALL APPLICATIONS TECH SATELLITE	--	1 YR	0 TO 90	555-5550 (300-3000)	180 (395)	--	--	SPIN STABILIZED	150W	SAB
EARTH RESOURCES SURVEY OPERATIONAL SATELLITE - I	--	2 YRS	SUN SYNCH	740 (400)	1130 (2500)	EARTH	1 SEC	3 AXIS WHEELS & N ₂ H ₄	600W	SOLAR ARRAY OR RADIOISOTOPE
EARTH RESOURCES SURVEY OPERATIONAL SATELLITE - II	--	2 YRS	SUN SYNCH	925 (500)	1310 (2900)	EARTH	1 SEC	3 AXIS WHEELS & N ₂ H ₄	700-1000W	SOLAR ARRAY OR RADIOISOTOPE
POLAR EARTH RESOURCES	1979	2 YRS	SUN SYNCH	925 (500)	1130 (2500)	EARTH	0.07 DEG	3 AXIS WHEELS & N ₂ H ₄	600W	SAB
POLAR ERS	1986	2 YRS	SUN SYNCH	925 (500)	1130 (2500)	EARTH	0.07 DEG	3 AXIS STAB N ₂ H ₄	600W	SAB

TABLE 1-A-II.- GEOSYNCHRONOUS MISSIONS

MISSION/VEHICLE	LAUNCH DATE	MISSION DURATION YEARS	ORBIT CHARACTERISTICS		WEIGHT Kg(LB)	POINTING		ATTITUDE CONTROL CONCEPT	POWER LEVEL	POWER CONCEPT
			INCLINATION DEGREE	ALT Km(nmil)		DIRECTION	ACCURACY			
EXPLORERS	1974	--	0	35,800 (19,300)	475 (1,050)	SUN & STARS	10 SEC		100W to 1.5 KW	SAB
SYNCHRONOUS EARTH SURVEY	1980	2 YRS	0		1290 (2,840)	EARTH	10 SEC	MOMENTUM WHEELS	400W	SOLAR ARRAY/ BATT (SAB)
SYNCHRONOUS EARTH OBSERVATION SATELLITE/PROTO	1990	--	0		1310 (2,890)	EARTH	10 SEC		400W	(SAB)
APPLICATIONS TECH SATELLITE	1973	5 YRS	0		4190 (9,240)	EARTH	0.05 - 0.2 DEG	3 AXIS	8 KW	(SAB) ALSO NUCLEAR
SMALL APPLICATIONS SATELLITE	1976	1 YR	0		585 (1,290)	EXPT DETERMINED	10 SEC	3 AXIS & SPIN	500W	(SAB)
TRACKING & DATA RELAY SATELLITE	1977	3 YRS	0		1290 (2,720)	EARTH	0.2 DEG	SPIN OR 3 AXIS	300/180W	(SAB)
DISASTER WARNING SATELLITE	1978	2 YRS	0		460 (1000)	EARTH	10 SEC	3 AXIS N ₂ H ₄	400W	(SAB)
SYSTEM TEST SATELLITE	1980	1 YR	0		1075 (2,370)	EARTH	0.2 DEG	3 AXIS OR SPIN	1 KW	(SAB)
COOPERATIVE APPLICATIONS	1975	2 YRS	0	35,800 (19,300)	915 (2,020)	EARTH	10 SEC	3 AXIS & SPIN	420W	(SAB)

TABLE 1-A-III.- PLANETARY MISSIONS

MISSION/VEHICLE	LAUNCH DATE	MISSION DURATION YEARS	ORBIT CHARACTERISTICS			WEIGHT kg(lb)	POINTING		ATTITUDE CONTROL CONCEPT	POWER LEVEL	POWER CONCEPT
			INCLINATION DEGREE	ALT km(A.U.)	AT		DIRECTION	ACCURACY			
MARS VIKING	1979	1 YR	ECLIPITIC	2.71×10^8 (1.52)	772 (a) (230) (b)	3500 (a) (772) (b)		1.0 DEG	3 AXIS H ₂ H ₄	80W	SAB
VENUS PIONEER	1976	1 YR		1.08×10^8 (0.72)	1075	1075		0.5	SPIN		SAB
VENUS RADAR MAPPER	1964	2 YRS		1.08×10^8 (0.72)	340	7,500	VENUS	0.1	3 AXIS H ₂ H ₄	1 KW	SAB
VENUS LARGE LANDER	1969	1 YR		1.08×10^8 (0.72)	4000	10,000		1.0	3 AXIS H ₂ H ₄	700W	SAB
MERCURY ORBITER	1967	2 YRS		0.58×10^8 (0.39)	660 (c) (335) (b)	1,630 (c) (740) (b)		1.0	SPIN CH ₂	200W	SAB
PIONEER - JUPITER FLYBY	1973	2 YRS		7.78×10^8 (5.20)	300	(705)		1.0	SPIN H ₂ H ₄	207W	RTIC
PIONEER - JUPITER ORBITER	1978	3 YRS		7.78×10^8 (5.20)	880 (c) (330) (b)	1,940 (c) (705) (b)		1.0	SPIN H ₂ H ₄	207W	RTIC
MARINER - JUPITER/SATURN FLYBY	1977	3 YRS		14.3×10^8 (9.54)	680	15,000		± .05	3 AXIS H ₂ H ₄	400W	RTIC
MARINER - JUPITER/URANUS FLYBY	1979	6 YRS		28.7×10^8 (19.18)	680	15,000		± .05	3 AXIS H ₂ H ₄	400W	RTIC
PIONEER - JUPITER PROBE	1982	2 YRS		7.78×10^8 (5.20)	545 (c) (330) (b)	1,200 (c) (705) (b)		1.0	SPIN H ₂ H ₄	220W	RTIC
PIONEER - SATURN PROBE	1984	3 YRS		14.3×10^8 (9.54)	485 (c) (270) (b)	985 (c) (541) (b)		1.0	SPIN H ₂ H ₄	180W	RTIC
MARINER - JUPITER ORBITER	1966	3 YRS		7.78×10^8 (5.20)	630	14,000		± .05	3 AXIS H ₂ H ₄	—	RTIC
URANUS PROBE/NEPTUNE FLYBY	1986	11 YRS		45.0×10^8 (30.06)	1115 (c) (625) (b)	2,460 (c) (1,100) (b)		± .05	3 AXIS H ₂ H ₄	—	RTIC
MARINER - SATURN ORBITER	1989	3 YRS	ECLIPITIC	14.3×10^8 (9.54)	1,090 (c) (490) (b)	2,400 (c) (1,050) (b)		± .05	3 AXIS H ₂ H ₄	—	RTIC
ENCKE SLOW FLYBY	1979	2 YRS	11.5	1.73×10^8 (0.14)	300	1770		1.0	SPIN CH ₂	200W	SAB
ENCKE RENDEZVOUS	1984	3 YRS	11.5	1.73×10^8 (0.14)	305	1800		1.0	SPIN CH ₂	200W	SAB
ASTEROID RENDEZVOUS	1989	4 YRS	ECLIPITIC	4.34×10^8 (2.9)	880	19,000		1.0	SPIN CH ₂	6.5 KW	SAB

(a) ADDESPACE FLEET MISSION PLAN

(b) ORBITER & LANDER

(c) ORBIT

(d) TRANSIT

(1) PIONEER POTENTIAL MISSION OPTIONS MARCH 14, 1972 NASA-JAMES RESEARCH CENTER

(2) N.R. SEP SURVEY DATED JULY 1, 1971

(3) PROJECT PLAN FOR HELIOS - A & B; GESCHLUSST FÜR WELTRAUMFORSCHUNG NIKH DATED MARCH '71

Therefore, the Mariner-Jupiter/Saturn Flyby Mission was selected because it is the first of the series of outer planet Mariner flights tabulated. Since this family of missions will be accomplished by the same vehicle, it is better to trade off IPACS for the first mission than assume that retrofitting IPACS can be cost-effective for later missions.

Thirty-Day Shuttle Missions.- IPACS applications could be made to either the shuttle vehicle or the shuttle payload. The shuttle could employ an IPACS for peaking power requirements, especially for the operation of landing gear and control surface hydraulics. However, hydrazine APU's have been selected for this specific application. Other peaking requirements are within the capability of the shuttle fuel cell assembly. Since the design decisions for the shuttle have been made and IPACS development time is inconsistent with that of the shuttle, use of IPACS on the shuttle itself was rejected. Use of IPACS as a shuttle payload energy storage device was examined in detail.

Table 1-A-IV lists the thirty-day shuttle payloads identified in the RAM (Reference 1-A-1) and the NR space station studies. Search of the literature was unable to identify any other thirty-day shuttle payloads formally defined. None of these missions lend themselves to an IPACS application. Power subsystem concepts formulated for all missions incorporate fuel cells with adequate capacity to handle defined average and peak loads. The RAM has its own 7 kw fuel cell which exceeds the load defined for its mission. All of the 30M series are dependent on the shuttle electrical power subsystem which can supply up to 6 kw to its payload.

Extension of the shuttle mission from 7 to 30 days requires additional fuel cell reactant storage as the power subsystems are currently configured. An alternative would be a solar array/IPACS kit for mission extension. Preliminary evaluation rejected this alternative on the basis of cost. A tank farm of up to 14 cryogenic tanks of the same design as currently defined for the shuttle can accommodate the 30-day sortie mission. Only recurring costs for the tanks and an installation cost are incurred. This amount will be much less than the development plus recurring costs of a solar array/IPACS concept.

A model 30-day shuttle sortie mission that has potential for an IPACS application was developed to examine this mission class. The mission is a combination of two sortie missions, the Earth Observation and Contamination Technology mission (30M-1) and a RAM material science payload, M1S2B. The power profile of M1S2B was superimposed on that of 30M-1. This power profile is similar to ten RAM payloads which have peak power levels that exceed the

TABLE 1-A-IV.- 30-DAY SHUTTLE MISSIONS

MISSION/VEHICLE	LAUNCH DATE	MISSION DURATION	ORBIT CHARACTERISTICS		WEIGHT Kg(LB)	POINTING		ATTITUDE CONTROL CONCEPT	POWER LEVEL KW	POWER CONCEPT
			INCLINATION DEGREE	ALT Km(ft)		DIRECTION	ACCURACY			
RAM LIFE SCIENCES	1990	30 DAY	ANY	450 (250)	97500 (215 000)	--	--	--	4.6	RAM FUEL CELL
EARTH OBSERVATION CONTAMINATION TECH	1979		55	500 (270)		EARTH	±.5°	CMG'S	2.96	SHUTTLE FUEL CELL SUPPORT
SPACE PHYSICS PHYSICS & CHEMISTRY	1979		28½	370 (200)		EARTH	2°	GIMBAL PLATFORM	3.06	
FLUID MANAGEMENT	1980		28½	555 (300)		--	--		3.22	
MEDICAL RESEARCH LIFE SUPPORT/MAN SYSTEMS	1980		28½	500 (270)		--	--		2.11	
X-RAY STELLAR ASTRONOMY	1980		28½	740 (400)		STELLAR	± 1 SEC	CMG'S	2.20	
ADV SOLAR ASTRONOMY	1980		SUN SYNCH	410 (220)		SOLAR	± 1 SEC	CMG'S	2.64	
INTERMEDIATE UV TELESCOPE	1981		28½	450 (250)		STELLAR	5 SEC	CMG'S	2.22	
HIGH ENERGY STELLAR ASTRONOMY	1981		28½	740 (400)		STELLAR	6 MIN	CMG'S	1.98	
INFRARED ASTRONOMY	1982		55	500 (270)		STELLAR	1 SEC	CMG'S	2.22	
COSMIC RAY PHYSICS	1980		28½	370 (200)		STELLAR	5°	SHUTTLE SUPPORT ONLY	2.47	
COMMUNICATIONS	1981	30 DAY	55	280 (150)	97500 (215 000)	EARTH	±.01°	GIMBALED PLATFORM	2.57	SHUTTLE FUEL CELL SUPPORT

available fuel cell power supply. M1S2B has the largest energy storage requirement of all and therefore provides an upper boundary for IPACS application. The 30M-1 sortie mission has pointing requirements reasonable for a vehicle of the size of the shuttle. Other 30-day missions were rejected because they either had no pointing requirement or too fine a pointing requirement. The resultant payload combination, then, has attitude control and peak power requirements that lend themselves to an IPACS application and is representative of the sortie class of missions.

RAM.- The RAM (reference 1-C-1) has three accommodation modes -- shuttle attached operations, space station attached, and free-flyers. The first two types of accommodation have been assigned a separate mission class in this study by the statement of work. Therefore, free-flying RAM's were the only accommodation mode considered for the RAM mission class. This accommodation mode also is the only RAM configuration which has both solar array power generation and momentum exchange devices for attitude control.

Table 1-A-V lists the free-flying RAM payloads. Only the astronomy missions are considered significant to further IPACS evaluation. Two of the technology experiments are subsatellites that are carried piggyback with other RAM experiments and therefore do not typify the mission class. The Fluid Management RAM was rejected because it does not have a pointing requirement.

Of the four astronomy free-flyers, there is little difference in characteristics. All vehicles require very accurate pointing, therefore not providing a discriminator. The Advanced Solar Observatory, A303B, was selected as the candidate RAM vehicle to subject the IPACS concepts to the highest power storage requirement possible while maintaining the tightest pointing requirement of all mission classes.

Modular Space Station.- Two modular space station studies have been accomplished (reference 1-C-2). Their characteristics are similar excepting size and configuration. Table 1-A-VI compares the two designs. The weight of the two designs is indicative of the design differences. Rockwell, Space Division developed a nine-module concept arranged in the shape of cruciform. McDonnell/Douglas (MACDAC) developed a design made up of only three modules shaped like an elbow. The asymmetrical shape of the MACDAC design led to a higher momentum storage requirement than the Rockwell design (11,400 n-m-sec versus 3000 n-m-sec). Conversely, the Rockwell design has a higher power requirement than the MACDAC, 19 kilowatts versus 15 kilowatts.

A significant difference between the two designs is the choice of energy storage concepts. Rockwell selected a regenerative fuel cell concept after trading it off against NiCd batteries. Design characteristics were developed for both designs, however. MACDAC adopted the more conventional battery approach.

The Rockwell design was selected for the IPACS evaluation because it would allow IPACS to be traded off against two electrical energy storage concepts and it has the largest energy storage requirements of all mission classes.

TABLE 1-A-V.- RAM FREE-FLYER MISSIONS

MISSION/VEHICLE	LAUNCH DATE	MISSION DURATION YEARS	ORBIT CHARACTERISTICS		WEIGHT Kg(LB)	POINTING		ATTITUDE CONTROL CONCEPT	POWER LEVEL	POWER CONCEPT
			INCLINATION DEGREE	ALT Km(ftmil)		DIRECTION	ACCURACY			
A103B X-RAY ASTRON OBS	1982	4-6 YRS	0-55	370 (200)	13400 (29,500)	STELLAR	1 SEC	3 AXIS N ₂ H ₄	2.27 KW	SOLAR ARRAY BATT
A203B ADV STELLAR OBS	1980	4-6 YRS	45-55	460 (250)	--	STELLAR	1 SEC	3 AXIS N ₂ H ₄	2.30 KW	SOLAR ARRAY BATT
A303B ADV SOLAR OBS	1986	4-6 YRS	45-55	500 (270)	12200 (27,000)	SUN	1 SEC	3 AXIS N ₂ H ₄	3.4 KW	SOLAR ARRAY BATT
A503B HI ENERGY STELLAR	1990	4-6 YRS	0-55	370 (200)	9050 (20,000)	STELLAR	± 2 SEC	3 AXIS N ₂ H ₄	2.5 KW	SOLAR ARRAY BATT
T103B CONTAMINATION MEAS		4-6 YRS	PIGGYBACK SUB SATELLITE			N/A	N/A		0.5 KW	SOLAR ARRAY BATT
T202B FLUID MGMT		6 m +	SUN SYNC	500 (270)		N/A	N/A		1.0 KW	SOLAR ARRAY BATT
T401A ADV S/C SYS			PIGGYBACK SUB SATELLITE			N/A	N/A		0.5 KW	

TABLE 1-A-VI.- SPACE STATION MISSIONS

MISSION/VEHICLE	LAUNCH DATE	MISSION DURATION YEARS	ORBIT CHARACTERISTICS		WEIGHT Kg(LB)	POINTING		ATTITUDE CONTROL CONCEPT	POWER LEVEL	POWER CONCEPT
			INCLINATION DEGREE	ALT Km(ftmil)		DIRECTION	ACCURACY			
NR SPACE STATION	1985	10 YRS	28.5-55°	370-555 (200-300)	~ 81500 ~ (180,000)	EARTH	0.25°	CMG'S H ₂ O	19 KW	SOLAR ARRAY REGEN FIC
MAC DAC SPACE STATION	1985	10 YRS	28.5-55°	370-555 (200-300)	~ 27200 ~ (60,000)	EARTH	0.25°	CMG'S N ₂ H ₄	15 KW	SOLAR ARRAY BATT

Mission Class Comparisons

The candidates identified for each mission class were then compared in their relationship to each other to assure that the IPACS would be exposed to as many issues as possible. Table 1-A-VII compares the candidates with respect to key IPACS design issues. Selection of the near-earth orbit satellite resulted from an evaluation of this comparison data.

Representative Missions Selected for Conceptual Design Studies

The TDRS and free-flying RAM vehicles were recommended for conceptual design penetration. This recommendation was subsequently accepted by the NASA/LRC.

Conclusions

The selected vehicles met both of the original objectives, i.e., that of being representative of the individual mission classes and exposing IPACS to a broad cross section of issues. Table 1-A-VII shows how well the selected vehicles expose the IPACS to design issues. The EOS satellite provides the coarsest pointing vehicle. It also required study of the effects of a sun synchronous orbit on IPACS. TDRS allowed understanding of the effects of geosynchronous orbit conditions on IPACS design. The planetary vehicle allowed examination of the usefulness of IPACS with a constant power generation concept. The shuttle mission enabled determination of the IPACS effectiveness with a very large vehicle. The RAM mission exposed the IPACS to extremely fine pointing requirements. Finally, the modular space station selection required examination of the impact of large electrical energy requirements and pitted the IPACS against the regenerative fuel cells, another promising energy storage alternative to the NiCd battery.

TABLE 1-A-VII.- MISSION CLASS COMPARISON

	LAUNCH DATE	MISSION DURATION	MANNING	ORBIT CHARACTERISTICS Km/(nmi)	WEIGHT Kg(LB)	POINTING ACCURACY DEGREE	MOMENTUM STORAGE/ TRANSFER REQUIREMENT N-m-sec FT-LB-SEC	POWER LEVEL WATTS	POWER DEMAND PROFILE	REMARKS
NEAR EARTH SATELLITE: EARTH OBSERVATIONS SATELLITE	1978	2 YRS	UNMANNED	1100 [SUN SYNCH] (600)	770 (1700)	1.0		100W	STEADY	EARTH OBSERVATORY SOLAR ARRAY/BATT
GEOSYNCHRONOUS SATELLITE: TRACKING & DATA RELAY SATELLITE	1977	3 YRS	UNMANNED	35,700 (19,300) 0°	1230 (2717)	0.2	.678 (10.5)	300/1800	STEADY POWER DOWN IN SHAPE	COMMUNICATIONS SATELLITE SOLAR ARRAY/BATT
PLANETARY SATELLITE: MARINER - JUPITER/SATURN	1977	4 YRS	UNMANNED	1.43 x 10 ⁸ (9.5A.U.) 30°	630 (1500)	0.05		400W	STEADY TILL PLANET ENCOUNTER THEN POWER UP	SCIENTIFIC SATELLITE RTG
SHUTTLE 30 DAY MISSION: EARTH OBSERVATION & CONTAMINATION TECHNOLOGY	1979	30 DAYS	MANNED	500 (270) 59°	97,500 (215,000)	0.5	9380 (6900)	10,840W	STEADY	EARTH RESOURCES FUEL CELL
RAM: ADVANCED SOLAR OBSERVATORY	1986	4-6 YRS	UNMANNED OPS, MAINTENANCE	500 (270) 45 to 55°	17200 (27,000)	1 SEC	2038 (1500)	3,400W	STEADY	ASTRONOMY SOLAR ARRAY/BATT
MODULAR SPACE STATION: NORTH AMERICAN DESIGN	1985	10 YRS	MANNED	500 (270) 59°	81500 (180,000)	0.25	3000 (2200)	19,000W	FLUCTUATE W/CREW DAY NIGHT CYCLE	GENERAL PURPOSE SOLAR ARRAY/REGEN FC

References

- 1-A-1. Research and Applications Modules (RAM) Phase B Study. Technical Data Document. Volume 1-4.1 Requirements Analysis and Definition.
Appendix A - Derived System Requirements. Convair Aerospace Division of General Dynamics, GDCA-DDA72-003B, Rev. B (May 12, 1972).

APPENDIX 1-B - SPACECRAFT REQUIREMENTS

Spacecraft requirements are presented below for each of the six selected reference missions.

Spacecraft requirements - EOS.-

Flight envelope: Payload capabilities to sun-synchronous orbit from Western Test Range (WTR) is 1088 kg (2400 lbs) to 976 km (525 nm) altitude. A proposed growth version with 3 Castor III solids and 6 Castor II has 1313 kg (2900 lb) capability to this altitude. Future growth versions go up as high as 1585 kg (3500 lb). The orbit is nominally high noon sun synchronous with an inclination of 1.74 rad (100 deg).

Mission duration: Vehicle lifetime is targeted for 2 years.

Reliability and maintainability: Subsystem reliability will be accomplished by providing redundancy to vehicle critical equipment. The vehicle will not be designed maintainable, however, the capability for shuttle retrieval and fault correction on the ground is being studied.

Spacecraft requirements - TDRS.-

Launch mode: The vehicle is boosted by a Thor-Delta 2914. The vehicle is spin stabilized during the transfer orbit with active nutation control.

Flight envelope: Two vehicles are nominally operated at synchronous altitude. One is positioned at a longitude of approximately 0.26 rad (15 deg) West and the other at a longitude of approximately 2.53 rad (145 deg) West. The selected orbit inclination is 0.0436 rad (2.5 deg).

Mission duration: The vehicle shall be designed for a minimum operational life of 5 years.

Reliability and maintainability - TDRS: The preliminary reliability apportionment is based upon a total vehicle reliability of 0.8.

The preliminary reliability apportionment for the electrical power subsystem is 0.95.

The preliminary reliability apportionment for the attitude control subsystem is 0.96.

The design shall attempt to eliminate all single point failures by redundancy where feasible.

The vehicle is not designed to be serviced or maintained in orbit.

Spacecraft requirements - MJS.-

Launch phase: The Titan/Centaur/Burner II launch vehicle will inject first into an earth parking orbit and then reignite to provide the mission injection velocity. The spacecraft will maintain communications via the S-band link and the launch vehicle telemetry system during the ascent.

Cruise Phase: The cruise flight phase is defined to include portions of a flight during which the spacecraft is in a relatively quiescent state. The purpose of cruise operations is to acquire science data, monitor the engineering status of the spacecraft, and to accumulate radiometric data for navigation. Some of these sequences will require commanded turn maneuvers of the spacecraft for extended periods of time.

At designated times during flight, the spacecraft will be required to perform trajectory correction maneuvers to improve navigation. The mission operations activity will increase significantly during this period.

Encounter phase: The encounter phase will begin about 40 days before the time of closest approach (encounter) to the planet when the frequency of activities and observations becomes very high. It will last until 40 days following encounter. Following closest approach, an earth occultation period will occur during which all data must be recorded for later playback when the down-link has been reestablished.

Reliability objectives: The mission will be designed to yield a high probability of mission success with a minimum degradation of the planned science return. The following reliability goals derived from a reliability prediction study will be used for the IPACS study.

<u>Subsystem</u>	<u>Reliability at Jupiter (1.5 years)</u>	<u>Reliability at Saturn (3.5 years)</u>
Power	0.944	0.881
Power distribution	0.99984	0.99915
Attitude control	0.983	0.951

Spacecraft requirements - 30 day Shuttle.-

Launch mode: The payload is launched by and remains attached to the shuttle orbiter.

Flight envelope: The experiments are conducted in a 500 km (270 n mi) circular orbit at an inclination of 0.96 rad (55 deg).

Mission duration: The mission duration is 30 days.

Reliability: All critical subsystems/functions (hardware whose failure could result in loss of crew or loss of module) will be designed for any credible combination of two component failures. Conservative factors of safety shall be provided where critical single failure points cannot be eliminated (pressure vessels, plumbing, etc.)

Spacecraft requirements - RAM.-

Launch mode: The vehicle is delivered to orbit by the shuttle.

Flight envelope : The desired orbit is circular with an inclination of less than 0.174 rad (10°) and an altitude of 740 km (400 n mi).

Acceptable orbit characteristics are a circular orbit with an inclination between 0.78 rad (45°) and 0.96 rad (55°) and an altitude of 500 km (270 n mi).

Mission Duration: The mission duration is 5 years.

Reliability: All critical subsystems/functions (hardware whose failure results in loss of crew or loss of module) will be designed for any credible combination of two component failures.

Conservative factors of safety shall be provided where critical single failure points cannot be eliminated (pressure vessels, plumbing, etc.)

As a goal, free flying RAMs will be designed to facilitate their retrieval and recovery by the shuttle in case of the failure of critical onboard systems.

Maintainability: The vehicle shall be designed for on-orbit maintenance in a shirtsleeve environment with a nominal service interval of 6 months.

Manning: The vehicle is manned periodically for on-orbit servicing but nominally operates unmanned.

Spacecraft requirements - MSS.-

Launch mode: The individual modules of the space station are delivered to orbit by the shuttle.

Flight envelope: The vehicle shall be capable of operating at altitudes between 445 and 500 km at an inclination of 0.96 rad (55 deg). Subsystem sizing shall be based on an orbital operating altitude of 445 km (240 nm).

Mission Duration: The operational life of the station shall be 10 years.

Reliability: The redundancy requirements utilized for the MSS subsystems are established by the application of the failure tolerance criteria and associated failure definitions. In addition to the failure tolerance criteria, specific requirements are established for areas that are considered unique. The following table defines the minimum allowable number of component failures which may result in the indicated operational mode.

<u>Operational Mode</u>	<u>Allowable Number of Component Failures to Reach Operational Mode</u>	
	<u>Station Operation (Manned)</u>	<u>Build-up (Unmanned)</u>
Normal	0	0
Nominal	1	-
Degraded	2	1
Emergency	3	2

Maintainability: The maintenance approach established for the MSS is 100 percent on orbit maintenance as a goal utilizing the in flight replaceable unit (IFRU) concept. Where on orbit replacement appears impractical, requirements for long life are established to minimize the need for module return.

The maximum envelope size for an IFRU is 100 x 100 x 127 cm (40 x 40 x 50 in) except IFRU's and expendables for critical functions which must be capable of passing through secondary access hatches of 56 x 56 x 127 cm (22 x 22 x 50 in.).

IFRU's which are part of time critical functions shall allow for two consecutive unsuccessful repairs before resulting in a critical condition.

IFRU's shall not exceed 27 kg (60-lb) where possible (1-g limit for one crew member), 54 kg (120-lb) as an upper limit (zero-g limit for one crew member where practical.

The subsystems shall be designed for the operational life of the station, with resupply of consumables and replaceable items of equipment. This operational life may be obtained through long-life design, and in-place redundancy for critical equipment whose failure could disable the space station or imperil the crew.

APPENDIX 1-C - COMPETITIVE ELECTRICAL POWER AND ATTITUDE CONTROL SUBSYSTEMS DEFINITION

The definition of the conventional electrical power and attitude control subsystems as defined in the original program documents is presented herein. Design data for the subsystems were taken from references 1-C-1 through 1-C-9.

Earth Observatory Satellite (EOS) Control Concept

Concept description. - The baseline attitude control system selected for the EOS was based on the goal of minimum weight using existing hardware or technology. The mechanization shown in figure 1-C-1 uses two reaction wheels installed in a "V" configuration for primary on-orbit stabilization and control. Horizon sensors integral to the reaction wheels are used for the separation, acquisition, correction and on-orbit phase as the basic feedback for the pitch and roll control loops. Yaw attitude errors are determined by gyro-compassing for the acquisition phase only since during normal orbit operations the roll control provided by the V-configuration will couple into yaw control for the earth oriented EOS. A sun sensor for yaw orientation is included to provide for reacquisition if required. A three axis rate gyro package is also included to provide rate stabilization and control during the acquisition and vernier velocity maneuver.

A reaction control system provides primary torque capability during separation, acquisition, vernier injection, and orbit makeup maneuvers. Both magnetic torquers and the reaction control system balance the disturbance torques during normal orbit operations.

Physical characteristics. - Weight and power requirements are summarized in Table 1-C-I.

Development considerations. - The control concept described above is based upon the use of existing technology. No component development is anticipated.

TDRS Control Concept

Concept description. - A functional diagram of the control concept is presented in figure 1-C-2.

The attitude control system selected in the trade studies is the "V" plus a third wheel system. The system was selected over the other candidates primarily on the basis of its reliability relative to the other candidates.

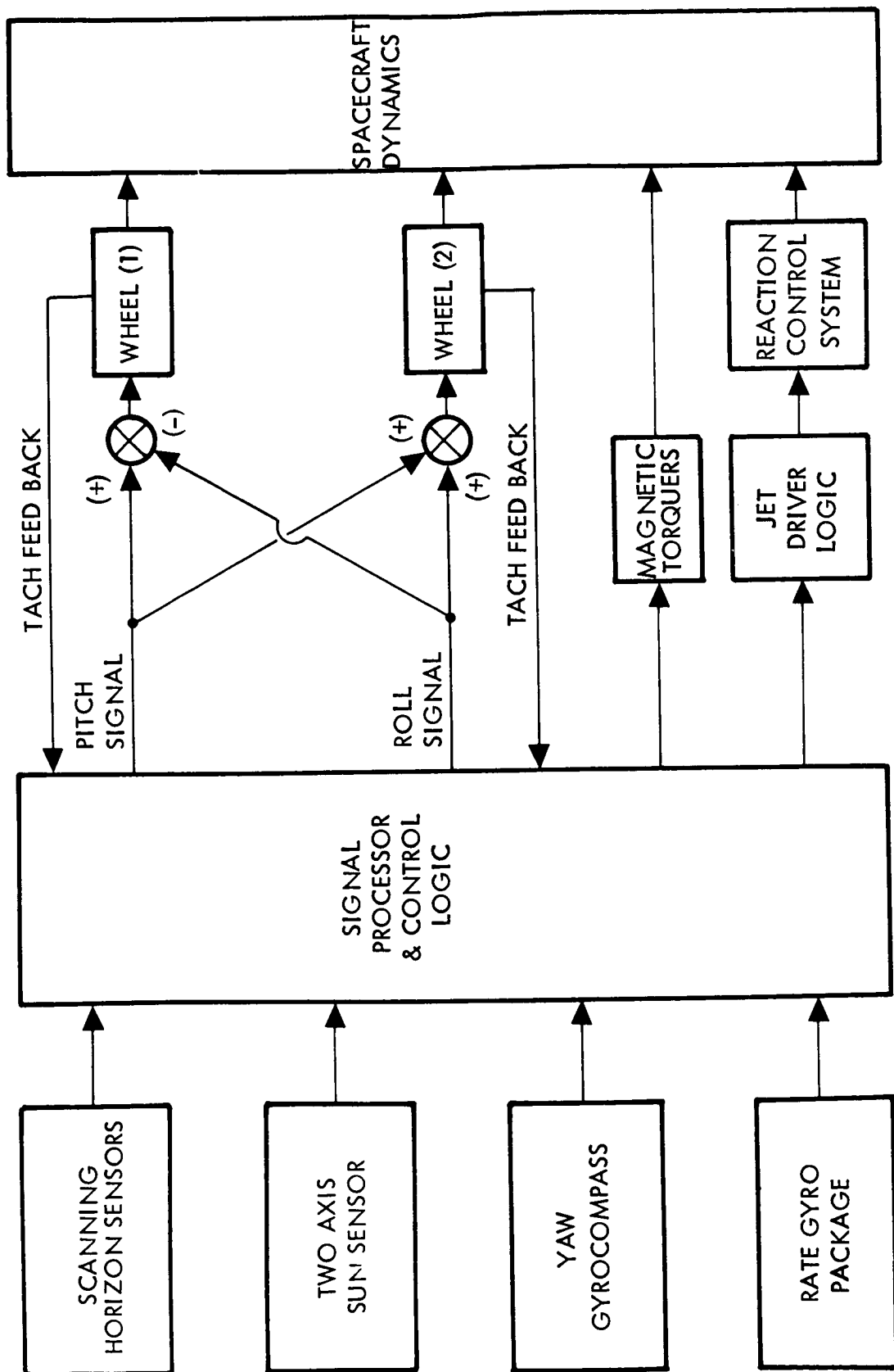


Figure 1-C-1. EOS Control Concept Functional Block Diagram

TABLE 1-C-1.- COMPETITIVE SYSTEM WEIGHT AND POWER SUMMARY

Components	Weight kg (lb)		Power (watts)
Rate gyros	2.3	(5)	20
Sun sensor	1.4	(3)	1
Reaction wheels & horizon sensors	21.8	(48)	16
Magnetic torquers	9.1	(20)	--
Reaction jet system (dry)	16.4	(36)	--
Electronics	5.4	(12)	8
Mounting and wiring	6.8	(15)	--
Solar panel drive	27.3	(60)	20
Total	90.5	(199)	65

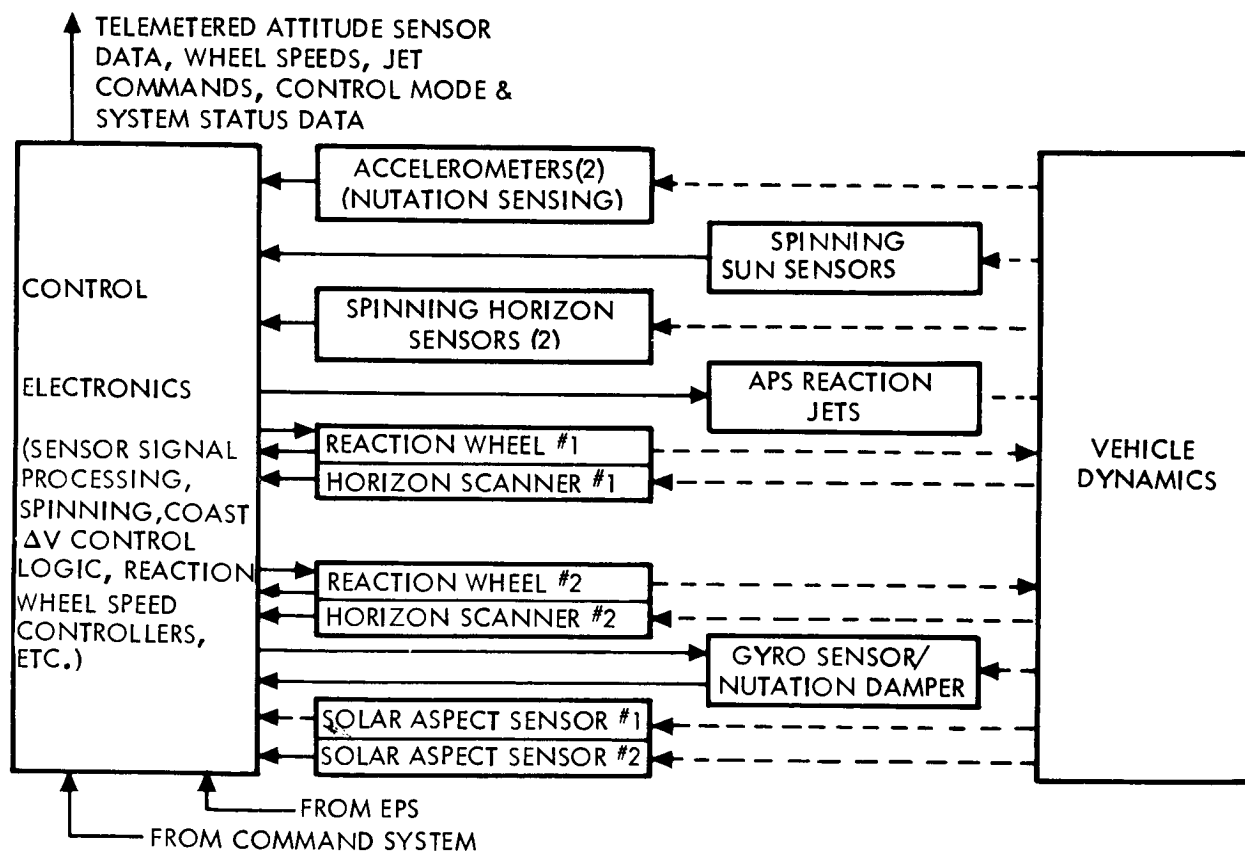


Figure 1-C-2. Functional Diagram - TDRS Control Concept

The system is the only one considered which had no single point failures which would cause the mission to fail. This absence of single point failures was found to produce a marked reliability improvement over the other candidates for the five year nominal satellite lifetime.

The system employs two momentum wheels which are operated with a nominal speed bias and are oriented in a shallow "V" in the Y-Z plane. A gyro is included as the third wheel and performs the dual function of attitude sensing during ΔV maneuvers and momentum transfer for nutation damping in the event of a failure of either momentum wheel in the V pair. The selected momentum wheels were originally developed for the Delta PAC mission and are derivatives of the Nimbus roll reaction wheel/earth scanner assemblies. The horizon scanning of the infrared bolometers is accomplished by the rotational motion of the momentum wheels. The horizon scanners must be modified to scan the earth from synchronous altitude.

A representative control logic for the coasting phase control of the "V" system is discussed below. Pitch and roll error data is derived from the horizon crossing pulses in the system electronics. Pitch control is achieved by driving the two momentum wheels in unison. Active nutation damping is provided by commanding the wheels differentially so as to obtain momentum transfer into the Z body axis. A pure derivative network is utilized in the roll feedback path to obtain nutation damping which is greater than critically damped. The pitch lead/lag network is similar to the Nimbus pitch control compensation.

For the on-orbit control the canted yaw torque RCS jets provide the momentum dumping required for the roll axis control of the momentum bias system. The disturbance induced yaw attitude errors are controlled through the dynamics of the quarter-orbit coupling in the momentum bias system, i.e., yaw error couples into roll after approximately 1.6 rad (90°) of pitch rotation and is removed in the roll channel. Relatively tight tachometer feedback control loops are utilized to provide a momentum command system rather than a torque command system.

The pitch and yaw axis reaction jet momentum dumping control logic will normally be disabled and will be activated no more frequently than once per day. The momentum storage capacity has been sized to permit this. Automatic momentum dumping at more frequent intervals is undesirable because of the larger power requirement of the reaction jet heaters and the jet pulsing duty cycle.

For coasting flight the momentum bias provides the necessary stiffness for passive yaw control. During ΔV maneuvers larger disturbance torques can occur due to the RCS thrust vector misalignment and mounting tolerances necessitating active three axis control. This necessitates the addition of a wide bandpass yaw sensor and the gyro has been selected for this purpose. This gyro has the feature that its spin rate can be modulated about the nominal spin rate thereby providing momentum transfer capability. The gyro is mounted with its spin axis along the X axis of the spacecraft. This permits the two degree of freedom gyro to sense pitch and yaw attitude data as well as transfer momentum into the X axis of the vehicle. Momentum transfer into the X axis is desirable for nutation damping because the closure of a roll sensing control loop into X axis momentum transfer produces very stable nutation damping without the necessity of lead filtering to obtain this stability. Nominally the gyro will not be operated except for ΔV maneuvers. In the event of a momentum wheel failure the gyro will be turned on full time for nutation damping. The

gyro may also be turned on to augment the attitude determination during the infrequent periods when the sun line and the nadir are nearly collinear.

Physical characteristics.- The physical characteristics of the system components are shown in Table 1-C-II.

Development considerations.- The horizon scanner, although previously used at lower altitudes requires minor modification for use at synchronous altitudes.

MJS Control Concept

Concept description.- A functional block diagram of the MJS control concept is presented in figure 1-C-3. This concept is the result of prior Rockwell research and development studies.

TABLE 1-C-II.- TDRS ATTITUDE CONTROL SUBSYSTEM COMPONENT
PHYSICAL CHARACTERISTICS SUMMARY

Component (number used)	Dimensions cm (inches)	Power (W)		Weight	
		av.	max.	kg	lb
Nutation sensing accelerometers (2)	5.8 x 4.3 x 30 (2.3 x 1.7 x 1.2)	2	2	0.27	0.6
Spinning horizon sensors (2)	8.4 x 10.9 x 20 (3.3 x 4.3 x 8)	2.7	2.7	1.82	4.0
Spinning sun sensors (2)	5.6 x 6.1 x 7.6 (2.2 x 2.4 x 3.0)	0.5	0.5	0.91	2.0
Solar aspect sensors (2)	9.4 x 9.7 x 2.3 (3.7 x 3.8 x 0.9)	0.5	0.5	2.04	4.5
Reaction wheel/earth Scanner assemblies (2)	20 dia x 17 (8.0 dia x 6.5)	7	40	12.98	28.6
Electronics	25 x 13 x 15 (10 x 5 x 6)	8	45	5.45	12.0
Yaw Gyro & Nutation Damper (1)	13 x 15 x 15 (5 x 6 x 6)	5	10	2.72	6.0
Total				26.19	57.7

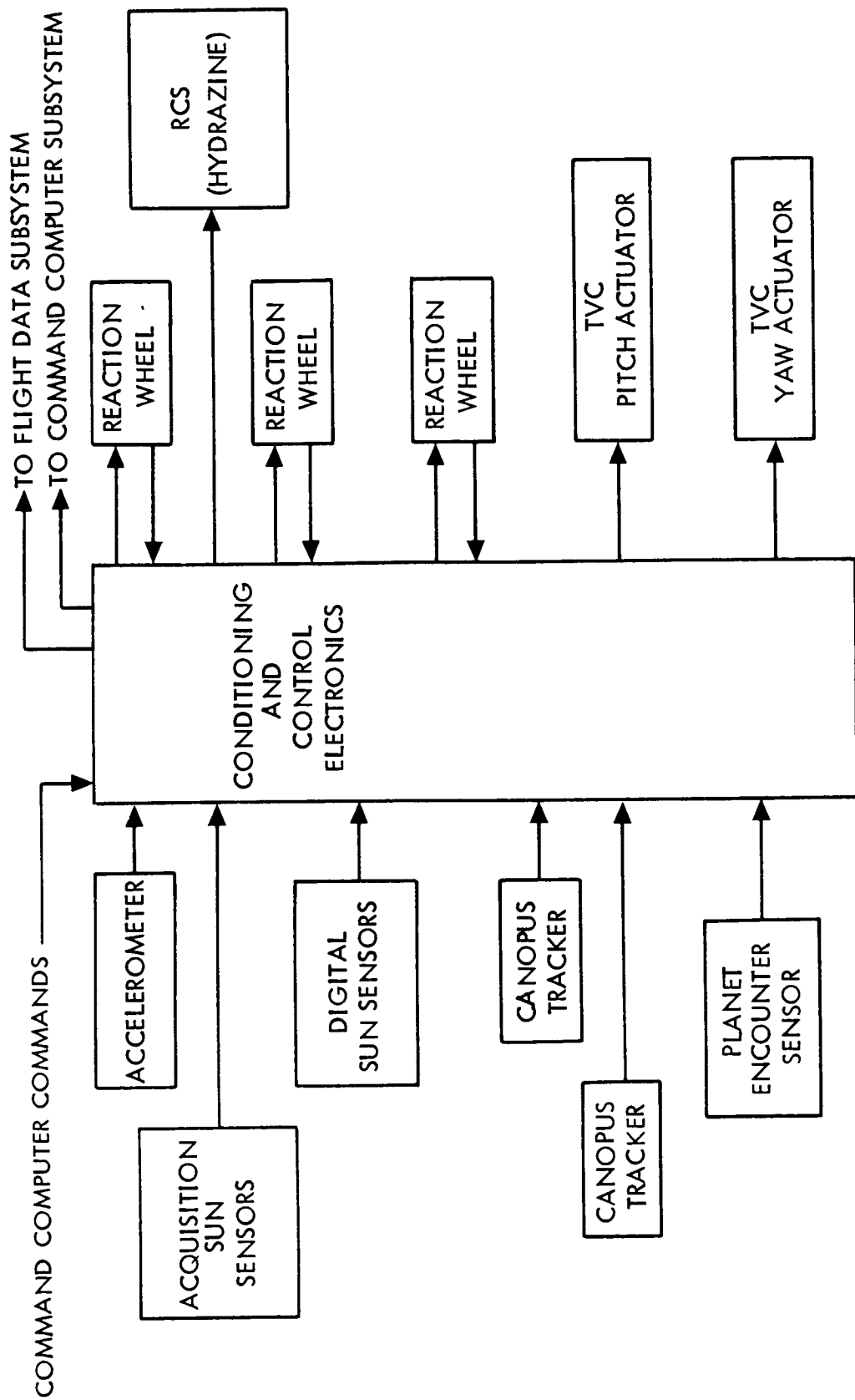


Figure 1-C-3. MJS Attitude Control Subsystem Functional Block Diagram

The wide angle digital sun sensor and redundant Canopus trackers are used as the reference for the long term cruise mode. The vehicle is stabilized in three axes with the boresight axis of the body fixed high gain antenna directed toward earth. Control torques are obtained from modified sensing gyros. These gyros are two axis, free rotor, gas bearing instruments. In the normal cruise mode the gyros are operated as biased reaction wheels. The same gyros are operated as sensing gyros for midcourse maneuvers. The reaction control jets are used for high rate maneuvers and damping booster separation transient. Attitude control during main engine burn is provided by either engine gimbaling or using jet vanes in the main engine exhaust. The accelerometer provides velocity measurements for the main engine burns. The planet encounter sensor is used to generate pointing commands for the science platform.

Thirty-Day Shuttle Control Concept

Concept description. - A functional diagram of the baseline control concept for this mission is presented on figure 1-C-4. The vehicle is controlled by three double gimbal CMG's (Skylab type and size). Orbiter sensors are used as the nominal vehicle reference. A gimbaled platform inertial reference, star trackers, and horizon sensors are available as elements of the basic orbiter. It may be necessary to provide a means of calibrating the orientation of the experiment sensors in the payload bay with respect to the orbiter reference orientation. Figure 1-C-4 shows a pallet mounted gimbaled star tracker used to accomplish this alignment transfer. The pallet tracker would be used to perform simultaneous sightings with the orbiter trackers and flight software would then derive the relative alignment.

Figure 1-C-4 shows typical experiment isolation platforms used to provide angular freedom with respect to the vehicle and improved stability. The RAM Phase B Study evaluated such isolation systems for astronomy experiments on sortie missions. These platforms are precision pointing units consisting of wide angle gimbals which are driven to payload aspect sensing acquisition accuracy. The azimuth and elevation axes are then locked and the experiment signal is used to drive pitch/yaw narrow angle fine point flex pivots. The external, wide angle portion of these platforms, or a modification thereof, should be adequate for the relatively coarse pointing required by the earth observation type experiments on this mission.

A potential concept for control of the CMG's was developed in the RAM study. That concept (extracted from reference 1-C-1) is presented below and diagrammed in figure 1-C-5.

The CMG steering law uses shuttle-supplied attitude and attitude rate error to generate a three-axis torque command vector proportional to attitude error plus attitude rate. The torque command vector is transformed into CMG command gimbal rates by the CMG control law (pseudo-inverse type). This law uses the matrix relating the six gimbal rates to the resultant torque output of the CMG. The inverse of this matrix enables calculation of the desired or command gimbal rates based on the torque command vector.

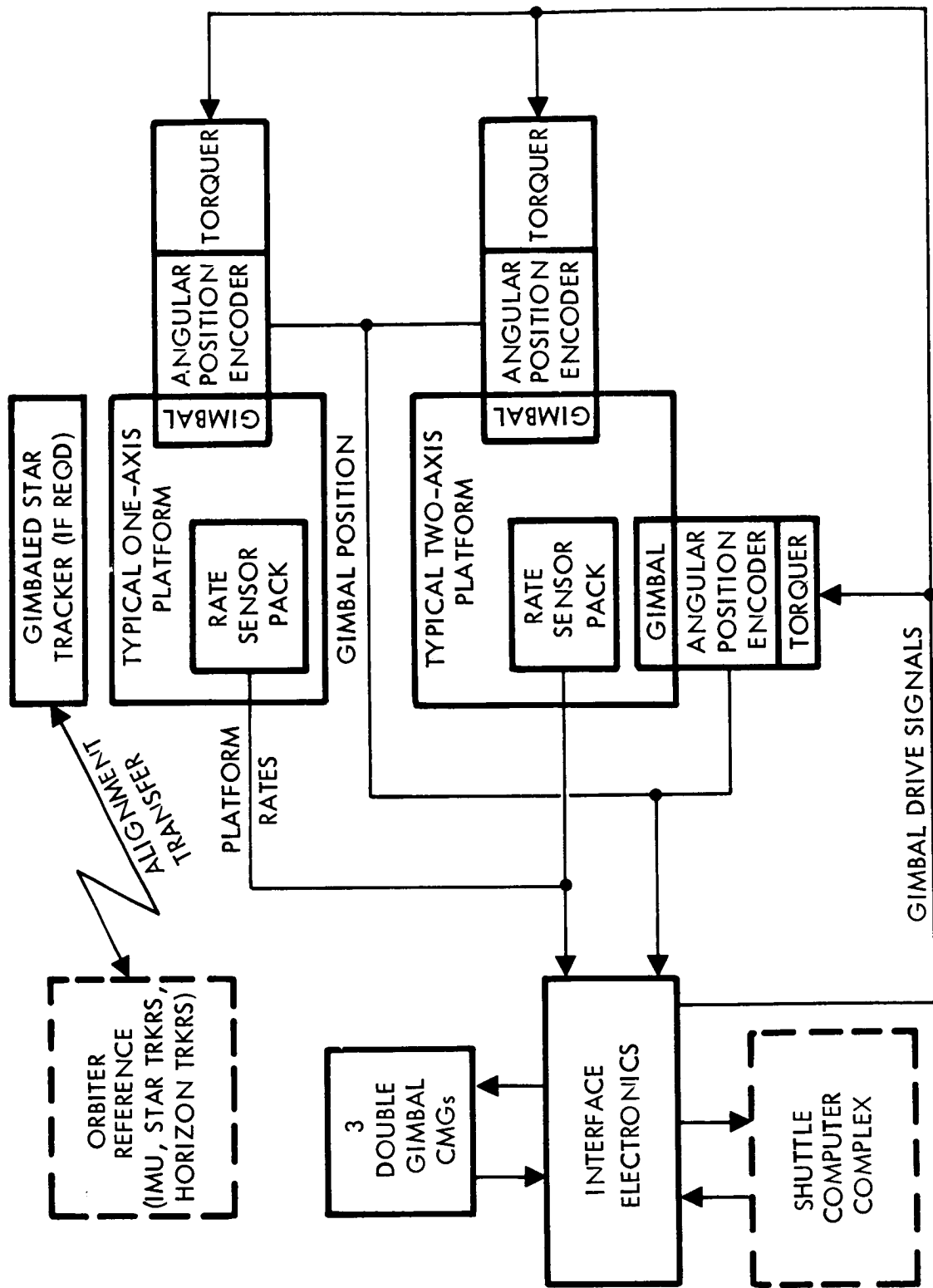


Figure 1-C-4. 30 Day Shuttle Payload Control Concept

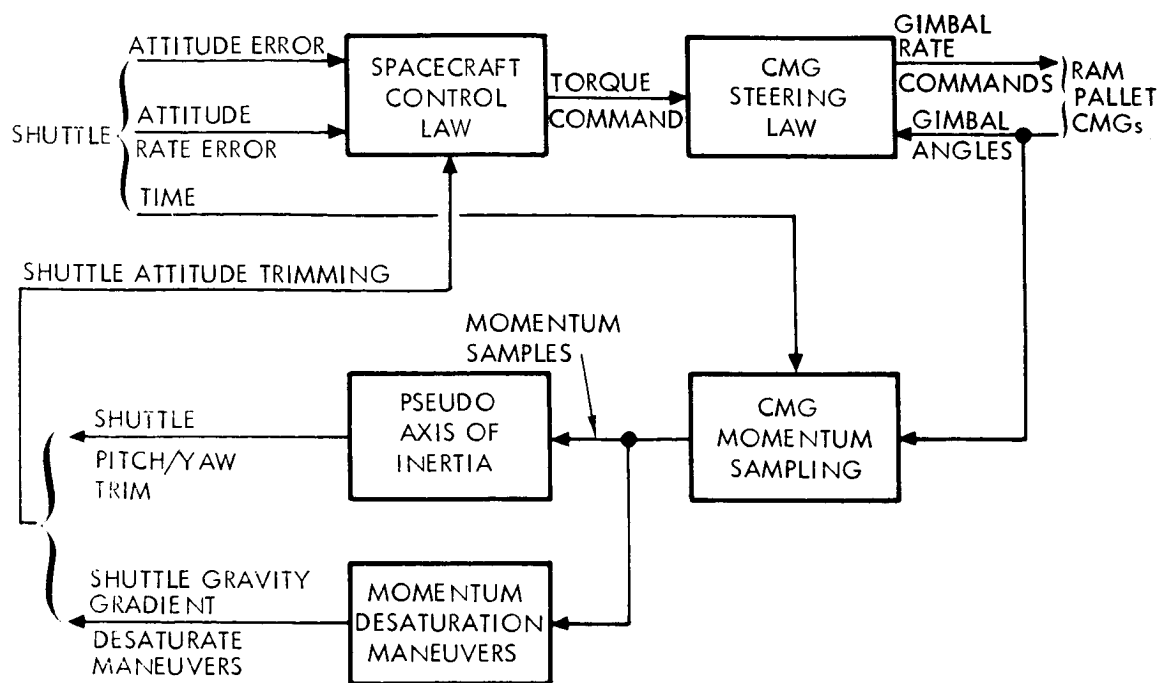


Figure 1-C-5. Shuttle CMG Control Software Flow

The function of shuttle trimming (shown on figure 1-C-5) is to utilize small, slow shuttle maneuvers relative to the nominal attitude to generate gravity gradient torques that, in turn, bound the CMG momentum. Basic data input is CMG system momentum time history generated by sampling the CMG gimbal angles over half-orbit periods. This data is used to develop two types of shuttle attitude maneuver commands. One, using the pseudo axis of inertia model, derives a pitch/yaw shuttle attitude change, which is based on the assumption that any biasing from a pure cyclic momentum time history is due to an expected slight difference in shuttle body roll axis and roll principal moment of inertia. The other, the momentum desaturation maneuver, generates three axis attitude increments, which are added to the pitch/yaw trim maneuvers to compensate for expected deviations from the ideal cyclic momentum caused by perturbation torques on the shuttle from other than gravity gradient in pitch/yaw and including gravity gradient in roll. Gravity gradient desaturation is also employed by Skylab.

CMG physical characteristics.— The per unit characteristics of the CMG momentum exchange system are summarized below. Three of these units are used.

Momentum	3130 n-m-sec	(2300 ft-lb-sec)
Weight	204 kg	(450 lb)
Size	0.53m ³	(18.7 ft ³)
Power (steady state)	48 watts	

Development considerations.- The momentum exchange units are the same size and type as used for Skylab. No development is required.

The experiment isolation platforms are development items. Cost estimates developed in the RAM study (reference 1-C-1) ranged from \$2.47M for a small gimbal platform to \$4.2M for a large gimbal unit. It should be noted that these platforms are precision pointing units designed to support astronomy requirements. A simplified version should be adequate for the subject mission without additional development.

RAM Control Concept

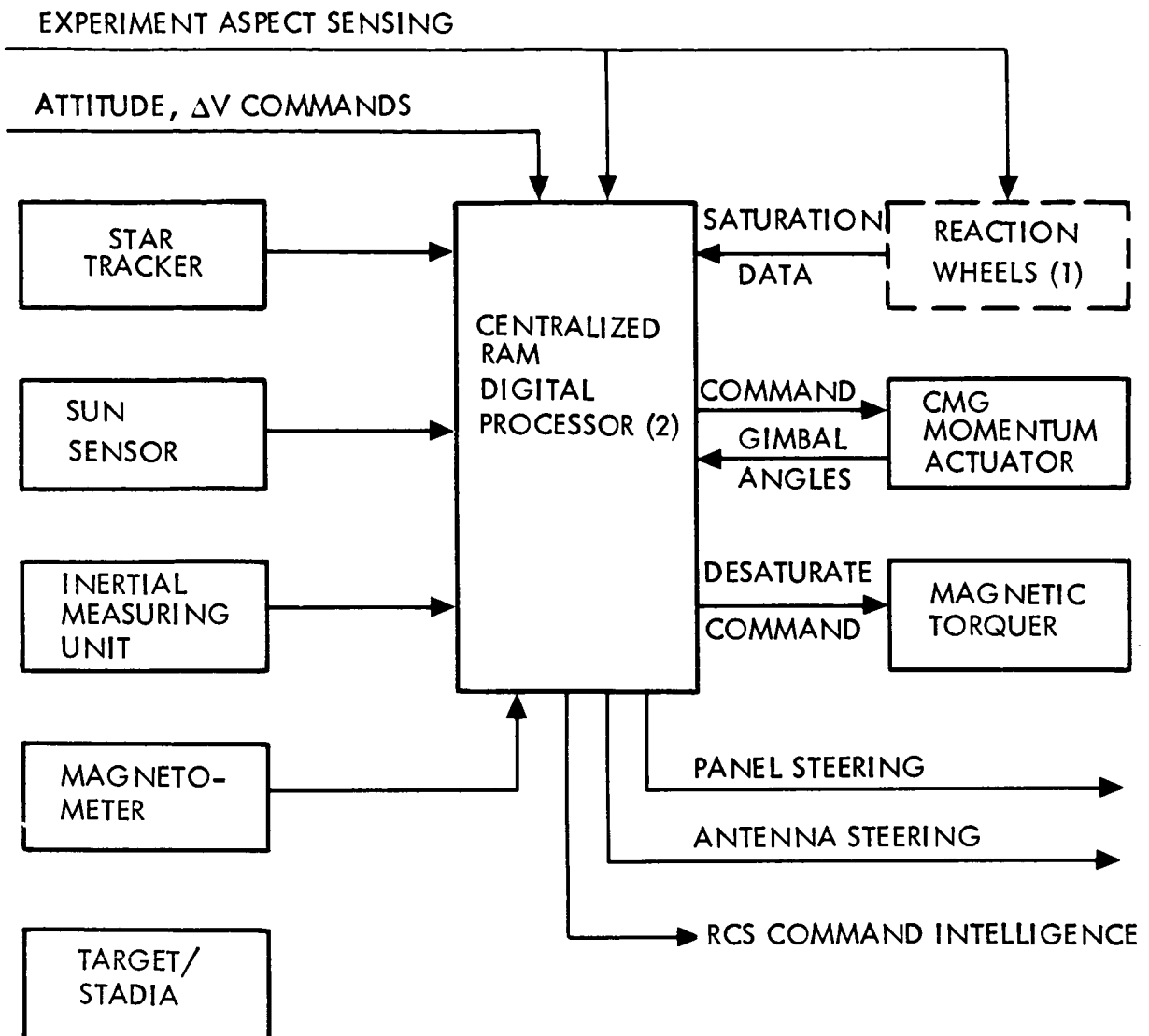
Concept description.- The selected RAM control concept is shown in the diagram on figure 1-C-6. This mechanization includes a set of sensory equipment and torque actuation equipment and provisions for intrasubsystem support functions. The diagram and descriptive text presented here were extracted from reference 1-C-1.

Star tracker referencing of an inertial measuring unit (IMU) provides an all-attitude continuous source of attitude and attitude rate data to support the observation acquisition accuracy requirement of $\pm 1.46 \times 10^{-4}$ rad (± 30 arc-sec).

A sun sensor is added to back up the star tracker system for module recovery purposes only, as it does not provide the accuracy required for observations. The magnetometer is used to provide a measurement of earth magnetic field for input to the magnetic desaturation torquer control.

All orientation and ΔV commands are processed by the digital computer to generate CMG torque and RCS torque and force commands. To minimize potential contamination from RCS exhaust, all orientation maneuvers excluding those of docking and other high ΔV applications are performed by the CMG's.

The magnetic torquer generates a magnetic field that interacts with that of the earth to produce a torque output comparable in magnitude to the maximum exerted by gravity gradient. This torque is used to desaturate or bound CMG accumulated momentum.



- (1) THIS IS AN EXPERIMENT PECULIAR ADD-ON TO PROVIDE IMPROVED POINTING PERFORMANCE IF NOT PROVIDED BY EXPERIMENT INTEGRAL IMAGE MOTION COMPENSATION (IMC).
- (2) IMPLEMENTS FLIGHT CONTROL AND FAILURE DIAGNOSIS SOFTWARE REQUIREMENTS.

Figure 1-C-6. Free-Flying RAM Control Concept

Experiment-integral aspect sensing, with CMG's only, provides body-pointing stability to $\pm 2.42 \times 10^{-6}$ rad (± 0.5 arc-sec). For the more stringent cases, this basic CMG control system is compatible with experiment-integral image motion compensation or improved body-pointing capability provided by modular addition of reaction wheels. In the body-point option, the reaction wheels become the primary torque disturbance reaction source with the CMG's continuously desaturating them, thereby limiting the required reaction-wheel momentum capacity. The reaction wheels represent experiment integration equipment.

Physical characteristics.— The physical characteristics for the guidance and control subsystem are presented in Table 1-C-III.

TABLE 1-C-III.— RAM CONTROL COMPONENT PHYSICAL CHARACTERISTICS

Assembly	Type/number	Per unit characteristics					
		Wt (kg)	Wt (lb)	Size (m ³)	Size (ft ³)	Av pwr (watts)	MTBF (k hr)
Basic							
CMG + Inv.	Double gimbal (3) (500 ft-lb-sec)	94.4	208	0.12	4.2	25	25
Star tracker	Fixed head (5)	9.1	20	.031	1.1	5.0	60
Magnetic Torquer	Double gimbal (1) (7-19) ft length	84.0	185	.056	2.0(b)	60	250
Rate gyro pkg.	Strapdown (1)	12.7	28	.028	1.0	66	50(a)
Magnetometer	Three-axis (1)	3.2	7	.004	0.15	2	500
Sun sensor	Wide angle (1)	0.9	2	.003	0.1	0	500
Experiment integration (c)							
Reaction wheels	High torque (3)	13.6	30	.048	1.7	10	100

Note: (a) Including one channel of internal redundancy.
 (b) Stowed volume. Operating corresponds to a hemisphere of radius 2.1m (7 ft) to 3m (10 ft).
 (c) For free-flying RAM's not containing IMC and requiring better than $\pm 2.42 \times 10^{-6}$ rad (± 0.5 arc-sec) pointing.

Development considerations.- The selection of fixed-head over gimbaled trackers is based on projected technology advancement enabling pattern recognition on sixth magnitude stars. A substantial improvement in reliability and life characteristics of the double gimbal type could reverse this selection.

The magnetic torquer is a new assembly with nonrecurring cost of \$1M including supporting analytical studies.

The reaction wheel is a new assembly differing from existing units in its requirement for high torque. Assembly nonrecurring cost is placed at \$300K.

The modification cost to convert an existing single gimbal CMG design to the proposed double gimbal design is estimated to be \$520K.

The above development costs are included in the costs for the competitive RAM system as shown in Module 3 to follow.

Modular Space Station Control Concept

Concept description.- A functional block diagram of the G&C subsystem is presented in figure 1-C-7. Items shown in the center of the diagram within the dashed lines represent information subsystem (ISS) hardware that perform G&C functions. The descriptive material presented below was extracted from reference 1-C-2.

Description of assemblies: The inertial reference assembly includes a strapdown inertial measurement unit (SDIMU) and a preprocessor. The SDIMU includes six gyros and six accelerometers in a skew-symmetric configuration. This concept provides satisfactory performance with any three gyros working and is more reliable than an orthogonal arrangement of nine gyros.

The optical reference assembly consists of two double-gimballed star trackers, a four-head horizon edge tracker, a sextant/telescope, three optical alignment units, and a preprocessor. This equipment is used to provide an attitude reference (both local level and inertial), alignment between the G&C equipment and experiment equipment, autonomous navigation measurements, and unknown target tracking for experiment support.

The RCS electronics assembly includes four RCS jet driver electronics units and two preprocessors. The driver units amplify the logic level outputs of the preprocessors to provide operating power for the solenoids and ignitors of the RCS jets. Each preprocessor is hardwired to all four quad driver units, and either is capable of controlling the vehicle without relying on the other. The preprocessors provide limited failure monitoring for the RCS.

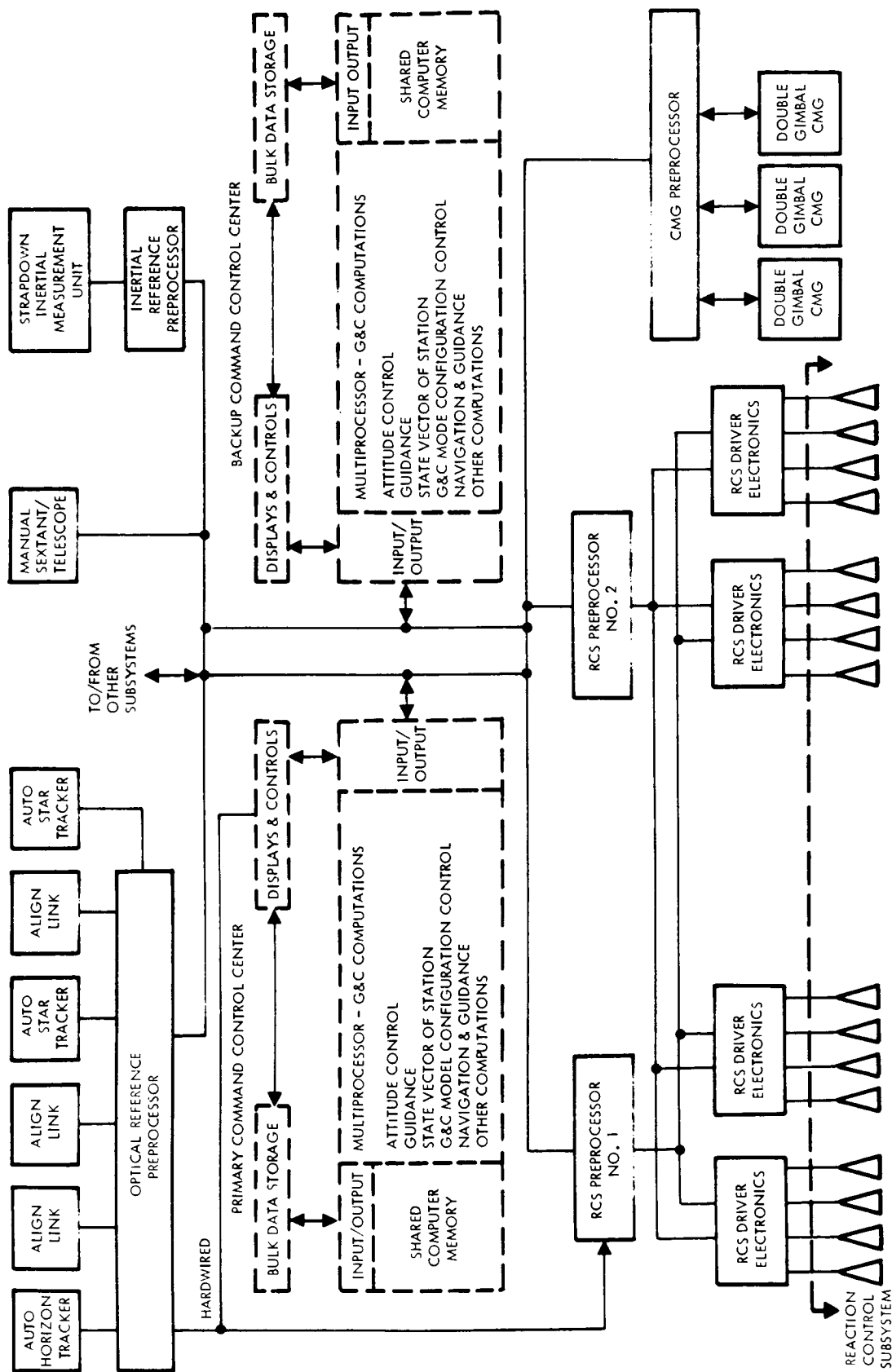


Figure 1-C-7. MSS G&C Functional Block Diagram

The momentum exchange assembly includes a planar array of three double-gimballed control moment gyros and a preprocessor. The angular momentum of each gyro is 1495 n-m-sec (1100 ft-lb-sec). The array will provide momentum exchange with one gyro down for repair. The CMG's are designed for on-orbit repair at the module level. The CMG's are desaturated by using the RCS or, when operations permit, gravity gradient torques.

The computation assembly represents the software for the G&C computations performed in the ISS. These computations are highly interrelated with other computations performed by the ISS to support such functions as flight control and experiment operations.

Operating modes: Local-level mode attitude control is accomplished with the star trackers and horizon trackers as the attitude reference. Yaw attitude is computed from star tracker data. Angular rates are derived from the attitude signals. Control torques are obtained from the CMG's, which are desaturated by using either the RCS or gravity gradient techniques. This mode is completely automatic. Crew attention is only required in case of an indicated failure.

Inertial mode attitude control is performed as described previously with the exception of the attitude reference function. The inertial mode attitude reference can be obtained by using either the SDIMU or both star trackers simultaneously.

Emergency power attitude control is the automatic mode used during an electrical power emergency when power is obtained from the fuel cells and the solar array is inoperable. The attitude reference is provided by the SDIMU. Control torques are provided by the RCS, and the CMG's are deactivated to conserve power. The optical reference is a potential lower power alternative to the SDIMU.

Orbit maintenance translation control is normally conducted simultaneously with local-level mode attitude control. The SDIMU is used for velocity measurements, and the translation thrusts are applied by using the attitude control jets.

Manual control with visual cues is an emergency mode that can be used to perform the only critical G&C function (stabilization for docking). In this completely manual mode, a hand controller and visual out-the-window cues are used. This control function can be performed from either volume in the core module. The hand controller switches are hardwired to the RCS electronics driver units, which activate the RCS jets. The only objective in this mode is to provide sufficient rate stabilization so that a rescue shuttle can dock.

CMG assembly: A functional block diagram of the CMG assembly is shown in figure 1-C-8. The assembly consists of a preprocessor and the momentum exchange devices.

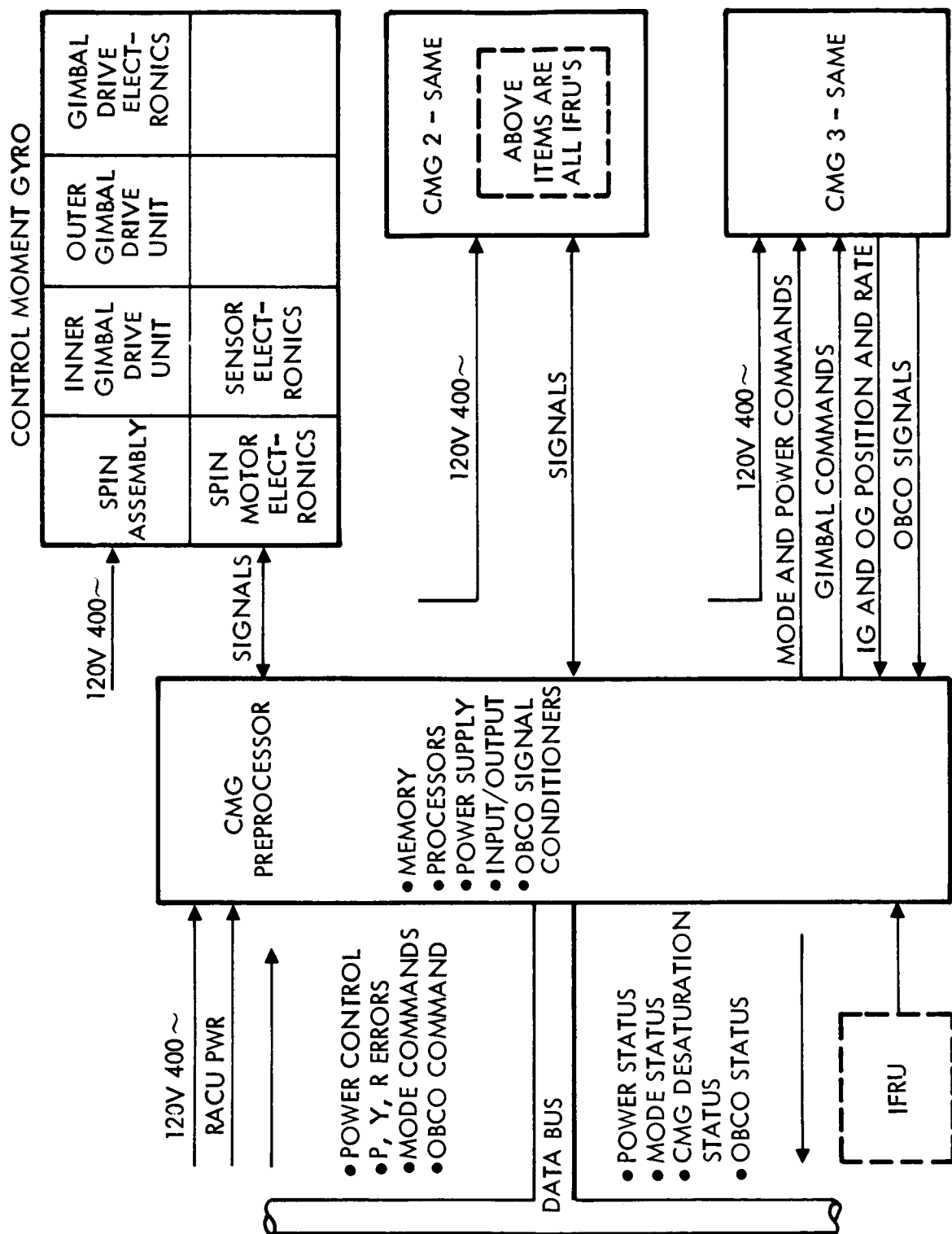


Figure 1-C-8. MSS Momentum Exchange Assembly

The CMG array selected for the Space Station was the result of a detailed and systematic comparison of likely candidates. The configuration is called 3 planar - DG or just 3 PM. The array has three 2-degree-of-freedom control moment gyros with parallel outer gimbals, the momentum vectors initially being in the orbit plane. Each CMG is mounted with its outer gimbal axis parallel to the X-axis and with the momentum vectors nominally in the y-z plane evenly spaced. The torque output along the axis parallel to the three outer gimbal axes is the sum of each gimbal drive unit.

Two basic design criteria were used in sizing the gyros:

1. With one gyro of the set not working, the remaining gyros must be capable of operating for at least one orbit without saturating. The purpose of this criterion is to ensure that, while a gyro is being maintained, the propellant saving capability of the CMG system is not lost.
2. With all gyros operating, desaturation of the system will not be required any more frequently than once every 12 hours. The purpose of this criterion is to minimize the effect of the reaction jet exhaust gases on the experiments.

The spin assembly module uses a spoked, single-material rotor having minimum weight, high stiffness, and good dimensional stability. The spin motor is a brushless dc motor with high efficiency, and its electronics devices are packaged in two modules and mounted directly on the inner gimbal to minimize leads. The inner gimbal is a conical structure with high stiffness and light weight. A stable and proven bearing preload method is provided by loading through a central rod.

The sensor and gimbal drive modules are replaceable. The gimbal drive uses a brushless torquer and tachometer for long life, and a roller-gear transmission is proposed since it combines high efficiency, low friction and backlash, high torsional rigidity, and short axial length. The sensor and gimbal drive contain the gimbal bearings. The outer gimbal is a box-shaped cross section of dip-brazed honeycomb construction.

Physical characteristics. - Physical characteristics of the G&C subsystem are summarized in Table 1-C-IV.

Physical characteristics of the CMG array are summarized below. These data were prepared for a system of three gyros, each having a momentum of 1495 n-m-sec (1100 ft-lb-sec).

TABLE 1-C-IV.- G&C PHYSICAL CHARACTERISTICS

Assembly	Weight kg (lb)	Average Power (watts)	Volume m ³ (ft ³)
Inertial reference	30 (65)	145	.013 (.450)
Optical reference	157 (346)	195	.1795 (6.336)
Momentum exchange	447 (984)	144	.229 (8.073)
RCS electronics	34.6 (75)	3	.013 (.451)
Computation	(0)	0	0
Total	669 (1470)	487	.434 (15.310)

1. Weight. Each gyro weighs 117 kg (258 pounds), excluding structural framework, trunnions, and cover. An estimate of the electronics weight is 15.9 kg (35 pounds), which includes spin motors, torque drives, and amplifiers.
2. Size. The wheel radius for each gyro is .24 m (9.5 inches). The swing diameter of the outer gimbal is 0.96 m (38 inches). Each gyro is 0.9 m (35.5 inches) long.
3. Power. The average operating power for the assembly is 144 watts; the peak power requirement is 504 watts. During spin-up, each gyro draws 128 watts.

Development considerations.- The CMG's in the MSS baseline concept are development items and their projected costs were estimated in the Phase B program and have been included in the data of Module 3. Development is felt to be required in at least the following areas.

Improved gimbal drive: Performance is limited by the gimbal drive unit. Goals are increased stiffness, reduced backlash, low breakaway torque, and a shorter axial length.

Improve spin bearings: Although non-contacting bearings have definite advantages over conventional ball bearing designs, the MSS concept utilizes an advanced ball bearing design to reduce noise and vibration and develop a constant flow lubrication method with sufficient reliability.

Control law development: The effort is analytical in nature and includes trade studies, simulation, and development of the selected concept.

Inflight replacement: This effort concerns the development of modules, procedures, and supporting tools or equipment required for inflight replacement of CMG modules.

Modular Space Station Power Concept

Concept description.- The electrical power system (EPS) provides primary electrical services by means of a 2 degree of freedom solar array. The MSS baseline defines an energy storage technique which consists of fuel cells operating from a stored reactant supply. The reactant is generated by water electrolysis during sunlight periods using solar array power. The solar arrays 650 square meters (7000 square feet) generate electrical power at +112 vdc. Each wing is divided into 47 power circuits (rated at ≤ 500 watts each) with on-array switching provisions controlled by the information management subsystem (ISS). Power transfer across the rotating interface at the turret is achieved by slip rings. Using slip rings in two axes permits continuous rotation of the array. Four power transfer circuits are required per wing. Two of these circuits support primary buses. The other two go directly to the electrolysis cells.

During normal long-duration operations, the electrical power requirements are supplied by the solar array-fuel cell/electrolysis combination. The solar array supports four electrical power channels as shown in figure 1-C-9. This network operates the primary buses in parallel under normal conditions; however, each bus can be isolated and the power can be supplied by four independent power buses. Each channel consists of a fuel cell and electrolysis cell with storage accumulators, a primary bus with inverters and regulators, an EPS control box, and secondary buses for local power distribution. The

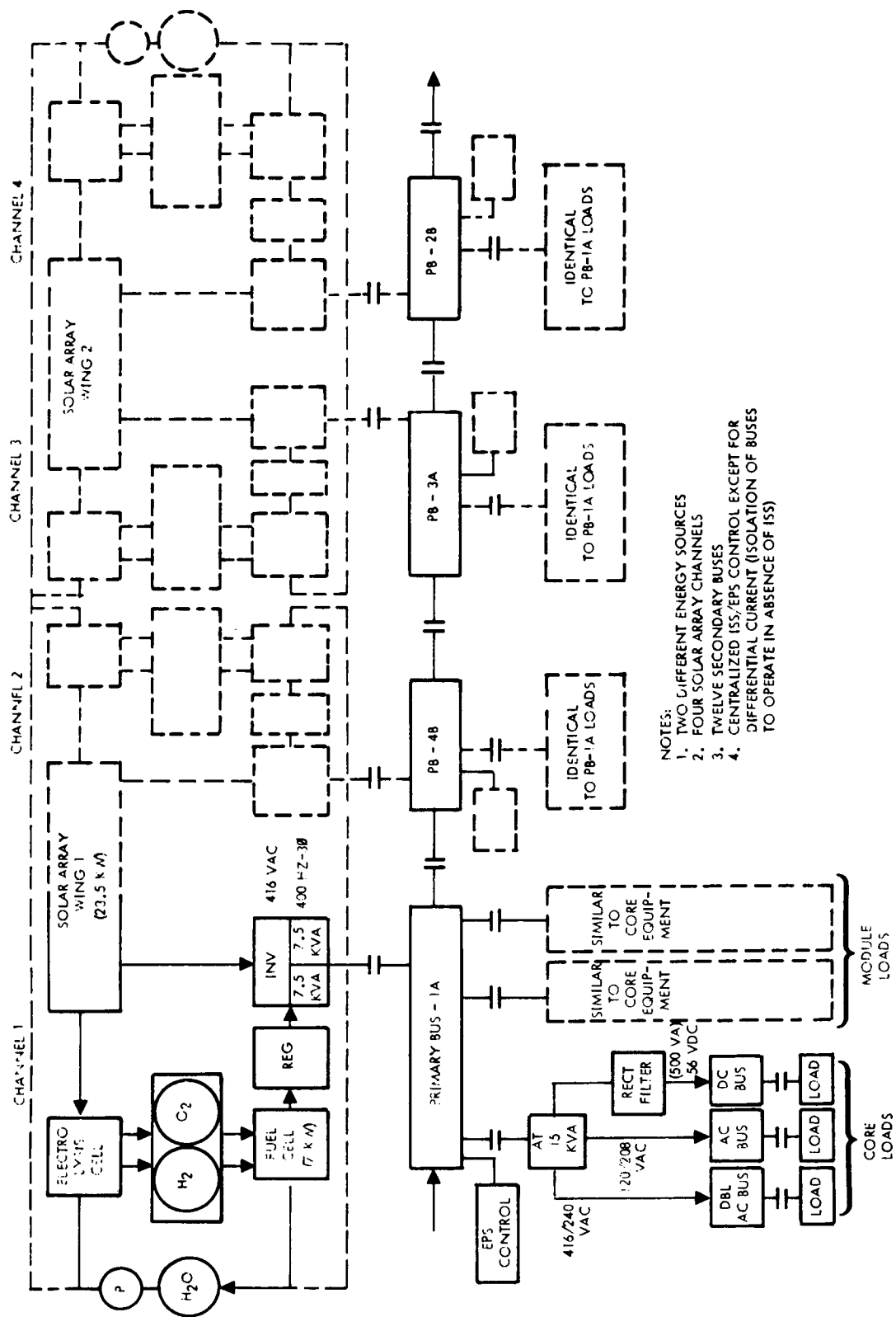


Figure 1-C-9. Modular Space Station Electrical Power Subsystem Functional Block Diagram

power is controlled by an integrated central processor in the information management subsystem (ISS). The ISS computer controls loads (i.e., load shedding, etc.), voltage regulation, and network stability. The EPS retains the ability to operate in the absence of ISS by isolating each bus and operating independently. Boot strap operations for initial startup are controlled with the EPS control box. Each station module contains dual secondary buses providing power to critical loads from both A and B systems. The secondary bus consists of power conditioning for voltage transformation and solid-state circuit breakers for load control and switching.

Physical characteristics.- Weight of each assembly is given in Table 1-C-V. Lifetimes of 2.5 years are taken for major energy storage equipment. A planned replacement of the solar arrays occurs at the end of the initial MSS lifetime of five years.

TABLE 1-C-V.- MSS (REGENERATIVE FUEL CELL) EPS
WEIGHT CHARACTERISTICS

Assembly description	Weight	
	Kg	lbs
Primary power	3031	6676
Energy storage	2255	4966
Conditioning & Distribution	1711	3768
	<hr/> 6997	<hr/> 15 410

Free-Flying RAM Power Concept

Concept description.- The RAM free-flying payloads are composed of technology and astronomy type experiments. These experiments are grouped in 10 different payloads with average power required varying from a few watts to 2180 watts per day. The latter power is required for the Advanced Solar Astronomy Observatory payload which has been selected for the IPACS study.

Figure 1-C-10 is a schematic of the free-flying RAM EPS.

Solar arrays are used for prime power generation. In addition to load power requirements, the sizing of solar arrays is a function of orbital parameters because the largest degradation is due to radiation damage. The array is a flexible rollout-type developed and already in-flight operation.

The free-flying RAM's with the larger power requirements feature dragon-fly systems with two tandem drums on each side; these extend four array panels on each side of the vehicle. The dragon-fly arrangement is required to minimize the length of the arrays for large areas. The 10 year power output is 6890 watts for an array area of 98.5 meters² (1060 ft²).

Power during periods of eclipse is provided by nickel-cadmium batteries. The batteries are rated at 36 amp-hr and sized for a depth of discharge of about 20 percent (20% results in minimum weight to orbit for such a system). The energy storage requirement is 2230 watt-hr.

Physical characteristics. - A weight breakdown for the system is presented in Table 1-C-VI.

TABLE 1-C-VI.- FREE-FLYING RAM EPS WEIGHT SUMMARY

Subassembly	Number of assemblies	Weight	
		kg	lb
Prime power source			
Solar array	2	223.4	492
Sun sensor		.91	2
Orientation mech.	2	22.7	50
Orientation cont. elec.		9.1	20
Installation hardware		34.5	76
Subtotal		290.61	640
Energy storage			
Batteries	8	351.	772
Battery chargers	8	91	200
Subtotal		442	972
Electrical cond. & distribution			
Power switch	2	31.8	70
Inverters	4	18.2	40
Line regulators	8	50.8	112
Dock interface con.		9.1	20
Manip conn PNL		9.1	20
Ground conn PNL		4.5	10
Busses		18.2	40
Outlets		9.1	20
Inst. hardware		15.0	33
Electrical wiring		249.8	548
Subtotal		415.6	913
Total		1148	2525

Shuttle 30-Day Sortie Power Concept

Concept description.— Primary power generation is accomplished by the Shuttle orbiter fuel cells using oxygen and hydrogen reactant, as required. The payload will provide the additional reactant quantities and its storage for power required in excess of a Shuttle 7-day mission. Shuttle will provide 50 kwh for emergency and/or contingency provisions. To handle peak power requirements above the available Shuttle power level the payload has a secondary (auxiliary) power generation assembly consisting of silver-zinc batteries, battery chargers, and delta power conditioning and distribution. The EPS delivers standard 28-volt dc and 115/200 volts ac, 3-phase, 400 Hz power. Nonstandard power conditioning will be part of the user equipment.

The Shuttle orbiter electrical power subsystem has a steady power generation capability of 14.0 kilowatts. An investigation of orbiter requirements showed that there is available, above the orbiter requirements, a power generation capability of 6.0 kilowatts which can be made available to the sortie payload.

A functional diagram for the system is presented in figure 1-C-11.

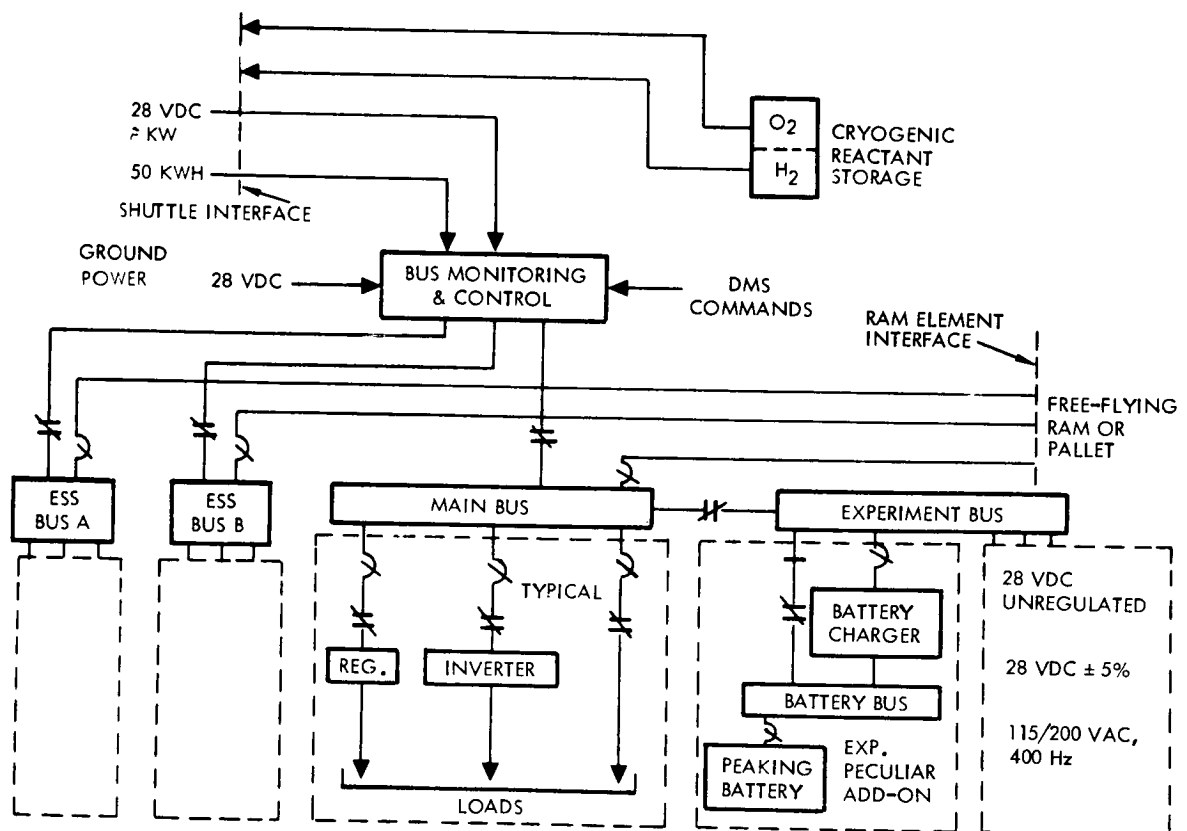


Figure 1-C-11. Sortie RAM Electrical Power Subsystem Schematic

Physical characteristics.- The physical characteristics for the system are summarized in Table 1-C-VII.

TABLE 1-C-VII.- 30-DAY SORTIE ELECTRICAL
POWER SUBSYSTEM WEIGHTS

Assemblies	Weight	
	kg	lb
Primary power generation ⁽¹⁾		
Cryogenic tanks, plumbing, etc.	907	2000
Consumables (2144 kwh)	835	1840
Power conditioning		
Sortie RAM	103	228
Power distribution		
Sortie RAM	356	784
Material science add-on ⁽²⁾	323	712
Energy storage ⁽³⁾		
Material science	284	625
Add-on (2 batteries)		
Total	2808	6189
(1) 6 kw power from Shuttle fuel cell (2) M1S1G (3) 2 batteries, chargers, and charge circuit		

Tracking and Data Relay Satellite Power Concept

Concept description.- The EPS provides primary electrical service by means of utilizing a single degree of freedom solar array. Power during sun eclipse periods is provided by nickel cadmium batteries. In addition to primary power generation, the EPS regulates, conditions and distributes electrical power to all TDRS loads.

The EPS block diagram is shown in figure 1-C-12. Power is supplied directly to the load with a central regulated 28 ± 1 volt dc bus. Voltage regulation is accomplished by a shunt regulator operating as a variable load across lower sections of the solar array panels. Each solar array panel is

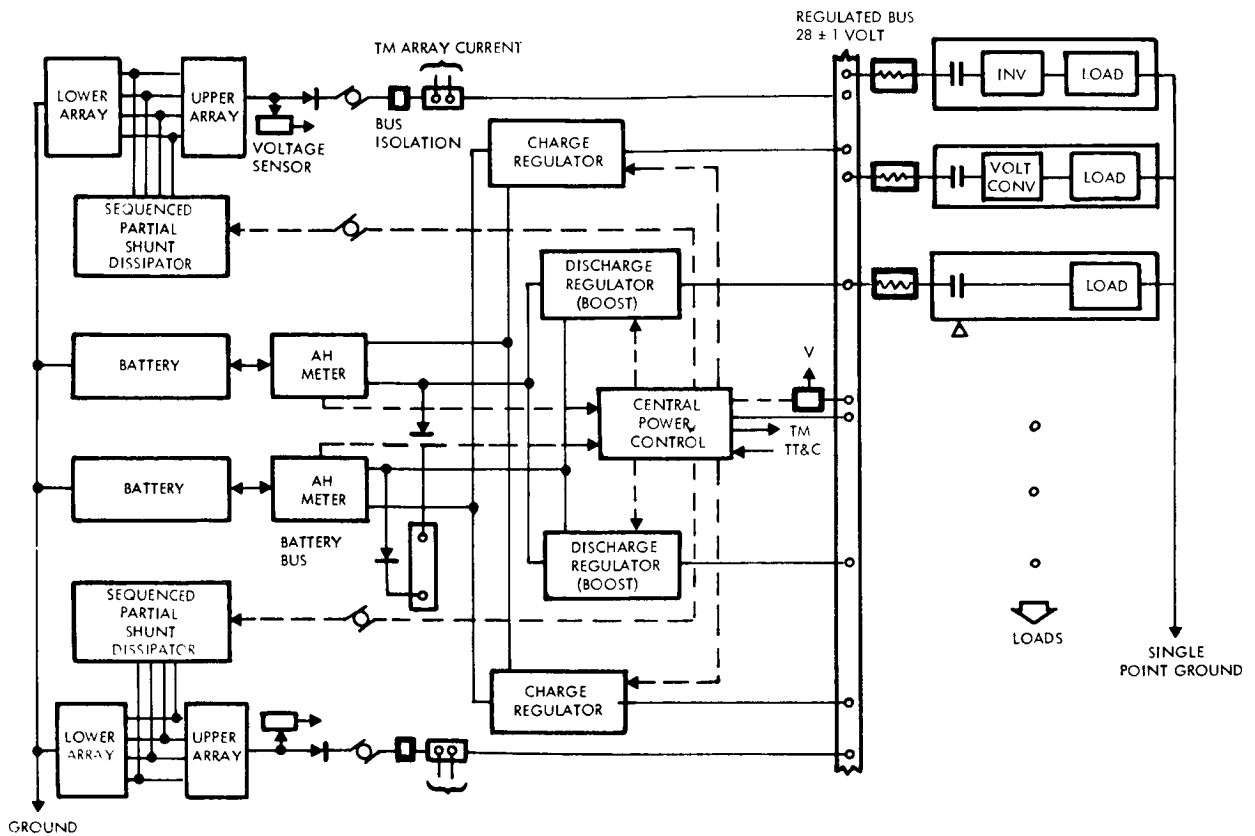


Figure 1-C-12. TDRS Electrical Power Subsystem Block Diagram

approximately 2.09 meters² (22.5 sq ft) in area for a total array area of 4.18 meters² (45 sq ft). Based on 10.35 watts/ft², a beginning of life power output of 466 watts is expected with an end of life power output of 400 watts.

The central power control unit controls the various EPS operational modes. It operates by detecting the difference between the main bus and reference voltage levels. Since the solar array is a constant power source, to supply larger amounts of power to subsystem loads, battery charging has to be inhibited and/or the boost regulator activated to supply power from the batteries.

Because of a constraint to utilize only flight proven technology and hardware (where possible) nickel cadmium batteries were selected for the energy storage assembly. The selection of two batteries for the baseline was made after an examination of the impact of a battery failure and considering system weight tradeoffs. The loss of one of the two batteries still permits an eclipse load of 115 watts for the full 72 minutes which is sufficient to operate both one forward low data rate (LDR) and one forward medium data rate (MDR) link. A direct energy transfer concept was selected since this permits power transfer directly from the solar array to the loads without any in-line

power conditioning. The majority of time (all but 80.2 hours per year) is spent in direct sunlight with spacecraft loads supported directly from the solar array; thereby this approach minimizes power conditioning losses.

The voltage converter (shown in figure 1-C-12) is required to provide 18 watts to the LDR for data transmission. This converter operates from the 28 volt regulated bus. As a general utility service, the EPS delivers regulated 28 volt dc power. With the exception of 18 volts dc for the LDR transmitters, all other nonstandard power conditioning will be part of the user equipment.

During transfer orbit an average power requirement of 44 watts up to a total of 27.5 hours must be provided. The baseline design utilizes the solar arrays in the stowed configuration. This is done by curving the panels and exposing the cells to simulate a body-mounted panel. The dependence on batteries is minimized by providing sufficient projected area for 44 watts output for the envelope of sunline/spacecraft orientations.

Physical characteristics: The physical characteristics for the system are summarized in Table 1-C-VIII.

TABLE 1-C-VIII.- TDRS ELECTRICAL POWER SUBSYSTEM WEIGHTS

Components/assemblies	Weight	
	kg	lb
Solar array	(27.09)	(59.6)
Panels (2)	18.0	39.6
Drive mechanism (2)	6.82	15.0
Linkage & fitting (2)	2.27	5.0
Power conditioning & distribution	(23.93)	(52.7)
Charge & discharge	5.13	11.3
Central control & logic	2.32	5.1
Packaging	2.22	4.9
Shunt dissipators	1.09	2.4
Amp HR meters	1.82	4.0
Voltage converter	2.27	5.0
Cabling	9.08	20.0
Energy storage		
Batteries (2)	(20.10)	(44.3)
Total	71.12	156.6
Note: Numbers in parentheses represent subsystem assembly total weights		

Mariner Jupiter/Saturn Power Concept

Concept description.- The spacecraft is to be capable of performing a Jupiter-Saturn flyby mission and navigate past these planets to a satellite at one, or at both, of the planets. The spacecraft will be designed for a flight time of four years; however, it is planned to gather and transmit science data beyond the last planet until equipment-operating ranges are exceeded or the spacecraft fails due to consumption of expendables or part failure.

The block diagram, figure 1-C-13, depicts the functional components of the power system design. All spacecraft electrical power will be supplied by three multi-hundred watt radioisotope thermoelectric generators (RTG). Power output from the RTG's basically is a function of the time rate of decay of the Plutonium-238 isotope fuel, the half-life of which is 87.5 years. The spacecraft will condition, regulate and switch the power before distributing it to the spacecraft loads.

In order to accommodate the use of Mariner/Viking hardware, power from the RTG's is converted and distributed in the following forms:

1. 2.4 kHz, 50V rms, single-phase, square wave power for engineering and science subsystems
2. 400 Hz, three-phase, quasi-square wave power for the gyros
3. Regulated dc power to the temperature control heaters and radio frequency subsystem (RFS) for the RF power amplifier power supplies and pyrotechnic subsystem for valve actuations.

The RTG sources provide primary direct power to the spacecraft main dc bus through a power source and logic (PSL). The PSL incorporates source isolating diodes, switches, relays and telemetry circuits necessary to control the RTG's and to interconnect the sources appropriately with conditioning equipment.

A shunt regulator maintains the main dc bus within 1 percent of 28 vdc. A battery is attached to the main bus for peak pulse loads through a charge/discharge controller which also is capable of exercising control of the shunt regulator, presumably for charging purposes.

A 24-kHz inverter conditions the power to the main ac bus for distribution to spacecraft loads. A standby inverter also is controlled by a failure detector (power control) unit. A separate 400-Hz 3-phase inverter provides gyro power.

Physical characteristics.- The mass of the MJS 77 power system components are listed in Table 1-C-IX.

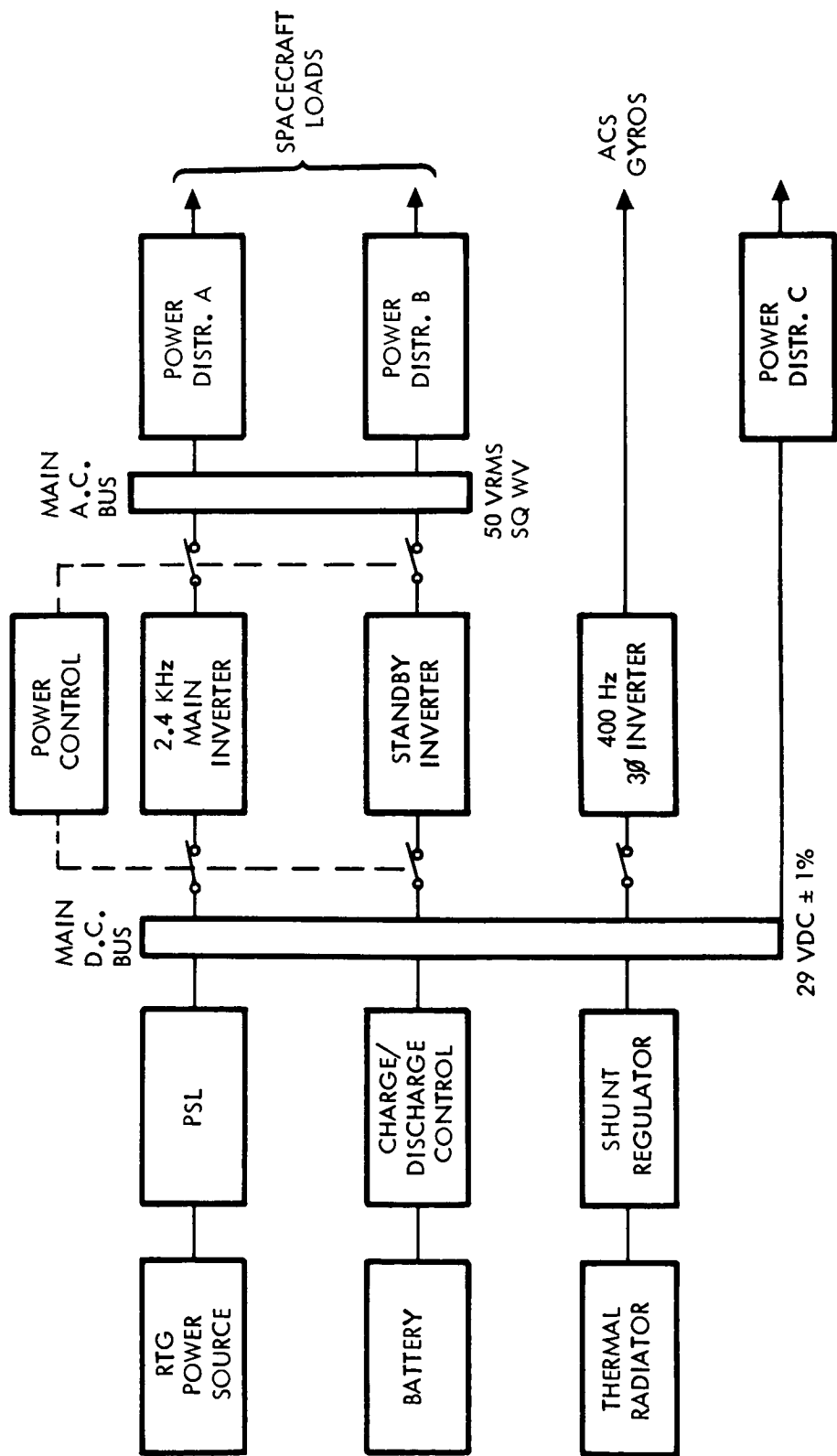


Figure 1-C-13. MJS77 Power System Functional Block Diagram

TABLE 1-C-IX.- MJS ELECTRICAL POWER SYSTEM WEIGHT SUMMARY

Component/assemblies	Weight	
	Kg	lb
Primary power	(118.92)	(262.17)
RTG's (3 required)	108.73	239.7
RTG gas venting	4.53	9.99
Power source & logic	5.66	12.48
Power conditioning & distribution	(25.26)	(55.69)
Shunt regulator	7.70	16.98
2.4-kHz inverter (2)	4.54	10.0
400 Hz, 3Ø inverter	1.81	3.98
Power control	3.18	7.0
Power dist. A	2.63	5.79
Power dist. B	1.80	3.98
Power dist. C	1.80	3.98
Power dist. D	1.80	3.98
Energy storage	(4.54)	(10.0)
Battery discharge/charge controller	2.27	5.0
Battery	2.27	5.0
Total	148.72	327.86
Note: Numbers in parentheses represent subassembly total weight		

Earth Observation Satellite Power Concept

Concept Description.- The electrical power subsystem for EOS is very similar in concept to the design developed in the TDRS Phase B study contract, i.e., EOS will utilize a solar array, batteries, and the direct energy transfer concept developed for TDRS array power utilization.

Figure 1-C-14 presents a functional block diagram of the electrical power subsystem. This represents the mechanization selected by GSFC for EOS and is called a direct energy transfer system. It essentially requires less solar array power than a series regulated system. The central control unit monitors the regulated bus and activates the particular electronic unit to maintain regulation. During eclipse, the control unit, sensing a falling bus voltage, turns on the boost battery discharge regulator. During sunlight, as the solar array begins to augment the battery power, the discharge regulator will begin to turn off. When the solar array can fully supply the load power, the discharge regulator is turned off and the buck battery charger is turned on. When the battery approaches full charge or the maximum charge current is reached the

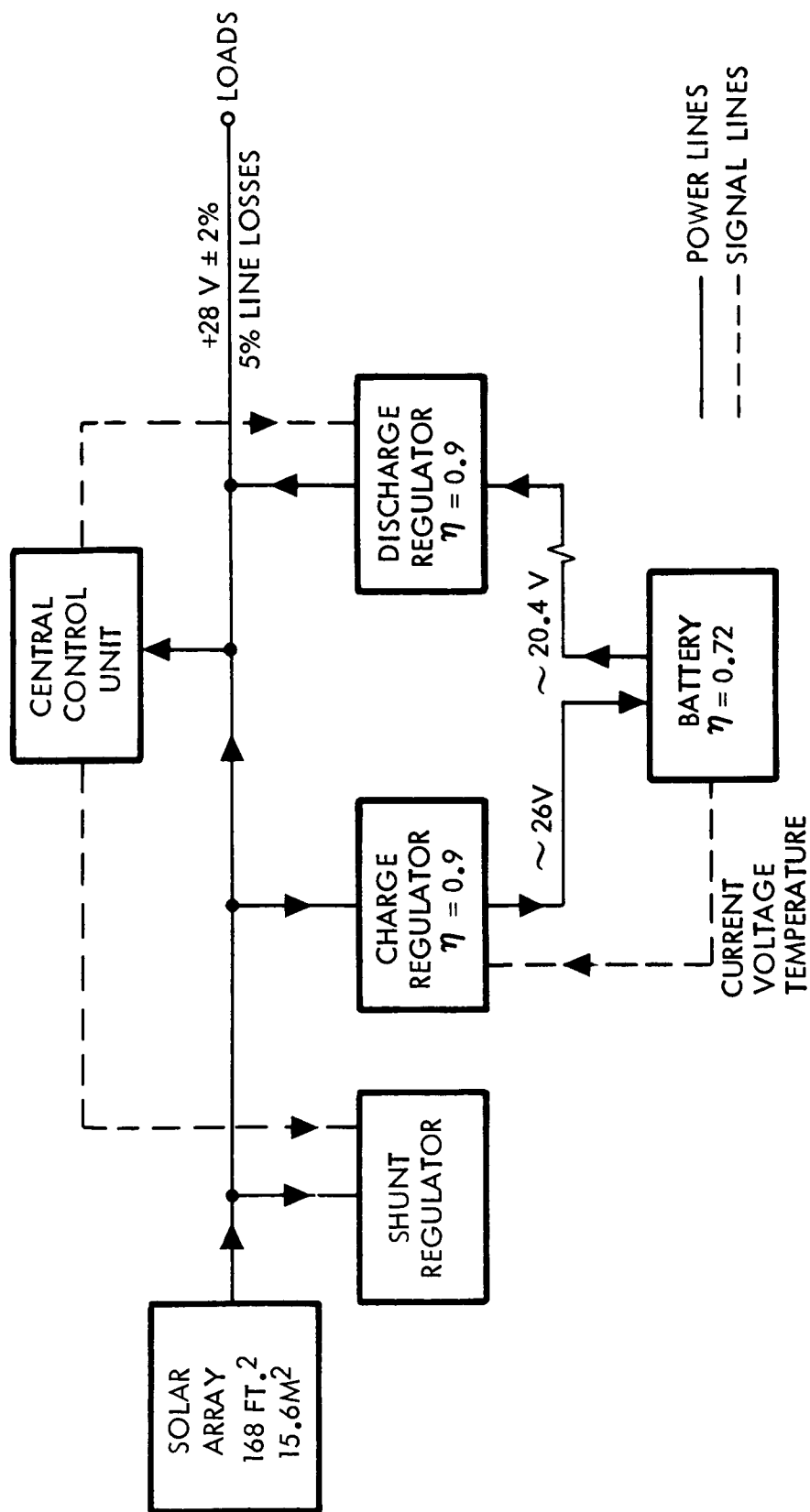


Figure 1-C-14. EOS Electrical Power Subsystem Block Diagram

regulated bus voltage will begin to rise. The control unit senses the rising voltage and turns on the shunt regulator sufficiently to maintain regulation within proper limits. All critical components are fully redundant. The regulator efficiencies shown are high, but are attainable. Any power factor corrections are assumed to be in the loads.

Physical characteristics: For the mission timelines analyzed, EOS housekeeping and payload power required varied from 537 to 727 watts average per orbit. Eclipse energy requirements (at the loads) varied from 279 to 367 watt hours. The orbit period is based on a 976 km (525 nm) sun synchronous orbit. Assuming a 5 percent line loss and a 90 percent battery discharge regulator efficiency, 430 watts is required from the energy storage subsystem. The resulting solar array area is 15.6 m²(168 sq ft). Allowing for 20 percent degradation over a two-year period, beginning of life power (BOL) is 1600 watts and end of life power (EOL) is 1280 watts. Solar array specific power at BOL is 9.5 watts per square foot. The NiCd batteries selected for energy storage use 20 AH cells (17 cells per battery). Four 19.6 kg (43.3 lb) batteries are required to limit depth of discharge to 25-30 percent of achieving the required two-year lifetime. Total EPS weight (not including harness) is estimated at 23.1 kg (510 lb).

Table 1-C-X summarizes electrical power system weights and characteristics. The solar array panel weight is based on a specific weight of 4.88 kg/sq m (1 lb/sq ft), which will allow use of comparatively thick solar cells and cover glass.

TABLE 1-C-X.- EOS ELECTRICAL POWER SUBSYSTEM WEIGHT SUMMARY

	Weight	
	kg	lb
Power generation		
Solar array	(112.8)	(248)
Panels (2)	76.4	168
Deployment yokes (2)	14.6	32
Panel hinges (4)	1.8	4
Panel/yoke hinges (4)	1.8	4
Deploy and drive system	18.2	40
Energy storage		
Batteries (4)	(79.1)	(174)
Power Distribution and Conditioning	(40.0)	(88)
Shunt regulators	3.6	8
Charge circuit regulators		
Chargers, contactors	5.0	11
Disch. circuit regulators, contactors	7.3	16
Wiring* and busses	15.0	33
Control unit	9.1	20
Total	231.9	510
*Does not include spacecraft wiring harness		

References

- 1-C-1. RAM Phase B Study, Vol. III, 4.4 Preliminary Design, Appendix A, Trade and Special Studies. General Dynamics, Convair Aerospace Division GDCA-DDA72-006 (May 12, 1972).
- 1-C-2. Modular Space Station, Phase B, Extension - Preliminary System Design Volume IV: Subsystems Analyses. NR, Space Division, MSC 02471 (SD 71-217-4) (January 1972).

MODULE 2 - CRITICAL COMPONENT DEVELOPMENT

This module addresses the IPACS developments associated with individual mission applications that were studied. The component development requirements are identified and discussed briefly together with schedule considerations. Estimated costs for these developments are presented in Module 3.

Development Requirements

The development requirements identified for each mission are summarized in Table 2-I. These requirements were reviewed to determine the common elements and also screen candidates considered least suitable for development. As indicated in the feasibility study, the MJS mission is a relatively poor IPACS application because of the extremely small energy storage function. Development requirements unique to the MJS mission application are therefore not recommended as high priority development candidates. The very high power, inside-out, permanent magnet generator required for the 30-day Shuttle is a unique case and the benefits of such a development would have limited value in terms of generalized applicability for other mission designs. This requirement was therefore also rejected as a development candidate. The remaining development candidates are:

(1) Present technology extensions

- Ball bearings and lubrication systems
- High-speed and power permanent magnet motor/generators
- Rotor balancing and induced vibration reduction

(2) Advanced technology developments

- High-speed magnetic suspension bearings
- Composite rotors

Note that the items are grouped into two classes. The first, developments which can be considered extensions of present technology, are associated with a first-generation IPACS. The second group includes the more extensive developments which are termed advanced technology; these are required for a second-generation IPACS.

Present Technology Extensions

Ball bearings and lubrication systems.- IPACS requirements indicate the use of high-speed ball bearing systems for some of the mission classes. Although the use of ball bearings at the IPACS speeds (50 000 rpm or less) is not unique, the combination of auxiliary requirements and high speed is.

TABLE 2-I.- DEVELOPMENT REQUIREMENTS SUMMARY BY MISSION

Mission	Development requirements	Comments
TDRS	<ul style="list-style-type: none"> • High speed, permanent magnet motor/generators • High-speed ball bearings and lubrication systems 	
RAM	<ul style="list-style-type: none"> • High speed and power permanent magnet motor/generator • Rotor balancing and induced vibration reduction • High-speed ball bearings and lubrication systems 	
MSS	<ul style="list-style-type: none"> • High speed magnetic suspension bearing • Composite rotor technology • High speed and power permanent magnet motor/generator 	
30-day Shuttle	<ul style="list-style-type: none"> • High speed, inside-out magnetic suspension bearing • Composite rotor technology • High speed, high power, inside-out permanent magnet generator 	High power requirement is not typical of other missions
EOS	<ul style="list-style-type: none"> • High speed, permanent magnet motor/generator • High speed magnetic suspension bearings 	No new problems not covered above
MJS	<ul style="list-style-type: none"> • Very high speed, low power, permanent magnet motor/generator • Very high speed, magnetic suspension bearings 	Mission is poor application for IPACS

Probably the more stringent requirement is lubrication. While the lubrication system must maintain bearing life and reliability, the power to run the bearing in the presence of lubrication drag must be consistent with the desired IPACS efficiency. As a result, flooded bearings cannot be used and the bearings have to be operated with minimum lubricant. Another important bearing requirement is for smooth operation with low acoustic noise and low broadband vibration.

Present bearing technology for these types of bearings has been limited to generally less than 12 000 rpm. The lubrication systems have generally been continuous-feed centrifugal oiling systems or solenoid-operated "spurt" systems having a sufficient capacity for the mission life. The high-speed ball bearing operating with minimum lubricant for IPACS is definitely a critical component because of the unknowns as far as bearing life calculation and the added threat of deterioration due to excess bearing heat or heat differentials.

Present bearings have been designed with race, retainer, and ball tolerances that are seemingly consistent with quiet, smooth, minimum-vibration performance. However, at high speeds, these tolerances tend to become more critical and bearing wear more significant. Vibrations at the retainer frequency (approximately 1/2 shaft speed), spin frequency, and twice the spin frequency will tend to become more pronounced and vary more with time and environment.

The development program for the high-speed ball bearings and associated lubrication system will consist of:

- (1) Evaluation of existing bearings for performance at IPACS speeds.
- (2) Design and evaluation of lubrication systems (including contact tests to assure adequate lubrication).
- (3) Bearing specification for minimum noise.
- (4) Test and evaluation of IPACS bearings.

Evaluation of existing bearings: The high IPACS speeds will necessitate bearings manufactured to higher than average standards. However, simply specifying special precision bearings in an effort to minimize wear, vibration, and noise would be a costly step which might not prove justified or effective. An evaluation of bearing specifications is required to define the tolerances important to the high-speed minimum lubrication application. Studies will be performed to define the relative importance of such factors as groove eccentricity, tolerances on bore and outer race, surface roughness, and concentricity of diametral dimensions. The goal will be to relax requirements where possible to lower bearing costs and delivery times while providing running characteristics comparable to ABEC 5 to 7 bearings.

The evaluation program will include tests of standard and preferentially specified bearings in a conformal test fixture. Test data would be used to correlate with preferential specification requirements.

Design and evaluation of lubrication systems: The IPACS lubrication system requires careful selection of oiler components to provide a consistent, but low, amount of lubricant to the bearings. Rotational speed, temperature, and housing seal configuration can be expected to be the major factors affecting nominal oiler operation. Lubrication system designs will be prepared and tested in a conformal seal, housing vacuum fixture to develop data defining oiler operation. Lubrication design effectiveness (which must be evaluated in the context of specific bearing designs) will be evaluated by means of elastohydrodynamic film analyses verified by contact conductivity tests. Film thickness requirements and effectivity will be evaluated. Evaporation or rate tests are planned. Heat loss and heat transfer calculations and tests will be required. Of special interest will be heat buildup rates and stabilization values for various rotor speeds as measured on inner and outer races. Race differential temperatures are critical to this evaluation.

Bearing specification for minimum noise: It can be expected that the preceding program will provide data necessary for the preparation of an IPACS bearing specification of general applicability.

Test and evaluation of IPACS bearings: As in any program, bearing tests will be required for the final design. Tests will include selection or screening, temperature, lubrication rate, drag torque, wear, and overspeed. Life tests are planned for continued operation through application phases.

This program is estimated to require one and one-half years.

High-speed and power permanent magnet motor/generators.- The permanent magnet motor-generators in the IPACS concepts are similar to those which have been designed, built, and tested for the last 7 years for momentum wheels and CMG's. They consist of a multipole permanent magnet main rotor, a multipole sensor rotor, Hall generators, and a two-phase wound stator.

The principal requirements that IPACS places on the motor/generators are operation at high-speed (20 000-50 000 rpm), high power (KW), and high efficiency at maximum power output (~97 percent). Although all of these requirements are judged to be compatible with the PM motor/generators, none has been demonstrated by hardware at this point. Spin motors for CMG's have been fabricated and tested for shaft power and speeds of approximately 200 watts and 10 000 rpm, respectively. Torque motors have been tested for shaft power and speeds of 1200 rpm and 1 KW. The chief development areas for the IPACS motor/generators are the structural design of the main rotor for high-speed operation

and the magnetic design of the stator/rotor combination to minimize power losses. Capability in these two areas should be demonstrated by hardware testing of one engineering model of an IPACS PM motor/generator.

The estimated duration of this development effort is approximately one year.

Rotor balancing and induced vibration.- The maximum IPACS rotor speeds, which range from 18 000 RPM to approximately 50 000 RPM, causes induced, or output, vibration to be a more significant design problem for IPACS than conventional CMG or MW systems operating at maximum speeds of 10-12 000 RPM. The requirements for rotor balance and control of spin bearing imperfections are both more stringent. In addition, the control of induced vibration over the IPACS 50% speed range is a development compared to conventional systems.

The major favorable impact of IPACS on induced vibration problems is the higher disturbance frequencies due to higher rotor speeds. This will allow better use of isolation than in conventional systems.

The development effort required is that of extending present balancing capability over a broad speed range. The displacement of the center of gravity of the rotating mass must be maintained in the range of 2.5×10^{-6} to 12.7×10^{-6} cm (1 to 5 μ -in.) as compared to the 51×10^{-6} to 76×10^{-6} cm (20 to 30 μ -in.) demonstrated by present technology. This includes initial balance, variation over the speed range and variations due to environment such as time, temperature, and launch vibration.

Initial balance of rotors to less than 2.5×10^{-6} cm can be obtained by present technology, but the control of variations requires design and development effort. Induced vibration variations due to rotor speed changes are caused by non-uniform expansion/contraction of the rotor due to the change in stress with speed. This can be either due to non-uniform cross-sections or non-homogeneity of the rotor material. Also, bending of the rotor/shaft can cause variations if the bending moments are not zero at the speed of balance. Variations with speed are controlled by initial rotor tolerances and material specifications.

To accomplish the control of induced vibration, it is expected that the total rotor assembly including its bearing, lubrication, spin-motor, and housing components will be balanced at full speed. The development effort is as follows:

- (1) Design and fabricate prototype isotropic rotor.
- (2) Balance rotor using conventional dynamic balance techniques at speed - repeat over speed range.
- (3) Trim balance in final assembly configuration over the speed range.

- (4) Measure vibration environment over operating speed range.
- (5) Analyze vibration isolation concepts to select most suitable configuration.
- (6) Fabricate isolation mount and assemble necessary test fixtures/instrumentation.
- (7) Conduct tests to measure performance of vibration isolation system.
- (8) Develop assembly design and balance requirements.

This effort is estimated to require one and one-half years.

Advanced Technology Developments

High-speed magnetic suspension bearings. - IPACS represents a natural application for non-contacting bearings as means of both prolonging system life and minimizing the power absorbed in the bearings. The most promising non-contacting bearing at this time is the magnetic bearing utilized in either the attractive or repulsive mode. During the past three years, magnetic bearings have been developed for momentum wheels and CMG's by NASA, but these bearings have largely been characterized by high power, low capacity, and relatively low speed ($<10\ 000$ rpm).

Present magnetic bearings have the following technical problems that must be solved prior to their use in an IPACS application:

- (1) Speed limitation - The active magnetic bearing is a shaft position servo that maintains the rotor in the center of a small gap (~ 0.025 cm or 10 mils) and must be able to control the rotor dynamics at the spin frequency and at the spatial coning frequency. Since most IPACS rotors will operate at or above several critical frequencies, this means that structural resonances will occur within the bearing position servo bandwidth and create servo stability problems.
- (2) Capacity/stiffness - Present bearings have been fabricated to support 45 kg (100 lb) with a wide band stiffness of 350×10^4 n/m (20 000 lb/in) which, while adequate for most momentum wheel applications, remains to be proven for the IPACS-type gimbaled units.

It is estimated that this development would require a two- to three-year effort.

Composite rotors.- Design studies, such as those documented in Module 1 of this volume, have shown that composite rotors present the potential for a significant improvement in rotor energy density. Considering the rotor configurations evaluated in this study, the tape-wound design using organic PRD-49-III in an epoxy matrix is considered the most promising concept. At present, however, it must be considered only a "paper" concept. A three-phase development program is required to bring composite rotor technology to the point where it can be applied to IPACS.

Phase I analysis and design: The products of this effort are detailed design drawings of a prototype rotor together with a specification for the manufacturing process. Detailed analyses must be performed to support this design effort. The most significant problem involves the interface between the isotropic shaft and hub and the composite disk.

Phase II component development: This phase includes the fabrication of prototype rotors, dynamic balancing of the rotors, and nondestructive testing.

Phase III component test: The prototype rotors are tested to evaluate their performance including tests specifically to evaluate the following:

- (1) Hub-disk interface integrity.
- (2) Energy at destruction (design margin verification).
- (3) Geometric stability (balance stability) over speed range.
- (4) Failure mechanisms.
- (5) Induced vibration.
- (6) Fabrication repeatability (uniformity).

Two iterations of the three-phase program are foreseen with a total program duration on the order of two to three years.

Recommended Development Priority

First priority developments.- Two problem areas are categorized in this class:

- Ball bearings and lubrication systems.
- High-speed and power permanent magnet motor/generators.

Both are recommended for early development as they are fundamental to the demonstration and verification of IPACS feasibility. The effort required is relatively modest, yet the results should be adequate to proceed with a first-generation space application of IPACS.

Second priority development.- One problem is categorized as slightly less important than the first two:

- Rotor balancing and induced vibration reduction.

This problem is fundamental to the application of IPACS to the precision pointing space applications such as the astronomy RAM or large space telescope. A program composed of both the first and second priority developments would be the minimum to support a precision pointing application.

Third priority developments.- The remaining two development areas are considered important but primarily with regard to the ultimate performance potential of IPACS. These are the longer duration, more costly developments:

- High speed magnetic suspension bearings.
- Composite rotors.

MODULE 3 - COST ANALYSIS

Introduction and Summary

One of the objectives of the study was to perform detailed cost comparisons to determine the cost effectiveness of the IPACS subsystem when incorporated into the TDRS, RAM, MSS, and the 30-Day Shuttle Sortie spacecraft. For this study, cost effectiveness is defined as the cost penalty or cost value resulting from the incorporation of IPACS into the above user vehicles. The cost effectiveness criteria provided by the statement of work (SOW) included guidelines as to system costs and penalty costs as defined in the costing groundrules and assumptions of this module. As discussed in Module 1 - Technical Feasibility Analysis, the EOS and MJS missions, although beyond the scope of the current contract, were added by Rockwell to better define the technical feasibility of IPACS for various types of satellite missions. Cost comparison studies of these missions were beyond the scope of the present study. It is clear, however, from the similarity in configurations that the EOS mission can be expected to enjoy at least the cost advantage of the TDRS example. The lower orbit of the EOS and consequent higher number of charge-discharge cycles per year favor the IPACS application over conventional battery systems and could therefore be expected to result in some cost advantage to the EOS IPACS. In the case of the MJS mission, the fact that IPACS was not considered competitive in a weight and performance sense makes cost comparison academic.

This module reflects the results of the cost analysis and the cost comparisons made between the IPACS and the competitive subsystems. Table 3-I shows the impact on cost of the IPACS configuration for the TDRS, RAM, MSS, and the 30-Day Shuttle Sortie. Development cost, first flight system cost, and cost effectiveness in terms of cost penalty and advantage are shown for all four programs. Mission operations costs were computed in accordance with the statement-of-work for comparative purposes for the TDRS and the RAM programs.

In each case, the present competitive power and control subsystem costs were taken from the original funded contract studies. The IPACS configuration cost reflects the results of the deletion of components from the present competitive subsystem and the addition of the IPACS components to the competitive subsystems.

Table 3-I reflects that the incorporation of IPACS into the four examined programs results in significant cost savings. The IPACS cost savings to the present competitive subsystems for the TDRS are just over 11 percent and for the RAM approximately 13 percent excluding penalty costs. The equipment cost savings for the MSS are approximately \$6.0M. The 30-Day Shuttle

TABLE 3-I.- COST SUMMARY AND COMPARISON

	Cost (\$ = M)					
	Development	First flight system	Missions operations	Equipment cost total	Penalty costs	Total cost comparison
TDRS						
Present competitive subsystem	\$ 3.254	\$ 0.800	\$ 7.648	\$11.702		
IPACS configuration	<u>2.869</u>	<u>0.657</u>	<u>6.861</u>	<u>10.387</u>		
Net*	(-) \$.385	(-) \$.143	(-) \$.787	(-) \$1.315	(+) \$.036	(-) 1.279
RAM						
Present competitive subsystem	20.080	8.400	12.833	41.313		
IPACS configuration	<u>20.663</u>	<u>7.746</u>	<u>7.693</u>	<u>36.102</u>		
Net	(+) \$.583	(-) \$.654	(-) \$5.140	(-) \$5.211	(-) 9.832	(-) 15.043
MSS						
Present competitive subsystem	226.400	136.800	NR**	363.200		
IPACS configuration	<u>222.312</u>	<u>135.150</u>		<u>357.462</u>		
Net	(-) \$4.088	(-) \$1.650		(-) \$5.738	(-) .855	(-) 6.593
30-Day Shuttle Sortie						
Present competitive subsystem	41.912	8.889	NR**	50.801		
IPACS configuration	<u>53.223</u>	<u>8.541</u>		<u>61.764</u>		
Net	(+) \$11.311	(-) \$0.348		(+) \$10.963	(-) .131	(+) 10.832

*(-) = IPACS advantage

*(+) = IPACS disadvantage

**Not required

Sortie has a cost penalty, which is traceable to the exceptionally high power required for the materials science experiment of the selected Shuttle mission. This high power makes the IPACS system costs inordinately high. It is shown in Module 5 that lower power requirements for Sortie missions result in cost effective IPACS applications. Because this experiment represents a worst case requirement which occurs rarely in the overall Shuttle missions, study results now indicate that a cost effective IPACS can be designed for the Shuttle Sortie missions with material science experiment peak power provided by conventional means when required. The penalty cost associated with using the cost effectiveness factors are also shown in Table 3-I. The penalty cost is then combined with the equipment cost to arrive at a total cost impact figure. Again, only in the case of the 30-day sortie is the cost impact not a potential savings.

Costing Groundrules and Assumptions

The major groundrules and assumptions for computing and comparing costs are as follows:

- (1) All costs, for IPACS and competitive subsystems, were normalized to GFY 1973 dollars.
- (2) Both IPACS and competitive subsystem costs include cost of tooling and special test equipment (STE) utilized by the factory for in-process checkout during fabrication.
- (3) Costs of assembly, checkout, and acceptance prior to installation into the user vehicle are included.
- (4) Competitive system costs were taken directly from original program documents.
- (5) Cost estimating techniques were matched to original program methods.
- (6) The following engineering and qualification test models are required:

	Unit Model	Subsystem Models
TDRS	1	1
RAM	1	1
MSS	1	2
Shuttle Sortie	1	2

Common costs.- The following costs were not considered in this study because it was felt that they are comparable or approximately the same for both the components deleted and the IPACS units added. They would, therefore, tend to cancel out or off-set each other in the comparative cost analysis conducted during the study:

- (1) Projected cost escalation and inflation factors beyond GFY 1973
- (2) User installation, test, checkout, and support
- (3) Ground support equipment (GSE) and facilities
- (4) Logistics support, parts, and documentation, except as shown in mission operations cost
- (5) Project management
- (6) Contract fee

Cost effectiveness factors.- The following factors were used in computing penalty costs and comparing the cost effectiveness of the IPACS configurations:

- (1) \$250/pound of launch weight
- (2) \$1400/pound of launch weight - geosynchronous orbit application
- (3) \$1500/cubic foot of occupied space
- (4) \$760/watt-year of power consumption

Work breakdown structure (WBS).- The highest level of WBS involvement during the IPACS study was at WBS level 5 - Subsystem Level. Figure 3-1 illustrates the position of level 5 in a typical program summary WBS. In a typical program summary-type WBS, level 2 is the top program designation. Level 3, Project Level, includes WBS items such as, but not limited to, launch vehicles, space vehicles, experiments, launch operations and services, and flight operation and services. Level 4 includes items such as design, development, test and engineering (DDT&E); flight hardware; major test hardware; ground support equipment; and facilities. Level 5, the subsystem level of the WBS, includes items such as structures, electrical power, attitude control, propulsion, and communications. Level 6 WBS items were deleted from the competitive subsystems and replaced by components added by the incorporation of IPACS. Also some level 6 components examined during the study were considered to be common to both the competitive subsystem and to IPACS requirements. Therefore, the WBS served as a means of structuring the IPACS costs for comparison to the competitive subsystem components deleted, and for reporting the results of the IPACS cost analysis.

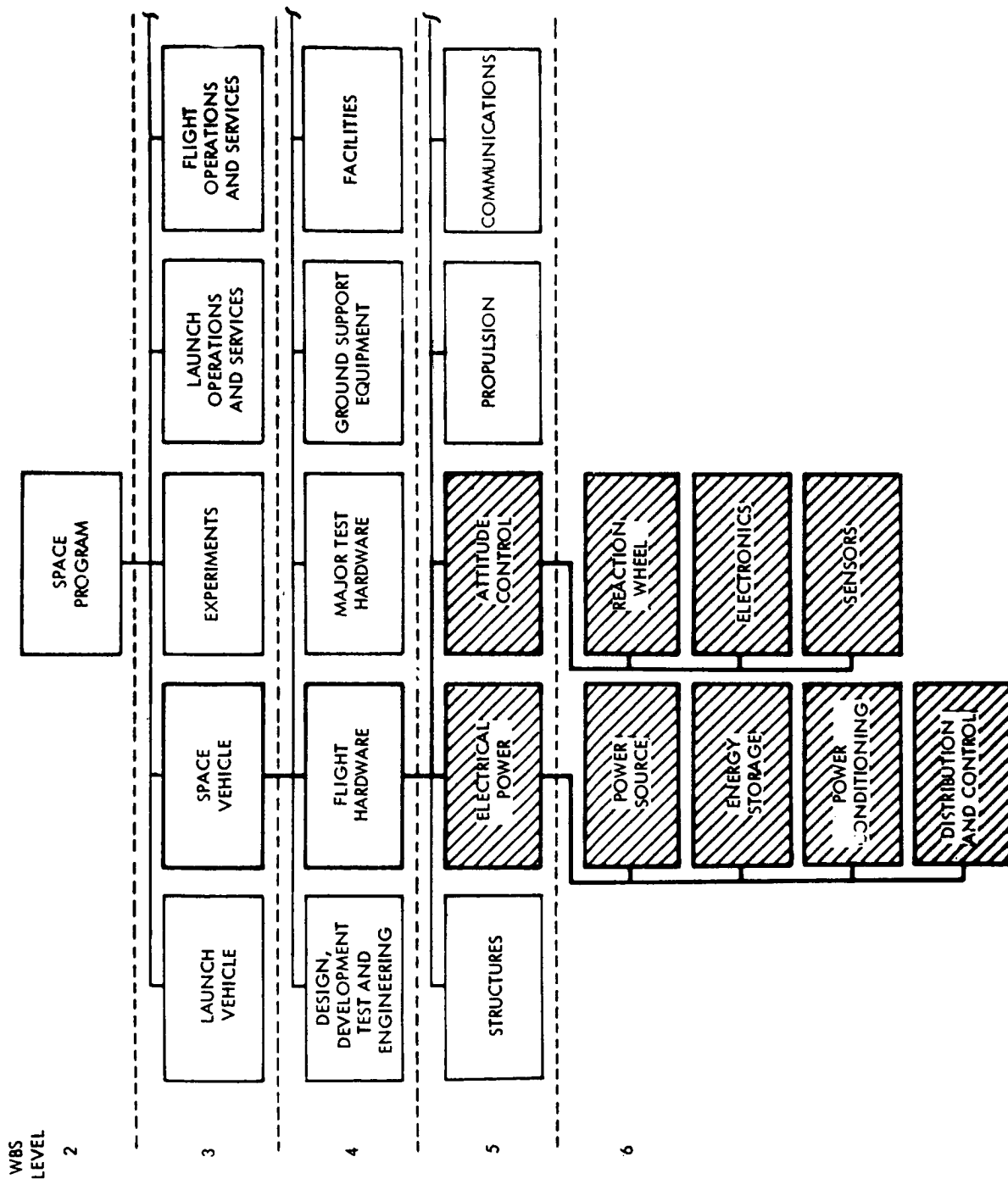


Figure 3-1. Summary Work Breakdown Structure (WBS)-Typical

Costing approach.- The overall approach to the task of costing the results of the IPACS study relates to the impact of incorporating IPACS into competitive subsystems of the candidate user vehicles, TDRS, RAM, MSS, and 30-Day Shuttle Sortie and to the state-of-the-art requirements and technology available for certain IPACS components.

The costing approach as it relates to the competitive subsystems was to identify and cost those components which would be replaced or eliminated by the incorporation of IPACS. Also, as mentioned above, it was determined for the purposes of this study that certain types of costs, such as ground support equipment, facilities, tooling, special test equipment, logistics support, user installation, test, checkout, and project management would be approximately the same for IPACS as for the components deleted. These types of costs were excluded since it was assumed that they would off-set each other in the comparisons performed during the study.

In most cases, the costs of the components deleted were calculated by the application of the parametric costing technique, which employs cost estimating relationships (CER's). The CER's, such as dollars per pound, were developed from the cost and technical data at the level available from the original program documentation. Where cost data were available for the components being deleted, the cost estimator utilized the exact cost reflected in the documentation.

Rockwell performed the task of calculating the cost of components deleted or eliminated from the competitive subsystems. The task of costing the design, development, testing, and fabrication of IPACS rotating assembly units was subcontracted to the Aircraft Equipment Division of General Electric of Binghamton, New York.

In the costing approach utilized, each mission system reflects the full cost of development of critical components. Possible benefits of technology carryover which may occur from an earlier development of a given critical component were not assumed because of uncertainties in NASA development priorities over the long term. Clearly, the early development of a critical component, such as a composite rotor for a RAM mission, would add appreciably to the IPACS advantage to the following systems.

The costs of IPACS units added are based upon estimates of manhours in terms of engineering, drafting, technicians, shop, reliability, and quality assurance requirements. Material costs and cost estimates of IPACS tooling, assembly and checkout, and acceptance tests were also determined.

The cost estimates were adjusted to include the same factors and mark-ups utilized in the original program costing, such as factors for growth, Rockwell supplier support, material procurement, and general and administrative (G&A). All IPACS costs were calculated in terms of GFY 1973 dollars. The costs of competitive subsystems were normalized to GFY 1973 dollars. (Refer to Groundrules and Assumptions.)

The mission operations costs are based upon an engineering analysis of mission operations requirements for the components deleted and the IPACS units added. More detailed data on mission operations requirements are provided below under each mission.

TDRS Cost Data

General.- Presented here are the programmatic information and cost data relating to the TDRS program. The programmatic information consists of the work breakdown structure (WBS) and the program development schedule. These data reflect the results of the cost analysis in terms of equipment cost, cost breakdowns, a comparison of development and first flight system cost, IPACS annual funding schedule, mission operations cost, and cost effectiveness tradeoffs. The comparisons show favorable cost reductions in all aspects of the TDRS program resulting from incorporation of IPACS. The development costs reflect slightly over 20 percent reduction (1.406M compared to 1.791M), while the first flight system and mission operations costs show approximately 30 percent savings (2.21M compared to 3.14M).

Work breakdown structure (WBS): Figure 3-2 sets forth the structure of the TDRS-IPACS-WBS prepared during the study. The WBS reflects those elements and components deleted as a result of the incorporation of IPACS, as well as the subsystem components unaffected and/or common to both the competitive subsystem and IPACS. The IPACS units and WBS elements added are shown also.

The TDRS-IPACS-WBS reflects design, development, test hardware (Engineering models), flight hardware, tooling and special test equipment, assembly and checkout, and mission operations for both the competitive subsystem and IPACS. The WBS shows an acceptance test separately for IPACS. It was assumed for this study that the competitive subsystem costs included the cost of acceptance tests. However, acceptance tests costs were not shown separately in the level of cost data examined during the study on the competitive subsystems.

IPACS development schedule: The TDRS IPACS utilizes a current technology flywheel subassembly. The IPACS TDRS Development Schedule (figure 3-3) to develop, test, and fabricate the TDRS IPACS units is planned to require a period of 3 years, excluding mission operations time. The design service life of the TDRS vehicle is 5 years. The program schedule identifies the development span

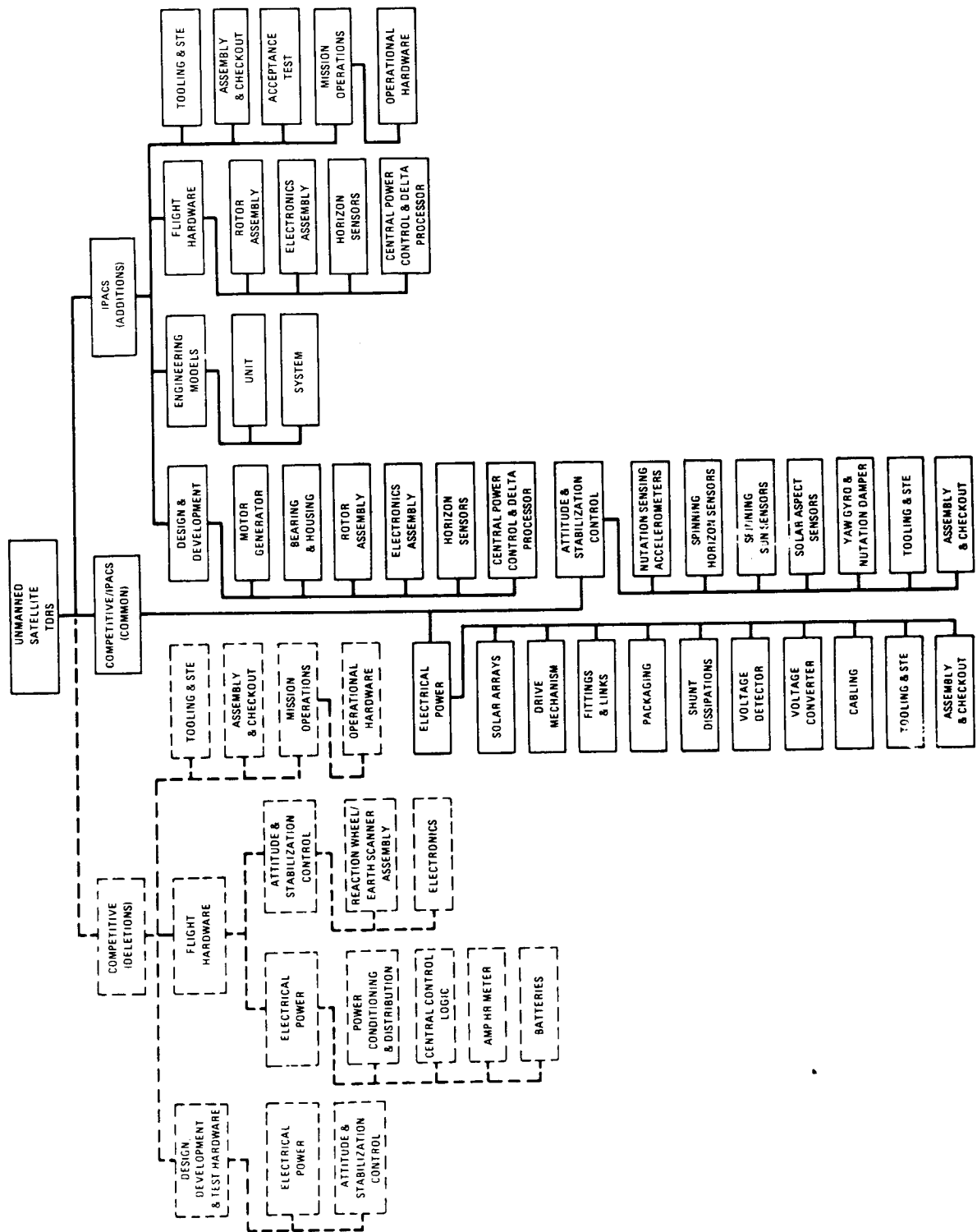


Figure 3-2. IPACS Work Breakdown Structure (WBS) for TDRS

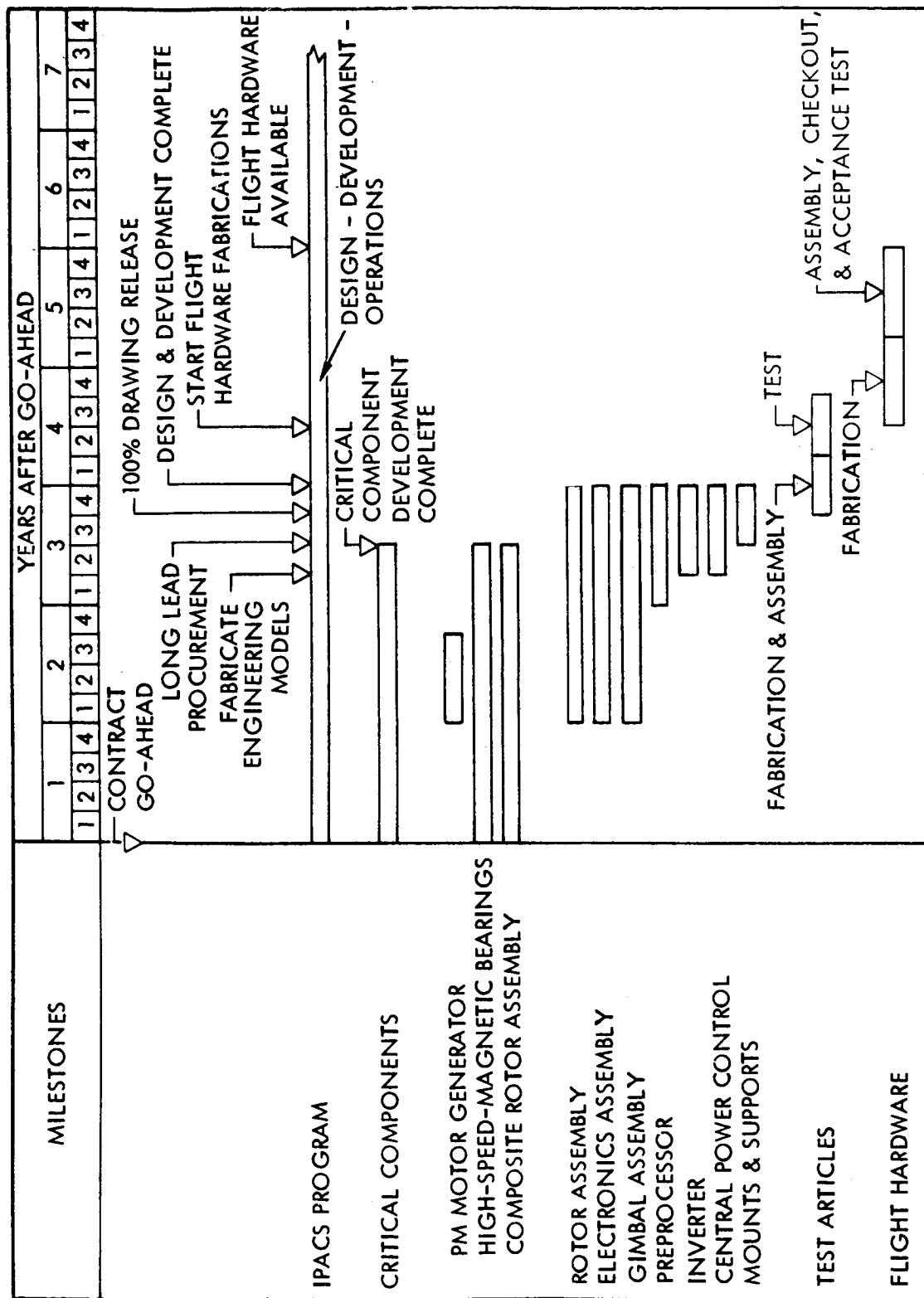


Figure 3-3. TDRS IPACS Development Schedule

time for the two IPACS components considered critical, the motor generator, and bearings. The estimated development times are 9 months for the motor generator and 15 months for the bearings. The development time span for the other IPACS units are shown. Drawing release and all design and development tasks are scheduled to be completed by the end of the second year. Fabrication, assembly, and test of the engineering models and the flight hardware are shown. The operational flight hardware is scheduled to be available during the first quarter of the fourth year after contract go-ahead. The flight operations time-span bar is not shown to be complete. However, it is assumed that it would cover 5 years.

Equipment cost.- Table 3-II reflects the impact on cost of the competitive subsystem as a result of incorporating IPACS into the TDRS vehicle. The costs are summarized separately for development (non-recurring), first flight system, and mission operations (recurring) for both the competitive subsystem and IPACS. The cost of the electrical power and the attitude control subsystems, as shown in the original program document, is \$3.254M for development and \$0.800M for the first flight system - a total of \$4.054M through the first flight system. Mission operations costs are \$7.648M, for a total of \$11.702M, including operational requirements of two sets of TDRS flight vehicles. Each set consists of two active and one on-orbit, spare TDRS vehicle.

The cost of the components deleted from the electrical power and the attitude control subsystems is \$1.791M for development, \$0.483M for the first flight system, and \$2.657M for mission operations. Approximately 60 percent of the cost through the first flight system of the competitive subsystem and approximately 35 percent of the cost of mission operations are deleted. The cost added by the incorporation of IPACS is \$1.406M for development, \$0.340M for the first flight system, and \$1.870M for mission operations. The net results show a reduction in subsystem cost of approximately 13 percent through the first flight system at \$3.526M, and a cost reduction of 10 percent in mission operations costs.

The TDRS mission operations costs include only the operational hardware required in addition to the first flight system cost. In the case of the TDRS, the total operational hardware requirements consist of two sets of flight vehicles. Each set consists of two active and one on-orbit spare vehicle, or a total of six TDRS vehicles. Therefore, the delta operational hardware cost shown in Table 3-II includes the cost of five additional TDRS vehicles worth of competitive components deleted and IPACS units added. It is assumed that there will be neither orbital maintenance nor ground spares. The cost of the five additional sets of components deleted amounts to \$2.657M. The cost of five additional sets of IPACS units added amounts to \$1.870M, a difference in mission operations cost of \$0.787M or approximately 30 percent. It was assumed in calculating the mission operations costs for both the competitive and the IPACS requirement that there would be neither refurbishment nor transportation cost. The TDRS application concept is based upon no maintenance nor spares.

TABLE 3-II.- COST SUMMARY - TDRS*

Cost levels	Development	First flight system	Sub-total	Mission operations	Total
Competitive subsystems**					
Electrical power	\$ 1.939	\$ 0.434	\$ 2.373	\$ 4.323	\$ 6.696
Attitude stabilization control	<u>1.315</u>	<u>0.366</u>	<u>1.681</u>	<u>3.325</u>	<u>5.006</u>
Totals	\$ 3.254	\$ 0.800	\$ 4.054	\$ 7.648	\$11.702
Less: Components deleted	(-) 1.791	(-) 0.483	(-) 2.274	(-) 2.657	(-) 4.931
Add: IPACS components	<u>1.406</u>	<u>0.340</u>	<u>1.746</u>	<u>1.870</u>	<u>3.616</u>
Net	(-) 0.385	(-) 0.143	(-) 0.528	(-) 0.787	(-) 1.315
New totals	2.869	\$ 0.657	\$ 3.526	\$ 6.861	\$10.387
* Dollars-in-millions					
**Source: Reference 3-1					

Components deleted: The costs of the components deleted are shown in detail in Table 3-III. The cost of the components deleted were determined by the application of CER's, such as dollars per pound, developed from the cost and technical data available from the original program documentation.

The non-recurring cost of \$1.791M includes \$1.725M for design and development, such as engineering analysis, design, preparation of drawings, specifications, plans, documentation, support, component development, laboratory testing, mockups and test hardware for the electrical power and attitude control subsystems, as well as \$0.066M of tooling and special test equipment (STE) utilized by the factory for in-process testing during fabrication.

The recurring cost (first flight system) of \$.483M includes flight hardware of \$.436M and assembly and checkout of \$.047M.

TABLE 3-III.-COST BREAKDOWN - COMPONENTS DELETED - TDRS

Cost Levels	Non-Recurring	Recurring	Totals
Non-recurring			
Design, development and test hardware			
Electrical power	\$0.800		\$0.800
Power conditioning and distribution			
Central control logic			
AMP hr meter			
Batteries			
Attitude and stabilization control	0.925		0.925
Reaction wheel/earth scanner assy			
Electronics			
Tooling and STE	0.066		0.066
Recurring (first flight system)			
Flight hardware			
Electrical power		0.179	0.179
Power conditioning and distribution			
Central control logic			
AMP hr meter			
Batteries			
Attitude and stabilization		0.257	0.257
Reaction wheel/earth scanner assy			
Electronics			
Assembly and checkout		0.047	0.047
Total	\$1.791	\$0.483	\$2.274

IPACS units added: Table 3-IV reflects a detailed cost breakdown of design, development, test, and fabrication by IPACS units, including cost of engineering models, tooling and STE, assembly and checkout, and acceptance tests cost. The non-recurring cost of \$1.406M includes \$0.842M of design and development, \$0.355M for engineering models, \$0.031M for tooling and special

TABLE 3-IV.- TABLE COST BREAKDOWN - TDRS IPACS UNITS ADDED
(DOLLARS IN M)

	Non- Recurring	Recurring	Total
Non-recurring			
Design & development			
Motor generator	\$.050		\$.050
Bearing & housing	.105		.105
Rotor assembly	.195		.195
Electronics assembly	.093		.093
Horizon sensors	.164		.164
Central power control	.235		.235
Engineering models			
Unit models			
Rotor assembly	.024		.024
Electronics assembly	.017		.017
Horizon sensors	.045		.045
Central power control	.052		.052
System model			
Rotor assembly	.072		.072
Electronics assembly	.048		.048
Horizon sensors	.045		.045
Central power control & delta processor	.052		.052
Tooling & STE	.031		.031
Assembly & checkout	.081		.081
Acceptance tests	.097		.097
Recurring costs (first flight system)			
Flight hardware			
Rotor assembly		\$.072	.072
Electronics assembly		.048	.048
Horizon sensors		.045	.045
Central power control		.052	.052
Assembly & checkout		.055	.055
Acceptance tests		.068	.068
Total	\$1.406	\$.340	\$1.746

test equipment, \$0.081M for assembly and checkout, and \$0.097M for acceptance tests. The unit models which are for component qualification and tests, consist of one each of the rotor assembly, the electronics assembly, the horizon sensors, and the central power control and delta processor. The systems models which are for TDRS vehicle systems verification and integration tests consist of one or the equivalent of one flight system: four rotor assemblies, four electronics assemblies, one set of horizon sensors, and one central power control and delta processor.

IPACS annual funding: Table 3-V shows the peak year funding for incorporation of IPACS into the TDRS. The funding is presented in government fiscal years (GFY's) after go-ahead. As shown in figure 3-3, IPACS Development Schedule, the time span of the IPACS development, test, and fabrication of flight hardware is 3 years. Table 3-V shows the peak year funding to occur in the second year after go-ahead at \$0.933M.

TABLE 3-V.- IPACS ANNUAL FUNDING SCHEDULE - TDRS

Description	Years after go-ahead			
	1	2	3	Total
TDRS IPACS	\$0.399	\$0.933	\$0.414	\$1.746
*Dollars-in-millions				

Cost effectiveness factors.- Table 3-VI reflects the cost resulting from the application of the cost effectiveness criteria. The weight saved by the incorporation of IPACS into the TDRS vehicle is 22.1 lb. IPACS occupies 1.778 cu ft more space than does the present components deleted by IPACS units. Also, IPACS increases the watt-years (W yr) consumption of power by 45. A minus (-) value reflects an IPACS advantage, and a plus (+) value shows an IPACS penalty. Therefore, the net results from the application of the cost effective weighting factors show a net IPACS cost disadvantage of \$.006M for each TDRS vehicle.

TABLE 3-VI.- COST EFFECTIVENESS TRADEOFF

Description	Delta amount	Factor	Cost (\$ = M)
Weight - lb	(-) 22.1	\$1400/lb	(-) \$.031
Space occupied - cu ft	(+) 1.778	\$1500/ft ³	(+) .003
Power consumption - Watt yr	(+) 45	\$760/W yr	(+) .034
Net			(+) .006

For the postulated mission of six TDRS vehicles, the total penalty costs would amount to a net IPACS cost disadvantage of \$.036M.

Total cost comparison.- A measure of the total program cost impact can be obtained by combining the equipment and penalty cost figures as shown in Table 3-VII. This table indicates that the IPACS approach could have a net savings effect of \$1.279M which is slightly greater than 10 percent of the total program cost for the electrical power and attitude control subsystems.

TABLE 3-VII.- TOTAL COST

Differential equipment cost	\$(-) 1.315M
Penalty cost	<u>(+) 0.036M</u>
Cost impact (net savings)	\$ 1.279M

RAM Cost Data

General.- This section presents data relating to the cost analysis conducted on the RAM program during the study. The RAM IPACS work breakdown structure, program development schedule, equipment cost, cost breakdowns, cost comparisons, annual peak year funding, and cost-effectiveness tradeoffs are shown and discussed in detail. The equipment cost analysis indicated a substantial IPACS cost reduction. The IPACS development and refurbishment costs are slightly higher than the cost of the components deleted. The IPACS first flight system costs also represent savings of \$0.654M, in excess of 35 percent. The IPACS mission operations costs are substantially less (\$5.140M) than the mission operations cost of the components deleted. Therefore, incorporation of IPACS into the RAM vehicle would result in overall cost reduction in excess of \$5.211M, Table 3-VIII.

Work breakdown structure: Figure 3-4 shows the RAM IPACS WBS prepared during the study. Included are the WBS items and hardware components of the competitive subsystem that were deleted. The WBS identifies the competitive subsystem components considered to be common to both subsystems or unaffected by the incorporation of IPACS. The IPACS units and WBS elements added also are shown.

The WBS includes design, development, test hardware (engineering models), flight hardware, tooling and STE, assembly and checkout, and mission operations for both the components deleted and IPACS units. Acceptance tests are shown separately for IPACS. It was assumed for this study that the competitive subsystem costs included the cost of acceptance tests; however, they were not shown separately in the level of cost data on the competitive subsystems examined during the study.

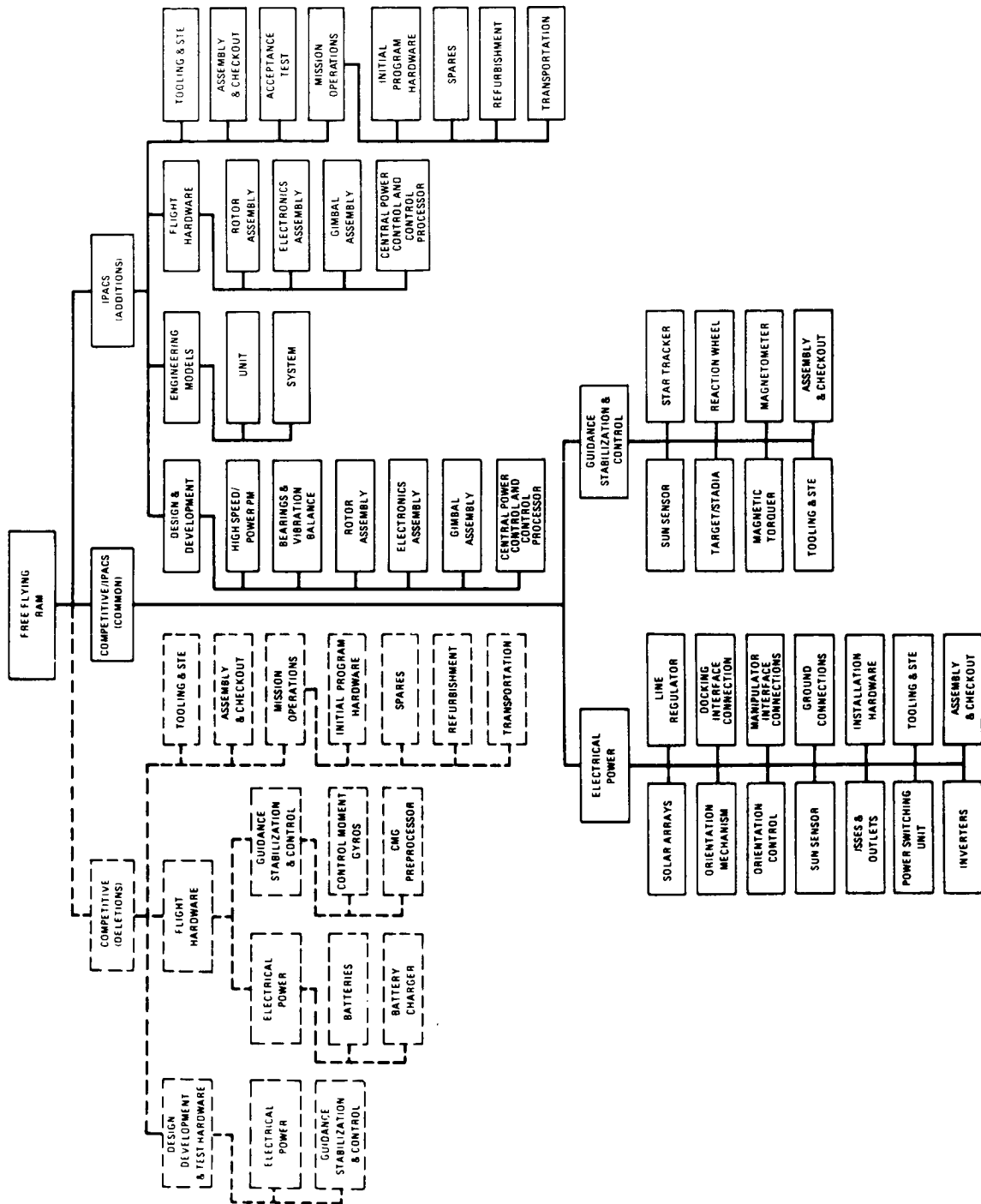


Figure 3-4. IPACS Work Breakdown Structure (WBS)-RAM

IPACS development schedule: The RAM IPACS utilizes a current technology flywheel assembly. Development, test, and fabrication of the RAM IPACS units would require a period of 4 years (figure 3-5). The program schedule identifies the development span for the two IPACS components considered critical: the high-speed permanent magnet motor and the rotor. The estimated development time is 1 year for the high-speed permanent magnet motor and 1 1/2 years for the high-speed rotor. The development spans for the other IPACS units are shown. Drawing release and all design and development tasks are scheduled to be completed by the end of the second year. Fabrication, assembly, and test schedules of the engineering models and the flight hardware are shown. The operational flight hardware is scheduled to be available during the latter part of the fourth year after contract go-ahead. It is assumed that flight operations would extend over a period of 11 years.

Equipment Cost.- Table 3-VIII shows the impact on cost of the competitive subsystem as a result of incorporating IPACS into the RAM vehicle. The costs are summarized separately for development (non-recurring), first flight system, and mission operations (recurring) for both the competitive subsystem and IPACS. The cost of the electrical power and the attitude control subsystems, as shown in the original program document is \$20.080M for development and \$8.400M for the first flight system, for a total of \$28.480M through the first flight system. Mission operations cost for the total electrical power and stabilization and attitude control competitive subsystem was not determined, except for the components added and deleted.

The cost of the components deleted from the electrical power and attitude control subsystems is \$2.156M for development, \$1.761M for the first flight system, and \$12.833M for mission operations. Less than 15 percent of the cost of the competitive subsystems through the first flight system is deleted by IPACS. The cost added by the incorporation of IPACS is \$2.739M for development, \$1.107M for the first flight system, and \$7.693M for mission operations. Table 3-VIII cost summary shows an insignificant reduction in cost through the first flight system resulting from the incorporation of IPACS into the RAM vehicle, \$0.071M. However, Table 3-VIII reflects a substantial difference in the mission operations cost at \$5.140M, or 40 percent.

The RAM mission operations costs associated with the components deleted and the IPACS units added are shown in Tables 3-IX and 3-X. The mission operations cost consists of operational replacement hardware and refurbishment. Cost of transportation of parts and supplies from the ground to earth orbit is included in penalty cost, Table 3-XV. The following ground rules and assumptions were used in costing mission operations:

- (1) The operational period was 11 years.
- (2) The flight program was that shown in figure 3-6.

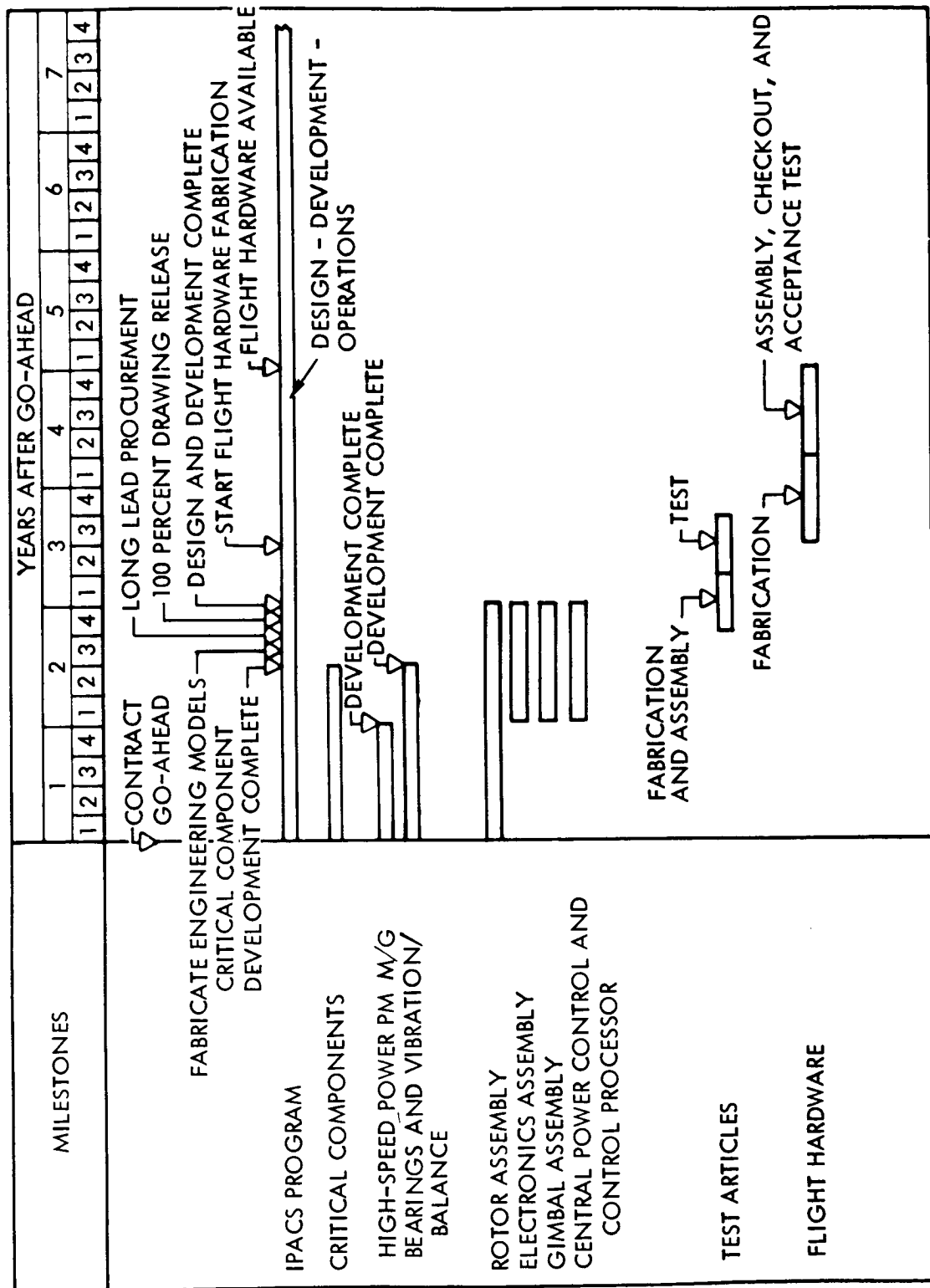


Figure 3-5. Free-Flying RAM IPACS Development Schedule

TABLE 3-VIII.- RAM COST SUMMARY

Cost level	Cost (\$=M)				
	Develop- ment	First flight system	Subtotal	Mission operations	Total
Competitive subsystems*					
Electrical power	\$ 5.050	\$5.460	\$10.510	**	\$10.510
Stabilization & attitude	15.030	2.940	17.970	**	17.970
Total	\$20.080	\$8.400	\$28.480	**	\$28.480
Minus: Components deleted	2.156	1.761	3.917	\$12.833	16.750
Plus: IPACS components	2.739	1.107	3.846	7.693	11.539
Net difference	+0.583	-0.654	-0.071	-5.140	-5.211
New total	\$20.663	\$7.746	\$28.409	\$-5.140	\$23.269
*Source: Reference 3-2 **Mission operations costs for the total competitive subsystem were not determined at this time					

TABLE 3-IX.-MISSION OPERATIONS COST - RAM COMPONENTS DELETED
(DOLLARS IN M)

Description	Replace- ment Hardware	Refurbish- ment	Total
Operational replacement hardware			
Battery packs	\$ 4.302		\$ 4.302
Control moment gyros	8.240		8.240
Refurbishment cost			
Control moment gyros		\$0.291	0.291
Total	\$12.542	\$0.291	\$12.833

TABLE 3-X.- MISSION OPERATIONS COSTS - RAM IPACS UNITS ADDED

Description	Cost (\$=M)
	Total
Operational replacement hardware	\$7.360
Refurbishment	0.333
Total	\$7.693

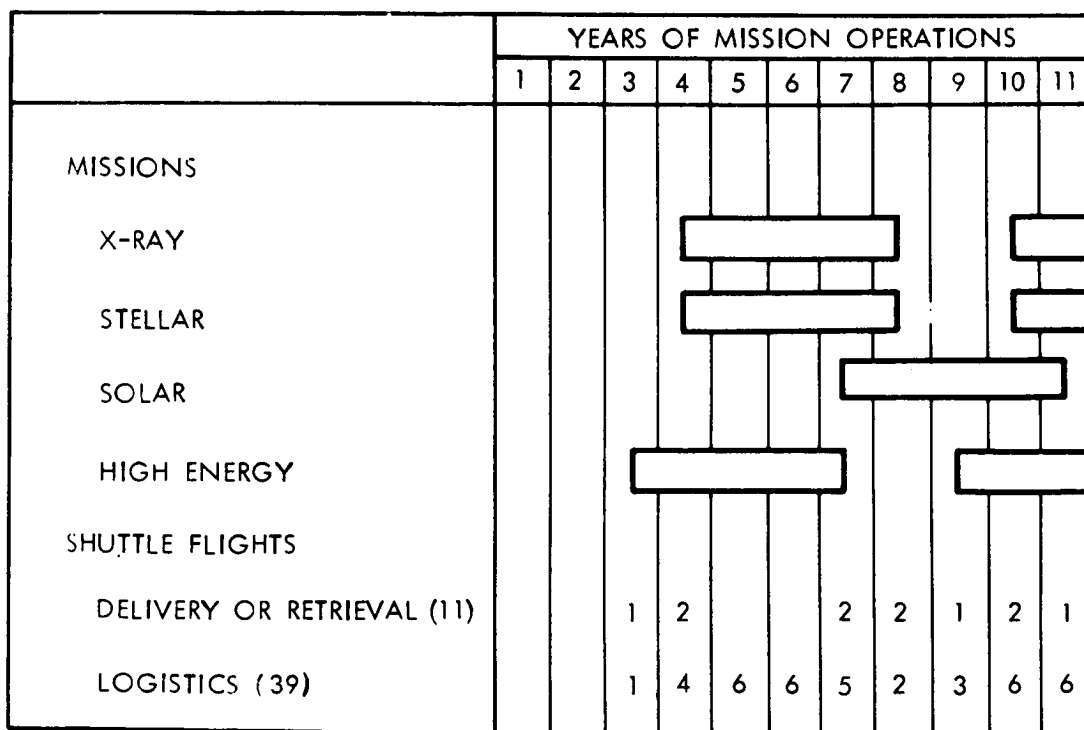


Figure 3-6. RAM Mission Logistics

- (3) Flight units (IPACS and CMG's) are exchanged in orbit and refurbished on ground for reflight.
- (4) IPACS units or CMG's are not flown after 5 years of operation.
- (5) Batteries are replaced after 3.3 years of flight use. The interval of 3.3 years was derived from battery cycle life test data with the battery sized for optimum depth of discharge.
- (6) Batteries are not refurbished.
- (7) The average replacement parts weight for computing transportation penalty costs is given in Table 3-XI.

TABLE 3-XI.- REPLACEMENT PARTS WEIGHT

Description	Sched maint. wt kg (lb)/6 months	Unsched maint. wt kg (lb)/6 months
Deleted components		
Batteries	52.6 (116)	2.3 (5)
CMG's	64.9 (143)	10.0 (22)
IPACS components	39.5 (87)	5.9 (13)

The scheduled maintenance weight requirements for the CMG's and IPACS units were based upon MTBF's of 118 000 and 154 000 hours, respectively. It was assumed that individual units would be replaced when their reliability dropped to 0.85. Both the CMG and IPACS failure rate estimates assume the use of high reliability parts, burn-in, and in-orbit stress levels. Single level standby redundancy was assumed for all electronics. The unscheduled maintenance estimate for the batteries is based on a battery pack MTBF of 260 000 hours.

- (8) The total program included three refurbishment operations.
- (9) CMG and IPACS unit refurbishment cost was 10 percent of the cost of a new unit.

(10) Flight replacement hardware requirements were:

Description	Flight replacement		Total
	units	Spares	
Battery packs	46	5	51
CMG's	27	4	31
IPACS units	20	4	24

Components deleted: The costs of the components deleted from the competitive subsystem are shown in detail in Table 3-XII. The cost of the components deleted were determined by the application of cost estimating relationships, such as dollars per pound, which were developed from the level of cost and technical data available from the original program documentation.

The non-recurring cost of \$2.156M includes \$1.886M for design and development, such as engineering analysis, design, preparation of drawings, specifications, plans, documentation, support, component development, laboratory testing, mockups, and test hardware for the electrical power and attitude control subsystems, as well as \$0.270M of tooling and special test equipment utilized by the factory for in-process testing during fabrication.

The recurring cost (first flight system) of \$1.761M includes flight hardware of \$1.560M and assembly and checkout of \$0.201M.

IPACS units added: Table 3-XIII gives a detailed cost breakdown of design, development, test, and fabrication by IPACS units, including cost of engineering models, tooling and STE, assembly and checkout, and acceptance tests. The unit models of the engineering models are for component qualification test purposes and consist of one each of the rotor assembly, the electronics assembly, the gimbal assembly, and the central power control and processor. The systems model is for RAM vehicle systems verification and integration tests and consist of the equivalent of one flight system (three rotor assemblies, three electronics assemblies, three gimbal assemblies, and one central power control and processor).

IPACS annual funding: Table 3-XIV shows the peak year funding for incorporation of IPACS into RAM. As shown in figure 3-5, the IPACS development, test, and fabrication period is 4 years. Table 3-XIV shows the peak year funding to occur in the third year after contract go-ahead at \$1.584M.

TABLE 3-XII.- COST BREAKDOWN, RAM COMPONENTS DELETED
(DOLLARS IN M)

Cost levels	Non-Recurring	Recurring	Total
Non-recurring			
Design, development and test hardware			
Electrical power	\$1.278		\$1.278
Batteries			
Battery charger			
Stabilization & control	0.608		0.608
Control moment gyros			
CMG preprocessor			
Tooling & STE	0.270		0.270
Recurring (first flight system)			
Flight hardware			
Electrical power		\$0.698	0.698
Batteries			
Battery chargers			
Stabilization & control		0.862	0.862
Control moment gyros			
CMG preprocessor			
Assembly & checkout		0.201	0.201
Total	\$2.156	\$1.761	\$3.917

TABLE 3-XIII.- COST BREAKDOWN, RAM IPACS COMPONENTS ADDED
(DOLLARS IN M)

Cost Levels	Non-Recurring	Recurring	Total
Non-recurring			
Design & development			
High-speed power PM M/G	\$0.058		\$0.058
Bearings and vib./balance	0.192		0.192
Rotor assembly	0.227		0.227
Electronics assembly	0.167		0.167
Gimbal assembly	0.201		0.201
Central power control & processor	0.171		0.171
Engineering models			
Unit models			
Rotor assembly	0.082		0.082
Electronics assembly	0.058		0.058
Gimbal assembly	0.093		0.093
Central power control & processor	0.106		0.106
Systems model			
Rotor assembly	0.196		0.196
Electronics assembly	0.137		0.137
Gimbal assembly	0.221		0.221
Central power control & processor	0.106		0.106
Tooling & STE	0.075		0.075
Assembly & checkout	0.10		0.310
Acceptance tests	0.339		0.339
Recurring costs (first flight system)			
Flight hardware			
Rotor assembly		\$0.196	0.196
Electronics assembly		0.137	0.137
Gimbal assembly		0.221	0.221
Central power control & processor		0.106	0.106
Assembly & checkout		0.214	0.214
Acceptance tests		0.233	0.233
Total	\$2.739	\$1.107	\$3.846

TABLE 3-XIV.- RAM IPACS ANNUAL FUNDING

Description	Years after go-ahead*				
	1	2	3	4	Total
RAM IPACS	\$.288	\$1.251	\$1.584	\$.723	\$3.846
*Dollars in \bar{M}					

Cost effectiveness.- Table 3-XV shows the cost resulting from application of cost-effectiveness factors. The weight saved by incorporation of IPACS into the RAM is 14 898 pounds. IPACS occupies 81.06 cubic feet less space than did the components deleted. Also, IPACS reduces the watt-years consumption of power by 7875. A minus value reflects an IPACS advantage and a plus value shows an IPACS penalty. The application of the penalty cost weighting factors show a net IPACS cost advantage of \$9.832 \bar{M} .

TABLE 3-XV.- COST-EFFECTIVENESS TRADEOFF

Description	Delta amount	Factor	Cost (\$ = \bar{M})
Weight, lb	-14 898	\$ 250/lb	-\$3.725
Space occupied, cu ft	-81.06	\$1500 cu ft	- .122
Power consumption, Watt yr	-7875	\$760 W yr	-5.985
Net			-9.832

Total cost comparison.- The combined cost savings possible through the use of the IPACS approach is shown in Table 3-XVI. This table combines both the equipment and penalty costs.

TABLE 3-XVI.- TOTAL COST

Item	Cost
Differential equipment cost	-\$5.211 \bar{M}
Penalty	-\$9.832 \bar{M}
Cost impact (net savings)	\$15.043 \bar{M}

MSS Cost Data

General.- This section presents the programmatic information and cost data relating to the MSS program, including the work breakdown structure, the program development schedule, equipment cost, cost breakdowns, a comparison of development and first flight system cost, IPACS annual funding schedule, mission operations cost, and cost-effectiveness tradeoffs. The incorporation of IPACS yields cost reductions in all aspects of the MSS program. The development cost reduction is approximately 15 percent and the first flight system cost savings is approximately 22 percent.

Work breakdown structure: Figure 3-7 sets forth the structure of the MSS IPACS WBS prepared during the study. It shows the elements and components deleted as a result of the incorporation of IPACS, as well as the subsystem components unaffected or common to both the competitive subsystem and IPACS. The IPACS units and WBS elements added also are shown.

The MSS IPACS WBS includes design, development, test hardware (engineering models), flight hardware, tooling and STE, assembly and checkout, and mission operations for both the competitive subsystem and IPACS. The WBS shows acceptance test separately for IPACS. It was assumed for this study that the competitive subsystem costs included the cost of acceptance tests; however, they were not shown separately in the level of cost data on the competitive subsystems examined during the study.

IPACS development schedule: The MSS utilizes an advanced technology fly-wheel assembly. Development, test, and fabrication of the MSS IPACS units (Figure 3-8) would require a period of 5 years. The program schedule identifies the development span for the three IPACS components considered critical: the PM motor generator, the high-speed magnetic bearings, and the composite rotor assembly. The estimated development period is 9 months for the PM motor generator and 2-1/2 years for the bearings and composite rotor. The development spans for the other IPACS units are shown. Drawing release and all design and development tasks are scheduled to be completed by the end of the third year. Fabrication, assembly, and test schedules of the engineering models and the flight hardware are shown. The operational flight hardware is scheduled to be available during the latter part of the fifth year after contract go-ahead. The flight operations time was not examined during this study and, therefore, is not shown to completion.

Equipment cost.- Table 3-XVII shows the impact on the cost of the competitive subsystem as a result of incorporating IPACS into the MSS vehicle. The costs are summarized separately for development (non-recurring) and the first flight system (recurring) cost for both the competitive subsystem and IPACS. The cost of the electrical power and the attitude control subsystems, as shown in the original program document (Reference 3-3), is \$226.400M for development and \$136.800M for the first flight system for a total of \$363.200M through the first flight system.

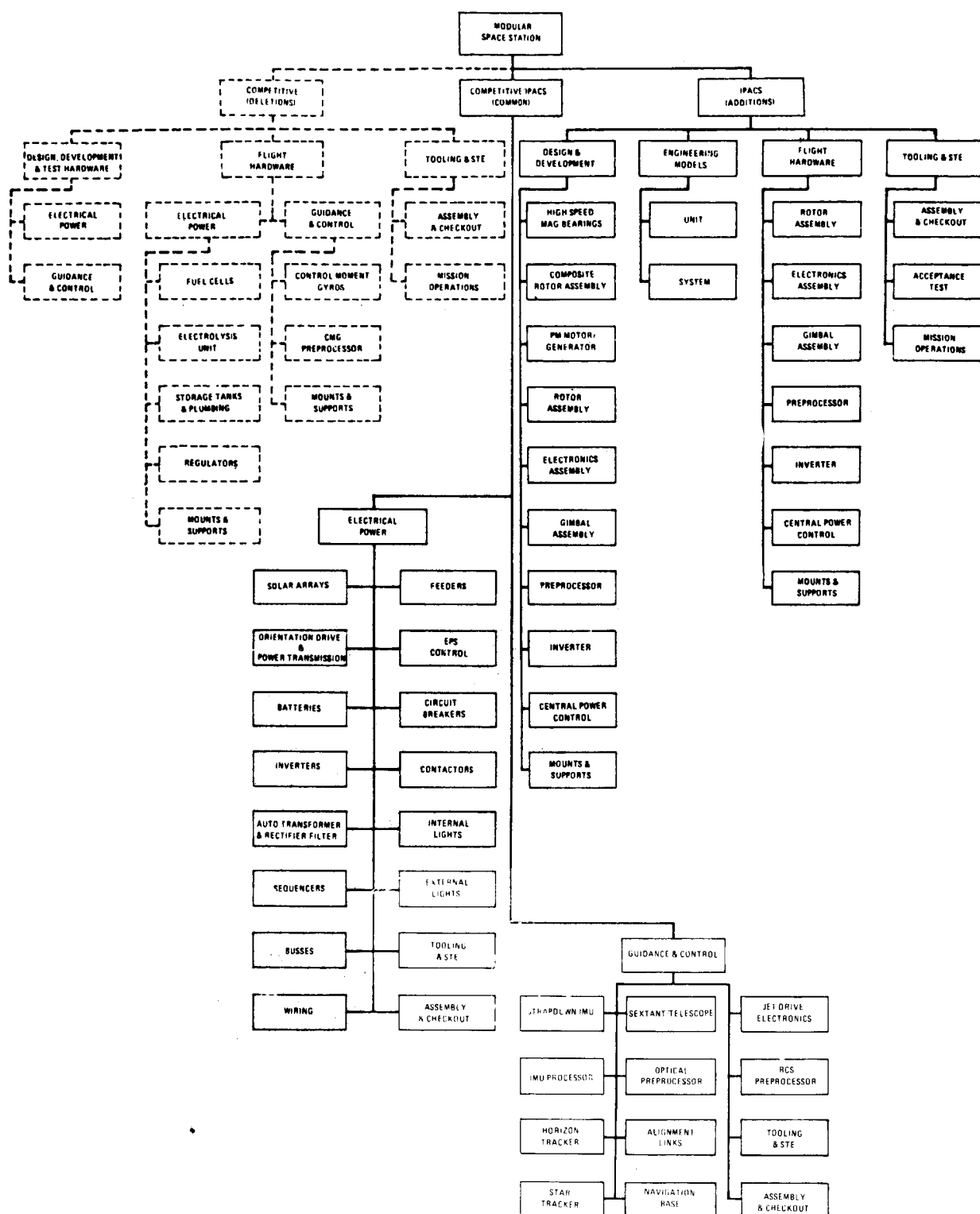


Figure 3-7. IPACS Work Breakdown Structure (WBS)-Modular Space Station

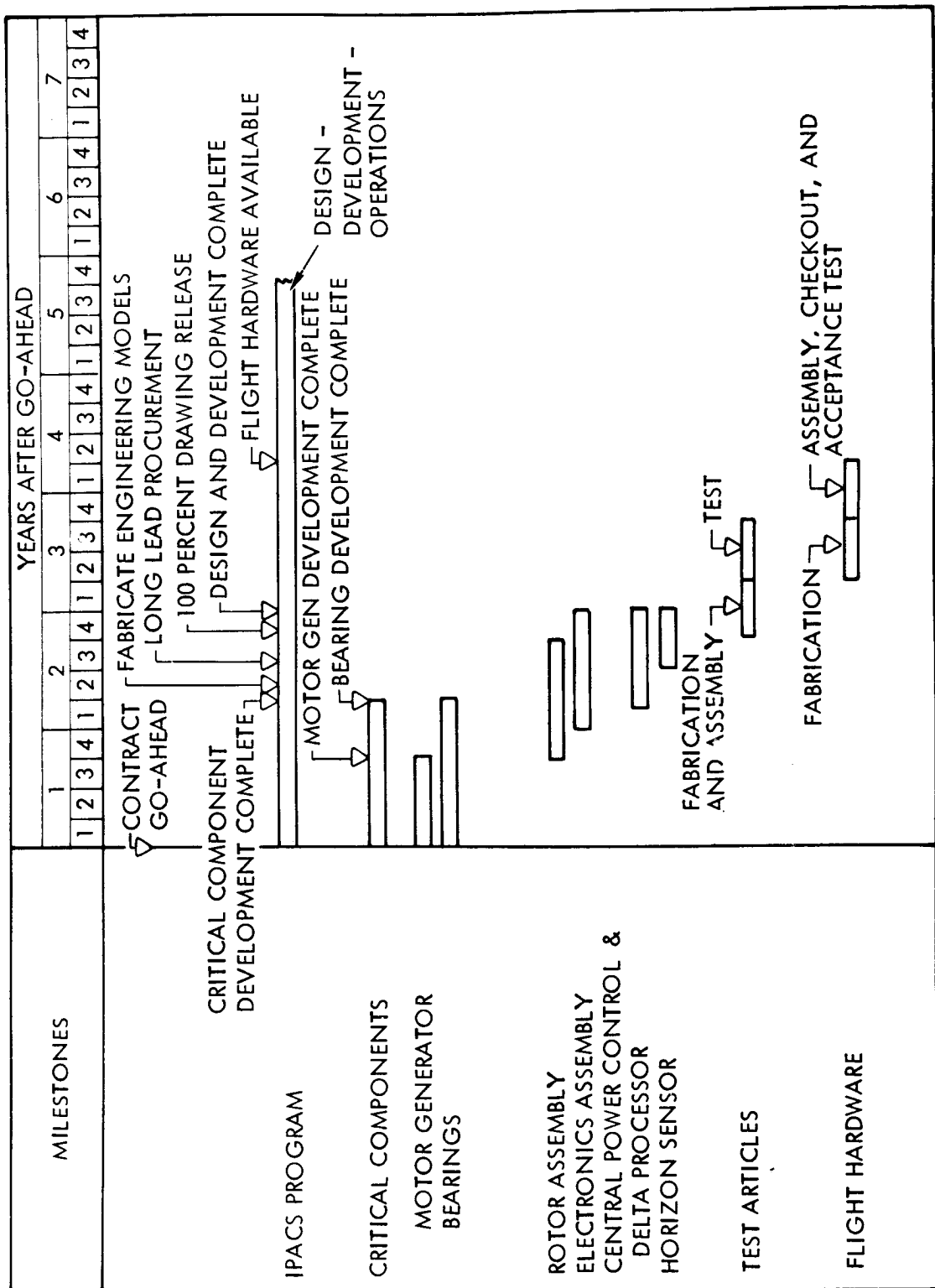


Figure 3-8. MSS IPACS Development Schedule

TABLE 3-XVII.- MSS COST SUMMARY*

	Development	First flight system	Sub-total
Competitive subsystems*			
Electrical power	\$165.500	\$126.500	\$292.000
Guidance and control	60.900	10.300	71.200
Total	226.400	136.800	363.200
Minus: components deleted	28.096	7.675	35.771
Plus: IPACS components	24.008	6.025	30.033
Net	-\$ 4.088	-\$ 1.650	-\$ 5.738
New total	\$222.312	\$135.150	\$357.462
*Dollars-in-millions *Source: reference 3-3			

The cost of developing, testing, and fabricating the first flight system of IPACS units is compared to the deleted components in Table 3-XVII. The cost of developing and testing IPACS units is \$24.008M, or \$4.088M less than the cost of the components deleted, a difference of approximately 15 percent. The difference in cost of the first flight system is approximately 22 percent less for IPACS. The overall cost difference is \$5.78 M, or 16 percent less for IPACS. Mission operations costs were not part of this study.

Components deleted: The costs of the components deleted (Table 3-XVIII) were determined by the application of cost estimating relationships, such as dollars per pound, which were developed from the level of cost and technical data available from the original program documentation.

The non-recurring cost of \$28.096M includes \$26.916M for design and development, such as engineering analysis, design, preparation of drawings, specifications, plans, documentation, support, component development, laboratory testing, mockups, and test hardware for the electrical power and attitude control subsystems, as well as \$1.180M of tooling and special test equipment utilized by the factory for in-process testing during fabrication.

The recurring cost (first flight system) of \$7.675M includes flight hardware of \$6.890M and assembly and checkout of \$0.785M.

TABLE 3-XVIII.- COST BREAKDOWN, MSS COMPONENTS DELETED
(DOLLARS IN M)

Cost level	Non-Recurring	Recurring	Total
Non-recurring			
Design, development and test hardware			
Electrical power	\$10.894		\$10.894
Fuel cells			
Electrolysis unit			
Tanks & plumbing			
Regulators			
Mounts & supports			
Guidance & control	16.022		16.022
Control moment gyros			
CMG preprocessor			
Mounts & supports			
Tooling & STE	1.180		1.180
Recurring (first flight system)			
Flight hardware			
Electrical power		\$4.816	4.816
Fuel cells			
Electrolysis unit			
Tanks & plumbing			
Regulators			
Mounts & supports			
Guidance & control		2.074	2.074
Control moment gyros			
CMG preprocessor			
Mounts & supports			
Assembly & checkout		.785	.785
Total	\$28.096	\$7.675	\$35.771

TABLE 3-XIX.- COST BREAKDOWN, MSS IPACS UNITS ADDED
(DOLLARS IN M)

Cost Levels	Non-Recurring	Recurring	Total
Non-recurring			
Design & development			
High-speed magnetic bearings	\$ 2.402		\$ 2.402
Composite rotor assembly	2.727		2.727
PM motor generator	.149		.149
Rotor assembly	.711		.711
Electronics assembly	.366		.366
Gimbal assembly	.359		.359
Preprocessor	.237		.237
Inverter	.731		.731
Central power control	.084		.084
Mounts & supports	2.829		2.829
Engineering test models			
Unit models			
Rotor assembly	.462		.462
Electronics assembly	.142		.142
Gimbal assembly	.204		.204
Preprocessor	.101		.101
Inverter	.219		.219
Central power control	.011		.011
Mounts & supports	.034		.034
System models			
Rotor assembly	3.695		3.695
Electronics assembly	1.131		1.131
Gimbal assembly	1.630		1.630
Preprocessor	.262		.262
Inverter	.438		.438
Central power control	.022		.022
Mounts & supports	.064		.064
Tooling & STE	.309		.309
Assembly & checkout	2.459		2.459
Acceptance test	2.292		2.292
Recurring (first flight system)			
Flight hardware			
Rotor assembly		\$1.847	1.847
Electronics assembly		.565	.565
Gimbal assembly		.816	.816
Preprocessor		.101	.101
Inverter		.219	.219
Central power control		.011	.011
Mounts & supports		.324	.324
Assembly & checkout		1.112	1.112
Acceptance tests		1.030	1.030
Total	\$24.008	\$6.025	\$30.033

IPACS units added: Table 3-XIX gives a detailed cost breakdown of design, development, test, and fabrication by IPACS units, including cost of engineering models, tooling and STE, assembly and checkout, and acceptance tests. The unit models are for component qualification test purposes and consist of one each of the rotor assembly, the electronics assembly, the gimbal assembly, the preprocessor, inverter, central power control, and mounts and supports. The systems models are for MSS vehicle systems verification and integration tests purposes and consist of two ships worth, or the equivalent of two flight systems. Each flight system consists of five rotor assemblies, five electronics assemblies, five gimbal assemblies, one preprocessor, one inverter, one central power control, and one set of mounts and supports.

IPACS annual funding: Table 3-XX shows the peak year funding associated with the incorporation of IPACS into the MSS. As shown in Figure 3-8, the IPACS development, test, and fabrication period is 5 years. Table 3-XX shows the peak year funding of \$9.851M to occur in the third year after go-ahead.

TABLE 3-XX.- MSS IPACS ANNUAL FUNDING SCHEDULE

Description	Years after go-ahead*					Total
	1	2	3	4	5	
MSS IPACS	\$1.262	\$6.067	\$9.851	\$9.160	\$3.693	\$30.033
*Dollars in M						

Cost Effectiveness - Table 3-XXI shows the cost resulting from the application of cost-effectiveness factors. The weight saved by the incorporation of IPACS into the MSS vehicle is 2,502.5 pounds. IPACS occupies 152.69 cubic feet less space than does the components deleted by IPACS units. Incorporation of IPACS into the MSS does not affect power consumption of the MSS. A minus value reflects an IPACS advantage and a plus value shows an IPACS penalty. The application of the cost-effective weighting factors show a net IPACS cost advantage of \$0.855M for each MSS vehicle.

TABLE 3-XXI. COST-EFFECTIVENESS TRADEOFF

Description	Cost Amount	Factor	Cost (\$ = M)
Weight, lb	-2,502.5	\$250/lb	-\$0.626
Space occupied, cu ft	-152.69	\$1,500/cu ft	-0.229
Power consumption*, W yr	-	-	-
Net			-\$0.855
*Mission duration factors excluded.			

Total cost comparison.— Table 3-XXII combines the equipment and penalty cost to arrive at a potential cost savings using the IPACS approach.

TABLE 3-XXII. TOTAL COST

Item	Cost
Differential equipment cost	-\$5.738M
Penalty cost	-0.855M
Cost impact (net savings)	\$6.593M

30-Day Shuttle Sortie Cost Data

General. This section presents the programmatic information and cost data relating to the Shuttle Sortie program, including the work breakdown structure, program development schedule, equipment cost, cost breakdowns, comparison of development and first flight system costs, IPACS annual funding schedule, and cost-effectiveness tradeoffs. The equipment cost comparison shows an overall penalty resulting from incorporation of IPACS. The development cost shows a penalty of \$11.311M, and the first flight system cost shows a slight reduction of \$0.348M.

Work breakdown structure: Figure 3-9 sets forth the structure of the Shuttle Sortie IPACS WBS prepared during the study. It contains the elements and components deleted as a result of the incorporation of IPACS, as well as the subsystem components unaffected or common to both the competitive subsystem and IPACS. The IPACS units and WBS elements added are shown also.

The Shuttle Sortie IPACS WBS contains design, development, test hardware (engineering models), flight hardware, tooling and STE, assembly and checkout, and mission operations for both the competitive subsystem and IPACS. The WBS shows an acceptance test separately for IPACS. It was assumed for this study that the competitive subsystem costs included the cost of acceptance tests; however, they were not shown separately in the level of cost data examined on the competitive subsystems during the study.

IPACS development schedule: The Sortie utilizes an advanced technology rotor assembly. Development, test, and fabrication of the Shuttle Sortie IPACS units would require a period of 4.5 years (Figure 3-10). The program schedule identifies the development span for the three IPACS components considered critical: the input-output (I-O) generator, bearings, and composite rotor. The estimated development period is 12 months for the I-O generator, and 30 months for the composite rotor and bearings. The development time spans for the other IPACS units are shown. Drawing release and all design and development tasks are scheduled to be completed by the end of the third year. Fabrication, assembly, and test of the engineering models and flight hardware

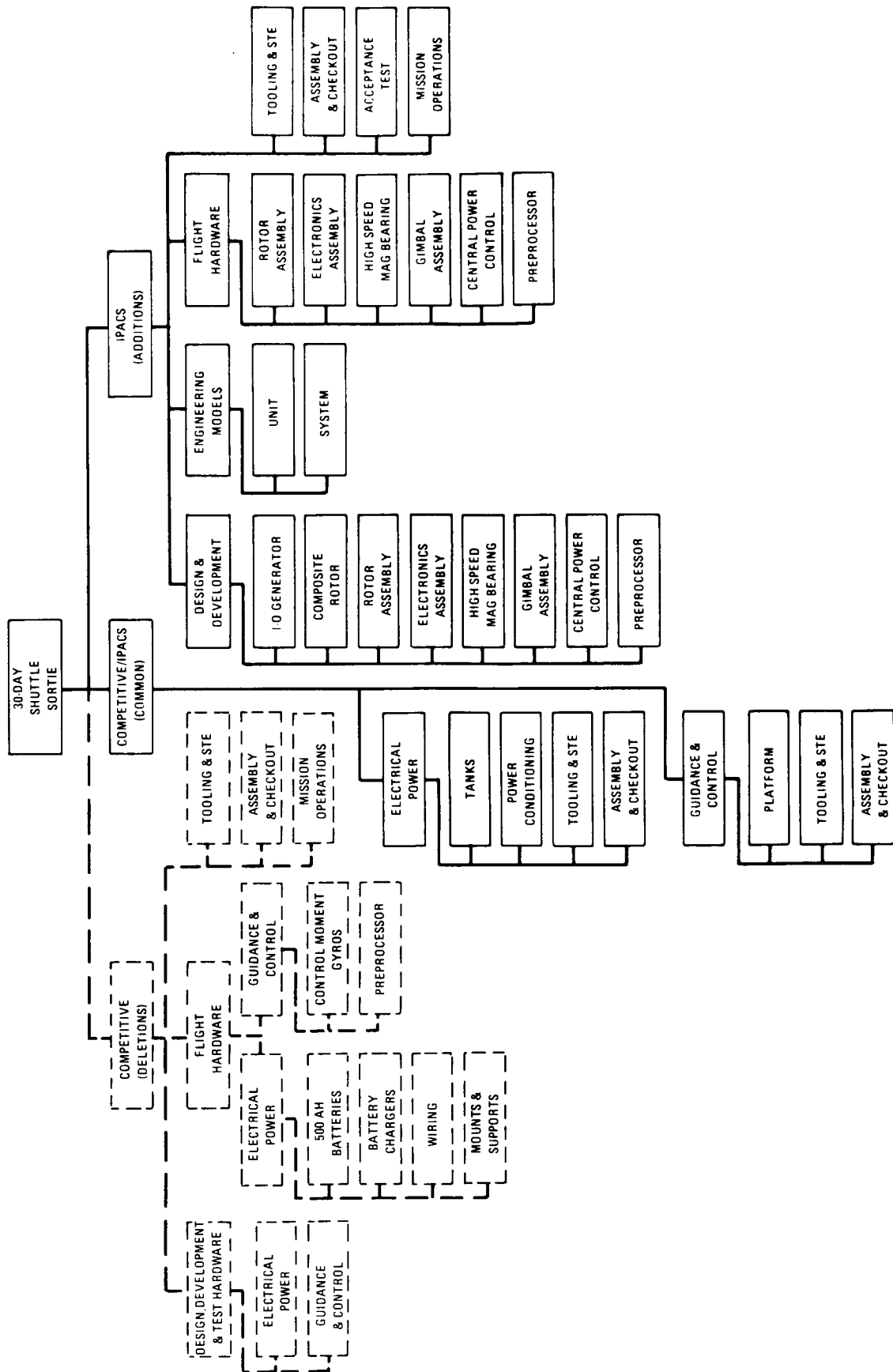
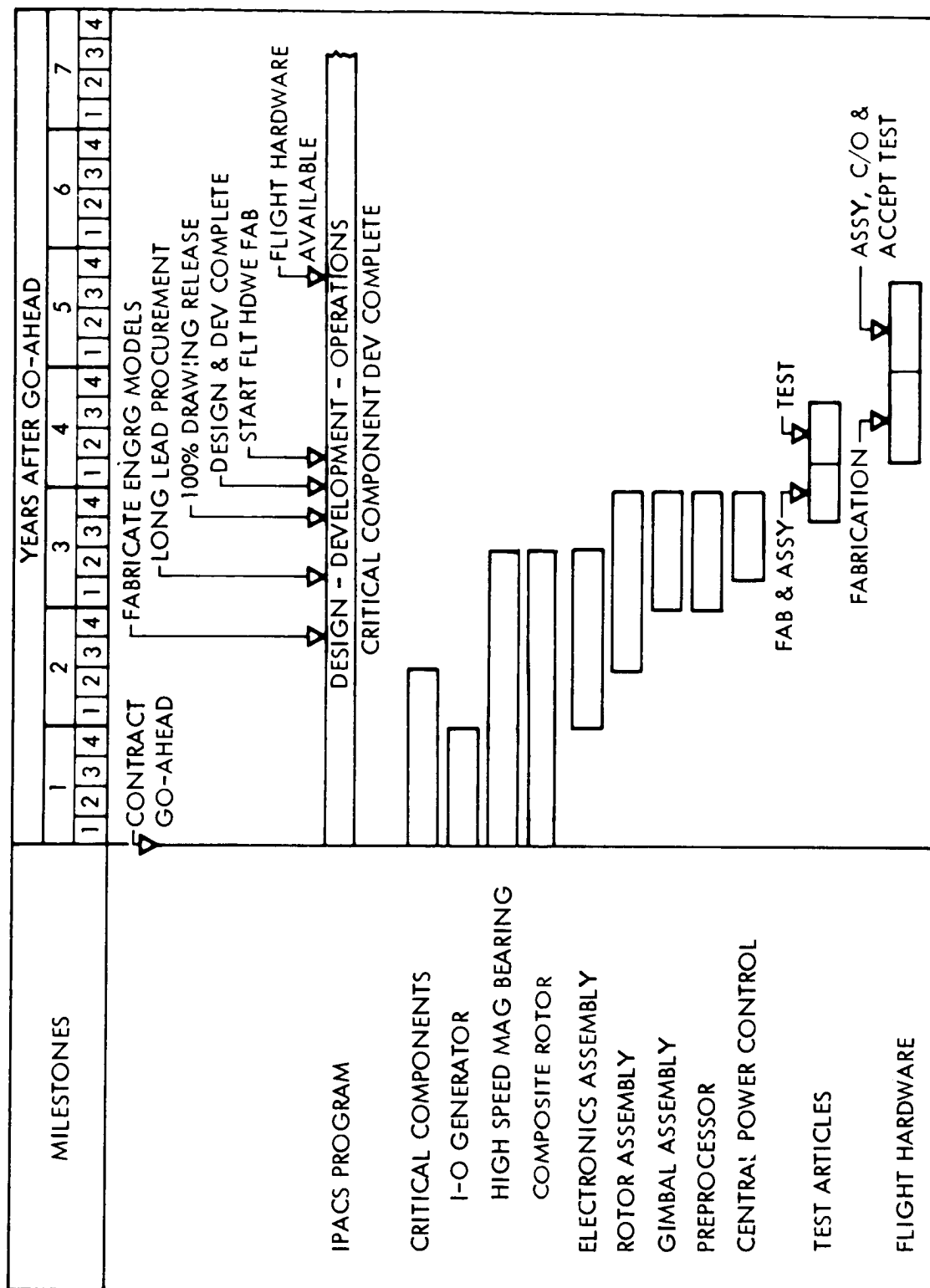


Figure 3-9. IPACS Work Breakdown Structure (WBS)-Shuttle Sortie - 30 Day



are shown. The operational flight hardware is scheduled to be available during the latter part of the fifth year after contract go-ahead. Mission operations were not examined during the study and are therefore not shown to completion.

Equipment cost.- Table 3-XXIII shows the impact on cost of the competitive subsystem as a result of incorporating IPACS into the Shuttle Sortie vehicle. The costs are summarized separately for development (non-recurring) and first flight system (recurring) for both the competitive subsystem and IPACS. The cost of the electrical power and attitude control subsystems, as shown in the original program document, is \$41.912M for development, and \$8.889M for the first flight system - a total of \$50.801M through the first flight system. The cost of developing, testing, and fabricating the first flight system of IPACS units also is compared to the deleted components. The cost of developing and testing IPACS units is \$15.055M or \$11.311M more than the cost of the components deleted. The difference in cost of the first flight system is insignificant, a decrease of about 10 percent for IPACS. The net result shows a penalty of \$10.963M associated with the incorporation of IPACS into the Shuttle Sortie vehicle. A lower level of detail for the electrical power and attitude control subsystems and the IPACS units added is provided below.

TABLE 3-XXIII.- SHUTTLE SORTIE COST SUMMARY

Cost levels	Cost (\$ = M)		
	Development	First flight system	Total
Competitive subsystem			
Electrical power	\$ 9.848	\$ 3.421	\$13.269
Guidance and control	32.064	5.468	37.532
Total	\$41.912	\$ 8.889	\$50.801
Minus: components deleted	3.744	3.245	6.989
Plus: IPACS components	15.055	2.897	17.952
Net	+\$11.311	-\$ 0.348	+\$10.963
New total	\$53.223	\$ 8.541	\$61.764

TABLE 3-XXIV.- COST BREAKDOWN, SHUTTLE SORTIE COMPONENTS DELETED
(DOLLARS IN M)

Cost level	Non- Recurring	Recurring	Total
Non-recurring			
Design, development and test hardware			
Electrical power	\$1.728		\$1.728
500-AH batteries			
Battery chargers			
Wiring			
Mounts and supports			
Guidance and control	1.495		1.495
Control moment gyros			
Preprocessor			
Tooling and STE	0.521		0.521
Recurring			
Flight hardware			
Electrical power		0.938	0.938
500 AH batteries			
Battery chargers			
Wiring			
Mounts and supports			
Guidance and control		1.975	1.975
Control moment gyros			
Preprocessor			
Assembly and checkout		0.332	0.332
Total	\$3.744	\$3.245	\$6.989

TABLE 3-XXV.- COST BREAKDOWN, SHUTTLE SORTIE IPACS COMPONENTS ADDED
(DOLLARS IN M)

Cost Level	Non-Recurring	Recurring	Total
Non-recurring			
Design and development			
Inside-out generator	\$0.175		\$ 0.175
Composite rotor	2.727		2.727
Rotor assembly	1.435		1.435
Electronics assembly	0.429		0.429
High-speed magnetic bearing	2.676		2.676
Central power control	0.084		0.084
Preprocessor	0.237		0.237
Engineering models			
Unit models			
Rotor assembly	0.462		0.462
Electronics assembly	0.221		0.221
Gimbal assembly	0.099		0.099
Central power control	0.011		0.011
Preprocessor	0.101		0.101
Systems models			
Rotor assembly	2.217		2.217
Electronics assembly	1.066		1.066
Gimbal assembly	0.458		0.458
Central power control	0.022		0.022
Preprocessor	0.202		0.202
Tooling and STE	0.206		0.206
Assembly and checkout	0.792		0.792
Acceptance tests	1.435		1.435
Recurring costs (first flight system)			
Flight hardware			
Rotor assembly		\$1.108	1.108
Electronics assembly		0.533	0.533
Gimbal assembly		0.230	0.230
Central power control		0.011	0.011
Preprocessor		0.101	0.101
Assembly and checkout		0.324	0.324
Acceptance tests		0.590	0.590
Total	\$15.055	\$2.897	\$17.952

Components deleted: The costs of the components deleted (Table 3-XXIV) were determined by the application of cost estimating relationships, such as dollars per pound, which were developed from the level of cost and technical data available from the original program documentation (Reference 3-4).

The non-recurring cost of \$3.744M includes \$3.223M for design and development, such as engineering analysis, design, preparation of drawings, specifications, plans, documentation, support, component development, laboratory testing, mockups, and test hardware for the electrical power and attitude control subsystems, as well as \$0.521M for tooling and special testing equipment (STE) utilized by the factory for in-process testing during fabrication.

The recurring cost (first flight system) of \$3.245M includes flight hardware of \$2.913M and assembly and checkout of \$0.332M.

IPACS units added: Table 3-XXV reflects a detailed cost breakdown of design, development, test, and fabrication by IPACS units, including cost of engineering models, tooling and STE, assembly and checkout, and acceptance tests. The unit models, for acceptance and component qualification tests, consist of one each of the rotor assembly, the electronics assembly, gimbal assembly, the central power control, and the preprocessor. The systems models, for Shuttle Sortie vehicle systems verification and integration tests, consist of one ship's worth, or the equivalent of a flight system, (three rotor assemblies, three electronics assemblies, three gimbal assemblies, one central power control, and one preprocessor).

IPACS annual funding: Table 3-XXVI shows the peak year funding for incorporation of IPACS into the Shuttle Sortie vehicle. As shown in Figure 3-10, the IPACS development, test, and fabrication period is 5 years. Table 3-XXVI shows the peak year funding of \$4.880M to occur in the second year after go-ahead.

TABLE 3-XXVI.- SHUTTLE SORTIE IPACS ANNUAL FUNDING SCHEDULE

Description	Years after go-ahead					Total
	1	2	3	4	5	
Shuttle Sortie IPACS	\$3.381	\$4.880	\$3.852	\$4.331	\$1.508	\$17.952
*Dollars in M						

Cost Effectiveness. Table 3-XXVII shows the cost resulting from application of the cost-effectiveness factors. The weight saved by the incorporation of IPACS into the Shuttle Sortie vehicle is 473.2 pounds. IPACS occupies 8.4 cubic feet less space than does the components deleted by the IPACS units.

TABLE 3-XXVII.- COST-EFFECTIVENESS TRADEOFF

Description	Amount	Factor	Cost (\$ = M)
Weight, lb	-473.2	\$250/lb	-\$0.118
Space occupied, cu ft	-8.4	\$1500 cu ft	- 0.013
Power consumption*, W yr	-		-
Net			-\$0.131

*Fuel cell power, therefore power factor excluded

A minus value reflects an IPACS advantage. Therefore, the net results from the application of the cost-effective weighting factors show a net IPACS cost advantage of \$0.131M for the Shuttle Sortie vehicle.

Total cost comparison.- The combined penalty and equipment cost are shown in Table 3-XXVIII. Although the penalty cost represents a savings for the IPACS approach it is not sufficient to overcome the differential equipment cost.

TABLE 3-XXVIII TOTAL COST

Item	Cost
Differential equipment cost	+\$10.963M
Penalty	- 0.131M
Cost impact (net increase)	+\$10.832M

The equipment cost penalty is readily traceable to the high power requirement (in excess of 60 kW), the relatively low (6 kW hr) energy storage requirement, and low number of charge-discharge cycles coupled with maintenance opportunity every 30 days. These requirements will allow short life and clearly favor a high energy density storage element of low cost.

Reference to the energy storage concepts section of Module 1 will show that applications such as this are now best satisfied by silver-zinc batteries. The particular requirements of the 30-day Shuttle, for the postulated system,

simply fall outside the IPACS boundaries of application from a cost viewpoint. As discussed in Module 5, the IPACS Shuttle application is better directed toward a power energy sizing more representative of the majority of missions where the lower development costs will allow the long-life and penalty cost advantages of an advanced IPACS to predominate.

Conclusions

This analysis has demonstrated that the IPACS concept can result in lower equipment cost as well as lower penalty cost than the competitive subsystems. These cost reductions occur with current and advanced technology units even though the IPACS is producing equal or superior performance. The only exception was the equipment cost for the 30-Day Shuttle previously discussed. As indicated, if the Shuttle requirement is handled differently, the IPACS concept can produce a cost savings for this application as well. In all cases, furthermore, the IPACS approach results in potential savings as calculated by the cost-effectiveness factors. It is reasonable to assume that these results are on the conservative side since the generic cost data used in the IPACS calculations were in some cases more detailed than that used in the competitive subsystem cost. As a result the competitive subsystem cost can be expected to grow at a faster rate than the IPACS cost data. Finally, the cost savings obtained by the IPACS approach appear well within allowable times to meet the flight schedules.

MODULE 4 - APPLICATIONS BOUNDARIES

Introduction

The purpose of this task was to evaluate some of the more important factors which have a potential impact upon the applicability of the IPACS concept. Previous studies have established the technical feasibility of IPACS for several classes of missions. Additional analyses have established a subset of missions for which the IPACS concept is cost effective compared with the currently defined momentum exchange and energy storage concepts.

The intent of this study was to generalize the previous results and supplement them as required to establish approximate bounds or limits beyond which IPACS would not be considered an appropriate concept. The potential boundary factors considered in the study include: momentum, energy, power, and pointing. In order to further define the region of applicability, cost trades with competitive systems were also considered.

Power Rating

The permanent magnet motor/generators used in IPACS are necessarily high speed and high efficiency devices. Development efforts for these units entail optimization to obtain the best balance of copper and core losses as well as design for minimum ripple. The requirement to operate at high speeds places restrictions on rotor diameter and construction. In order to quantize the development problem as a function of power level, relative cost estimates were prepared and are presented in figure 4-1. The costs presented have been normalized to the development cost associated with a low power machine which operates with a maximum speed of 40 000 rpm. The practical power limit for a machine with this top speed is approximately 13 kW. The comparable limit for a 50 000 rpm machine is about 5.5 kW. The higher speed machine must be built with a smaller diameter and longer stack length. It will have higher core losses and the interface problems between the wheel and the motor/generator can be expected to be more severe.

Figure 4-2 presents normalized recurring costs for the same range of machines. These curves also reflect the rapid increase in cost as the power feasibility limit is reached.

Based upon the cost data presented, it is concluded that the power output for a single IPACS unit should be 13 kW or less. Assuming arrays of up to six machines comprising a subsystem, the total power capability would be on the order of 80 kW. The Lundell type brushless machines can deliver higher power at somewhat lower efficiencies, however, the 80 kW capability of brushless dc machine arrays exceeds any known spacecraft requirements.

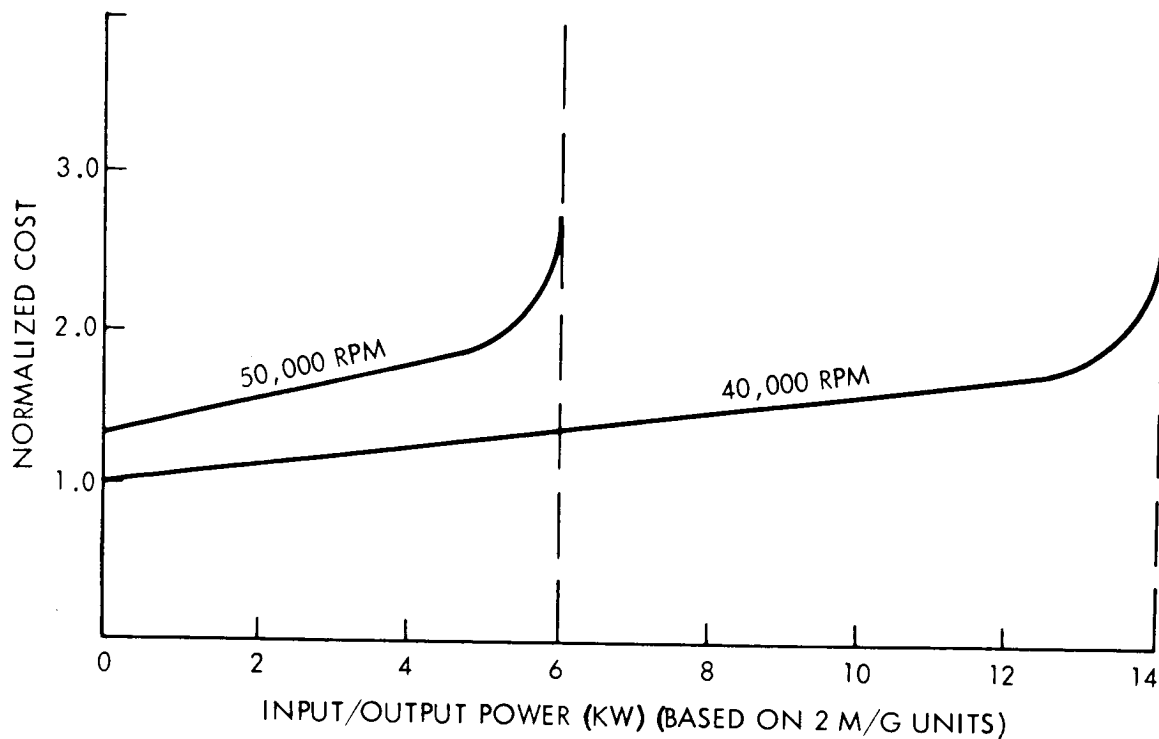


Figure 4-1. Normalized Non-Recurring Cost of PM Motor-Generators VS Power Level

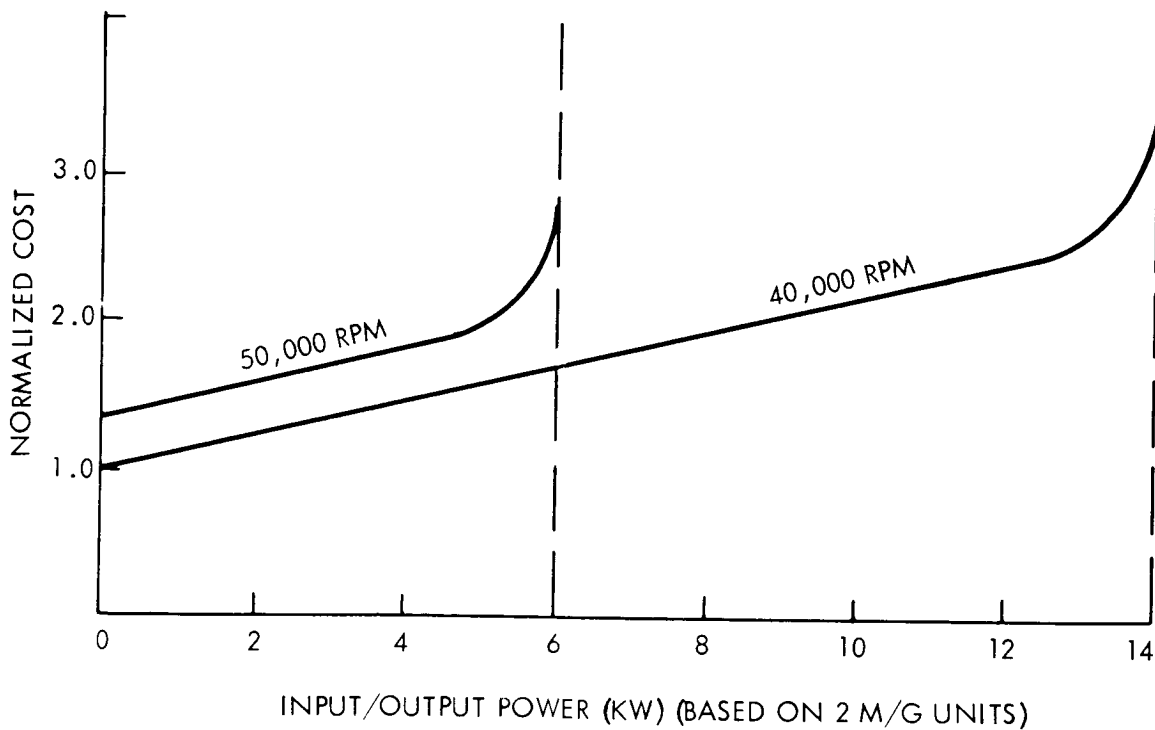


Figure 4-2. Normalized Recurring Cost of PM Motor-Generators Vs Power Level

Energy Storage

One upper limit on energy storage capability for a single IPACS machine can be derived from physical limitations on the external dimensions of the units. In the feasibility study an upper limit of 102 cm (40 in.) was adopted as the maximum overall dimension for a single unit. This constraint allows equipment to be moved through internal hatches in large manned spacecraft such as a space station. On a double gimbaled unit, the maximum dimension occurs along the mounting axis for the outer gimbal. The best way to move a unit would be with this axis oriented along the direction of motion through the hatch. The constraining size is then the larger of the two dimensions normal to this axis. This would be the length along the inner gimbal axis. A reasonable estimate of this dimension is 150 percent of the rotor diameter. If we constrain this dimension to be 102 cm (40 in.), a rotor diameter constraint of approximately 68.6 cm (27 in.) results. In order to maximize packaging efficiency, the axial length of the rotor assembly should not exceed the rotor diameter. Thus an absolute limit on rotor hub thickness would be the rotor diameter. Allowances must be made, however, for the motor length, bearing oiler and preload subassemblies. Design studies have shown approximately 35 percent of the axial length is devoted to subassemblies. This reduces the rotor hub thickness to 43.2 cm (17 in.) or less. Assuming a steel rotor and a constant stress profile the speed limit would be 24 900 rpm and the rotor would be able to store about 12 000 watt-hr. An array of such units would have an energy storage capability in the 30 to 70 kW-hr range. This capability exceeds any known spacecraft energy storage requirement.

The minimum energy storage capability is perhaps best defined by a cost trade which identifies the point at which IPACS is no longer cost effective as the complexity of an IPACS unit would not be warranted for very small energy storage functions. The feasibility study has shown that IPACS is cost effective for units as small as 70 watt-hr per wheel. Thus the lower bound is known to be under this level; how much lower has not been established. It is considered significant to note, however, that of all the spacecraft missions reviewed in the process of selecting reference missions for this study only four were found to have an energy storage requirement of less than 100 watt-hr. A further consideration is the potential impact of cycle life. IPACS could be cost-effective for a mission with a very small energy storage requirement if a high number of charge-discharge cycles were required. Thus the lower bound on energy storage can be expected to drop as the cycle life requirement increases.

Angular Momentum Storage

There exists an upper bound on angular momentum storage per unit that is derived from the physical size constraint discussed above. The 68.6 cm

(27 in.) diameter rotor has a low speed angular momentum of approximately 21 700 N-m-sec (16 000 ft-lb-sec). Considering the momentum storage requirements for even the large manned spacecraft (either shuttle or space station) it is concluded that there is not a significant momentum storage upper bound for IPACS. Figure 4-3 presents a plot of energy storage versus angular momentum capability. The shaded region indicates the area covered by individual mission designs in the feasibility study. As seen from the chart, IPACS has been shown to be cost effective over several boundary points of the feasibility region.

Pointing

The objective of this segment of the study is to evaluate the potential applicability of IPACS to precision pointing missions. Although many elements of a control system can influence the pointing capability of the system the torque source (IPACS) is the element of concern herein. Thus attitude and angular rate sensors together with their associated noise are excluded, vehicle flexibility is excluded, and electronics non-linearities are excluded. Study results would indicate that IPACS is applicable to body point a vehicle to an accuracy on the order of 4.8×10^{-6} rad (1 $\overline{\text{sec}}$). This conclusion is based on a comparison of IPACS to the present technology control moment gyros being postulated and proposed for vehicles such as the free-flying astronomy RAM or large space telescope (LST). Preliminary performance analyses have been conducted to evaluate some of the more important factors impacting pointing and stability. These factors are listed below and each will be discussed with respect to IPACS. The reference vehicle for purposes of the analysis will be the free flying RAM a relatively large fine pointing vehicle.

IPACS factors potentially impacting pointing performance:

- Excess angular momentum.
- Control non-linearities such as gimbal static and running friction or gimbal rate deadband.
- Vibration forces and torques induced by rotor static and dynamic unbalance or bearing eccentricity.
- Power delivery action causing disturbance torques - where IPACS power response affects IPACS control response.

Vibration. - A potential problem regarding IPACS applicability to precision pointing missions concerns the vibration input to the vehicle due to static and/or dynamic unbalance of the IPACS rotor, bearing eccentricity, or other errors. The major vibration inputs will occur at the rotor spin frequency and higher harmonics of the spin frequency. The vehicle response will be attenuated but the pointing of elements within the vehicle can be

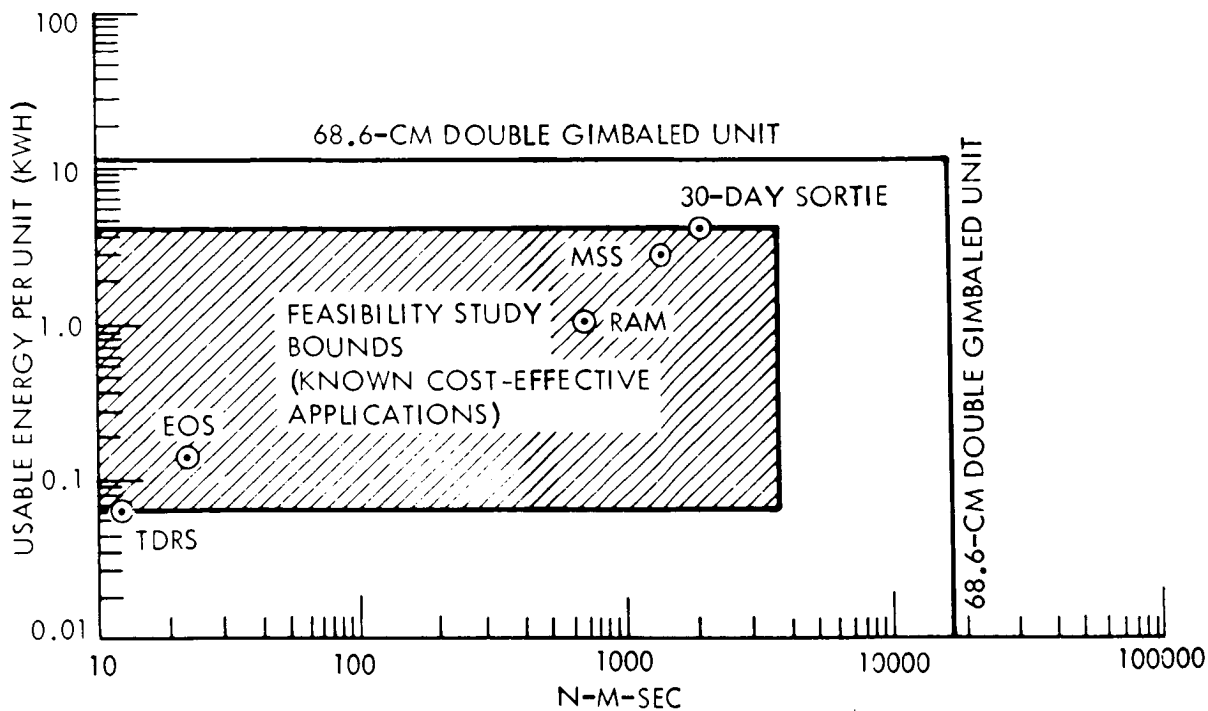


Figure 4-3. Usable Energy Per Unit Vs Low Speed Angular Momentum

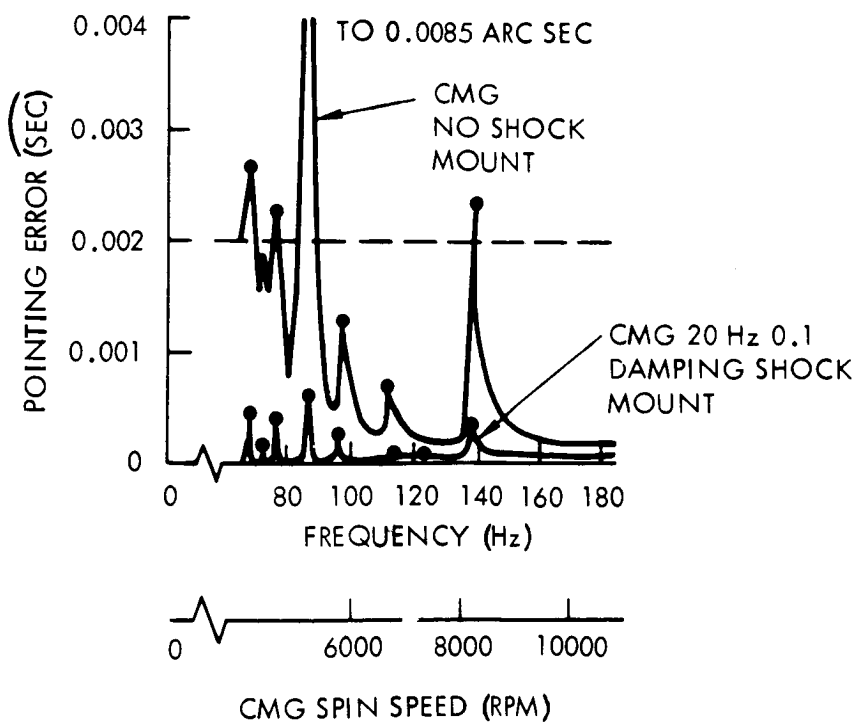


Figure 4-4. CMG Vibration Effects

significantly influenced. In the case of an astronomy RAM such as the LST, vibration of the primary mirror or instrumentation packages can have a major impact upon image motion stability. The requirements for this vehicle are vehicle pointing to an accuracy of 4.8×10^{-6} rad (1 $\overline{\text{sec}}$) (1σ) with image motion stabilization to 2.4×10^{-8} rad (0.005 $\overline{\text{sec}}$) (1σ). Thus the applicability of IPACS must be considered not only in light of the IPACS units meeting the 4.8×10^{-6} rad (1 $\overline{\text{sec}}$) requirement but also these units must not be a source of vibrational disturbances that exceed the image motion stability requirement. Preliminary studies have been conducted to assess this problem for control moment gyros (NASA TMX-64726 Volume V, dated December 15, 1972, MSFC) and to evaluate the suitability of shock-mounting the CMG's to alleviate the problem. Dynamic models of the CMG's, shock mounts, and vehicle were formulated. The system was subjected to the vibrational forces and torques generated by the CMG's and the structural response was determined. These structural deformations were then applied to an optical model to establish pointing error for both force and moment inputs from the CMG's as a function of CMG rotor speed. The shock mounts that were assumed for the analysis are 20 hertz mounts with a damping factor of 0.1 critical. The first two modes of the primary mirror occur at approximately 16 Hz and the bending modes of the instrumentation package occur at approximately 19 Hz.

Figure 4-4 which presents the results of the MSFC study has been extracted from the above mentioned report for reference. It is clear from the plots that the shock mounts represent a significant factor in improving the potential pointing stability. The mounts can be expected to be even more significant for IPACS which must operate at variable speeds (with CMG's an advantageous spin speed could be selected to minimize the pointing error).

A brief study was conducted to extrapolate the above results to the IPACS region of interest. The IPACS design for RAM operates at a maximum speed of 45 000 rpm and a speed reduction of 50 percent. Thus rotor mass unbalance will introduce fundamental disturbances in the range of 375 to 750 Hz.

The IPACS rotor mass will be greater than the mass of the CMG rotor by perhaps a factor of 1.5, and it will be assumed both rotors can be balanced to an equivalent center-of-mass offset. For comparison purposes it will be assumed that the CMG would use a spin speed of 6000 rpm. As the impressed vibration force varies as the square of the rotor speed and directly with the mass offset, the IPACS unit can be expected to generate forces in the range of 20 to 80 times greater than the CMG. However, the shock mount will have higher attenuation due to the higher frequency separation. The additional attenuation should range from 12 db at the low IPACS speed to 20 db at the upper speed. Thus the net torques transmitted to the vehicle through the shock mount are expected to be from 5 to 8 times those transmitted for the CMG's.

A more thorough evaluation of the vibration problem, although certainly worth while, is considered to be beyond the scope of the present effort.

Excess angular momentum.- In some IPACS designs the rotors when sized to perform the necessary energy storage function are found to have excess momentum storage capacity. In one sense this is an advantage in that the required gimbal motion is reduced. A potential disadvantage however concerns the impact on gimbal compliance considerations. A brief analysis was conducted to quantize this problem for a single gimbal IPACS design such as the modular space station design.

The gimbal dynamics of an IPACS unit are in a large part determined by the stiffnesses of the gimbal assembly structure and the gimbal drive system. Both the effective gimbal inertia and the allowable bandwidth are dependent upon these stiffnesses. Figure 4-5 is a block diagram model of a single gimbal IPACS which includes a spring between the wheel inertia and the gimbal shell inertia. The stiffness of this equivalent spring, K_B , is made up of the following stiffnesses:

- * Spin bearing stiffness
- * Gimbal shell stiffness
- * Rotor stiffness about an axis normal to the spin axis

In order to determine the effects of the springs it is necessary to write the relationship between torque motor (or drive system) torque, T_M , and the IPACS output torque, T_V , and compare this with the case where $K_B \rightarrow \infty$ (infinitely stiff structure).

As $K_B \rightarrow \infty$, T_M and T_V are related by

$$T_V = \frac{HT_M}{s(I_G + I_W)} \quad (\text{no tack feedback})$$

so that the apparent gimbal inertia is the sum of the inertia of the gimbal shell (I_G) and the inertia of the rotor about an axis normal to the spin axis (I_W). H is the angular momentum of the rotor.

As K_B becomes finite, the total gimbal inertia becomes larger by the addition of a term proportional to $(H^2)/(K_B)$, and the bandwidth is reduced because of the addition of wheel nutation dynamics to the effective transfer function as shown below.

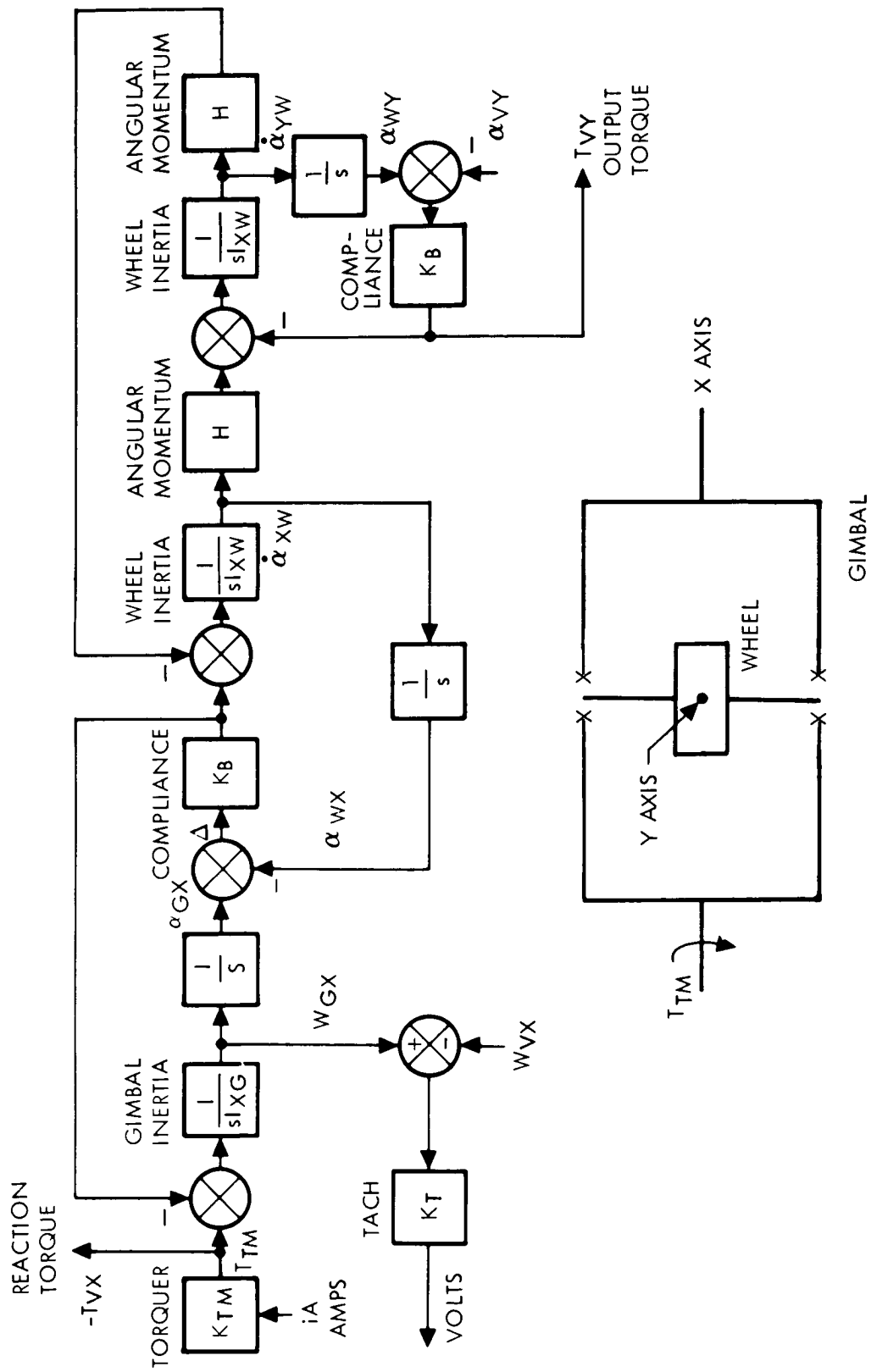


Figure 4-5. Single Gimbal IPACS with Compliance

Referring again to figure 4-5, the general transfer function can be shown to be

$$T_V = \frac{HT_M}{s \left(I_W + I_G + \frac{H^2}{K_B} \right) \left[1 + \frac{s^2 I_W}{K_B} \frac{\left(I_W + 2I_G + \frac{H^2 I_G}{K_B I_W} \right)}{\left(I_W + I_G + \frac{H^2}{K_B} \right)} + \frac{s^4 I_W^2 I_G}{K_B^2 \left(I_W + I_G + \frac{H^2}{K_B} \right)} \right]}$$

The apparent total gimbal inertia is given by

$$I_{eff} = I_W + I_G + \frac{H^2}{K_B}.$$

The usable bandwidth of the unit can be found by factoring the denominator polynomial into two quadratics and using the lowest frequency to establish the maximum allowable bandwidth, which is dependent on both H and K_B .

Substitution of parameters representative of the IPACS design for space station indicate that the allowable bandwidth would be on the order of 70 rad/sec - well above that required for 4.8×10^{-6} rad (1 sec) body pointing. It is therefore concluded that excess momentum storage capacity is not significantly detrimental from a gimbal compliance standpoint.

Control non-linearities. - Analyses to-date indicate that gimbal static and running friction should not preclude the attainment of 4.8×10^{-6} rad (1 sec) body pointing.

Studies by General Electric including hardware in the loop simulations (Control Moment Gyros Characteristics and Their Effects on Control System Performance; AIAA Paper No. 68-875; Phillips, J.P.; AIAA Guidance, Control, and Flight Dynamics Conference - Pasadena, California, August 12-14, 1968) have indicated that friction effects are not as significant as originally thought with regard to precision pointing. The study demonstrated a dynamic range of gimbal speed control from 5.8×10^{-3} rad/sec (0.0033 deg/sec) up to the limit established by the output torque rating. It was also concluded that the gimbal should run smoothly at even lower speed. There was no rough starting or stopping of the gimbal which would cause vehicle perturbations.

Bendix analyses conducted for the RAM study led to the conclusion that CMG's alone could provide 2.4×10^{-6} rad (0.5 sec) body pointing for the RAM free-flyer (RAM Phase B Study; GDCA-DDA 71-004; Vol II, Appendix A, Part IX). This conclusion was based upon a simulation including flexible body dynamics, non-linear CMG dynamics, A/D and D/A interfacing, and experiment induced disturbances. CMG deadbands were studied in the range of 1 to 5 percent of maximum gimbal rate.

The current Rockwell simulation of the RAM IPACS system indicates that the projected gimbal non-linearities will not prevent the required body pointing.

Power interaction with control.— The problem of concern is the attitude disturbance presented to the vehicle by the IPACS system performing a power function -- either charge or discharge. The RAM IPACS simulation (discussed in Module 3 of Volume II) indicates steady-state pointing errors well under 4.8×10^{-6} rad (1 sec) during either maximum charge or discharge of the IPACS wheels.

Pointing summary.— A preliminary analysis was conducted to evaluate the precision pointing potential of IPACS systems. An absolute lower bound was not established and cannot be established in a generalized sense.

It is concluded that the application of an IPACS system to a vehicle requiring 4.8×10^{-6} rad (1 sec) body pointing is reasonable. Further analyses and development would perhaps show finer pointing to be possible for a specific mission application.

System Cost Comparisons

The results of a preliminary investigation of system costs is presented in figure 4-6. The data are best used for generalized comparisons as specific costs are subject to variation depending upon qualification test requirements, installation complexity, reliability requirements, and other factors.

The two lowest curves show a comparison between a present technology IPACS system with a relatively coarse control requirement and a Ni Cd battery system combined with a momentum bias reaction wheel control system. The crossover of the curves is not felt to be significant considering the generalized nature of the data. A reasonable conclusion is that IPACS is cost competitive with the conventional power and control system over the energy range considered.

The second group of curves indicates that IPACS remains cost effective when the control requirements become more stringent. Once again, the crossover of the curves should not be considered significant.

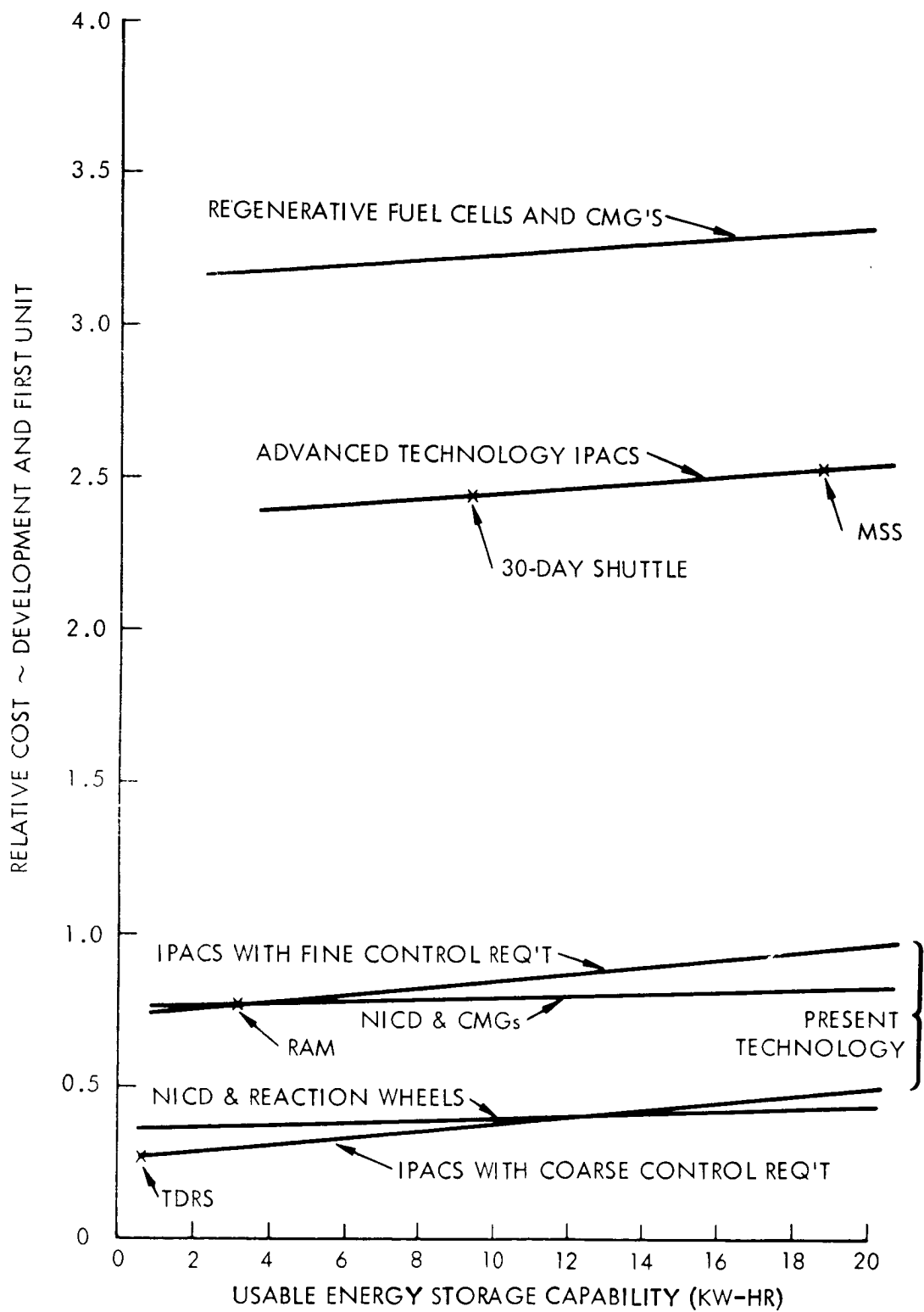


Figure 4-6. System Cost Comparison

The two top curves on the figure compare advanced technology systems; here the IPACS concept includes composite rotors and magnetic suspension bearings. The competitive power and control systems were assumed to be regenerative fuel cells and advanced generation control moment gyros. A clear cost advantage is shown for the IPACS.

Summary

The results of the applications boundaries study are summarized in Table 4-I.

TABLE 4-I.- IPACS PERFORMANCE BOUNDARIES

Factor	Upper bound	Lower bound
Power rating	13 kW/unit 50 - 80 kW/array	$P < 100 \text{ W}$
Energy storage	10 - 12 kWhr/unit 30 - 70 kWhr/array	$E < 100 \text{ Whr}$
Momentum storage	108 500 N-m-sec (80 000 ft-lb-sec)	Not significant
Pointing	(Coarse Pointing) Not significant	$4.8 \times 10^{-6} \text{ rad (1 sec)}$

In general, the study did not indicate that IPACS significantly differs in capability and constraints from the present CMG designs with the exception of rotor imbalance and consequent induced vibration. In this case, balancing to an accuracy five to ten times better than current designs with shock mounting is required to approximate current large sized CMG's. Both shock mounting to this level and balancing are considered extensions of the current art, using current machines. An amount of additional design and test development cost can be expected to be incurred in the larger IPACS units to achieve the balancing or isolation required.

Standardization Considerations

Standardization was not a subject of the current study. The general applicability of IPACS as determined by the feasibility study, however, posed interesting questions as to standardization potential of the units. Study results were reviewed to estimate standardization potential. The review included mission requirements power and control distribution, a determination of requirements density by region and a parametric sizing of two "best fit" units.

Requirements.— The mission requirements originally utilized in the process of selecting representative missions for IPACS were used as mission models. These requirements are summarized in Tables 1-A-1 - 1-A-VI of Appendix 1-A of this volume. The planetary missions were excluded because of the feasibility study results which indicated these missions to be relatively poor IPACS applications. The 30-day shuttle missions were excluded because of an anticipated separate study task which will be devoted solely to the application of IPACS to these sortie missions. The remaining mission categories include: near earth satellite missions, geosynchronous missions, RAM, free-flyer missions, and space station missions. The range of requirements encompassed by these missions is shown in Table 4-II. The number of cases represented by each range are indicated in the first column of the table. Momentum storage requirements were intentionally excluded from the survey in order to simplify the problem. This is not considered a limitation affecting the results as the feasibility study designs generally showed that an IPACS rotor sized for the energy storage requirement would have adequate momentum exchange capacity for control.

TABLE 4-II.— RANGE OF REQUIREMENTS BY MISSION CLASS

Mission class (cases)	Finest pointing	Power range	Energy storage range
Near earth satellites (23)	4.8×10^{-6} rad (1 sec)	100 W → 5 kW	50 W-hr → 2.5 kW-hr
Geosynchronous (9)	4.8×10^{-5} rad (10 sec)	100 W → 8 kW	100 W-hr → 8 kW-hr
RAM (7)	4.8×10^{-6} rad (1 sec)	500 W → 3.4 kW	250 W-hr → 1.7 kW-hr
Space station (2)	4.4×10^{-3} rad (0.25 deg)	15 kW → 19 kW	11 → 15 kW-hr

Based on the Table 4-II data, it was concluded that an IPACS unit designed so that it would not preclude the achievement of 4.8×10^{-6} rad (1 sec) body pointing should be adequate for the entire control mission spectrum. Note also that it was concluded in the applications boundaries study that the 4.8×10^{-6} rad (1 sec) requirement is achievable with IPACS. The remainder of the standardization analysis will therefore be concentrated on the power and energy storage factors.

The power and energy storage requirements associated with the individual missions are identified on figure 4-7. A single application is denoted by a point. Where multiple applications have identical requirements, the number of applications is noted by the point.

Design considerations.- In attempting to group the requirements into regions which could potentially be satisfied by a relatively few standardized IPACS units, the following considerations were utilized.

- (1) The energy storage requirement will tolerate less latitude than the power requirement when system weight is a significant factor. This stems from the fact that motor/generator weight represents typically 8 percent of an IPACS unit weight whereas the rotor represents anywhere from 50 to 80 percent of the unit weight. Thus a standardized unit could cover a relatively wide power range without incurring an excessive weight penalty.
- (2) Variations in the IPACS wheel array might be tolerated in an attempt to fit a standard unit into a spectrum of missions. This partially violates the standardization philosophy as the system software will change as the array changes. Allowing the array to vary would lead to the use of perhaps seven or eight skewed single gimbal units to satisfy a large requirement and perhaps an array of four skewed units for a smaller requirement. The use of an array with more than eight units is considered marginal from the standpoint of complexity and an array with less than four units will normally not satisfy the failure criteria for the mission. Thus it can be concluded that variation of the number of wheels in the array allows perhaps a factor of 2 latitude in the energy storage requirement. Note that even allowing a change from single gimbaled to double gimbaled units (where an array of 3 DG could be used) for the smaller sizes only increases this latitude from a factor of 2 (the range between 4 units and 8 units) to a factor of 2.6 (the range between 3 units and 8 units).

Using the above considerations, figure 4-7 was inspected and regions of requirements were defined by energy storage ranges where the upper limit was approximately twice the lower limit. A most promising region appears to be the one bounded by 500 watt-hr at the top and 250 watt-hr at the bottom (region A). This region contains 16 out of the possible 42 cases or 38 percent of the cases. Three other regions were established such that the majority of the population is included within the four regions.

Table 4-III shows the percentage of missions falling within each class or region.

TABLE 4-III.- POPULATION DENSITY BY REGION

Region	Percent of total population
A	38
B	21
C	7
D	21
Excluded	<u>13</u>
	100

Two of these regions were then selected for further analysis. Region A was selected because of its large percentage of the population. Region C was selected to evaluate the penalties incurred if a region C unit were to be used to satisfy region B requirements, which would mean covering the entire mission population with three standard IPACS designs.

Potential standardized configurations.- Consider first the problem of a standardized design for region A. The maximum requirements for this region are a power level of 1 kW and 500 W-hr energy storage. An array of 6 non-gimbaled opposed wheels will be assumed. Trade studies conducted previously for the TDRS application showed gimbaled units to be significantly heavier than non-gimbaled arrays in this size range. Each wheel is sized to provide

$$\frac{500}{6} = 83.4 \text{ W-hr.}$$

The power rating per wheel is sized at

$$\frac{1000}{4} = 250 \text{ watts.}$$

This allows full power delivery with one wheel failed (failure of one wheel forces shut down of the opposing wheel from an energy storage standpoint - it remains functional for control however). The estimated characteristics of a unit-designed to meet these requirements is presented in Table 4-IV.

TABLE 4-IV.- STANDARD IPACS FOR REGION A

Component	Weight	
	kg	lb
Rotor	3.45	7.6
Motor/generator	0.91	2.0
Case & mounts	1.73	3.8
Electronics	1.0	2.2
	7.09	15.6
Characteristics: <ul style="list-style-type: none"> • Steel rotor • Max. speed 50 000 rpm • Rotor diameter - 34 cm (13.4 in) • Ball bearings 		

An array of six of these units would weigh 42.5 kg (93.5 lb). Four of the units could be used for the TDRS application. The standardized array would weigh 28.3 kg (62.4 lb) compared to the estimated 25.9 kg (57 lb) for the custom designed IPACS for the feasibility study. Comparing the standardized array with the competitive energy storage and control subsystems of TDRS it is found that the IPACS is still weight competitive.

Consider next a standardized IPACS sized to handle the region C requirements. In this case an array of six single gimbaled units was sized to handle maximum requirements of 20 kW power and 15 kW-hr energy storage with one of the six units in-operable. Thus each unit is sized for 4 kW and 3 kW-hr. The estimated characteristics of the unit are presented in Table 4-V.

A full array of six standard units represents a weight penalty of 23.6 kg (52 lb) when compared with the array of five units sized precisely for modular space station (MSS) requirements. This weight difference is not considered significant although the six-unit array would be expected to be slightly less weight efficient than a five-unit array. For example, the six-unit array would require more total housing or case weight than the five-unit array.

Let us consider now the application of these standard units beyond their design region down into region B. RAM requirements fall at the upper extreme of region B. The "standard" array for RAM would be four of the units sized above. The number of units is dictated by the requirement to store energy with one unit failed and not the power or energy requirements. Actually the array of standardized units will have excessive power and energy storage capability.

TABLE 4-V.- STANDARD IPACS FOR REGION C

Component	Weight	
	kg	lb
Rotor	75.9	167
Motor/generator	11.8	26
Electronics	1.4	3
Housing, Bearings	29.5	65
Drives & sensors	7.3	16
	125.9	277
Characteristics: <ul style="list-style-type: none"> * Composite rotor * Magnetic suspension bearings * Max. speed - 35 000 rpm * Rotor diameter - 58 cm (22.8 in) 		

The standardized array of four single gimbale units would weigh 503 kg (1108 lb) compared with 225 kg (495 lb) for the array of three double-gimbale units sized specifically for RAM. Although the standardized array would be weight effective compared with the competitive baseline systems, it is felt that the weight penalty of 272 kg (600 lb) compared to a custom IPACS design is unreasonable. Considering the fact that RAM requirements fall at the upper range of this region the weight penalty would be even more severe for other missions. It is concluded that it is not reasonable to design a single standardized IPACS to cover both regions C and B.

Standardization summary and recommendations.- The brief analysis presented above has shown that the concept of standardized IPACS requires several unit sizes, perhaps three or four to cover the potential spectrum of missions. The study also indicated that two standard designs could cover approximately 60 percent of the mission population. A more detailed analysis (beyond the scope of this contract) is required in order to reach a conclusion regarding the cost effectiveness of standardization. Such a study should include consideration of the actual number of flights anticipated for each identified mission. For example, TDRS in the study above is considered as a single application where in fact several vehicles will be flown. Thus in the selection of requirements for standardized designs TDRS should be weighed heavier than a mission that will be completed with a single vehicle. Reusage of hardware as is feasible for missions like RAM is also important. In addition to the incorporation of a more extensive mission model a further study should evaluate the standardization penalties for various specific missions to establish better standardization bounds.

MODULE 5 - SPACE SHUTTLE ADVANCED TECHNOLOGY LABORATORY APPLICATIONS

The six mission/vehicle selections originally chosen for the IPACS study included a Shuttle sortie mission of 30 days duration. As the study progressed it became apparent that the IPACS should be evaluated within the context of a 7-day Shuttle mission. This module of the report presents study results of the analysis of power and pointing requirements for three Advanced Technology Laboratory (ATL) payloads.

Advanced Technology Laboratory Requirements

ATL study and mission requirements are summarized in this section.

Study requirements.- The evaluation of IPACS application to the ATL sortie missions was accomplished by defining the physical and performance factors of the competitive baseline system, developing an IPACS system concept, and comparing the two systems for physical, performance, and cost differences.

Mission requirements.- Mission power and pointing requirements along with study ground rules are summarized below.

Electrical power: The power source is a single fuel cell with power output of 7.0 kW continuous and 10.0 kW peak for 2.0 minutes. Power conditioning and distribution losses are assumed to be 20 percent, yielding an average power of 5.6KW for subsystems and experiments.

The power allocation is 3.6 kW for subsystems and 2.0 kW for experiments.

Stability and control: The orbiter attitude is to be controlled by a momentum exchange technique (either CMG's or IPACS). Experiment pointing and stability requirements which exceed the capability of the vehicle momentum exchange system will be satisfied using gimbale platforms.

The gimbale platforms will be capable of the following performance:

Pointing 0.24×10^{-6} rad (± 0.5 arc-sec) over 1/2 orbit
Stability 0.48×10^{-6} rad (± 0.1 arc-sec) over 1/2 orbit
Maximum payload size 3.05 m diam. x 4.57 m long
(10.0 ft diam. x 15.0 ft long)
Payload weight 454 kg to 2718 kg (1000 lb to 6000 lb)

Mission model: The study mission model consists of two ATL sortie flights per year for the years 1980 through 1990 inclusive.

ATL power profiles: The power profiles for three typical ATL missions are presented in figure 5-1.

Energy storage requirements: Table 5-I lists stored energy required for the three ATL payloads. The largest daily requirement of stored energy is for 2017 W-hr (ATL No. 2). Excess energy available from the fuel cell is more than adequate to recharge the batteries. For example, during the 8-hour sleep period, 11 000 W-hr of fuel cell energy is available for battery recharge. Assuming a combined battery and charger efficiency of 70 percent, 2880 W-hr will be required.

Energy storage requirements that size the energy storage assembly are summarized by Table 5-II. These requirements are taken from Table 5-I, which lists power requirements above the fuel cell capability of 5600 W (allows for conditioning and distribution losses) and corresponding time intervals.

Momentum storage requirements: The momentum storage requirements for this mission are essentially the same as those established for the 30-day Shuttle sortie mission. Vehicle mass properties were assumed to be identical. The momentum storage requirement of 2370 N-m-sec (1750 ft-lb-sec) per wheel is calculated for six orbits of continuous operation without desaturation. The vehicle is constrained to fly with the longitudinal axis normal to the orbital plane.

Control torque requirements are assumed to be equivalent to the torque capability of the competitive control system [163 N-m (120 ft-lb) per torquer] such that the systems will have comparable performance.

Backup power requirements: The analysis discussed in Appendix 5-A (Criteria for Sortie Lab Backup Power) estimates time required to power down a sortie lab in case of fuel cell failure. A total time of 45 minutes to power down is shown. No attempt is made to allocate power requirements for the events used to arrive at the power-down timeline shown by figure 5-A-2 (Appendix 5-A).

Figure 5-2 shows an estimate of sortie lab emergency power requirements based on a total power down time of 45 minutes. At the time of primary power loss, it is assumed the load requirement is the maximum peak required by the ATL payload. It is assumed that the loads can be turned off to the 3.5 kW

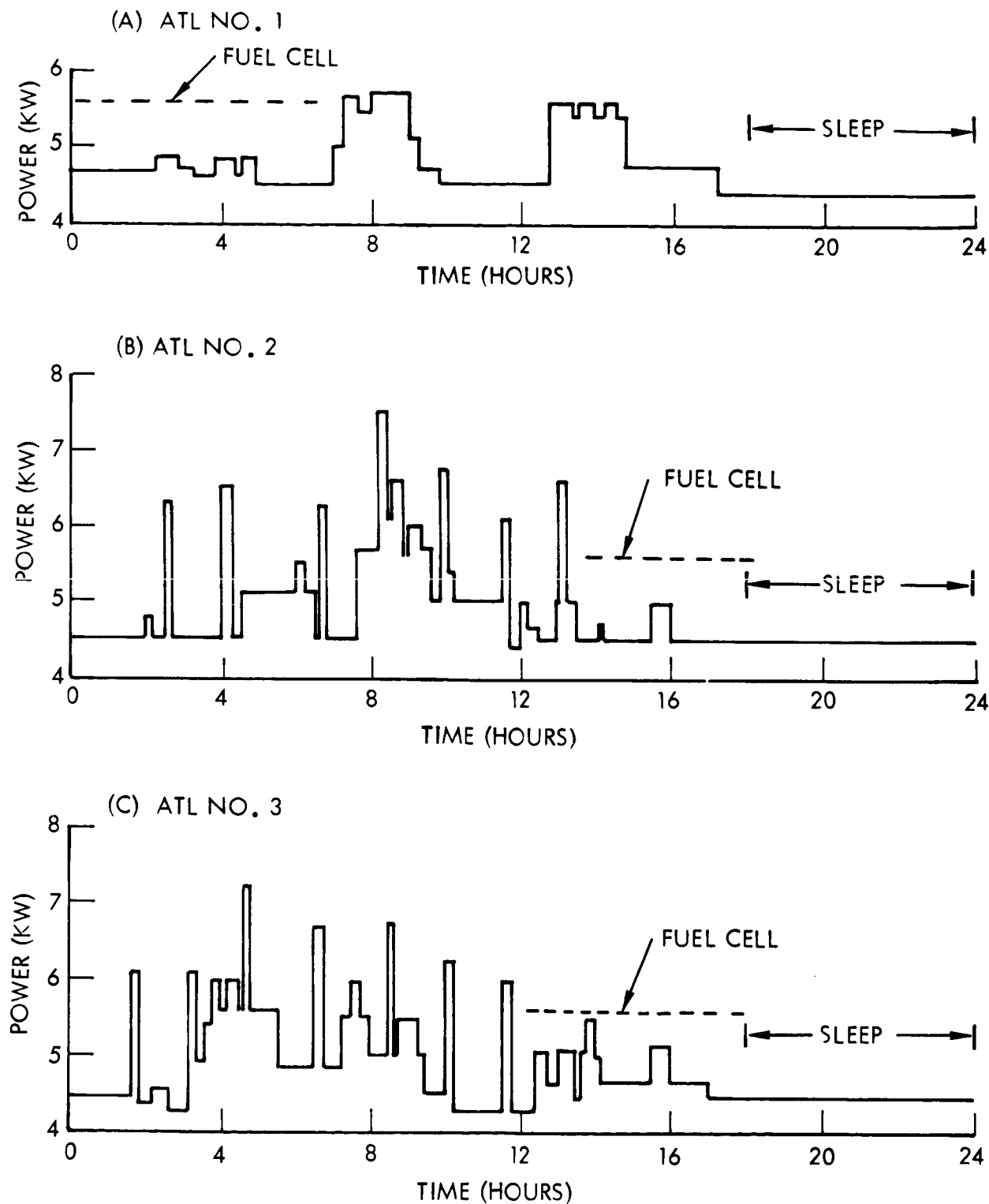


Figure 5-1. Representative Advanced Technology Lab Payload Power Requirements

TABLE 5-I.- ATL PAYLOAD ENERGY STORAGE REQUIREMENTS
(DOES NOT INCLUDE POWER CONDITIONING AND DISTRIBUTION LOSSES)

ATL 1				ATL 2				ATL 3			
Mission Time (hr)	Power Req. (W)	Stored Power Req. (W)	Stored Energy Req. (W-hr)	Mission Time (hr)	Power Req. (W)	Stored Power Req. (W)	Stored Energy Req. (W-hr)	Mission Time (hr)	Power Req. (W)	Stored Power Req. (W)	Stored Energy Req. (W-hr)
7.25-7.65	5650	50	20	2.5-2.65	6300	700	105	1.7-1.85	6100	500	75
8.0-9.0	5700	100	100	4.0-4.25	6500	900	425	3.2-3.35	6100	500	75
				6.6-6.75	6250	650	97	3.8-4.0	6000	400	80
				7.55-8.15	5650	50	30	4.0-4.15	5600	0	0
				8.15-8.40	7500	1900	475	4.15-4.5	6000	400	140
				8.40-8.50	6100	500	50	4.5-4.6	5600	0	0
				8.50-8.85	6600	1000	350	4.6-4.75	7250	1650	238
				8.85-8.90	5600	0	0	6.5-6.75	6700	1100	(458)
				8.90-9.30	6000	400	160	7.5-7.7	6000	400	275
				9.30-9.55	5700	100	25				80
				9.85-10.0	6750	1150	(1090)	8.5-8.6	6750	1150	115
				11.50-11.65	6100	500	75	10.0-10.15	6250	650	97
				13.1-13.25	6600	1000	150	11.55-11.70	6000	400	60
Daily total			120	Daily total			2017	Daily total			1235
Note: The subtotals shown in parentheses indicate cumulative energy storage requirement for the bracketed periods due to the lack of charging opportunities											

TABLE 5-II.- ENERGY STORAGE REQUIREMENTS SUMMARY*

ATL Payload	Peak Power (W)	Maximum Discharge Power Required (W)	Maximum Discharge Energy Required (W-hr)	Minimum Discharge Energy Required (W-hr)	Maximum Charge Power Available (W)	Number Daily Charge/Disch. Cycles
1	5700	100	100	20	1200	2
2	7500	1900	1090	75	1200	7
3	7250	1650	458	60	1350	8
*Power conditioning and distribution losses not included.						

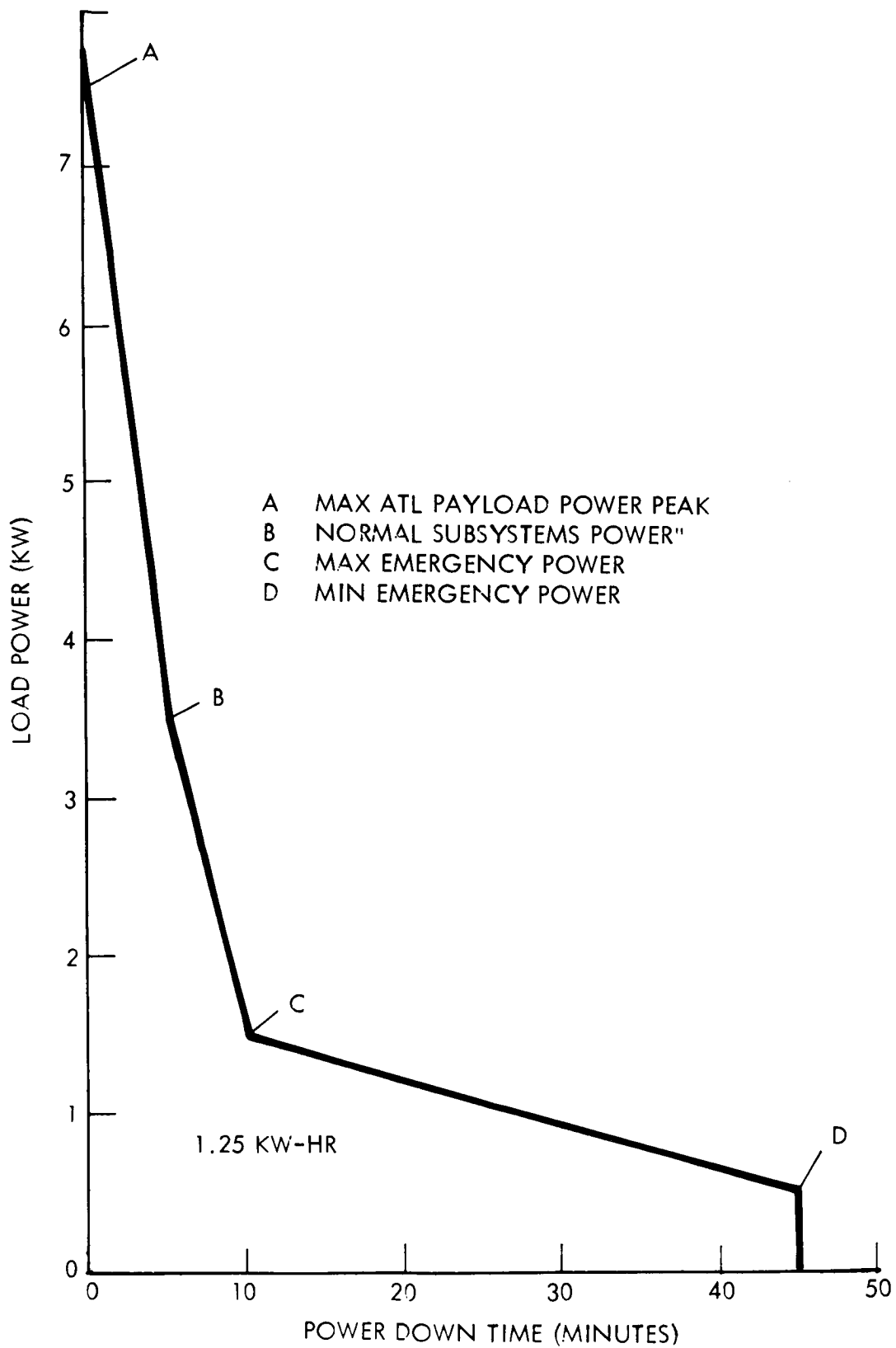


Figure 5-2. Estimated Emergency Requirements

level in 5.0 minutes and to the 1.5 kW level in another 5.0 minutes. The reference listed by figure 5-2 estimates RAM emergency power requirements to be 750 W average. This value is used to obtain the required energy for the remaining 35 minutes time to power down. Allowing a 20-percent loss for power conditioning and distribution, 1.56 kW-hr of energy is required.

Competitive Power and Control Concepts

Advanced Technology Laboratory payload power requirements have been analyzed to define a competitive energy storage concept for comparison with IPACS. The following energy storage devices were considered:

- (1) Currently available - nickel cadmium (NiCd), silver cadmium (AgCd), and silver zinc (AgZn) batteries
- (2) Advanced - nickel cadmium and nickel hydrogen batteries and integrated regenerative fuel cells

Nickel cadmium and primary and secondary silver zinc batteries were evaluated on a weight and cost basis as secondary power sources to meet the ATL power requirements. Weight data were generated for both design point and modular type batteries. For example, in the first case, battery sizes were chosen to most nearly fit the requirements of each payload. In the modular approach the batteries were chosen for the ATL payload No. 3 requirements and the same battery, charger, and regulator modules used to meet the ATL 1 and 2 loads. Based upon the results of this analysis, secondary AgZn batteries recharged in flight were selected for comparison with the IPACS concept. Study details are presented below.

Battery energy storage assembly parametric analysis.- Inspection of battery cycle life data (figure 5-3) indicates that there are optimum depths of discharge for different type batteries. These data are based on continuous charge-discharge cycles at a fixed depth of discharge until battery failure. The low number of charge-discharge cycles required for the ATL, the varying depths of discharge, and the 11-year program life necessitates another approach to establishing battery cycle life.

Assuming a 60-percent maximum depth of discharge, battery cycle lives are estimated from figure 5-3 for the ATL No. 3 payload. These are shown by Table 5-III.

The method used is considered to be approximate since the battery life data of figure 5-3 are not based on cycling batteries at various depths of discharge. Also, most battery testing is based on continuous cycling except

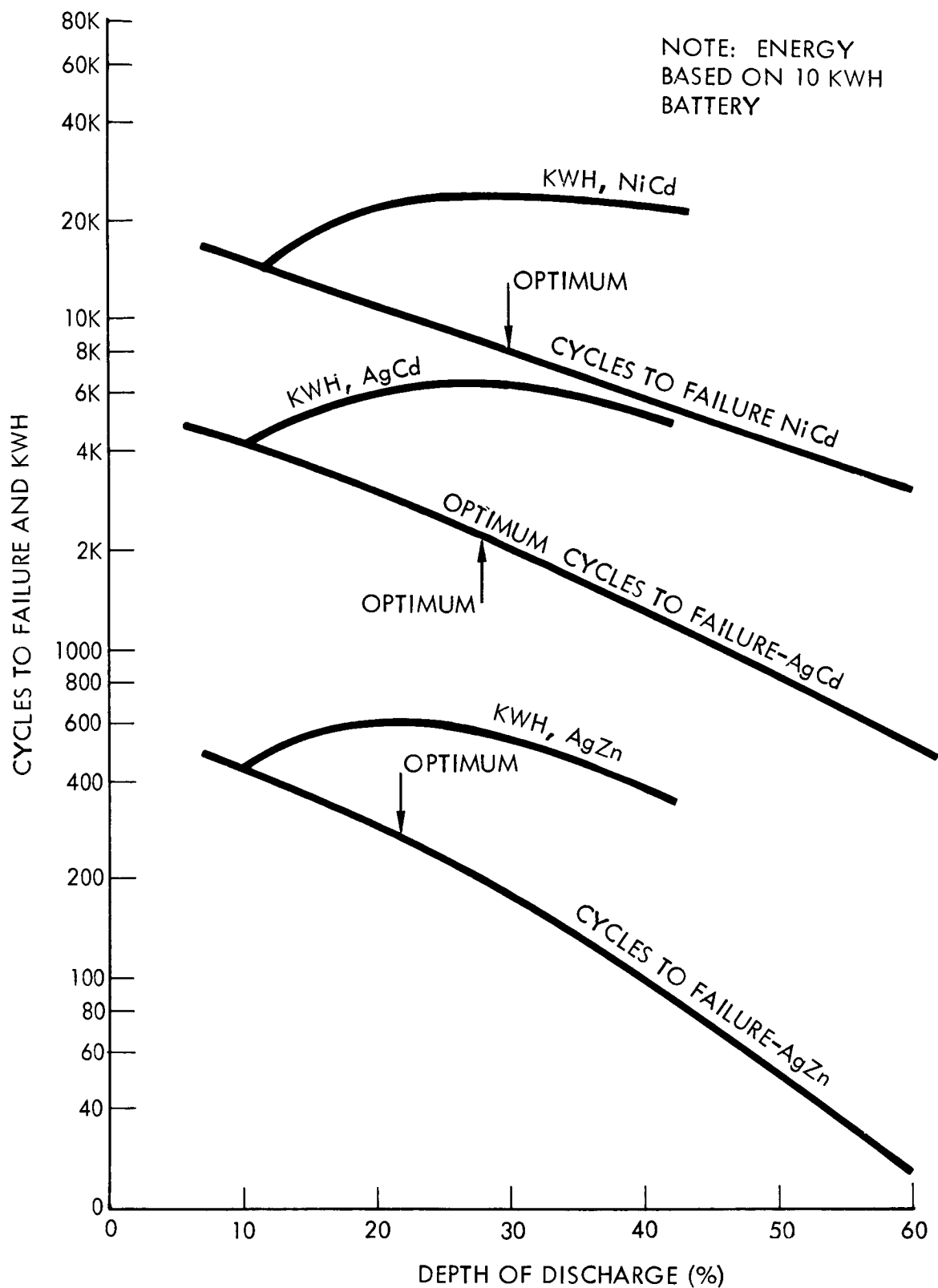


Figure 5-3. Battery Cycle Life and Total Energy Characteristics

TABLE 5-III.- BATTERY CYCLE LIFE ESTIMATION, ATL NO. 3 PAYLOAD
BASED ON MAXIMUM 60-PERCENT DEPTH OF DISCHARGE (DOD)

Daily Cycle	Discharge* (W-hr)	Depth of Discharge (percent)	NiCd		AgCd		AgZn	
			Cycle Life	Battery Life Used (percent)	Cycle Life	Battery Life Used (percent)	Cycle Life	Battery Life Used (percent)
1	75	9.8	15 200	$\times 10^{-3}$ 6.58	4300	$\times 10^{-2}$ 2.32	450	0.22
2	75	9.8	15 200	6.58	4300	2.32	450	0.22
3	458	60.0	3100	32.20	510	19.60	26	3.85
4	275	36.0	6600	15.15	1600	6.25	130	0.77
5	80	10.5	15 000	6.67	4200	2.38	430	0.23
6	115	15.1	13 000	7.70	3600	2.78	360	0.28
7	97	12.7	14 000	7.14	3900	2.56	400	0.25
8	60	7.8	16 200	6.18	4600	2.17	480	0.21
Battery life used, 1 day (percent)			88.20		40.38		6.03	
			$\times 10^{-3}$		$\times 10^{-2}$			
Total days for 100-percent cycle life			1132.00		248.00(1)		17.00**	
<p>*Power conditioning and distribution losses not included. **Limited to activation period of one year (1)Cycle lives are from figure 5-3</p>								

for simulated geosynchronous orbit. For the 11-year program of 22 sorties there would be 132 days of battery cycling. It is indicated that this could be met by the NiCd or AgCd batteries. However, in the case of both AgCd and AgZn cells, degradation, and their service life, starts when electrolyte is added. Deterioration of separator and dissolution of the negative electrode begin immediately and continue with time, regardless of cycle life, until end of service life.

Communications with a battery manufacturer have indicated that NiCd batteries could possibly approach an 11-year service life with intermittent use. Between sortie missions the batteries could be stored dry, discharged, and open circuit at a 10°C (50°F) temperature. They also recommended that either AgZn or AgCd be limited to two sortie missions within any one-year period.

Tables 5-IV and 5-V show battery weights required for the ATL payloads considered. Battery replacement assumptions are listed at the bottom of each table. The weights of Table 5-IV are obtained by sizing the batteries to each payload energy requirement (Table 5-I). Battery cell sizes were selected which result in actual maximum depths of discharge being closest to 60 percent for NiCd and AgZn cells recharged in flight, 80 percent for AgZn cells recharged once on the ground, and 100 percent for primary AgZn cells used once. Table 5-V weights represent a modular energy storage approach, where the batteries and associated regulator and charger are sized for the ATL 3 payload requirement. The following assumptions are used to obtain complete energy storage assembly weight for each mission:

- (1) Battery charger and regulator weights are scaled from Skylab for the ATL 2 and 3 payloads:

Battery charger = 4.4 kg/kW (9.7 lb/kW)

Battery regulator = 2.95 kg/kW (6.5 lb/kW)

These were increased by a factor of two for the ATL No. 1 payload to account for scale effect (design point).

- (2) Battery weights are obtained by increasing cell weights by 25 percent to account for cases, connectors, etc.
- (3) Charger and regulator weights are increased 50 percent above mission values to obtain 11-year program weights.
- (4) Power conditioning and distribution losses are neglected for purposes of parametric analysis.

It can be noted that the Shuttle fuel cell is capable of operating at 10 kW continuously if additional radiator area is added. For the ATL payload 2 peak power requirement of 1900 watts, an increase of 3.35 m² (36 ft²) is

TABLE 5-IV.- ATL PAYLOAD PEAK POWER APPROACHES (DESIGN POINT)

ATL Payload	1						2						3					
	Battery			Weight (kg)			Battery			Weight (kg)			Battery			Weight (kg)		
	No.	AH	DD	Mission	Program		No.	AH	DD	Mission	Program		No.	AH	DD	Mission	Program	
Secondary NiCd (25 cells)	1	6.0	0.56	10.9	13.6		3	20	0.61	92.9	115.7		2	12.0	0.64	46.3	59.4	
Secondary AgZn Recharge during flight (21 cells)	1	5.3	0.63	4.09	27.7		2	30	0.61	31.2	210.5		2	11.5	0.66	21.9	110.2	
Recharge on ground (21 cells)	1	30.0	0.80	9.53	96.2		5	115	0.70	140.1	1459.7		3	115.0	0.72	86.2	879.5	
Primary AgZn (20 cells)	1	25.0	0.96	9.53	191.0		4	105	0.96	110.2	2246.7		4	65.0	0.95	77.2	1526.0	
Fuel Cell Radiator Delta				1.81	2.27					32.6	39.51					20.0	24.0	

TABLE 5-V.- ATL PAYLOAD PEAK POWER APPROACHES (MODULAR)

ATL Payload	1						2						3					
	Battery			Weight (kg)			Battery			Weight (kg)			Battery			Weight (kg)		
	No.	AH	DD	Mission	Program		No.	AH	DD	Mission	Program		No.	AH	DD	Mission	Program	
Secondary NiCd (25 cells)	1	12.0	0.29	23.1	33.2		5	12.0	0.61	115.6	145.6		2	12.0	0.64	46.4	59.4	
Secondary AgZn Recharge during flight (21 cells)	1	11.5	0.29	10.9	58.6		5	11.5	0.63	54.4	272.1		2	11.5	0.67	21.8	110.2	
Recharge on ground (21 cells)	1	115.0	0.21	29.9	296.2		5	115.0	0.71	149.6	1472.0		3	115.0	0.72	89.8	886.0	
Primary AgZn (20 cells)	1	65.0	0.37	20.9	386.1		6	65.0	1.03	125.2	2300.0		4	65.0	0.95	83.4	1536.0	

No. = number, AH = cell ampere hours, DD = battery depth of discharge. 20% replacement of NiCd batteries during 11-year program. Secondary AgZn replaced every other mission, primary AgZn replaced every mission. Mission represents one 7-day sortie, Program represents total 22 sorties (11 years).

required. Increased weight is estimated at 36.65 kg (72 lb) including tubing, heat exchanger, and pumps. Since this approach was not included in the ground rules for this analysis, it will not be considered. It remains, however, an interesting and potentially significant alternative to batteries for energy storage on ATL missions.

Table 5-VI compares energy storage assembly weights for both the modular and design point approaches. Two different bases are used for the weight comparison. Mission weights are the complete energy storage weight required for a single seven-day sortie. Program weights are based on the total weight of energy storage components required for 22 7-day sorties over the 11-year period.

The weight penalty for the modular approach is greatest for the ATL 1. This could be decreased by using smaller charger-battery sets for the ATL 3 with a small penalty in specific power.

Table 5-VII shows energy storage assembly costs for the modularized approach. The costs shown do not include development, test, and engineering, material procurement, and general and administrative costs. Therefore, they should be used for relative comparisons only. The cost relationships used are shown in Table 5-VIII and the following notes:

- (1) Cell costs are increased by 40 percent to obtain complete battery costs. This allows for the battery case, connector, etc.
- (2) Charger and regulator costs were based on \$4400/kg (\$2000/pound) from Skylab. To allow for launch into orbit cost, a Shuttle launch cost of \$10 M was taken with a 29,848-kg payload, or \$339/kg (65,000 lb payload, \$154/lb). For 22 launches, logistic cost is then \$7458/kg (\$3390/lb) times mission weight.
- (3) The program costs include mission hardware and replacements. Total cost is obtained by adding launch and program costs.

The costs shown by Table 5-VII are total costs which have been normalized to the minimum costs for each payload and power approach. The costs shown can only be considered significant in terms of relative parametrics.

From the weight and cost considerations presented, secondary AgZn batteries recharged in flight now appear as the preferred approach to meeting ATL peak power requirements.

TABLE 5-VI.- ATL PAYLOAD PEAK POWER APPROACH WEIGHT COMPARISON

ATL Payload		1		2		3	
Design Approach		Modular	Design Point	Modular	Design Point	Modular	Design Point
		Weight (kg)		Weight (kg)		Weight (kg)	
Peak Power Approach		Weight Basis		Weight (kg)		Weight (kg)	
Secondary NiCd	Mission Program	23.1	10.9	115.7	93.3	46.3	46.3
		33.1	13.6	145.6	115.7	59.4	59.4
Secondary AgZn Recharge during flight Recharge on ground	Mission Program	10.9	4.1	54.4	31.3	21.8	21.8
		58.5	27.7	272.2	210.5	110.2	243.0
	Mission Program	29.9	9.5	149.7	140.2	87.5	86.2
		296.2	96.2	1472.0	1460.0	886.8	880.0
Primary AgZn	Mission Program	20.9	9.5	125.2	110.2	83.5	77.1
		386.0	191.0	2301.0	2083.0	1537.0	1526.0
Note: Mission is defined as one 7-day sortie; Program is 22 sorties over 11-year period							

TABLE 5-VII.- ATL PAYLOAD PEAK POWER APPROACH COST COMPARISON
(MODULARIZED)
(22 missions including launch costs)

ATL Payload Peak Power Approach	1	2	3
Secondary NiCd batteries	1.61	1.69	1.65
Secondary AgZn			
Recharge during flight	1.0	1.0	1.0
Recharge on ground	1.96	2.16	3.20
Primary AgZn batteries	1.49	1.92	3.12
Note: Numbers presented are ratios of cost to least related cost of each payload.			

TABLE 5-VIII.- BATTERY CELL COSTS AND COST RELATIONSHIPS

Type	AH Rating	Cost (\$)
NiCd	6.0	195.00
	12.0	230.00
	20.00	275.00
Secondary AgZn	5.3	18.00
	11.5	31.20
	30.0	54.00
	115.0	127.10
Primary AgZn	25.0	34.80
	65.0	54.00
	105.0	81.60

Advanced energy storage devices.— Energy densities shown in references 5-1 through 5-3 have been used to compare advanced energy storage devices with AgZn batteries selected for the ATL 3 sortie payload. Peak power and energy storage requirements are as follows:

Energy peak (daily)	458 W-hr
Maximum charge power available	1350 W
Maximum discharge power required	1900 W

Assumptions used to obtain a comparison of advanced energy storage devices (Table 5-IX) are summarized:

- (1) No development, test, and engineering; material procurement; general and administrative; etc., in costing.
- (2) Advanced NiCd and Ni-H₂ batteries are costed at current NiCd (6 to 12 AH cells) battery costs of \$660/kg (\$300/lb).
- (3) Regenerative fuel cells are costed at \$2200/kg (\$1000/lb).
- (4) Charger and regulator based on current Skylab costs at \$4400/kg (\$2000/lb).
- (5) Launch costs at \$339/kg (\$154/lb).
- (6) AgZn batteries are replaced every other mission based on total of 22 missions.
- (7) It is assumed the advanced energy storage devices will last 11 years with 50-percent replacement or refurbishment.
- (8) Battery weights include 25 percent of cell weight for case, interconnectors, etc.
- (9) Power conditioning and distribution losses are neglected.

The battery W-hr/kg values shown are based on single cells. Allowing 25 percent of the cell weight for case, connectors, etc., results in a battery specific energy of 35.2 W-hr/kg (16 W-hr/lb) for the advanced NiCd, and 72.6 W-hr/kg (33 W-hr/lb) for the Ni-H₂ units. The energy densities shown for the regenerative fuel cell are based on the weight of the complete package.

TABLE 5-IX.- ADVANCED ENERGY STORAGE DEVICES FOR
ATL NO. 3 PAYLOAD

Selected AgZn Candidate	Advanced Device		Advanced NiCd Battery (1)		Ni-H ₂ Battery (2)		Regenerative (3) Fuel Cells	
	Reference		5-1		5-2		5-3	
0.67	Depth of Discharge		0.70		0.70		0.70	
Mission	Program	Relative Performance	Advanced NiCd Battery (1)		Ni-H ₂ Battery (2)		Regenerative (3) Fuel Cells	
			Mission	Program	Mission	Program	Mission	Program
1.0		Mission weight	1.48		1.04		0.58	
	1.0	Program weight		0.43		0.31		0.17
1.0		Mission hardware cost	1.14		1.06		0.71	
	1.0	Program hardware cost		0.98		0.63		0.49
	1.0	Total cost (including launch)		1.29		0.88		0.56
Notes: (1) 44 W-hr/kg (20 W-hr/lb) (2) 88 W-hr/kg (40 W-hr/lb) (3) 132 W-hr/kg (60 W-hr/lb)								

It is assumed that only a boost regulator is required for the regenerative fuel cell. Voltages would be matched to the unregulated bus voltage in the charging mode.

When compared on a mission weight basis, only the 132 W-hr/kg (60 W-hr/lb) regenerative fuel cell offers a substantial reduction in weight, and a large part of this is due to elimination of a charger.

Substantial reduction in program weights are shown by all advanced energy storage devices. However, this is not considered to be a heavily weighted parameter. There is no substantial reduction in mission hardware cost. An increase of regenerative fuel cost from \$2200 to \$4400 per kg (\$1000 to \$2000 per lb) would close this gap. This also is the case for program hardware cost and total cost.

In conclusion, if program weight is not an important factor and considering uncertainties in the assumed regenerative fuel cell costs, the selected AgZn energy storage assembly is competitive with the advanced devices considered.

Competitive electrical power characteristics.- The electrical power subsystem mechanization selected for the ATL payloads is a modification of the one previously defined for the Shuttle 30-day sortie. For the latter mission, payload power is supplied by the orbiter fuel cells. The payload provides for its own power conditioning, distribution and control, energy storage and fuel cell reactant (cryogenic H₂ and O₂) requirements.

Figure 5-4 shows a schematic for an ATL electrical power subsystem using batteries for energy storage (secondary power). A 7-kW fuel cell is added to the sortie lab. Fuel cell heat will be rejected by the laboratory environmental control system (not shown). Silver-zinc batteries have been selected for the ATL sortie lab 7-day mission. Battery discharge voltage may vary from 1.3 to 1.8 V per cell depending upon discharge rate. The ATL power profiles for the various payloads require a large range of discharge rates. Therefore, a regulator is included in the battery discharge circuit. Charge voltages of 1.96 to 1.98 V per cell are required.

The Shuttle power interface shown for the 30-day sortie has been retained for the ATL 7-day mission; 50 kW-hr of energy has been allocated to payloads. During the sortie mode approximately 6 kW of Shuttle fuel cell power will be available for the payload. During normal ATL operations it is not planned to use orbiter power. However, in case of ATL fuel cell failure, Shuttle power along with energy remaining in the ATL energy storage assembly (depending on state of charge) would be desired for emergency operation. This is treated further in a following discussion. The ATL payload data management subsystem (DMS) will use the orbiter communications for data relay to ground. The RAM element interface for the Shuttle 30-day sortie is deleted from the ATL payload EPS mechanization. Any pallets will be supplied by the experiment bus.

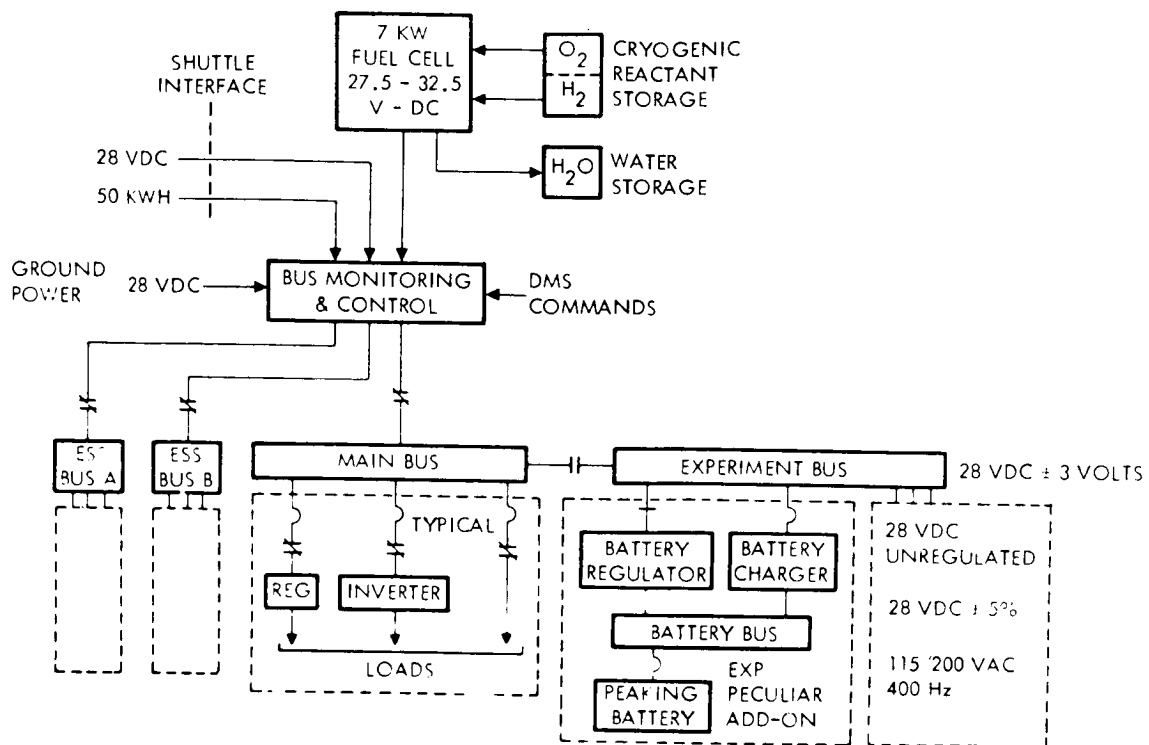


Figure 5-4. ATL Electrical Power Subsystem Schematic With Peaking Batteries

Table 5-X summarizes ATL electrical power subsystem weights. The primary power generation, power conditioning, and power distribution weights are independent of payload. The primary power generation is based on a single fuel cell and a single set of cryogenic tanks. The reactant tank weights are based on those currently being specified for the orbiter. The tank characteristics are as follows:

Reactant	Tank External Dim				Capacity				Tank Weight	
	Length		Diameter		Total		Usable			
	M	(in.)	M	(in.)	kg	(lb)	kg	(lb)	kg	(lb)
H ₂	1.27	(50)	1.17	(46)	49.8	(109.7)	44.5	(98)	103.3	(227.7)
O ₂		Sphere	1.02	(40)	414.4	(913.6)	378.1	(833.6)	112.4	(247.8)

TABLE 5-X.- ATL PAYLOAD ELECTRICAL POWER SUBSYSTEM WEIGHTS (MISSION)
(BATTERY SECONDARY POWER)

Components/Assemblies			Weight											
			kg		lb									
Primary power generation			(406.4)		(896)									
Fuel cell (1)			91.6		202									
Cryogenic H ₂ tank (1)			103.4		228									
Cryogenic O ₂ tank (1)			112.5		248									
Plumbing, valves, ext. pressurization			72.1		159									
Water pump (1)			4.1		9									
Water tank (1)			22.7		50									
Power conditioning			(103.4)		(228)									
Inverters, main (1)			20.4		45									
essential (2)			20.4		45									
experiment (1)			20.4		45									
Regulators, main (1)			0.9		2									
essential (2)			16.3		36									
experiment (3)			25.0		55									
Power distribution			(355.6)		(784)									
Electrical monitoring and control (1)			42.6		94									
Buses, diodes and contactors			13.2		29									
Wiring (13.7 kW rated)			299.8		661									
Subtotal			865.4		1908									
ATL Payload			1		2		3							
			kg		lb		kg		lb					
Secondary power generation			(10.9)		(24)		(65.4)		(144)		(32.6)		(72)	
AgZn batteries**			4.1		9		24.5		54		12.2		27	
Chargers			3.2		7		19.1		42		9.5		21	
Regulators			3.6		8		21.8		48		10.9		24	
Total			876.3		1932		930.8		2052		898.0		1980	
**Twenty-one 11.5 AH cells														

Assuming a fuel cell specific reactant consumption of 0.41 kg/kW-hr (0.9 lb/kW-hr), the above tankage results in 980 kW-hr available for the ATL payload; 720 kW-hr are required at a 5-kW average load power for 6 days on orbit. Full cryogenic tanks will permit operation at close to the 7-kW level for 6 days on orbit.

Power conditioning and distribution weights are the same as those used in the 30-day Shuttle sortie.

In order to account for power conditioning and distribution losses, the parametric battery weights are increased by one battery each for the ATL 2 and 3 payloads. The following battery maximum depths of discharge result when allowing for 20-percent power conditioning and distribution losses.

ATL Payload	Number of Batteries*	Maximum Discharge Energy (W-hr)	Maximum Depth of Discharge (%)
1	1	125	36
2	6	1362	66
3	3	585	57

*AgZn (11.5 AH), 345 W-hr

Table 5-XI shows an estimate of EPS component weights required for a program of twenty-two 7-day missions over an 11-year period. Footnote 1 shows the assumed mission mix. Total maximum equipment operating time is 3168 hours. An engineering model of one of the orbiter fuel cells has run 5080 hours on test without a failure. For those components showing program weight equal to mission weight, it is assumed their operating lifetimes are equal to or greater than that required for the 11-year program.

For the purpose of defining the competitive power system, the AgZn batteries will be changed each mission, whereas the parametric studies assumed every other mission. This is based on the premise that ground handling requirements to expeditiously remove the batteries from the spacecraft and place them in cold storage will be more expensive than new batteries.

Secondary power subsystem component weights and dimensions are summarized in Table 5-XII.

Competitive control concept and characteristics.— The competitive control concept and associated physical characteristics for this mission are identical to those presented previously for the 30-day Shuttle sortie mission - refer to Module 1 of this volume.

TABLE 5-XI.- ATL PAYLOAD ELECTRICAL POWER SUBSYSTEM WEIGHTS (PROGRAM)⁽¹⁾
(BATTERY SECONDARY POWER)

Item	Weight		Δ Mission (%) (6)
	kg	lb	
Fuel cell (2)	91.6	202	0
Cryogenic H ₂ tank	103.4	228	0
Cryogenic O ₂ tank	112.5	248	0
Plumbing, valves, external pressurization	90.7	200	25
Water pump	4.1	9	0
Water tank	22.7	50	0
Inverters	81.6	180	33-1/3
Regulators (load)	51.3	113	21-1/2
Monitoring and control	53.1	117	23
Buses, diodes and contactors	13.2	29	0
Wiring	299.8	661	0
Chargers (7-lb each)	22.2	49	1 spare
Regulators (8-lb each)	25.4	56	1 spare
Batteries (78 total)	318.4	702	(3)
Installation structure (10%) ⁽⁴⁾	65.8	145	

(1) Assume 6 ATL payload 1 missions
8 ATL payload 2 missions
8 ATL payload 3 missions

(2) Maximum equipment operating time = 3168 hr

(3) Use 1 mission each, cost = \$920 each
Based on Eagle Picher data and assuming cell and case cost equal on weight basis

(4) Based on mission EPS weight less wiring

(5) Program based on 22 sorties (11 years). Experiments powered-up 6 days each sortie, one day allowed for ascent to and descent from orbit.

(6) Percentage increase in the mission weights shown in Table 5-X.

TABLE 5-XII.- SECONDARY POWER SUBSYSTEM COMPONENTS PHYSICAL CHARACTERISTICS

Component	Dimensions		Volume		Weight	
	cm	(inch)	cm ³	(in ³)	kg	(lb)
AgZn battery	12.7 x 12.7 x 25.4	(5 x 5 x 10)	4098	(250)	4.1	(9)
Battery regulator	20.3 x 20.3 x 17.8	(8 x 8 x 7)	7212	(440)	3.6	(8)
Battery charger	17.8 x 17.8 x 15.2	(7 x 7 x 6)	4917	(300)	3.2	(7)

IPACS ATI Concept

The ATL electrical power subsystems schematic using IPACS for secondary power is shown in figure 5-5. The IPACS units have been substituted for the peaking battery and its associated components of the competitive power system shown in figure 5-4. The motor/generator wheels are a planar array of 3 double-gimbed units. The IPACS discharges directly to the experiment bus instead of an equivalent battery bus (figure 5-4). IPACS charge power is switched directly from the fuel cell. The central control unit will receive bus voltage status from bus monitoring and control and deliver power to the experiment bus when the fuel cell power goes below 7 kW (5.6 kW delivered to busses). When power required by the loads is less than 5.6 kW (determined by bus voltage), fuel cell power will be available for adding energy to the IPACS momentum wheels. The control unit will determine which units that power should be supplied to, depending on their current energy levels.

The ATL IPACS weights are summarized by Table 5-XIII. Primary power generation, power conditioning, and distribution weights are the same as the competitive electrical power system. Energy storage and attitude control weight results were extracted from the conceptual design effort documented below.

TABLE 5-XIII.- ATL IPACS WEIGHT SUMMARY

Component/assemblies	Weight	
	kg	lb
Primary power gen. (Table 5-X)	406.4	896
Power conditioning (Table 5-X)	103.4	228
Power distribution (Table 5-X)	355.6	784
Subtotal	(865.4)	(1908)
Energy storage/attitude control*	(334.7)	(737.8)
Energy momentum units (3)	313.3	690.6
Motor-generator electronics (3)	4.1	9.0
2 drive electronics (3)	7.3	16.2
Central control	10.0	22
Total	1200.1	2646
*See Table 5-XIV		

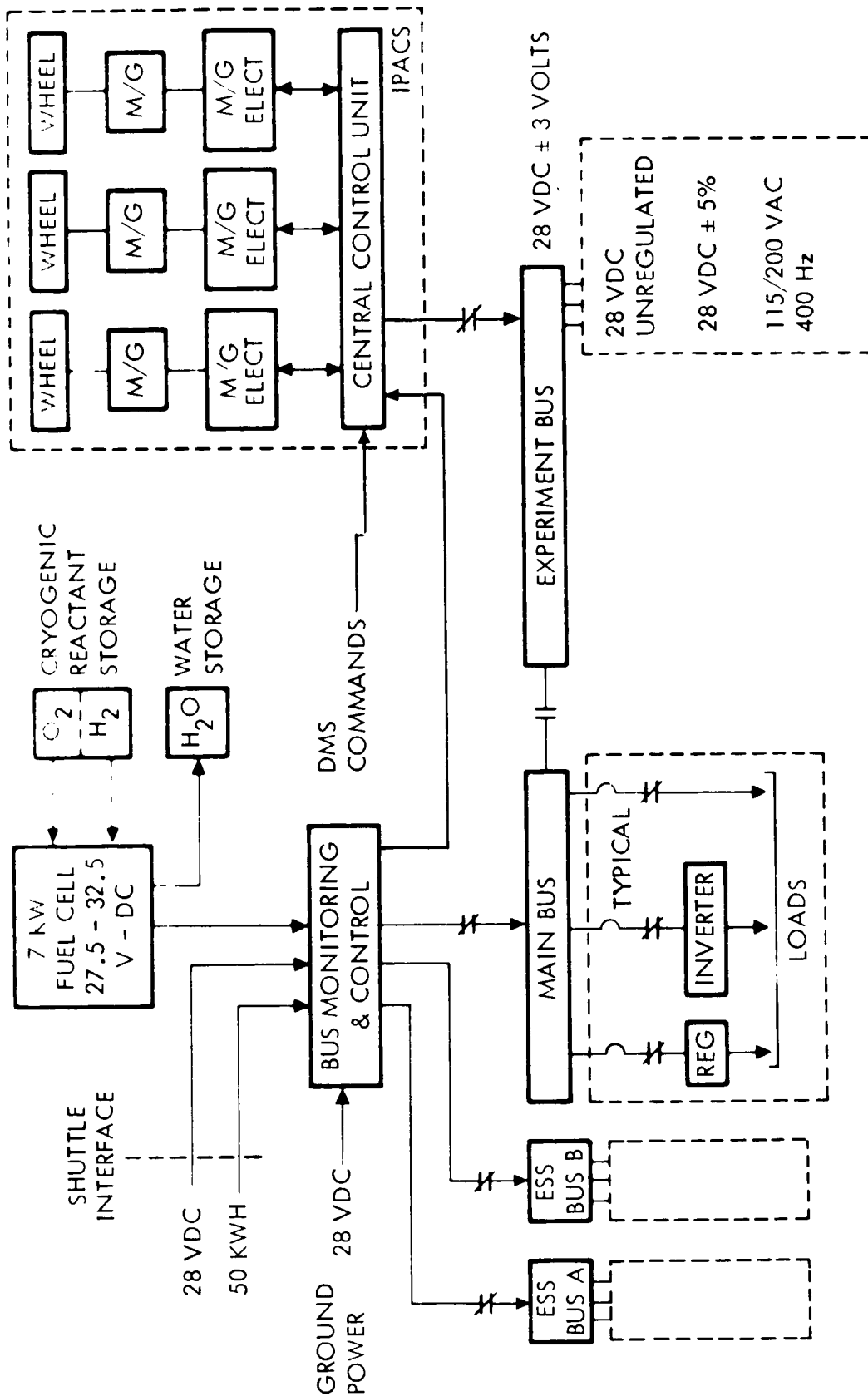


Figure 5-5. ATL Electrical Power Subsystem Schematic With IPACS

ATL IPACS design.— The following presents a conceptual design of a weight-optimized, two-gimbal CMG for the ATL mission. From the standpoint of wheel speed, it is a conservative design; however, from the overall volume standpoint, a considerable penalty is paid by this approach.

Inner gimbal: The inner gimbal design is similar to that of the RAM shown by drawings in Module 2, Volume II, of this report. The rotor selected was a 0.68 m (27 in.) diameter titanium disk rotating at 18 500 rpm maximum. This disk is only 2.44 cm (0.96 in.) thick to satisfy momentum and energy storage. Its cross section has been thickened near the shaft to increase the linear resonant frequency perpendicular to the spin axis. This increases the rotor weight from 41.05 kg (90.5 lb) to 43.45 kg (95.8 lb). The rotor has an integral hollow shaft 6.35 cm (2.5 in.) in diameter which houses the motor-generator rotor. The rotor is supported on 206H ball bearings (rotor weight is almost identical to that of the RAM CMG) with a 133.4 N (30 lb) preload. At the maximum rotor speed of 18 500 rpm, the bearing losses are 31 W total with an estimated windage loss of 4 W at 0.133 N/m^2 (1.0 micron) air pressure in the enclosure. Bearing lubrication is by centrifugal oiler in a manner similar to that used on the RAM. The bearing preload is by means of a "long travel" spring with a launch lock mechanism as developed for the RAM IPACS unit.

The gimbal enclosure consists of two conical housings fastened to a central mounting ring. The gimbal pivots are fixed to this ring. The conical housings are of 2.03 mm (0.080 in.) thick aluminum alloy, and the central mounting ring and gimbal pivot mounting pads are also aluminum. Housing thickness was selected based on required stiffness about an axis perpendicular to the spin axis.

The motor generator unit of 1200 W is mounted within the enclosure. It is a two-phase, permanent magnet rotor machine having an efficiency varying between 96 and 98 percent over the operating conditions. The lowest efficiency point is when operated as a generator and delivering full load at half speed. The motor is 12.07 cm (4.75 in.) in diameter and 6.35 cm (2.5 in.) long with a stack length of 3.8 cm (1.5 in.). Samarium-cobalt is used as a permanent magnet material allowing a total radial gap of 2.54 mm (0.100 in.). The PM rotor is housed in the titanium shaft having a wall thickness of 2.29 mm (0.090 in.). The MG weight is 4.54 kg (10 lb). Output can be doubled by adding a second MG unit on the opposite side of the rotor with no design changes; total weight would be increased by <5 kg (<11 lb) including electronics.

Outer gimbal: The outer gimbal has a hollow box-type construction 5.08 cm (2 in.) by 10.16 cm (4 in.) with reinforced mounting surfaces at the gimbal axes.

Gimbal drive: The gimbal drive module consists of a dc torque motor, a gear reduction unit, gimbal bearings and shaft, and the housing and flange. To keep weight and power requirements to a minimum, the gimbal torque of 162.7 N-m (120 ft-lb) is supplied through a transmission. The transmission ratio was selected as $N = 18$ using star planetary gearing with two meshes. The selection of the transmission ratio is a compromise between power, motor size and speed, reflected inertia, backlash, transmission complexity, etc.

To obtain the peak motor torque of 9.03 N-m ($\frac{120}{18} = 6.66$ ft-lb) would require 121 W using a 9.5 N-m (7 ft-lb) dc torquer of advanced design and weighing 3.18 kg (7 lb). This power can be reduced with a relatively small increase in gimbal drive weight (figure 5-6). The torque motor selected has a weight of 5.13 kg (11.3 lb) and a peak power of 56 W. This gives a total gimbal drive weight of 14.79 kg (32.6 lb) per unit. The gimbal drive module is 19.68 cm (7-3/4 in.) in diameter and 15.24 cm (6 in.) long. A flange is added for mounting.

Sensor module: The sensor module provides gimbal position and rate information, contains gimbal bearings and an internal spline coupling to minimize thrust loading and misalignment torques. It is identical to the sensor unit of RAM.

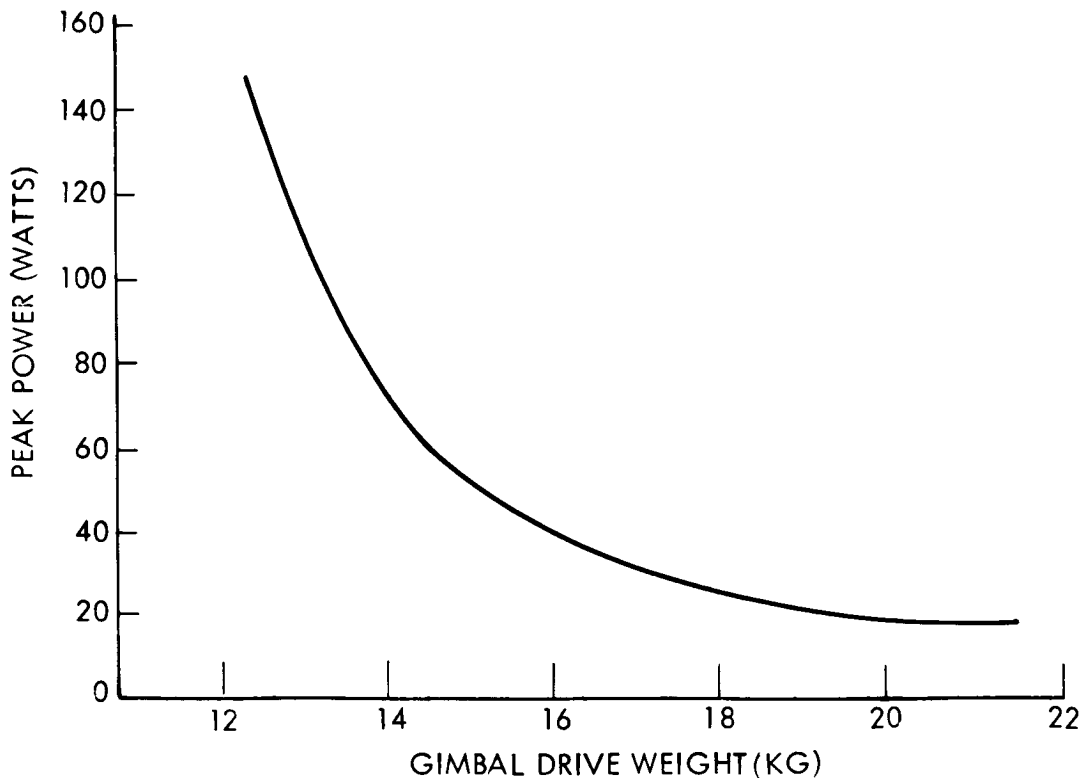


Figure 5-6. Gimbal Drive Power Weight Trade

CMG assembly: The CMG assembly consists of the inner gimbal, the outer gimbal, and two each of gimbal drive modules and sensor modules similar to the RAM. The clearance volume (assignable spacecraft volume) is 1.11 m (43.6 in.) in diameter by 1.12 m (44.25 in.) long for a total of 1.08 m³ (38.2 ft³).

The modular construction of the CMG facilitates assembly and repair.

CMG characteristics: The weight estimate for the ATL CMG is given in Table 5-XIV. This weight reflects the added weight of the gimbal drive to reduce torque motor power. Weight of the MG and gimbal electronics is included.

TABLE 5-XIV.- ATL WEIGHT ESTIMATE

Item	Weight	
	kg	lb
Inner gimbal		
Wheel	43.45	95.8
Shaft	2.86	6.3
Motor/generator	4.54	10.0
Spin bearings, oilers, housings	2.81	6.2
Enclosure	8.80	19.4
	62.46	137.7
Outer gimbal	8.66	19.1
2 sensor assemblies (with gimbal bearings)	3.72	8.2
2 drive assemblies (with gimbal bearings)	29.57	65.2
CMG assembly	104.41	230.2
MG electronics	1.36	3.0
2 drive electronics	2.45	5.4
Sensor electronics are part of control law computer		
Total weight with electronics	108.22	238.6
Note: CMG weight has been increased to minimize T.M. power		

Table 5-XV gives the power requirements. The estimated average power includes both gimbal torque motors at a 10 percent duty cycle, two sensor units, total spin power, and standby power of three electronic sets.

Table 5-XVI lists critical dimensions and volumes, while Table 5-XVII gives other characteristics not categorized in the three prior tables.

IPACS and Competitive System Comparisons

The comparison analysis included consideration of physical characteristics, performance characteristics, and operational differences.

TABLE 5-XV.- POWER REQUIREMENTS

Peak power - gimbal drive unit	56 W*
Rotor losses at 18 500 rpm	
Bearings	31 W
Windage (at 1 micron)	4 W
	<hr/>
Total	35 W
Maximum motor input	1200 W
Maximum generator output	1150 W
Usable energy (50% speed reduction)	957 W-hr
Motor efficiency	97% Min.
Generator efficiency	96-98%
Estimate average power	<58 W
<hr/>	
*If this power is doubled, CMG weight is reduced by 3.54 kg (7.8 lb)	

TABLE 5-XVI.- CMG SIZE AND VOLUME

Rotor diameter	68.58 cm, 27 in.
Inner gimbal - diameter	73.66 cm, 29 in.
axial length	53.85 cm, 21.2 in.
spin bearing spacing	40.64 cm, 16 in.
Maximum radius about outer gimbal axis	55.37 cm, 21.8 in.
Maximum length along outer gimbal axis	112.40 cm, 44.25 in.
Gimbal drive module dimensions	19.68 cm diameter by 15.24 cm long, 7.75 in. by 6 in.
Clearance volume	1.08 m ³ , 38.2 ft ³

TABLE 5-XVII.- PERFORMANCE CHARACTERISTICS

Minimum spin-up time (from rest)	1.1 hr
Maximum coast time	38.3 hr
Minimum spin momentum	2374 N-m-sec, 1751 ft-lb-sec
Gimbal friction (% of peak torque)	1/2%
Gimbal backlash	0.00029 rad, 1 arc min
Maximum spin speed	18 500 rpm
Minimum spin speed	9250 rpm
Rotor balance	0.254 μ m, 10 microinches
Rated gimbal torque	162.7 N-m, 120 ft-lb
Spin bearing preload	133.44 N, 30 lb

Physical characteristics comparison.- The weight and volume differences between the IPACS and competitive designs are summarized in Table 5-XVIII. Both the weight and volume data are presented as system deltas. Components common to both systems have been excluded. The comparison is therefore made on the basis of three double-gimbaled IPACS energy-momentum units compared with three Skylab CMG's and a complement of batteries, chargers, and regulators which varies as a function of the mission. Volume data for the IPACS units and the CMG's are based upon an equivalent spherical volume of the rotors.

Inspection of the table shows IPACS to be significantly lighter than the competitive system. The weight saving is 288.4 kg (636 lb) or more for some missions. IPACS volume is indicated as higher than the competitive system volume in all cases. This is not considered a problem as the large volume of the orbiter cargo bay is not expected to constrain the ATL design. Should volume become a problem, an alternate IPACS design could be used that provides lower volume at the expense of weight. An IPACS design with volume smaller than the competitive system could be provided with a weight increase of 9.5 kg (21 lb) per unit or total system weight increase of 28.6 kg (63 lb). Note that the IPACS design would still be at least 260 kg (573 lb) lighter than the competitive system.

Performance characteristics comparison.- A summary of the performance characteristics of the IPACS and competitive systems is presented in Table 5-XIX. The momentum storage capability of the competitive systems is larger because existing design CMG's are used, contrasted with IPACS units tailored specifically for the orbiter vehicle. The IPACS units are sized to provide at least six orbits of continuous operation without desaturation. The competitive system (using a comparable sizing methodology) would be capable of eight orbits without desaturation.

The available energy storage data differ between missions in that the IPACS units are sized for the worst-case missions and the battery system is tailored to the individual mission. In each case a battery depth of discharge of 66 percent was used to calculate the data shown in the table. Although this depth of discharge is not necessary to meet the current requirements for Payloads 1 and 3, it does provide an indication of the growth potential available before additional batteries must be used.

The attitude control performance for both systems is considered essentially equivalent. Precision control capability (pointing accuracy and rate stability) is dictated by the performance of the experiment isolation platforms which are a common element of both systems. The control torque levels were specified to be equal in both systems. If the ATL payloads are sensitive to induced vibration the IPACS units may require shock mounting or it may be possible using precision balancing techniques to keep the IPACS-induced vibration level comparable to that associated with the CMG's. This would require a factor of three improvement in the balancing capability.

TABLE 5-XVIII.- PHYSICAL CHARACTERISTICS COMPARISON

Parameter	IPACS design	Competitive Design		
		Payload 1	Payload 2	Payload 3
Δ System weight \sim kg (lb)*	334.67 (737.8)	623.80 (1374)	678.28 (1494)	645.59 (1422)
Δ System volume \sim m ³ (ft ³)	0.507 (17.9)	0.289 (10.2)	0.371 (13.1)	0.323 (11.4)
*Delta from common primary power generation, conditioning, and distribution.				

TABLE 5-XIX.- PERFORMANCE CHARACTERISTICS COMPARISON

Parameter	IPACS design	Competitive Design		
		Payload 1	Payload 2	Payload 3
Momentum storage n-m-sec (ft-lb-sec)(per array)	7130 (5250)	\longleftrightarrow	9360 (6900)	\longleftrightarrow
Available energy storage W-hr	2925	228	1370	685
Attitude control performance	\longleftrightarrow	Equivalent	\longleftrightarrow	\longleftrightarrow
Control torque nm- (ft-lb) (per torquer)	163 (120)	\longleftrightarrow	163 (120)	\longleftrightarrow

Operational consideration comparisons.- There are operational differences between the IPACS and the competitive battery - CMG system which are significant considering the projected 11-year program of flight operations. The total program is assumed to consist of 22 flights, including six Payload 1 missions, eight Payload 2 missions, and eight Payload 3 missions.

The physical characteristics comparison indicated IPACS to be lighter than the competitive system. Over the total program, and including consideration of the payload mix discussed above, the net weight saving of IPACS over the competitive system is 6960 kg (15 340 lb). This saving is due to the difference of launch weight between IPACS and the competitive system. The associated cost saving is evaluated in the cost analysis portion of this module.

A second operational difference between the systems concerns the inventory of hardware required to complete the program. A summary of the flight hardware and spare requirements is presented in Table 5-XX. The regulators and chargers are reused from mission to mission. One flight set of CMG's was assumed to be adequate for the entire program (less than 154 days of operation). Two spare units are considered adequate allowing one unit at the flight depot and one unit at the vendor in rework. In the case of the IPACS design similar requirements were assumed - three flight units and two spares. The cost impact of these inventory requirements are considered in the mission operations portion of the cost section.

A final operations consideration in the comparison between the IPACS and competitive system is the "between flight" or pre-flight operations differences. The delta functions to be performed are summarized in Table 5-XXI. Operations that are common for both designs have been excluded. It is felt that the operational checks of the IPACS units are not much more complex than the checks required for the CMG's. Thus the IPACS design is considered less complex than the competitive system from the ground operation standpoint. This factor was not included in the operational cost evaluation.

System comparison summary.- In summary, the weight-optimized IPACS design was found to provide a significant weight saving with some increase in volume. Alternative IPACS designs could provide a volume saving with a slight decrease in the weight saving. Attitude control performance is considered essentially equivalent between the systems. The momentum storage capability in the competitive system exceeds the mission requirements and the energy storage capability in the IPACS design exceeds the mission requirements - both are considered secondary benefits. Evaluation of the operational considerations for the 22-flight program indicates IPACS should provide significant advantages in terms of transportation cost reduction, flight hardware inventory reduction, and simplification of ground operations.

TABLE 5-XX.- HARDWARE REQUIREMENTS - FLIGHT AND SPARE

Component	Flight units	Spares	Total
IPACS	3	2	5
CMG's	3	2	5
Batteries	78	0	78
Chargers	6	1	7
Regulators	6	1	7

TABLE 5-XXI.- PRE-FLIGHT OPERATIONS COMPARISON

IPACS design	Competitive design
<ul style="list-style-type: none"> • Checkout IPACS units 	<ul style="list-style-type: none"> • Checkout CMG's • Remove old batteries • Install new batteries • Add or remove chargers and regulators, as required • Checkout energy storage subsystem

ATL Systems Cost Analysis

General.- This section presents the programmatic information and cost data relating to the ATL program, including the work breakdown structure (WBS), program development schedule, cost summary, cost breakdowns, IPACS annual funding schedule, and cost-effectiveness tradeoffs. The development cost data indicate an IPACS penalty of \$4.090M. The first flight system cost reflects a reduction of \$0.692M for IPACS. Thus cost through the first flight system shows an IPACS penalty of \$3.398M. When the operational costs associated with replacement hardware are considered, the IPACS penalty drops to an overall \$0.947M. Consideration of cost-effectiveness factors such as transportation result in a net IPACS saving of \$2.682M.

Work breakdown structure: Figure 5-7 gives the WBS for the ATL IPACS. The WBS shows the elements and components deleted as a result of the incorporation of IPACS, as well as the subsystem components unaffected or common to both the competitive subsystem and IPACS. The IPACS units and WBS elements added also are shown.

The ATL IPACS WBS reflects design, development, test hardware (engineering models), flight hardware, tooling and STE, assembly and checkout, and mission operations for both the competitive subsystem and IPACS.

IPACS development schedule: The development, test, and fabrication of the ATL IPACS units is shown to require a period of 4-1/2 years (figure 5-8), excluding mission operations time. The program schedule gives the development span for the two IPACS components considered critical, the high-power PM motor/generator and rotor balance and bearings. The estimated development period for the motor/generator is 12 months and 1-1/2 years for the rotor balance and bearings. The development span for the other IPACS units are shown. Drawing release and all design and development tasks are scheduled to be completed by the end of the third year. Fabrication, assembly, and test of the engineering models and the flight hardware are shown. The operational flight hardware is scheduled to be available during the early part of the fifth year after contract go-ahead. Flight operations are not shown to completion; however, the mission operations time was assumed to be 11 years.

Equipment cost.-

Summary: Table 5-XXII gives the impact on cost of the competitive subsystem as a result of incorporating IPACS into the ATL vehicle. The costs are summarized separately for development (non-recurring), first flight system, and mission operations (recurring) for both the competitive subsystem and IPACS.

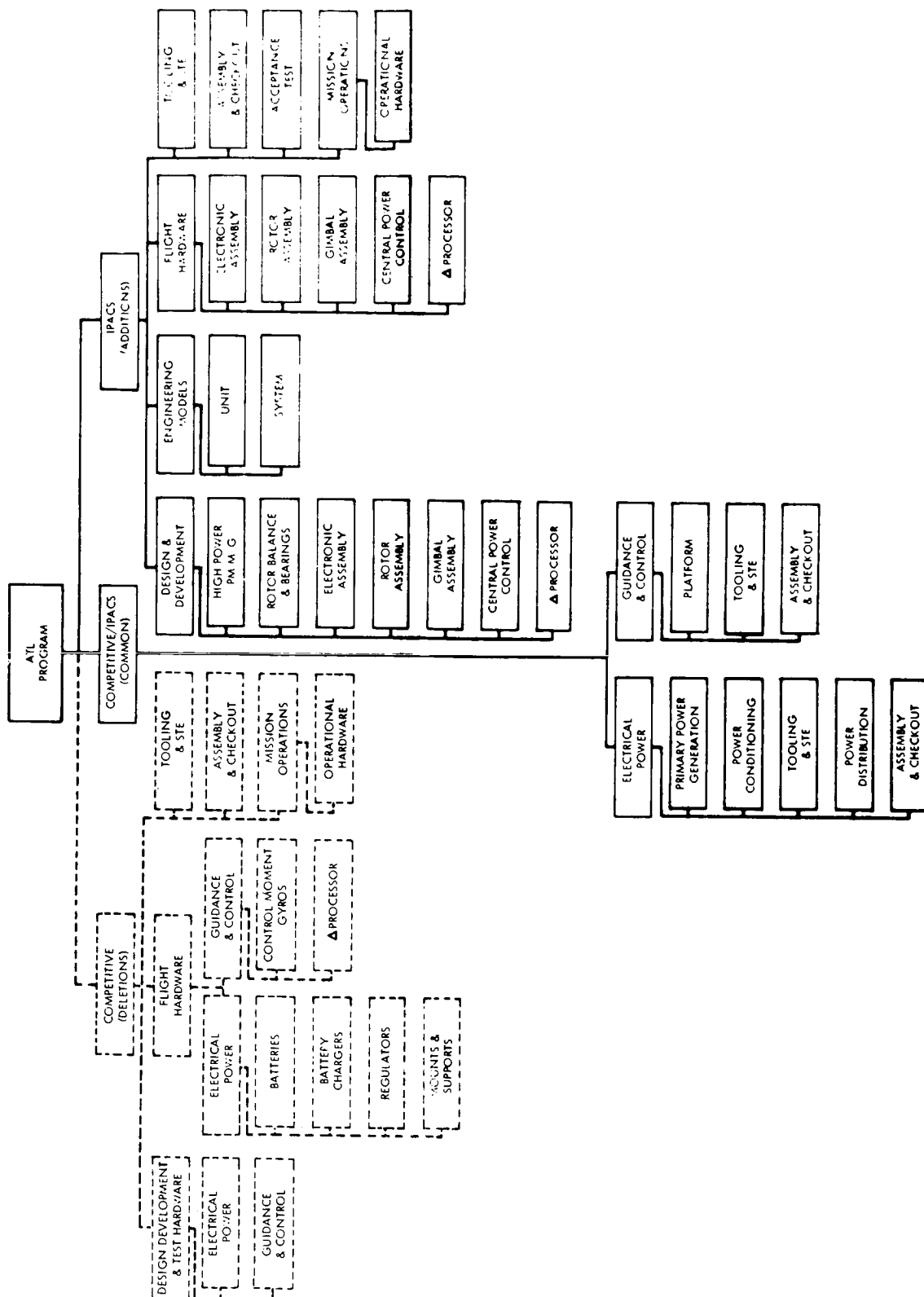


Figure 5-7. ATL Program Work Breakdown Structure

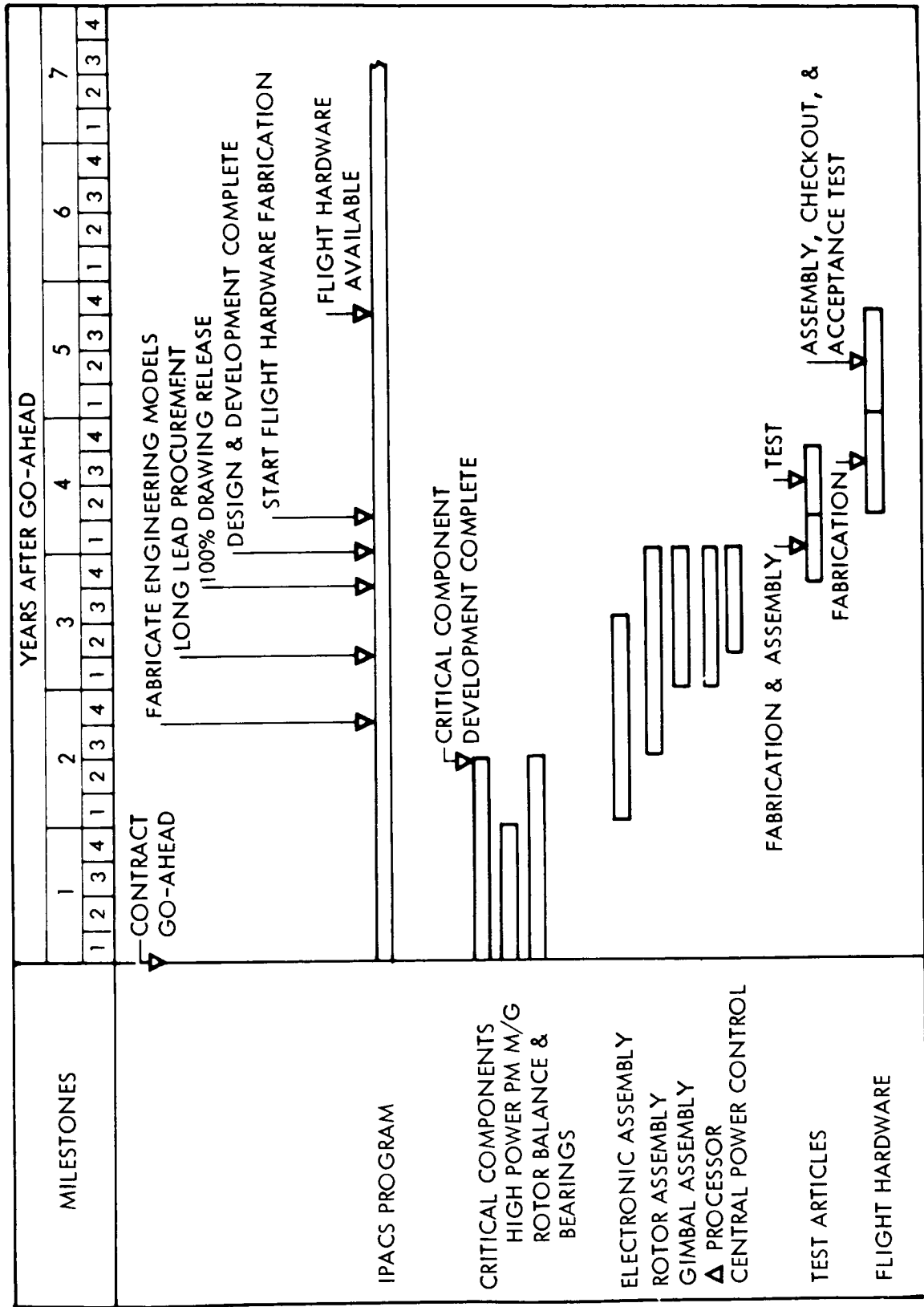


Figure 5-8. ATL Program IPACS Development Schedule

TABLE 5-XXII.- COST SUMMARY - ATL

Cost levels	Development	First flight system	Cost (\$ = M) Subtotal	Mission operations	Total
Competitive subsystem					
Electrical power	\$ 6.471	\$13.573	\$20.044	ND*	\$20.044
Guidance & control	32.064	5.468	37.532	ND	37.532
Total	\$38.535	\$19.041	\$57.576	ND	\$57.576
Less: components deleted	-4.238	-3.167	-7.405	-4.101	-11.506
Net	\$34.297	\$15.874	\$50.171	-4.101	\$46.070
Plus: IPACS components	+8.328	+2.475	+10.803	+1.650	+12.453
New total	\$42.625	\$18.349	\$60.974	-2.451	\$58.523
*ND = not determined during the study					

Mission operations costs: The ATL mission operations costs associated with the components deleted and the IPACS units added are shown in Tables 5-XXIII and 5-XXIV. The mission operations costs consist of operational replacement hardware. The cost of transportation of parts and supplies from the ground to earth orbit is covered in the cost-effectiveness tradeoff. The following ground rules and assumptions were utilized in the costing of mission operations:

- (1) The operational period was assumed to be 11 years.
- (2) Batteries are replaced after every flight.
- (3) No refurbishment is required.
- (4) Flight replacement hardware requirements are as shown in Table 5-XXV.

TABLE 5-XXIII.- MISSION OPERATIONS COSTS -
COMPONENTS DELETED - ATL

Description	Cost (\$-M)
Operational replacement hardware	
Chargers	\$0.055
Battery packs	2.592
Regulators	0.062
Control moment gyros	1.392
Total	\$4.101

TABLE 5-XXIV.- MISSION OPERATIONS COSTS -
IPACS UNITS ADDED - ATL

Description	(\$ = M)
	Total
Operational replacement hardware	\$1.650
Total	\$1.650

TABLE 5-XXV.- FLIGHT REPLACEMENT HARDWARE - ATL

Description	Flight replacement units	Spares	Total
Chargers	0	1	1
Battery packs	72	0	72
Regulators	0	1	1
CMG's	0	2	2
IPACS units	0	2	2

Table 5-XXIII reflects the mission operations cost related to the components deleted. The total cost is \$4.101M, consisting of replacement hardware of chargers, battery packs, regulators, and control moment gyros.

Table 5-XXIV shows the mission operations costs related to the IPACS units added. The total mission operations cost is \$1.650M, consisting of operational replacement hardware.

Cost breakdown - components deleted: The cost of the components deleted, shown in Table 5-XXVI, were determined by the parametric costing approach which employs cost estimating relationships such as dollars per pound. The CER's were developed from the same cost and technical data associated with the 30-day Shuttle sortie program.

The non-recurring cost of \$4.238M includes \$3.714M for design and development, such as engineering analysis, design, preparation of drawings, specifications, plans, documentation, support, component development, laboratory testing, mockups, and test hardware for the electrical power and attitude control subsystems, as well as \$0.524M of tooling and special testing equipment utilized by the factory for in-process testing during fabrication.

The recurring cost (first flight system) of \$3.167M includes flight hardware of \$2.843M and assembly and checkout of \$0.324M.

TABLE 5-XXVI.- COST BREAKDOWN, COMPONENTS DELETED - ATL
(DOLLARS IN M)

Cost Level	Non Recurring	Recurring	Total
Non-recurring			
Design, development & test hardware			
Electrical power	\$2.219		\$2.219
500 AH batteries			
Battery chargers			
Wiring			
Mounts and supports			
Guidance and control	1.495		1.495
Control moment gyros			
Δ processor			
Tooling and STE	.524		.524
Recurring			
Flight hardware			
Electrical power		\$.868	.868
500 AH batteries			
Battery chargers			
Wiring			
Mounts and supports			
Guidance and control		1.975	1.975
Control Moment gyros			
Δ processor			
Assembly and checkout		.324	.324
Total	\$4.238	\$3.167	\$7.405

TABLE 5-XXVII.- COST BREAKDOWN - IPACS COMPONENTS ADDED - ATL

Cost Level	Non Recurring	Recurring	Total
Non-recurring			
Design and development			
High power PM M/G	\$.129		\$.129
Rotor balance and bearings	.248		.248
Rotor assembly	.329		.329
Electronics assembly	.377		.377
Gimbal assembly	.715		.715
Central power control	.084		.084
Δ processor	.237		.237
Engineering models			
Unit models			
Rotor assembly	.172		.172
Electronics assembly	.130		.130
Gimbal assembly	.316		.316
Central power control	.011		.011
Δ processor	.102		.102
Systems models			
Rotor assembly	.820		.820
Electronics assembly	.617		.617
Gimbal assembly	1.503		1.503
Central power control	.022		.022
Δ processor	.204		.204
Tooling and STE	.139		.139
Assembly and checkout	1.133		1.133
Acceptance tests	1.040		1.040
Recurring costs			
(First flight system)			
Flight hardware			
Rotor assembly		\$.410	.410
Electronics assembly		.309	.309
Gimbal assembly		.752	.752
Central power control		.011	.011
Δ processor		.101	.101
Assembly and checkout		.466	.466
Acceptance tests		.426	.426
Total	\$8.328	\$2.475	\$10.803

Cost breakdown - IPACS units added: Table 5-XXVII shows a detailed cost breakdown of design, development, test, and fabrication of IPACS units, including cost of engineering models, tooling and STE, assembly and checkout, and acceptance test cost. The unit models are for component qualification test purposes and consist of one each of the rotor assembly, the electronics assembly, gimbal assembly, the central power control and Δ processor. The systems models are for ATL vehicle systems verification and integration test purposes and consist of the equivalent of two flight systems, each set including 3 rotor assemblies, 3 electronics assemblies, 3 gimbal assemblies, 1 central power control, and 1 Δ processor.

The recurring costs (first flight system) of \$2.475M includes \$1.583M for flight hardware, (3 rotor assemblies, 3 electronics assemblies, 3 gimbal assemblies, 1 central power control, and 1 Δ processor), \$0.466M assembly and checkout and \$0.426M for acceptance tests.

IPACS annual funding: Table 5-XXVIII shows the peak year funding for incorporation of IPACS into the ATL vehicle. As shown in figure 5-8, the time of the IPACS development, test, and fabrication of flight hardware is 5 years. Table 5-XXVIII shows the peak year funding to occur in the third year after go-ahead at \$3.543M.

TABLE 5-XXVIII.- IPACS ANNUAL FUNDING SCHEDULE - ATL

Description	Years after go-ahead*					Total
	1	2	3	4	5	
ATL IPACS	\$0.454	\$2.182	\$3.543	\$3.295	\$1.329	\$10.803
*Dollars in M						

Cost-effectiveness tradeoffs.- The following factors were provided by NASA for use in computing penalty cost and value cost resulting from incorporation of IPACS into the ATL vehicle:

\$250/lb of launch weight

\$1500/ft³ of occupied space

\$760/W-yr of power consumption

Table 5-XXXIX gives the cost resulting from the application of the above factors. Table 5-XXX shows the weight breakdown used to estimate transportation costs. These weights represent the flight hardware for the total program of 22 missions with hardware common to both the IPACS and competitive systems excluded. The difference between the IPACS component weight and the deleted component weight yields the program flight weight saved by the incorporation of IPACS, which is 6962 kg (15,334 lb). This weight when multiplied by the \$250/lb factor yields the transportation or weight penalty cost. Over a total of 22 missions, IPACS occupies 3.86 m³ (136.6 ft³) more space than did the components deleted, resulting in a small penalty for IPACS.

TABLE 5-XXIX.- COST-EFFECTIVENESS TRADEOFF

Description	Amount	Factor	Cost (\$ - M)
Weight (lb)	-15 334	\$250/lb	-\$3.834
Space occupied (ft ³)	+136.6	\$1500/ft ³	+.205
Power consumption (W-yr)	Nil	\$760/W-yr	Nil
Net			-\$3.629

A minus figure reflects an IPACS advantage and a plus value shows an IPACS penalty. Therefore, the net results from the application of the cost-effective weighting factors show a net IPACS cost advantage of \$3.629M for the ATL vehicle.

TABLE 5-XXX.- TRANSPORTATION WEIGHT SUMMARY

Description	Total weight kg (lbs)
Deleted components	14,334 (31 572)
Chargers	248 (546)
Batteries	319 (702)
Regulators	283 (624)
CMG's	13,484 (29 700)
IPACS components	7,372 (16 238)

Total cost comparison.- Table 5-XXXI indicates the total cost impact of using the IPACS concept. The cost savings associated with cost-effectiveness factors significantly outweigh the loss associated with differential equipment costs. The total cost savings are on the order of 4 percent of the program cost (excluding operations) for the two competitive subsystems. The conclusion drawn is that the systems are essentially equivalent from a cost standpoint. It should be noted, however, that the transportation cost savings and the other operational advantages of the IPACS concept would make its use cost-effective if the development costs were partially shared by either another program or technology development activities.

TABLE 5-XXXI.- TOTAL COST COMPARISON

Factor	Cost
Differential equipment	+\$0.947M
Penalty	- 3.629
Total cost impact (savings)	-\$2.682

ATL Summary

The IPACS concept for ATL resulted in an 18-percent weight saving and 4-percent cost saving over the competitive system. The cost saving is not significant and both systems are considered cost equivalent.

Development cost penalties overrode significant transportation cost savings. Development cost sharing should make IPACS cost-effective for ATL.

The low energy storage requirement for ATL resulted in a suboptimal IPACS design which more approximated a CMG than an energy momentum wheel both in its design and low operational speeds.

Further studies are recommended to define a more optimum design size for an IPACS with the ATL momentum requirement. It can be expected that higher energy storage capability will result at no cost in weight. The resulting design may then be developed to have broader sortie lab applicability.

References

- 5-1 Chaskey, A., and M. Klein, "High Energy Density Nickel - Cadmium Cells," Intersociety Energy Conversion Engineering Conference Paper No. 709065 (1970).
- 5-2 Stockel, J. F., et al, "A Nickel-Hydrogen Secondary Cell for Synchronous Orbit Application," Intersociety Energy Conversion Engineering Conference, Paper No. 729019 (1972).
- 5-3 Dunlop, J. D., et al, "Analysis of the Single Cell Concept for a Rechargeable H₂-O₂ Fuel cell," Intersociety Energy Conversion Engineering Conference Paper No. 719120 (1971).

APPENDIX 5-A - CRITERIA FOR SORTIE LAB BACKUP POWER

If experiments and subsystems are operating normally, but there is a sudden loss of primary power, it is assumed that backup power would be provided only to allow termination of the mission. Since no hazard is implied, and crew safety is not a concern, the mission objectives from this point should be to:

- (1) Preserve the validity of accrued scientific data and specimens.
- (2) Protect the sortie lab and its equipment from damage during mission termination.
- (3) At a minimum, configure the sortie lab and save its equipment to permit Shuttle entry and landing.

The requirements for the above will vary as a function of crew size and actual experiment payloads (Table 5-A-I). This analysis is based on a crew size of two, which appears to be a nominal case for sortie lab. A larger crew size could effect shutdown more quickly in some cases but might take slightly longer to express.

The experiment complement has various effects on planning for the contingency. For example, loss of primary power could be used to shut down the main bus and switch critical subsystems to a contingency bus. However, payloads for each mission would require customized consideration. Therefore, in this analysis it was baselined that power shutdown would be accomplished by the crew. An important payload effect is the condition of certain experiments at the time primary power is lost. Environmental or meteoroid detectors may be deployed, imaging sensors may be extended, and casting metals may be in a molten state. The above mentioned examples (plus subsystems load until

TABLE 5-A-I.- BASELINE CONSIDERATIONS

- | |
|--|
| <ul style="list-style-type: none">. Crew Size - Two. Power Down Accomplished by Crew. Experiment Payload Varied, e.g.,<ul style="list-style-type: none">- Materials Processing- Life Sciences- Observational |
|--|

crew evacuation) tend to size the magnitude of the power load. Life sciences experiments could dictate duration of the power load. Some specimens would require refrigeration, freezing, or life support. If the validity of scientific data are to be retained (objective 1, above), then power requirements may extend past Shuttle landing and rollout until ground power can be applied to the sortie lab.

In order to meet the specified mission contingency objectives, the crew must perform certain activities or control various functions which can be identified as power users until the function is completed. These are summarized in Table 5-A-II as a function of mission objective. Figure 5-A-1 is an integrated timeline for power down which meets all stated objectives. In the event that retention of scientific data is not an objective (despite the investment in a Shuttle launch) a different and shorter sequence could be followed. This would allow shutdown of the continuing power shown for the life sciences specimens. An additional option would appear to be that securing of the sortie lab is not an objective and that configuring for Shuttle entry is the only objective. In this case, deployed arrays or sensors could be jettisoned and eliminate the power required for retraction motors. The overall time-to-crew evacuation could be reduced from about 45 minutes to about 30 minutes. The power continued until after landing includes the means to provide caution and warning data to the Shuttle. If Shuttle power can be transferred to the sortie lab, then this power for pickoffs, transducers, and alarms could in fact be Shuttle provided.

Cryo dumping was not included in the timeline since it is not a Shuttle operational requirement.

TABLE 5-A-II.- SUMMARY OF CREW ACTIONS AND FUNCTIONS

Mission Objective	
1	<ul style="list-style-type: none"> A. Place life science specimen in freezer, refrigerator or life support canister. B. Shut down oven, deposition equipment, etc., and allow specimen to harden so that it can be stowed or restrained. C. Dump computer memory and in-process data to tape storage; make pertinent log entries and notes.
2 and 3	<ul style="list-style-type: none"> A. Safe sortie lab high-pressure systems B. Stow or secure loose equipment. C. Retract any externally deployed sensors.
All	Continue life support system, lighting, voice communications, and caution and warning until crew evacuation.

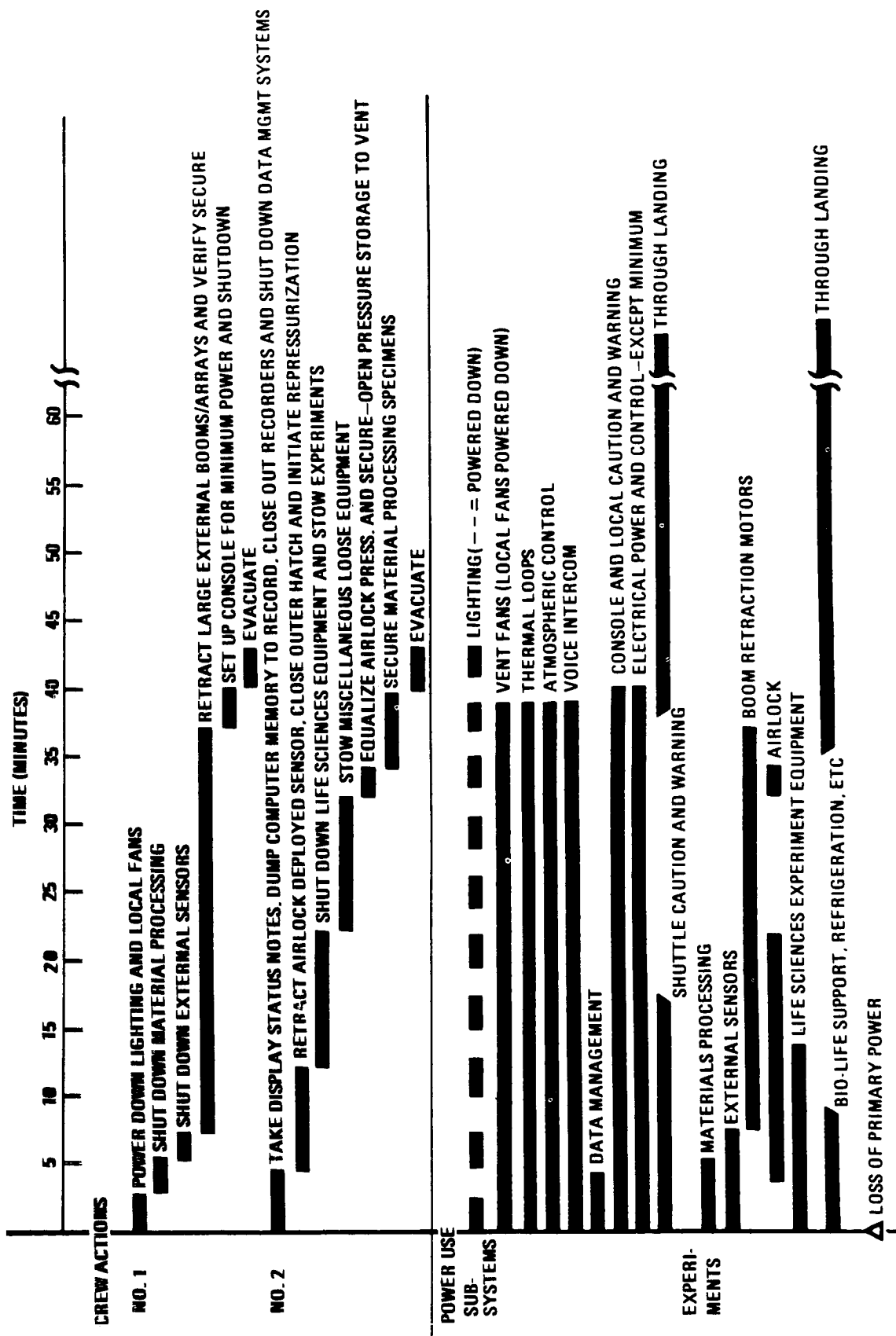


Figure 5-A-1. Power-Down Timeline

MODULE 6 - FEASIBILITY STUDY CONCLUSIONS AND RECOMMENDATIONS

Feasibility Study Conclusions

Simultaneous electrical energy storage and attitude control by means of flywheel arrays appeared technically feasible and satisfied performance requirements for all missions studied.

The flywheel units were found to weigh less than the competitive battery or fuel cell systems studied for all but the RTG-powered planetary MJS mission. Competitive flywheel assemblies, assembled from either current or advanced technology components, are predicted to produce about twice the energy density of the competitive battery systems at comparable development levels.

As energy storage elements, current technology flywheels were found to range between 9.5 and 22 W-hr/kg, with advanced technology wheels ranging between 18 and 37 W-hr/kg. This compares with 2.6 to 13 and 6.7 to 22 W-hr/kg for current and advanced technology NiCd systems, respectively. When considered as an integrated power and control subsystem, weight savings over the conventional subsystems ranged from 215 kg (473 lb), a 6 percent saving, to 100 kg (222 lb), or 36 percent, for the EOS mission. The RAM mission studies resulted in an IPACS advantage of 497 kg (1096 lb), a 31-percent weight savings.

The flywheel energy-momentum units were found readily adaptable to both gimbaled and nongimbaled arrays of conventional control usage.

The weight advantages of the flywheel systems increased as mission life and charge-discharge cycles increased. With proper design, IPACS energy density, unlike batteries, is relatively unaffected by increases in the number of charge-discharge cycles for realistic spacecraft lifetimes. IPACS lifetimes in excess of five years appear readily attainable with only small weight changes over that of a one-year mission.

IPACS operational factors were found to be comparable to those of current systems.

Development, first unit, and penalty cost data were estimated for IPACS and compared with the data from the original studies for the TDRS, RAM, MSS, and 30-day Shuttle sortie missions. Mission operations costs also were estimated for the two missions of the conceptual design studies, TDRS and RAM. Equipment cost savings were indicated at \$1.3M for TDRS, \$5.2M for RAM, and \$5.7M for MSS; these savings represented 11, 13, and 2 percent, respectively. Penalty costs for the TDRS did not significantly change the cost advantage. Penalty costs for the RAM systems, however, resulted in a significant savings increase of \$9.8M, resulting in an overall cost advantage for the RAM IPACS of \$15M which amounts to a 36 percent decrease over competitive systems costs.

The 30-day Shuttle sortie mission resulted in a \$10.8M (20 percent) cost penalty for IPACS use. The 30-day Shuttle mission selected had a very high (60-kW) power requirement and moderate (5 kW-hr) energy storage requirement with a low number of charge-discharge cycles. The increase in development costs to obtain IPACS (\$11.1M) outweighed the low cost of high energy density Ag Zn batteries for this mission.

The ATL Shuttle sortie mission subsequently studied utilized a lower power and energy requirement. The IPACS has shown comparable costs (4 percent advantage for IPACS) to the Ag Zn competitive system. Again, development costs were higher for IPACS but operational costs lower for the 11-year mission period studied.

The studies did not show any inherent power, energy, or control boundaries which significantly limit IPACS in spacecraft application. Power levels to 80 kW per array and energy storage to 70 kW-hr per array are obtainable for units sized to space station dimensional constraints. Momentum storage capability exceeds requirements and control pointing is expected to parallel that of current CMG's.

The developments required for the current technology designs include: demonstration of ball bearing system life and power capability at speeds to 50 000 rpm with light film lubrication through centrifugal oilers; fabrication and demonstration of high speed and efficiency for permanent magnet rotor generator-motor units; and, demonstration of the capability to balance rotors about a factor of seven better than common for CMG's over the wider high-speed range. These developments are verified by calculations but remain to be demonstrated.

The advanced technology designs require the development of high energy density composite rotors and magnetic suspension bearings capable of 50 000 rpm operation. Composite designs have been built and tested in other research programs but delivered performance is lower than design prediction. Predictable designs must be developed and tested for performance and producibility. Magnetic suspension bearings have been built and tested to 8000 rpm. Improvements in bearing field control electronics bandwidth and stability are required to achieve the higher rpm.

Development costs vary among programs but, for the current technology, approximate those required for a new CMG design without power return capability.

An advanced technology composite rotor development for MSS and 30-day Shuttle was estimated at \$2.7M for a three-year program. The magnetic suspension bearing development for the same missions was estimated at \$2.5M for the same missions.

Recommendations

Feasibility studies indicate the IPACS concept to be a cost-effective method of increasing subsystem life and energy density with only moderate development cost. The IPACS designs appear especially suited to the requirements of Shuttle-era spacecraft such as the RAM where long life and refurbishment capability can result in decisive savings for multiple mission usage. It is, therefore, recommended that IPACS development continue.

Studies are recommended to define the more optimum IPACS designs for application to selected missions. Specific parameters should be studied to define the sensitivities of the IPACS designs to changes in requirements and operating ranges. Cost-effectiveness studies are required to define the preferred technology approach for IPACS design.

Overall system electrical design optimization studies are recommended. The benefits of higher voltage arrays and efficiencies of control circuits are to be defined.

Control studies defining elastic body and nonlinear control effects are recommended for continuance.

From the standpoint of design it is recommended that a current technology energy-momentum wheel be fabricated and tested to validate development design calculations and performance estimates.

The testing of the current-technology unit can be expected to provide the design data base for the development of the advanced technology composite rotor and magnetic suspension bearing.

NATIONAL AERONAUTICS AND SPACE ADMINISTRATION
WASHINGTON, D.C. 20546

OFFICIAL BUSINESS
PENALTY FOR PRIVATE USE \$300

FIRST CLASS MAIL

POSTAGE AND FEES PAID
NATIONAL AERONAUTICS AND
SPACE ADMINISTRATION
451



POSTMASTER: If Undeliverable (Section 158
Postal Manual) Do Not Return

"The aeronautical and space activities of the United States shall be conducted so as to contribute . . . to the expansion of human knowledge of phenomena in the atmosphere and space. The Administration shall provide for the widest practicable and appropriate dissemination of information concerning its activities and the results thereof."

—NATIONAL AERONAUTICS AND SPACE ACT OF 1958

NASA SCIENTIFIC AND TECHNICAL PUBLICATIONS

TECHNICAL REPORTS: Scientific and technical information considered important, complete, and a lasting contribution to existing knowledge.

TECHNICAL NOTES: Information less broad in scope but nevertheless of importance as a contribution to existing knowledge.

TECHNICAL MEMORANDUMS: Information receiving limited distribution because of preliminary data, security classification, or other reasons. Also includes conference proceedings with either limited or unlimited distribution.

CONTRACTOR REPORTS: Scientific and technical information generated under a NASA contract or grant and considered an important contribution to existing knowledge.

TECHNICAL TRANSLATIONS: Information published in a foreign language considered to merit NASA distribution in English.

SPECIAL PUBLICATIONS: Information derived from or of value to NASA activities. Publications include final reports of major projects, monographs, data compilations, handbooks, sourcebooks, and special bibliographies.

TECHNOLOGY UTILIZATION PUBLICATIONS: Information on technology used by NASA that may be of particular interest in commercial and other non-aerospace applications. Publications include Tech Briefs, Technology Utilization Reports and Technology Surveys.

Details on the availability of these publications may be obtained from:

**SCIENTIFIC AND TECHNICAL INFORMATION OFFICE
NATIONAL AERONAUTICS AND SPACE ADMINISTRATION
Washington, D.C. 20546**